Interaction between sulfur (S) and nitrogen (N) assimilation pathways in response to S and N supply in onion (*Allium cepa* L.)

A thesis presented in partial fulfilment of the
requirements for the degree of
Doctor of Philosophy in Plant Molecular Biology
At Massey University, Palmerston North, New Zealand

Srishti Joshi 2014

Abstract

This thesis investigates the extent of interdependency between the sulfur (S) and nitrogen (N) assimilation pathways in the commercially important, S-accumulating, monocot species, onion CUDH2107 (*Allium cepa* L.), to elucidate some of the regulatory points of cross-talk between these two pathways.

To test the interactions between the two pathways, a factorial S x N depletion experiment was set up. Plants were grown in short day conditions to maintain the pre-bulbing stage after which they were transferred to long day conditions to promote bulbing. At the end of the short day conditions, the plants were harvested as leaf, pseudo stem and root and at the end of the long day conditions, as leaf, bulb and roots, for each of the four treatments. The four treatments comprised of control treatment (designated C; comprising 14 mM N and 2 mM S), low S treatment (designated –S; comprising 14 mM N and 0.25 mM S), low N treatment (designated –N; comprising 3.5 mM N, 2 mM S) and coupled low S and N treatment (designated –S-N; comprising 0.25 mM S and 3.5 mM N).

In terms of changes in biomass, both the root and the shoot biomass tended to be higher under the –S treatment at the bulbing stage, although these changes were only significant for the root biomass. Under the – N and the –S-N treatments, the shoot biomass was much lower when compared with the control plants at both the pre-bulbing and the bulbing stage, although no change in the root biomass was observed. The exception was at the bulbing stage under the –S-N treatment where the root biomass was significantly higher when compared with the control plants.

At the transcriptional level in response to the -S treatment, the relative transcript abundance of commonly used S-starvation marker genes, *AcHAST1;1LIKE1* and *AcAPSR1* increased in both root and the leaf tissue and was more marked at bulbing. In contrast, transcript abundance of *AcAPSK1,* which marks a bifurcation in the S-assimilation pathway, decreased. At bulbing, a decrease in the relative transcript abundance of *AcATPS1, AcSIR1* and *AcOASTL3* in the leaf tissue and *AcATPS1, AcAPSK1, AcOASTL2, AcNRT2;1LIKE1* and *AcNiR1* in the root tissue was observed in response to the –S treatment. However, in response to N deprivation, under the –N as well as –S-N treatment, the transcript abundance of *AcHAST1;1LIKE1* and *AcAPSR1* was dramatically reduced in the roots with a significant induction in the leaf tissue at both the stages. In addition, relative transcript abundance of *AcATPS1 , AcAPSK1* and *AcSOX1* also increased whereas *AcOASTL2, AcNR1*

and *AcNiR1* decreased under the –N and the –S-N treatments in the leaf tissue, at pre-bulbing. However, at bulbing, transcript levels of *AcOASTL2 and AcNR1* also increased under both, the –N and the –S-N treatments. In the roots, at pre-bulbing, the relative transcript abundance of *AcHAST1;1LIKE1, AcNRT2;1LIKE1* and all the down-stream reductive S and N assimilation genes investigated declined, while the transcript abundance of *AcAPSK1* increased. A similar response was observed at the bulbing stage for most genes except *AcSOX1* and *AcOASTL3* which increased and *AcOASTL1, AcOASTL2* and *AcNRT2;1LIKE1* showed no change. Similar to the leaf under the –S-N treatment, the transcriptional profile of the genes investigated in the roots under the –S-N treatment also showed a dominant response to N depletion.

In terms of protein accumulation and enzyme activity, AcSiR1 declined in the –S treatment but accumulated in the –N and the –S-N treatment in the leaf tissue at pre-bulbing whereas at bulbing, a decline in protein accumulation was observed under all three treatments. The AcSiR1 enzyme activity declined under the –S and the –N treatment but remained unchanged under the –S-N treatment in the leaf tissue at the pre-bulbing as well as the bulbing stage. In the roots, AcSiR1 accumulated under the –S treatment in both the stages whereas activity remained unchanged. No AcSiR1 protein could be detected under the –N treatment at both stages and in the –S-N treatment at pre-bulbing, whereas the activity increased under these treatments at both stages. Under the –S treatment in the leaf tissue, AcNiR1 accumulated slightly at both pre-bulbing and bulbing whereas the activity remained unchanged. Under the –N and the –S-N treatments, AcNiR1 declined in the leaves at pre-bulbing but accumulated at the bulbing stage. However, the activity remained unchanged at the pre-bulbing stage and was below the assay detection limit at bulbing. In the roots, the AcNiR1 accumulation response was similar to that in the leaf tissue under each treatment at both the stages, whereas the activity declined under all treatments at both stages except at the pre-bulbing stage under the –S treatment where it remained unchanged.

The accumulation of a set of targeted metabolites was also compared over the four treatments. A decline in the S containing flavour precursors, including the lachrymatory factor, thiopropanal-S-oxide, was observed in all tissues in response to low S supply. However, glutathione only declined in the leaf at the bulbing stage. An effect of the –S treatment on the accumulation of N-containing metabolites was observed as an accumulation of the amino-acids in the pseudo-stem and the bulb. In contrast, a decline in the accumulation of the amino-acids and derivatives was observed in the leaf at bulbing. In

response to the –N treatment, most of the N-containing metabolites declined systemically, including the N-pathway cysteine precursor, *O*-acetylserine and serine. Flavonol glucosides accumulated in a tissue-specific manner in the pseudostem at the pre-bulbing stage but declined in the bulb tissue. Generally, sugars accumulated systemically at both developmental stages whereas sugar phosphates accumulated only in the leaf and root tissue at the pre-bulbing stage. The lachrymatory factor thiopropanal-S-oxide, accumulated in the leaf at the pre-bulbing stage but declined at the bulbing stage in response to the –N treatment. The metabolite accumulation profile in the plants under the –S-N treatment was similar in all tissues to that of the –N treatment at both the stages.

The results from the factorial experiment suggest a hierarchy of N nutrition over S nutrition in *A. cepa,* where the incorporation and accumulation of S metabolites as well as bulb formation is regulated by N availability.

A putatively novel point of interaction between the S-assimilation and the N-assimilation pathways *via* sulfite reductase (AcSiR1) and nitrite reductase (AcNiR1) was also investigated. Recombinant AcSiR1 and AcNiR1 were each able to reduce both sulfite and nitrite, although with a higher specific activity for the physiological substrate in each case. Further, solid phase binding assay indicated a positive interaction between the two recombinant proteins, although this could not be confirmed by Isothermal titration calorimetry (ITC). In addition to this, in a short term S x N depletion experiment with *Arabidopsis, AtSiR1* transcripts only declined in the –S-N treatment in the leaves whereas *AtNiR1* transcripts declined in the –S, -N as well as –S-N treatment in wild type plants. In the roots, *AtSiR1* transcripts decline in both the –N and the –S-N treatment in the roots whereas no significant change was observed in the *AtNiR1* transcripts. In a *sir1* T-DNA knock-down line of *Arabidopsis,* the *AtSiR1* and the *AtNiR1* transcripts did not change in response to any treatment in both leaf and the roots.

Substrate redundancy between AcSiR1 and AcNiR1, *in vitro,* along with the other interaction studies suggest that although both AcSiR1 and AcNiR1 can reduce both substrates, the possibility of this being a direct point of cross-talk between the two pathways is not conclusively established.

Acknowledgements

I would like to thank my supervisor Prof. Michael McManus, for accepting me into this PhD program and guiding me every step of the way, for instilling in me the love for science and critical thinking and above all, for being a supremely patient mentor. I cannot thank you enough for all that I have learnt these past four years. I also would like to thank my co-supervisor Dr. John McCallum for all the resources provided during the PhD, for his timely suggestions and for always being encouraging and positive about my work and progress.

I am grateful for the support from Dr. Daryl Rowen and Martin Hunt from Plant & Food Research for helping me in the volatile GC-MS analysis, teaching me the nitty gritties of volatile extraction and patiently answering any queries. I thank Dr. Bruce Searle, Dr. Stephen Trolove and the Plant & Food Research, Hawkes bay as well as Jonathan Crawford at the climate lab for helping me with the factorial experiment. A special thanks to Dr. Ryo Nakabayashi and the metabolomics group in RIKEN, Japan, for performing the targeted metabolomics and helping me with the analysis. Huge thanks to Ann Truter and Cynthia Cresswell who were always there, smiling, to sort out any problem outside the lab, making this a relatively smooth ride for me.

Warm thanks to all my labmates: Alvina, Afsana, Aakansha, Diantha, Faisal, Julia, Jay, Jibran, Matt, Happy, Rachael, Rama, Sam and Tina for making the lab such a happy place to work in. Susanna and Afsana deserves a very special thanks for their unconditional assistance and friendship, for letting me make the important mistakes and saving me from making the time-consuming ones.

Thanks to Plant & Food Research and HortNZ for the PhD scholarship and also the resources during the period of study. Thanks to Institute of Fundamental Sciences and the New Zealand Society of Plant Biologists for additional assistance and financial support for attending conferences.

Last but not the least; I would like to thank my parents, grandparents and siblings for all the encouragement and love and my partner for showing such strong conviction in my capabilities and always being by my side.

Abbreviations

1-PRENCSO	Trans-S-1-propenyl-$_L$-cysteine sulfoxide
2-CPGTH	*S*-2-carboxypropyl glutathione
APSK1	Adenosine-5´-phosphosulfate kinase
APSR/APR	Adenosine-5´phosphosulfate reductase
ATPS/APS	Adenosine-5´-triphosphate sulfurylase
BLAST	Basic logical alignment search tool
bp	Base-pair
bZIP	Basic leucine zipper
cDNA	Complimentary DNA
DMF	*N,N*-dimethyl formamide
DNA	Deoxyribonucleic acid
DNase	Deoxyribonuclease
dNTP	2´-deoxynucleotide 5´ triphosphate
DTT	Dithiothretiol
E. coli	*Escherichia coli*
EDTA	Ethylenediaminetetraacetic acid
FW	Fresh weight
g	Acceleration due to gravity
gDNA	Genomic DNA
g	Gram
h	Hour
HAST1;1/ SULTR1;1	High affinity sulfate transporter
IPTG	Isopropyl-β-D-thiogalactopyranoside
ITC	Isothermal titration calorimetry
kb	Kilo base-pair
kD	Kilo daltons
L	Litre
LB	Luria-Bertani (media or broth)
LF	Lachrymatory factor
M	Molarity (moles per litre)
MCSO	Methyl cysteine sulphoxide
mg	Miligram
Milli-Q-water	Water purified by Milli-Q-ion exchange chromatography
min	Minute
ml	Millitres
mol	Mole (Avagadro's number)
Mpa	Mega Pascal
mRNA	Messenger RNA
NBT	*P*-nitro blue tetrazolium chloride
NCBI	National Centre for Biotechnology Information
ng	Nanogram
NiR	Nitrite reductase
NR	Nitrate reductase
NRT2;1	High affinity nitrate transporter 2;1
*O*AS	*O*-acetylserine
*O*ASTL/*O*AS-TL	*O*-acetylserine(thiol) lyase
°C	Degree celsius
PAGE	Polyacrylamide gel electrophoresis
PAPS	3´- phosphoadenosine-5´-phosphosulfate
PBS	Phosphate buffer saline

PCR	Polymerase chain reaction
pH	-Log (H+)
qRT-PCR	Reverse transcriptase-polymerase chain reaction
Rnase	Riboxynuclease
RO	Reverse osmosis
SAT	Serine acetyltransferase
sec	Second
SEM	Standard error mean
SiR	Sulfite reductase
SOX	Sulfite oxidase
Tm	Melting temperature at which DNA strands separate prior to annealing
Tris	Tris (hydroxymethyl) aminomethane
Tween-20	Polyoxyethylenesorbitan monolaurate
U	Unit (based on enzyme activity)
V	Volt
v/v	Volume per volume
w/v	Weight per volume
w/w	Weight per weight
X-Gal	5-Bromo-4-chloro-3-indolyl-β-D-galactopyranoside
µg	Microgram
µl	Microlitre
µM	Micromolar

List of Figures and Tables

Chapter1: Introduction

1.1 Project overview

Sulfur (S) and nitrogen (N) are two of the essential macronutrients required by plants to sustain growth and reproduction. These nutrients are incorporated in plants *via* the multistep S and N-assimilation pathways respectively. This process is an integral part of the planet's natural recycling system, the sulfur and the nitrogen bio-geological cycles. Since the drop in SO_2 emissions across the globe, especially in the western Europe, S deficiency in crop species such as wheat and rapeseed has become a major agricultural concern (Hawkesford & De kok, 2007). This has led to increasing interest in studying S incorporation mechanism and the genes involved in the S-assimilation pathway in plants. However, the S-assimilation pathway is indirectly regulated by optimal N supply as the precursor to cysteine, *o*-acetylserine is a product of acetylation of the amino acid serine (Droux et al., 1998). Due to its low bioavailability as a nutrient in the soil, farming practices of un-capped N fertilization has led to excessive leaching of N through the soil and into water-bodies which has, in-turn, increased the problem of eutrophication (V. H. Smith & Schindler, 2009). Hence nitrogen availability and increasing nitrogen use efficiency (NUE) in plants with limited N-fertilization has been a long standing goal of agricultural research.

For S-accumulating commercially important species such as the members of the *Brassicaceae*, a lot of research studying the interaction between the S and N-assimilation pathway has been done, as members of this family accumulate S-containing secondary metabolites known as glucosinolates which are nutritionally important for their antioxidant properties (Kliebenstein et al., 2001). In another commercially important plant genus, the *Alliums*, S is also important as it is a major component of the flavour compounds known as the cysteine sulfoxides which also contribute towards the characteristic pungency of the bulb (Eady et al., 2008; McCallum et al., 2011; McManus et al., 2012). The bulbs in Alliums form a sink for reduced sulfur compounds which are then mobilized during flowering (Lee et al., 2013). The reduced S-compounds stored in the bulbs are also nutritionally important, adding to the commercial value of the bulb.

As the reductive assimilation of S is dependent on precursors from the N-assimiliation pathway, it is important to study the interactions between these two assimilation pathways in an effort to understand how cross-talk might regulate the assimilation of down-stream metabolites under limiting S or N conditions. Interestingly, the N and S-assimilation

pathways also share an uncanny similarity, as an enzyme in the S-assimilation pathway, sulfite reductase (SiR) has a structurally and functionally similar counterpart in the N-pathway, nitrite reductase (NiR) (Krueger & Siegel, 1982; Nakayama, Akashi & Hase, 2000; Lukat et al., 2008). Both of these enzymes are co-localized in the plastids and assist in the six electron reduction of sulfite/nitrite to sulfide/ammonia. Although some functional redundancy *in vitro,* between these two enzymes has been shown in prokaryotes (Lukat et al., 2008), as well as in higher plants such as spinach (Krueger & Siegel, 1982), the possibility of interaction between the N and S-assimilation pathway through this commonality has not been investigated before. Thus the focus of this study has been to examine the effect of S and/or N depletion on key enzymes of the S and N-assimilation pathways and the down-stream accumulation of metabolites. A secondary aim is to explore the possibility of interaction between the S and N pathway indirectly as enzyme recruitment or directly as protein-protein interaction between AcSiR1 and AcNiR1.

For the first part of the study, a factorial experiment was designed with four different combinations of N and S concentrations leading to a N and S replete treatment (C; 14 mM N and 2 mM S), low S treatment (-S; 14 mM N and 0.25 mM S), low N treatment (-N; 3.5 mM N and 2 mM S) and a low S and N treatment (-S-N; 3.5 mM N and 0.25 mM S). the response of key S and N assimilation genes was investigated at the transcriptional and translational level for two developmental stages, the pre-bulbing stage and the bulbing stage in roots and leaves. Accumulation of major S and N metabolites and also the S-containing volatiles were then determined for roots and leaves and, where possible, also the pseudo-stem and the bulb.

For the second part of the study, recombinant AcSiR1 and AcNiR1, generated using the *E. coli* expression system, were used to establish enzyme redundancy and to study the possibility of a direct interaction as a protein-protein complex. As reverse genetics approaches could not be explored as a means to study the recruitment of AcSiR1 or AcNiR1 under limited expression of the either of the genes for *A. cepa,* an *Arabidopsis SIR* knock-down line (*sir1-1*), recently characterized by Khan et al., 2010, was used to study the repercussions of limited *AtSiR1* expression on the N-assimilation pathway, mainly *AtNiR1* expression. A short term S and N deprivation factorial experiment was also conducted for both the wild type and the *sir1-1* line to investigate any transient recruitment at the transcriptional level.

1.2 Overview of the essential elements of plants

A fascinating and rather important capability of living cells is to take up substances from the environment and subsequently assimilate these to synthesize their own cellular components. This phenomenon of taking up chemical compounds needed for growth and metabolism may be defined as nutrition and the substances required, as nutrients. Various specific metabolic processes help convert these nutrients into cellular components or substances required for energetic reactions. The term “metabolism” thus encompasses all of the chemical reactions that occur in a living cell to sustain life. Nutrition and metabolism are therefore interconnected phenomena.

The exclusivity of plants is in the fact that all of the essential nutrients required are inorganic. Plants use solar radiation as an energy source and convert it to chemical energy in the form of organic compounds, a process supported by the uptake of inorganic nutrients from the soil and the atmosphere (Mengel and Kirkby 2001).

A precise set of criteria for an element to be essential, as opined by Arnon and Stout (1939), states that:

1- It must be required for the completion of the life cycle of the plant.
2- The deficiency is specific for the element in question.
3- The element is directly involved in the nutrition of the plant (e.g. required for an enzyme to work or constituent of an essential metabolite).

Based on the growth requirement for a given nutrient, the essential elements are divided into two groups namely the macronutrients and the micronutrients. The macronutrients, as suggested by the name, are consumed in larger quantities and make up between 0.2% to 4% each of plant dry weight. These are nitrogen (N), phosphorous (P), potassium (K), calcium (Ca), sulfur (S) and magnesium (Mg) (Mengel and Kirkby 2001).

The micronutrients are required only in very minute quantities, and mainly are constituents of enzyme co-factors and prosthetic groups and are required for catalytic activities of different enzymes such as the Mo-dependent enzyme nitrate reductase and the Fe-dependent class of oxido-reductases (Mengel and Kirkby 2001).

1.3 Sulfur (S) as an essential macronutrient

Sulfur constitutes between 0.1 to 1% of plant dry weight and is required for synthesis of the amino acids cysteine and methionine (Khan et al., 2008). Sulfur containing compounds are important for numerous aspects of crop quality and for the natural resistance of plants to various bacterial and viral pathogens as well as insect pests. Plants require sulfur to synthesize a spectrum of S compounds with diverse physiological functions. For example, the tripeptide glutathione, an S-containing compound, is required for plant response to abiotic stress (increase in reactive oxygen species, uptake of heavy metals). Another example is the secondary S metabolite group, the glucosinolates, which are pathogen-directed defense compounds synthesized by plants. Finally, The thiol group of cysteine in proteins maintains protein structure by the formation of disulfide bridges between two cystine residues. Sulfur is also found in vitamins and co-factors (Saito, 2004) and is also incorporated into sulfoquinovosyl diglycerol (SQDG), a sulfolipid, which is a component of the thylakoid-membrane, found in all photosynthetically active organisms. Given the importance of this macronutrient, much research has been directed towards understanding the pathway leading to its uptake and incorporation in plants, which will be discussed in further detail in the next section.

1.4 Sulfur assimilation in plants

Sulfur assimilation in plants plays a key role in the sulfur cycle in nature. The incorporation of sulfur into cysteine in plants can begin by the uptake of sulfate by the roots *via* specialized transporters or as inorganic sulfur from the soil or as sulfur dioxide gas from the atmosphere. In the recent times, depletion of sulfur-containing air pollutants has led to sulfur deficiency in many agriculture areas of the world, such as Western Europe (Saito, 2004).

S assimilation by plants as an integral part of the global sulfur cycle

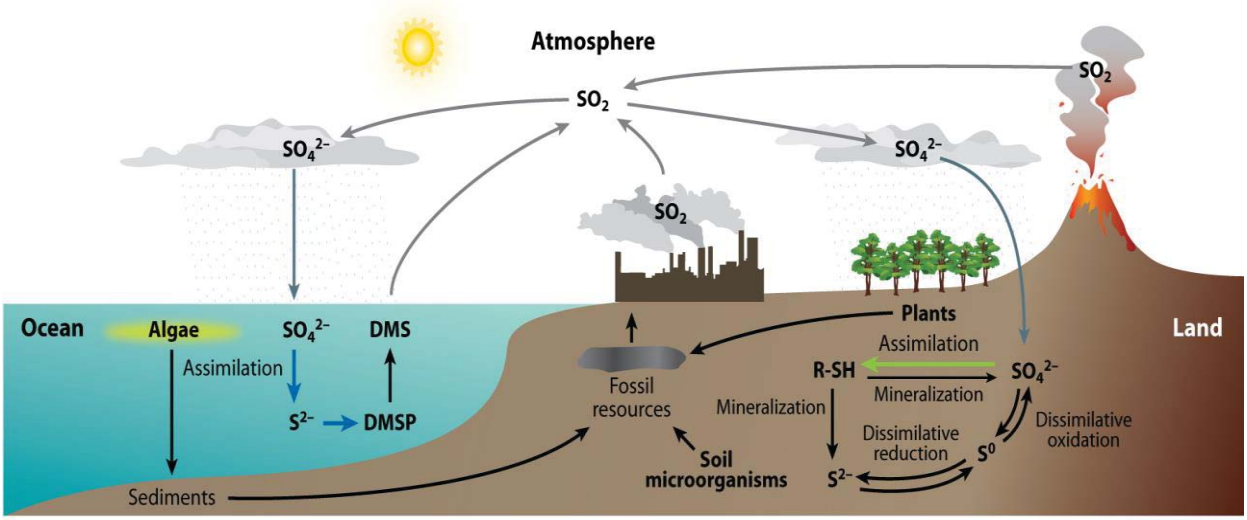

Figure 1.1 Sulfur cycle in nature Sulfate taken up by the soil is assimilated by plants (*green arrow*) and algae. Soil microorganisms mineralize organic sulfur to sulfate *via* dissimilatory metabolism. Volatile dimethylsulfide (DMS) made by algae by conversion of dimethylsulfoniopropanoate (DMSP) is also released into the atmosphere along with volatile compunds from volcanoes and SO_2 gas as industrial pollutant. These compounds are then oxidized back to sulfate in the atmosphere and are recycled *via* precipitation as rain. From Takahashi et al. (2011)

The need to understand the mechanisms of sulfur assimilation in detail has been readily recognized and much work has been done in terms of understanding the mechanisms involved at a molecular and biochemical level. A simplified representation of sulfur assimilation pathway in plants, with the enzymes involved and their cellular localization, is depicted below:

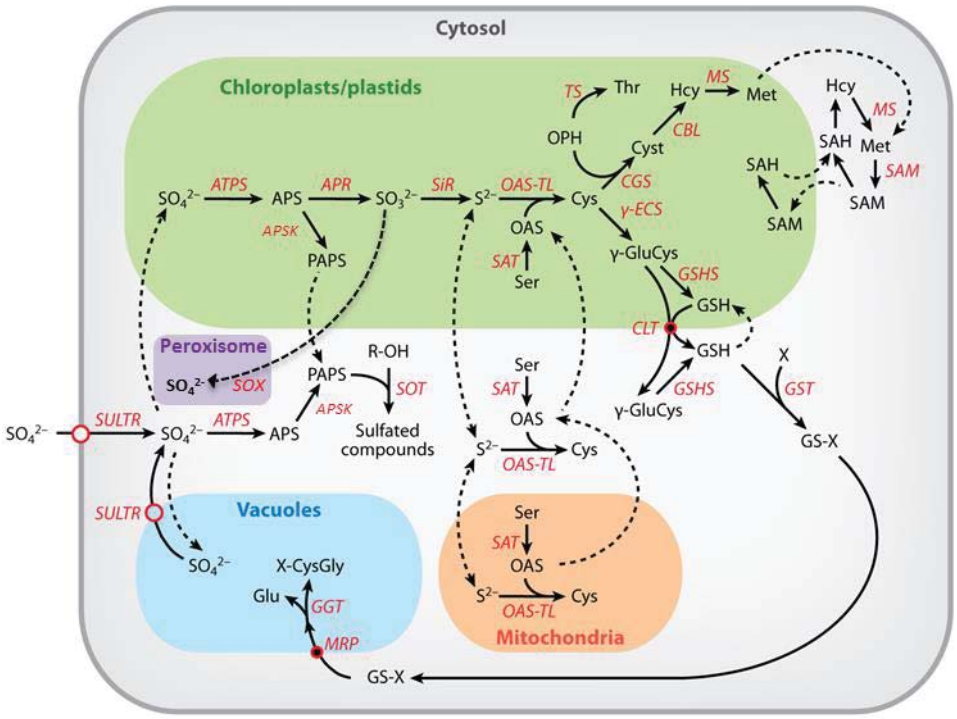

Figure 1.2 Schematic representation of plant sulfur assimilation and subcellular localization of its major enzymes The genes are abbrev*ia*ted as *SULTR* (sulfate transporter), *ATPS* (ATP sulfurylase), *APR* (APS reductase), *SIR* (sulfite reductase), *SAT* (serine acetyltransferase), *OAS-TL* (O-acetylserine thiollyase) *γ-ECS* (γ-glutamylcysteine synthetase), *GSHS* (glutathione synthetase) *APSK* (APS kinase), *SOX* (Sulfite oxidase), *SOT* (sulfotransferase). Dashed lines represent multiple reaction steps; dotted lines indicate unconfirmed transport steps. Modified from Takahashi et al., 2011.

1.4.1 Uptake mechanisms of sulfate from the soil

Sulfate (SO_4^{2-}) is the most oxidized and the most common form of sulfur in nature. Plants primarily make use of the proton gradients across the membrane (proton/sulfate co-transport system) to mediate sulfate influx into plants and within the plant compartments (Takahashi et al., 2011). Specialized membrane proteins called sulfate transporters, distributed throughout the plant, are involved in this process. The sulfate transporters possess 12 membrane-spanning domains and belong to a large family of cation/solute co-transporters (Hawkesford, 2003). In addition, these proteins also contain a STAS (sulfate transporter and antisigma factor antagonists) domain which has been shown to be involved in protein-protein interactions between SULTR1;2 and OAS-TL in *Arabidopsis,* and may have a regulatory function in sulfur sensing (Shibagaki & Grossman, 2010). Twelve genes have been identified to encode the sulfate transporter family in *Arabidopsis* and rice *(Oryza sativa*), whereas 10 transporter genes have been characterized in wheat (*Triticum aestivum)*. Studies, *in silico,* have suggested a 14 gene family for poplar and 15 for grape (*Vitis vinifera).* The members of the multi-gene sulfate transporter family are classified under four subfamilies from *SULTR1* through to *4* according to their amino acid sequences. A fifth group of transporters has also been proposed which shares low, but definite similarities with the other transporters based on the genome database for *Arabidopsis* and wheat. However, more recently a member of this group, SULTR5:2, was shown to be a high affinity molybdate transporter (Tomatsu et al., 2007).

SULTR1 gene family is designated as high affinity transporters which are induced under S starvation (Buchner et al., 2010). The group comprises of three members, *SULTR1;1, 1;2 and SULTR1;3* in *Arabidopsis, V.vinifera, T. aestivum* and *O. sativa* and only one member has been identified so far in poplar. The *SULTR1;1* and *1;2* are involved in the initial sulfate uptake from the rhizosphere (Saito, 2004). SULTR1;3 , a phloem localized high affinity transporter, is involved in long distance source to sink translocation (Yoshimoto et al., 2003). The most strongly represented member of the family *SULTR1;1* shows species specific variation in localization and expression under S limiting conditions. For example, *SULTR1;1* in wheat, is duplicated and expressed as *SULTR1;1a* and *SULTR1;1b* and is expressed in multiple tissues in both root and the shoot (Buchner et al., 2010). In *Arabidopsis,* expression of *AtSULTR1;1* is confined mainly to lateral root cap, root hairs, cortex and the epidermis of the roots with low level expression in auxiliary buds of leaves

under low external sulfate (Takahashi et al., 2000). In rice, four splice variants have been suggested for this gene with tissue specific expression of at least one of the variants, *OsSULTR1;1b* .

Group 2 transporters are low affinity transporters localized in vascular tissues and are involved in the uptake of sulfate from the plant apoplast into vascular cells. *SULTR2;1* along with root to shoot transport, is also involved in transport of S to the seed as indicated by presence in the base of the silique (Awazuhara et al., 2005). The group consists of two members, *SULTR2;1* and *2;2* in *Arabidopsis, O. sativa, V.vinifera* and *P. trichocarpa* and one member in *T. aestivum.*

Group 3 transporters are described as leaf expressed and have five representatives in the *Arabidopsis*, *T. aestivum, P. trichocarpa* and *V. vinifera* transporter families. In common with group 2, these too are low affinity transporters (Hawkesford, 2003). A member of the group, *SULTR3;1*, has been recently characterized as a chloroplast localized sulfate transporter in *Arabidopsis* (Cao et al., 2013) . The members of the group 3 family may also be involved in sulfate translocation within the various compartments in developing seeds, as T-DNA lines of different members of this group show an increased ratio of sulfate to total sulfur with a decline in cysteine content indicating reduced sulfate metabolism in seeds (Zuber et al., 2010).

The group 4 family contains two transporters, at least, in *Arabidopsis,* one each in *O. sativa* and *T. aestivum,* six in *P. trichocarpa* and five members in *V. vinifera*. This group is responsible for sulfate transport from the vacuole to the cytoplasm, especially under sulfate limitation, when the demand for S increases (Kataoka et al., 2004).

Species	Group 1	Group 2	Group 3	Group 4
Arabidopsis. sp	3	2	5	2
O. sativa	3	2	6	1
T. aestivum	3	1	5	1
P. trichocarpa	1	2	5	6
V. vinifera	3	2	5	5

Table 1.1 Sulfate transporter gene family members for different species classified into four different groups, with the number of members in each group for each species indicated (From Buchner et al., 2004, 2010, Kopriva et al., 2009). For *V. vinifera* reference *Arabidopsis* sequences were also aligned against *V.vinifera* sequences using the NCBI database.

1.4.2 S-reductive assimilation

Sulfate reduction and cysteine biosynthesis is a multistep process involving a series of enzyme-catalyzed steps, cross-talk with other metabolic pathways and certain regulatory mechanisms. The role played by each enzyme in this process is discussed in detail below.

1.4.2.1 1.4.2.1 Adenosine-5´-triphosphate sulfurylase (EC 2.7.7.4)

ATP sulfurylase (ATPS) characterizes the entry point for sulfate into the sulfur assimilation pathway. Sulfate, before assimilation, needs to be activated to adenosine-5´-phosphosulfate (APS). This is brought about by linking sulfate to a phosphate residue *via* an anhydride bond with the consumption of ATP and release of pyrophosphate (Takahashi et al., 2011). This reaction is catalyzed by ATPS.

In most higher plants investigated so far, ATPS activity has been found both in the chloroplast as well as cytosol (Lunn et al., 1990; Klonus et al., 1994; Rotte & Leustek, 2000) . Most photosynthetic organisms investigated so far contain at least two copies of the ATPS gene except *S moellendorffii* . In *A. cepa,* although only one ATPS gene copy exists, protein fractionation of chloroplasts followed by spot alignment using 2D-PAGE suggested the existence of two isoforms (Thomas, 2008). In *Arabidopsis* and *Populus trichocarpa,* four genes coding for ATPS gene have been found. All four genes from the *Arabidopsis* family have been reported to encode only the plastidic form, and so it is hypothesized that the cytosolic form is produced by translation from an alternate start codon (Yi et al., 2010). However, the existence of both cytosolic and plastidic forms is not universal in all species. The role of the cytosolic ATPS, if present, is also still unclear, as activated APS needs to be transported to plastid for further reduction. As APS is also required for the sulfation reaction *via* adenosine 5´ phosphosulfate kinase (APSK; EC 2.7.1.25) to form 3-phosphoadenosine 5´ phosphosulfate (PAPS), the activity of the cytosolic isoform may be linked to cytosolic APS kinase and involved in provision of PAPS for secondary metabolism (Rotte & Leustek, 2000). A possible post-transcriptional regulation for ATPS, at least in *Arabidopsis,* has been suggested. Three out of the four genes (excluding *ATPS2*) of *Arabidopsis* are targeted by microRNA (mir395) which is in turn regulated by the

transcription factor SLIM1 that is inducible by sulfate deficiency (Kawashima et al., 2011). Cleavage of specific *ATPS* transcripts by mir395, leading to reduction in translation and hence activity, has also been predicted for *O. sativa, M. trunculata, S. bicolor, S. lycopersicum, P. trichocarpa, Z. mays* and *V. vinifera* (Liang, Yang, & Yu, 2010). This specific regulation suggests a differential function of the three targeted isoforms from *ATPS2*. In wheat however, *ATPS* has not been found to be a target for mir395 (Li, Zheng et al., 2013), indicating that regulation by mir395 might not be universal in all plant species. In addition, R2R3-MYB transcription factors have also been found to target *ATPS1* and *ATPS3* in *Arabidopsis* (Kopriva et al., 2012). Therefore it can be safely said that even though there is a functional redundancy at some level, the different ATPS isoforms have differential and specialized biological functions (Kopriva et al., 2009).

1.4.2.2 Adenosine-5´-phosphosulfate reductase (EC 1.8.4.9)

APS is reduced to sulfite by APS reductase (APSR). In common with *ATPS*, APSR gene also encodes a transit peptide to direct the mature protein into the plastids. The mature protein of APSR consists of 2 domains. The N domain resembles PAPS reductase and the C-terminal domain exhibits homology similar to the redox protein, thioredoxin (Bick et al., 1998). Unlike the APSR found in sulfur-reducing bacteria, plant APSRs contains a 4Fe-4S cluster as a sole co-factor (Kopriva et al., 2001). In most vascular plants, APSR is encoded by a small gene family (Kopriva et al., 2009). The two-electron reduction of APS to sulfite, catalyzed by APSR is thiol-dependent. A reduced cysteine residue of APSR reacts with APS to form an enzyme-(Cys)-S-SO_3^- intermediate releasing AMP, which is then reduced with GSH to liberate SO_3^{2-}. The enzyme is later regenerated by a second GSH molecule (Saito, 2004). For sulfur accumulating species like the Alliums, where GSH-derived reduced compounds are accumulated, it has been shown that ATPS and APSR form a supra-molecule *in-vitro*, suggesting that the assimilation flux may be preferentially directed in favor of reductive assimilation instead of the oxidative pathway *via* APS kinase (Cumming et al., 2007).

APSR is strongly regulated at the transcriptional level through feedback inhibition from thiol-containing compounds such as cysteine and GSH, nitrate deficiency and CO_2 deficiency. Conversely, an increase in transcript level of the APSR gene family is observed under *O*AS accumulation and sulfate deficiency (Lee et al., 2011). More recently, a bZIP

transcription factor, long hypocotyl 5 (*HY5)*, was identified as a key regulator of *APSR* transcription, specifically targeting *APSR1* and *2*. The regulation of *APSR* by *O*AS or nitrate deficiency was disrupted in the *HY5* mutants, suggesting its involvement in nitrate to sulfate assimilation signaling (Lee et al., 2011)

1.4.2.3 Sulfite reductase (EC 1.8.7.1)

Sulfite reductase (SiR) catalyzes the six-electron reduction of sulfite to sulfide. It is a plastid-localized enzyme which uses ferredoxin as electron donor in photosynthetic cells and NADPH in non-photosynthetic cells (Saito, 2004). *Arabidopsis* and most other species have only a single gene copy for *SiR* which encodes a protein product with a transit peptide to direct the mature protein into the plastids. It shares structural and functional similarities with another enzyme, nitrite reductase, which operates in the nitrogen-assimilation pathway. Considering the cytotoxic nature of sulfite, the importance of this enzyme as a regulatory milestone in the sulfate assimilation has gained importance only recently. The recent finding has corroborated its importance in the assimilatory pathway where *SiR* knockouts were found to be all seedling lethal (Khan *et al*., 2010). *SiR* knockdowns in *Arabidopsis thaliana* are either seedling lethal or strongly retarded in growth. The surviving line *sir1-1,* exhibited an activity of 17-28% compared to wild type, suggesting that a minimum threshold expression and activity is required in plants for survival and growth. Radioactive labeling experiments showed a 28-fold decrease in incorporation of ^{35}S into S containing amino acids and metabolites, mainly cysteine and GSH. Complementation of mutants with *35S:SiR* restored the wild type thiol levels corroborating the evidence for the significance of SiR as a control point in the pathway (Khan *et al*., 2010). Similar work done in tomato using RNAi generated *SiR* knock-down lines has shown the importance of this gene in preventing early senescence by keeping sulfite accumulation below cytotoxic level in plants (Brychkova et al., 2013), hence reinforcing the cytotoxic nature of sulfite and the functional importance of *SiR* as an essential sulfite scavenger.

1.4.2.4 The serineacetyl transferase (SAT) (EC 2.3.1.30)-*O* acetylserine (thiol) lyase (*O*AS**T**L) (EC 4.2.99.8) Complex

The final step in the pathway is the incorporation of sulfide in the *O*AS backbone, leading to formation of cysteine. This crucial step also links carbon and nitrogen assimilation with sulfur assimilation. This step is achieved conjointly by two enzymes, namely serine acetyltransferase (SAT) and *O*-acetyl serine (thiol) lyase (*O*ASTL) which do so by forming a complex called the cysteine synthase complex. Both these enzymes are found in three major compartments of the cell: the cytosol, the mitochondrion and the plastid. SAT catalyzes the formation of *O*-acetyl serine (OAS) from serine and acetyl-CoA. OAS, being the connecting link for S, N and C pathways, plays a major regulatory function and has been shown to be a limiting factor for S assimilation (Saito, 2004).

The *Arabidopsis SAT* family encodes five genes, three of which play a major role in *O*AS formation (Kopriva *et al*., 2009). These major isoforms of SAT have been shown to be functionally redundant (Watanabe et al., 2010). The group produced quadruple mutant combinations for all five genes, three of which then showed dwarfism. The quintuple mutant however, was embryo lethal. The three cytosolic isoforms have been shown to play a major role during seed development, whereas the mitochondrial isoform was shown to play the dominant role in cellular *O*AS formation.

*O*ASTL catalyzes the formation of cysteine from *O*AS and hydrogen sulfide. This catalytic reaction requires pyridoxal phosphate as a cofactor. The enzyme *O*ASTL belongs to a large family comprising nine isoforms in *Arabidopsis.* Other higher plants possess six to ten *OASTL* genes (Kopriva *et al*., 2009). As a part of the hetero-oligomeric complex cysteine synthase, *O*ASTL is found to be inactive but the excess of free *O*ASTL present as a homodimer seems to be required to achieve full SAT activity and conversion of *O*AS to cysteine (Takahashi et al., 2011). Excess *O*AS can dissociate the complex but this event can be overcome by the stabilizing effect of sulfide, indicating a mechanism of regulation in the pathway (Takahashi et al., 2011). Cysteine can be synthesized in three major compartments of the plant, the cytosol, mitochondria and chloroplasts (Heeg et al., 2008). Null mutants of all of the major *O*ASTL isoforms are able to develop normally and so this along with studies done on SAT isoform mutants suggests that there is free exchange of sulfide, *O*AS and

cysteine across these organelle membranes. The results also suggest that the cytosol and not the plastid is the major cysteine synthesizing compartment (Watanabe et al., 2010).

Assimilation *via* the cysteine synthase complex is not the only assimilaton pathway for sulfate existing in plants. APS kinase (E.C 2.7.1.25) forms a divergent oxidative pathway from APSR and catalyzes the formation of PAPS, which is exported from the chloroplast. In *Arabidopsis* and other members of the *Brassicaceae*, PAPS is a substrate for the formation of an array of S-containing glucosinolate compounds whereas in non-glucosinolate accumulating species it is the sulfate donor for brassinosteroids, jasmonates and other sulfonated compounds (Mugford et al., 2009; Raviliouset al., 2012).

1.4.2.5 Sulfite oxidase (EC 1.8.3.1)

Sulfite oxidase (SOX), a fairly recent addition to the well characterized S-assimilation pathway genes, is a molybdenum-containing enzyme localized in the peroxisomes. The reaction catalysed uses molecular oxygen as an electron donor to oxidize sulfite back to sulfate releasing a molecule of hydrogen peroxide (Hänsch et al., 2007). The enzyme has been shown to function to protect plants from sulfite toxicity. For example, over-expression of *ZmSO* in tobacco lines has been shown to increase tolerance to sulfite stress while the enzyme in tomato has been shown to induce sulfite accumulation under no-light conditions (Xia et al., 2012; Brychkova et al., 2013). SOX activity has also been shown to protect plants against exposure to high concentration of SO_2. Recently, the importance of *SOX* for sulfite detoxification in seed germination has also been elucidated by Xia et al (2014) showing its expression to be crucial for timely germination of *Arabidopsis* seeds exposed to sulfite.

	SULTR	***ATPS***	***APSR***	***SiR***	***SAT***	***OASTL***
Arabidopsis	12	4	3	1	5	9
O. sativa	12	2	2	2	5	9
S.bicolor	9	2	1	1	3	6
P. trichocarpa	14	4	2	3	5	10

Table 1.2 Summary of the reductive S-assimilation genes and members in the gene family in different plant species. *SULTR*: sulfate transpoter, *ATPS*: ATP sulfurylase, *APSR*: adenosine 5' phosphosulfate reductase, *SiR*: sulfite reductase, SAT: serine acetyl transferase, *OASTL*: *O*-acetylserine thiolyase (From Kopriva et al., 2009)

1.5 S-starvation responses and pathway regulation in plants

In the past decade, the technological advancement in sequencing and especially the streamlining of the "omics" platform has led to a much more precise understanding of responses involved in sulfur starvation in plants at the genetic level.

At a physiological level, the sulfur starvation response is characterized by pale green young leaves and an increase in root to shoot ratio (Ferreira & Teixeira, 1992; Hell, 1997). This phenotype at the transcriptional and post-transcriptional level, relates to an initiation of a whole network of responses involving genes not only from the S-assimilation pathway but also the N and the C assimilation pathways.

At a transcriptional level, the genes involved in S reductive assimilation are induced by S limitation *via* a feedback mechanism involving the accumulation of downstream products of the pathway such as *O*AS, cysteine and GSH (Takahashi et al., 2011). This is seen as an up-regulation in the sulfate transporter genes, mainly the members of the high affinity sulfate transport family, *SULTR1;1* and *SULTR1;2* which are responsible for uptake of sulfur from the roots. Of these, *SULTR1;1* is more responsive to S limitation and is more highly induced compared to *SULTR1;2* as the protein encoded by it has been shown to have a lower K_m for sulfate (Takahashi et al., 2000) . However, the expression of *SULTR1;1*, differs between monocots and dicots as unlike dicots, *SULTR1;1* is expressed in both the root and the shoot in monocots and no *SULTR1;2* homolog has been found in monocots. Thus in monocots, *SULTR1;1* in induced in both the roots as well as the shoots as shown by S-deprivation studies in wheat and rice (Buchner et al., 2010). The de-repression of the S-assimilation pathway in response to S limitation is also characterized by the up-regulation of *APSR* and *SAT* (Hirai et al., 2003; Takahashi et al., 2011).

An additional layer of complexity is added by the integration of the S-responsive transcription factor *SLIM 1* and microRNA miR395, which accumulate under S limiting conditions and regulate the expression of several sulfate transporters and *ATPS* for increased uptake and flux of SO_4^{2-} under S limiting conditions (Kawashima et al., 2011). Although much work has been undertaken to dissect the regulation of the pathway the sensory mechanism for S status is still unclear (Rouached et al., 2009). Only very recently,

two allelic mutants of *AtSULTR1;2* have been characterized and shown to exhibit an S-deprivation response independent of internal SO_4^{2-} status, thus hinting at the possibility of the protein encoded, SULTR1;2 being a part of the external SO_4^{2-} sensory complex in plants (Zhang et al., 2014). The fact that AtSULTR1;2 has also been shown to interact with *O*ASTL *via* the AtSULTR1;2 STAS domain may give indications as to how internal SO_4^{2-} sensing is achieved in plants (Shibagaki & Grossman, 2010; Zhang et al., 2014).

Apart from the transcriptional regulation, down-stream mechanisms, such as protein-protein interaction and to some extent post-translational modifications are also responsible for pathway-regulation. The importance of cysteine-synthase complex in the regulation of the S starvation response has already been discussed but not much is known about the importance of post-translational modifications in S-assimilation pathway regulation, although some evidence hints at more species specific role *via* this mechanism (Durenkamp, De Kok & Kopriva, 2007).

1.6 Nitrogen (N) assimilation in plants

Nitrogen is required for synthesis of amino acids, proteins, ATP, chlorophyll, nucleic acids, lipids and a number of plant metabolites (Kusano et al., 2011). Approximately 20-50 g of nitrogen is required per kg of dry biomass in all non-leguminous plants. This high requirement in non N_2 fixing plants makes it the limiting factor for growth in most cropping systems (Xu et al., 2012). Nitrogen from various sources is incorporated into the organic form *via* the assimilation of ammonia. Plants are capable of taking up nitrogen from the environment in various forms. From the soil, it can be taken up as ammonium or amino acids by plants adapted to low pH and reducing soils such as in arctic/tundra region but more commonly, it is taken up as nitrate under higher pH and aerobic soil conditions (Fig 1.2) (Masclaux-Daubresse et al., 2010). The nitrate assimilation pathway and enzymes involved are depicted below:

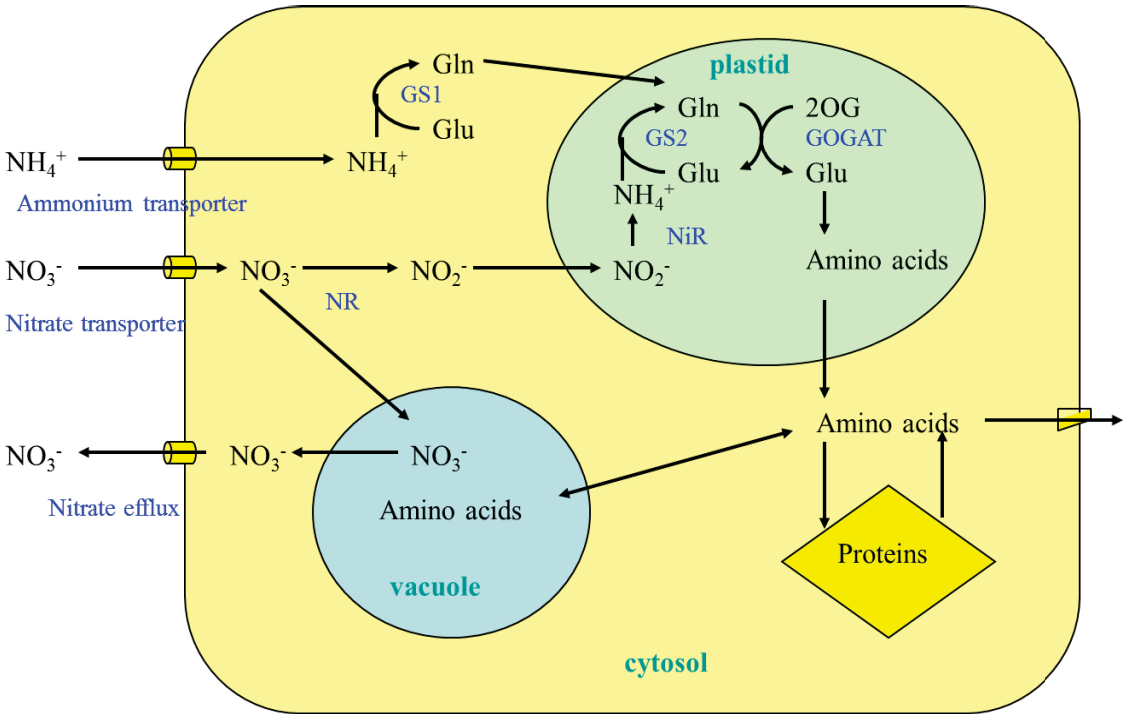

Figure 1.3 Schematic representation of nitrate assimilation and the enzymes involved in plants. NR- nitrate reductase, NiR- nitrite reductase, GS- glutamine synthase, GOGAT- glutamine-oxoglutyrate amino transferase. From Ohyama et al; 2012

1.6.1 Uptake mechanisms of nitrate from the soil

Nitrate available in the soil is taken up *via* a specialized family of membrane proteins called the nitrate transporters. In plants, two groups of nitrate transporters (NRT1 and NRT2) have been found to facilitate the uptake and distribution of nitrate. The *NRT1* gene family mediates a low-affinity transport system (LATS) with the exception of *AtNRT1.1* in Arabidopsis, which is a dual affinity transporter and also a nitrate sensor (Ho et al., 2009). *NRT1* comprises a large family of 53 genes in *Arabidopsis,* 51 of which are expressed and show different tissue patterns in the plant (Masclaux-Daubresse *et al*., 2010).

The *NRT2* gene family, mediating a high-affinity transport system, is yet to be fully functionally characterized in higher plants. In *Arabidopsis,* the *NRT2* group comprises of 7 genes of which *AtNRT2.1* has been shown to be involved in induced high affinity nitrate transport. Nitrate reductase (*NR)* mutant in *Arabidopsis,* which accumulated a high level of NO_3^- but reduced amount of downstream N metabolites, exhibited elevated *AtNRT2.1* expression indicating that NO_3^- itself is the inducer for the gene (Tsay et al., 2007). Very recently, *AtNRT2;1* has also been shown to be involved in a negative feedback loop with ethylene biosynthesis where *AtNRT2;1* plays a positive role in ethylene signaling, but ethylene production down-regulates *AtNRT2;1* (Zheng et al., 2013). Another member of the family, *NRT2;4* has been characterized to encode as a plasma membrane localized high affinity nitrate transporter expressing in both roots and shoots and involved in sulfate uptake and translocation under N limiting conditions (Kiba et al., 2012).

1.6.2 Nitrate assimilation

Nitrate, after being taken up by the roots, is assimilated into ammonia, which is further metabolized to form glutamate *via* the glutamate synthetase-glutamine-oxoglutyrate amino transferase (GS/GOGAT) pathway. The pathway involved in nitrate reduction up until ammonium synthesis is described in detail in the following section.

1.6.2.1 Nitrate reductase (NR) (E.C 1.7.99.4)

Nitrate reduction takes place in both roots and shoots but is spatially separated between cytoplasm, where nitrate reduction takes place, and the plastids/chloroplast where the nitrite reduction occurs. The first step in the pathway, the reduction of nitrate to nitrite is catalyzed by nitrate reductase (NR) in the cytosol. NR is found to be active as a homodimer in which each monomer comprises three prosthetic groups: flavin adenine dinucleotide (FAD), a molybdenum cofactor (MoCo) and a heme group (Masclaux-Daubresse et al., 2010). In higher plants, two main forms of NR are found: a NADH - specific form which is the most common and a NAD(P)H bi-specific form which is present either in conjunction with the former one, as in maize, barley, rice and soybean, or as the sole isoform, as in *Betula pendula.* A third NADPH specific form is found in fungi and mosses, but has not yet been discovered in any higher plant species (Meyer & Stitt, 2001). The two classes of genes encoding the NR apoenzyme and the *cox* gene encoding the Mo cofactor have been identified and although the enzyme is thought to be localized in the cytosol, an association with the plasma membrane (PM-NR) has been reported in corn roots and barley (Masclaux-Daubresse *et al*., 2010).

The expression of the *NR* gene is inducible by light and is regulated by the bZIP transcription factors *HY5* and *HYH* (Jonassen et al., 2008). Interestingly, *HY5* has also been shown to regulate the *APSR* response to nitrate deficiency, thus forming a common regulatory point between the two pathway and highlighting a possible link of nitrate to the S-assimilation pathway (Lee et al., 2011) .

1.6.2.2 Nitrite reductase (NiR) (E.C 1.7.2.1)

After nitrate is reduced, the nitrite is translocated to the chloroplast/plastid where it is further reduced to the ammonium ion. This reaction, catalyzed by the second enzyme in the pathway, nitrite reductase (NiR) is a six-electron reduction utilizing ferredoxin as an electron donor, in common with the SiR in the sulfate assimilation pathway discussed previously. The gene encodes a transit peptide for translocation of the mature protein into the chloroplast. In roots, NiR is plastid localized and uses NADPH as the electron donor. NiR, unlike NR, is a holoenzyme and has two redox centers: a siroheme-Fe centre and an iron-

sulfur cluster (Crawford, 1995). The *Nii* genes (*NiR*) encoding the NiR enzyme have been characterized in many plant species including *Arabidopsis* where only one *NiR* copy exists and the gene number for most species varies from one to two (Meyer and Stitt, 2001).

Ammonium, from nitrite reduction, is then assimilated in the plastid/chloroplast by GS/GOGAT cycle by which ammonium is fixed onto a glutamate molecule by GS to form glutamine. Glutamine then reacts with 2-oxoglutarate to form 2 molecules of glutamate, in a reaction catalyzed by GOGAT. Glutamate, the most diverse product of nitrogen metabolism can then be used as a metabolite, a signaling molecule, an energy-yielding substrate, a nutrient or a structural determinant in proteins (Forde & Lea, 2007).

1.7 N-starvation response and pathway regulation in plants

At a physiological level, the N starvation response comprises pale green old leaves and an increase in primary root length over lateral root growth (Castaings et al., 2009). This response is different from that seen in S starvation where the younger leaves exhibit the pale green phenotype and not the old tissue. This has been attributed of re-mobilization of N from older tissues and incorporation into new leaves to contribute to growth (Bieker & Zentgraf, 2013) .

At the transcriptional level, unlike S-assimilation pathway, the primary N-assimilation pathway is de-repressed under nitrate replete conditions and thus genes involved in primary N assimilation, such as nitrate reductases and the nitrite reductase, are down-regulated under nitrate deficiency when the pathway is repressed (Bieker & Zentgraf, 2013). The N-assimilation pathway is feedback-regulated by its downstream products, such as ammonium and amino acids. A 150 bp cis-acting element in the promoter region of *NRT2;1* has been shown to be responsible for both the positive regulation by nitrate deficiency and the negative regulation by N metabolites (Girin et al., 2007). This also forms a point of cross talk between the N and C metabolism, as *NRT2;1* expression has also been shown to be activated by the addition of sugars (Lejay et al., 2008).

Another point of regulation in the pathway is the molybdenum containing enzyme NR, which is also nitrate responsive, but another layer of regulation is added by light as in the dark it is inactivated by phosphorylation of a conserved serine residue and the binding of 14-3-3 proteins (Lillo & Appenroth, 2001).

From a review of both N and S-assimilation pathways, it is evident that regulatory mechanisms, though specific, are not always exclusive to a certain pathway but are more often points of cross-talk between two or more pathways. Therefore, to dissect any regulatory mechanism in a pathway, it is also important to appreciate its position in a network of signalling pathways.

1.8 Similarities between plant SiRs and NiRs : Structure, function and localization

Sulfite reductase (SiR) and nitrite reductase (NiR) each belong to a family of oxidoreductases with conserved siroheme and iron-sulfur cluster domains (Appendix 1 and 2). While functional redundancy has been characterized extensively between the two enzymes in prokaryotes, not much work has been done in characterizing the functional redundancy between assimilatory SiR and NiR in plants. Interestingly in the unicellular red algae *Cyanidioschyzon merolae,* a novel variant of the ferredoxin-dependent sulfite reductase with substrate specificity for nitrite has been identified (Sekine et al., 2009). Conversely, in *Wolinella succinogenes* cytochrome *c* nitrite reductase has been shown to reduce sulfite (Lukat et al., 2008). In plant, although this redundancy has only been investigated in crude spinach so far, studies done on recombinant maize sulfite reductase by the Nakayama group in Japan have shown that a single amino acid substitution at the distal site of the siroheme can drastically change the substrate specificity to nitrite (Krueger & Siegel, 1982; Nakayama et al., 2000).

At a structural level, both enzymes share the same prosthetic groups with a siroheme and 4Fe-4S cluster and both utilise reduced ferredoxin as an electron donor for the six electron reduction of sulfite or nitrite in chloroplasts (Fig 1.4A). Alignment of SiR and NiR sequences from different monocot and dicot species, including onion (Fig 1.4B), not only show the four highly conserved cysteine residues which form the point of the 4Fe-4S ligation (Crane

& Getzoff, 1996), but also the conserved α-helix and β-strands flanking the conserved cysteine residues in the predicted secondary structure (appendix 2).

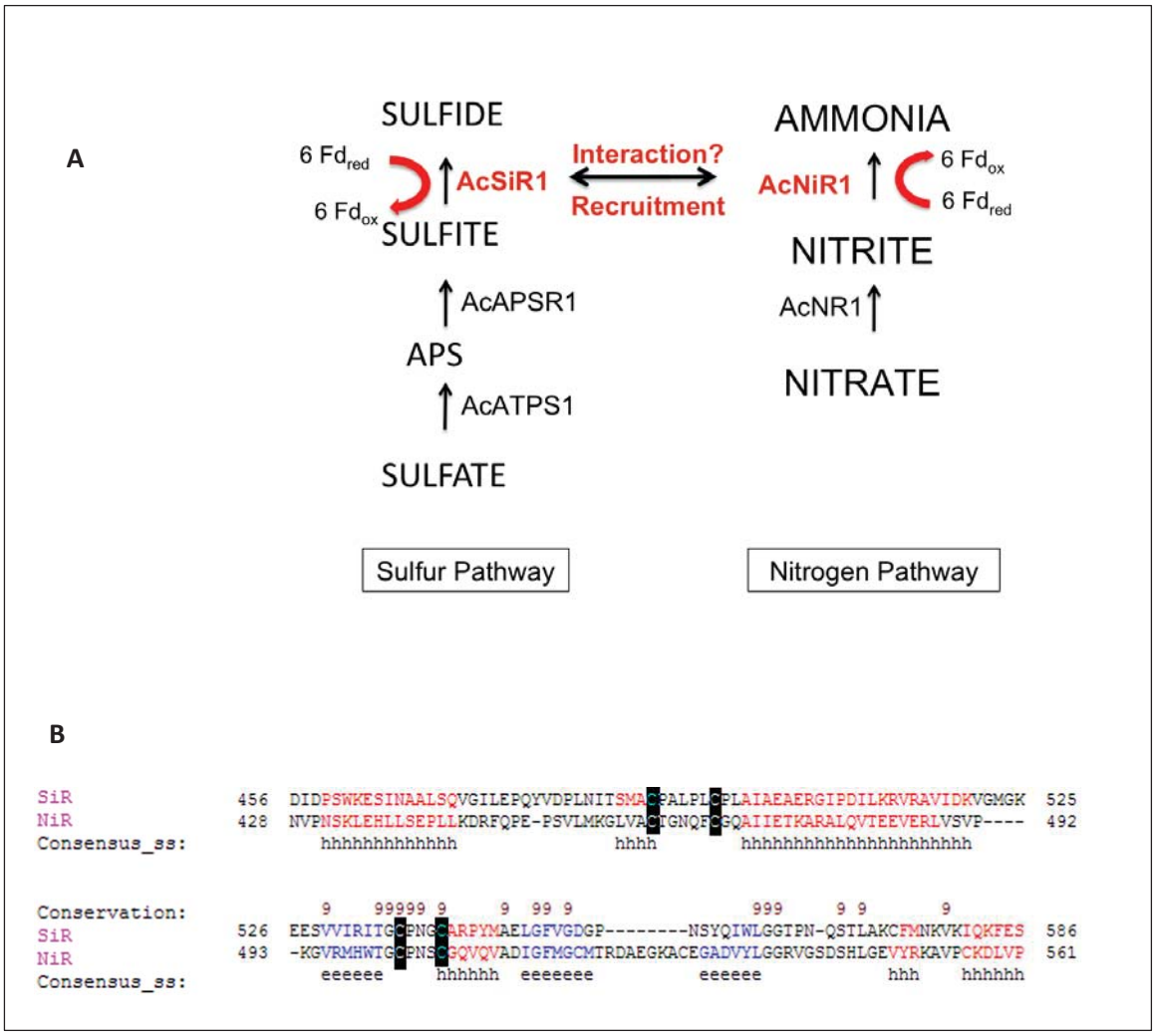

Figure 1.4 Schematic representation of the S and N-assimilation pathway with sequence similarity between AcSiR1 and AcNiR1. A. Similarity between the six electron reduction of sulfite and nitrite shown with an indication of interaction between the two enzymes (modified from Davidian et al., 2012, Ohyama et al., 2012). **B.** CLUSTAL alignment of AcNiR1 and AcSiR1 sequences showing conserved cysteine residues highlighted in black. In the secondary structure, the blue colour and letter e denotes the α-helix, while the red colour and letter h denotes the β-sheet.

Phylogenetic comparison of *Ac*SiR1 and *Ac*NiR1 with other monocot and dicot sequences (Fig 1.5) shows both enzymes group distinctly. However, it should be noted that the distance from other monocot sequences might be due to a lack of annotated SiR sequences from monocot species, other than the grasses, in the NCBI database.

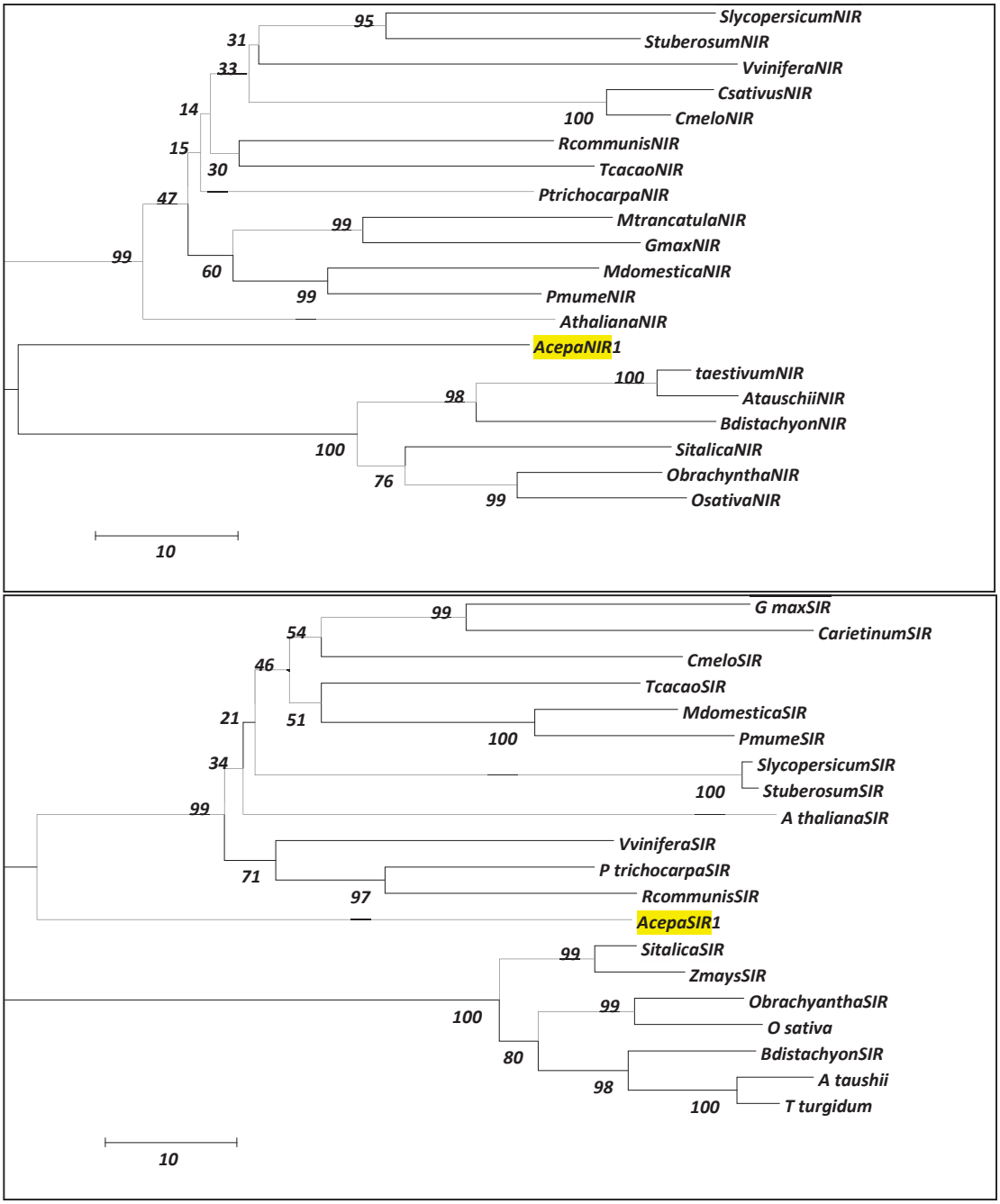

Figure 1.5 Evolutionary relationships of SiR and NiR portein sequences analyzed using the MEGA6 software. The evolutionary history was inferred using the Neighbour-Joining method. The percentage of replicate trees in which the associated taxa clustered together in the bootstrap test (1000 replicates) are shown next to the branches. The evolutionary distances were computed using the number of differences method and are expressed as the number of amino acid differences per sequences

The sulfur and nitrogen assimilatory pathways are two major metabolic pathways in plants, which assimilate and incorporate these macronutrients. Proper functioning of these two multi-step pathways has been shown to be essential for plant survival. However, some of the intermediates of the N and S-assimilation pathways such as sulfite and nitrite are strong nucleophiles and can cause extensive damage to the plant upon accumulation (Gruhlke & Slusarenko, 2012). Adaptive measures to counter the accumulation of sulfite include its oxidation to the less toxic state, sulfate, by peroxisome-localized sulfite oxidase (Brychkova et al., 2007). Sulfite is also diverted to other pathways such as formation of sulfolipids by UDP-Sulfoquinovose synthase (Sanda et al., 2001). In contrast, not many nitrite consumption pathways exist in plants other than the recently elucidated nitrate reductase (NR)-dependent conversion of nitrite to nitric oxide (Zhao et al., 2009). Thus the substrate redundancy between SiR and NiR could be exploited as an alternative pathway for consumption of both sulfite and nitrite by plants (Crane & Getzoff, 1996). In onion, a preferentially sulfur accumulating species, it is therefore hypothesized that this redundancy could have a further important role during N or S stress where either enzyme could be recruited to provide a demand driven increased reduction of sulfite or nitrite.

1.9 The genus *Allium*

Allium comprises a large growing genus with around 750 known species with the latest, *Allium akirense*, having been discovered only very recently (Friesen & Fragman-sapir, 2014). The taxonomic classification is complicated, with the genus first being placed under the family Liliaceae in the older angiosperm classification. However, under the latest APGIII classification, the following hierarchy has been adopted (Khedim et al., 2013):

Clade	Monocot
Order:	Asparagales
Family:	Amaryllidaceae
Subfamily:	Allioideae
Genus:	*Allium*

Members of the genus are broadly described as perennial plants with formation of a storage organ, mostly a bulb but also a rhizome or swollen root (Fritsch & Friesen, 2002). A

striking characteristic of the members of this genus is the synthesis of unique glutathione derived secondary metabolites, collectively referred to as *S*-alk(en)yl-$_{L}$-cysteine-sulfoxides (ACSOs) (Randle et al., 1995). The most notable of these are *trans*-(+)-*S*-(1-propenyl)- $_{L}$-cysteine-sulfoxide (1-PRENCSO; isoalliin) and -(+)-*S*-(2-propenyl)- $_{L}$-cysteine-sulfoxide (2-PRENCSO; alliin) found in *A. cepa* (onion) and *A. sativum* (garlic), respectively. These are major contributors to the characteristic aroma and pungency commonly associated with the garlic and onion respectively. Upon tissue disruption, the ACSOs react with an enzyme released called alliinase (E.C 4.4.1.4), giving rise to a range of thiosulfinates. It is the combination of these thiosulfinates which produces the characteristic flavour and aroma properties associated unique to some allium species (Kopsell & Randle, 1999). Within the genus, however, there is a large variation in accumulation of these compounds. Some species produce only a few cystiene sulfoxides (CSOs) and inactive alliinase such as the members of subgenus *Melanocrommyum*, hence lacking any odour while other species such as *A. sativum, A. cepa, A. fistulosum* accumulate large quantities of ACSOs (Fritsch & Friesen, 2002).

The genus is globally distributed with some members, such as *A. schoenoprasum* ,even existing in the sub-arctic belt. The greatest amount of species variation is seen for Alliums stretching from the Mediterranean basin to central Asia. Another centre of species diversity exists in the western North America that comprises of several subgroups of the genus. This widespread occurrence with local centres of diversity indicates adaptation to diverse ecological niches (Kamenetsky & Rabinowitch, 2006).

Following the discovery of the anti-bacterial activity of allicin, a cysteine derived organosulfur compound which is also responsible for the characteristic garlic flavour (Cavallito & John, 1944), characterization of other flavour compounds became increasingly important for different species in this genus. One of the more commercially important Allium, that has been extensively studied and also accumulates the active organosulfur compounds, the ACSOs, *Allium cepa,* has been the crop of choice for this study and has been discussed in detail in the following section.

1.9.1 Onion (*Allium cepa* .L)

A. cepa, commonly known as onion, is one of the oldest cultivated vegetables with records hinting at domestication of this species reaching as far back as 2700 B.C in Egypt and the 6th century BC in Indian writings (Fritsch & Friesen, 2002). It is now cultivated as a biennial with the bulb forming in the first year leading to emergence of an umbel in the second growing season. As one of the principle Alliums and also an economically/horticulturally important crop, onion owes its culinary value to a series of volatile sulfur compounds arising from the amino acid cysteine which is the first (S)-containing product of the reductive assimilation pathway. Four major ACSOs have been found in *A. cepa* so far. These are *trans*-(+)-*S*-(1-propenyl)-$_L$-cysteine-sulfoxide (1-PRENCSO; isoalliin), (+)-*S*-methyl-$_L$-cysteine-sulfoxide (MCSO), (+)-*S*-proyl- $_L$-cysteine-sulfoxide (PCSO) and cycloallin. Of these, 1-PRENCSO is the most abundant (Kopsell & Randle, 1999). The earliest work describing a protein involved in the enzymatic degradation of ACSOs in *A. cepa* was done by Kupiecki & Virtanen (1960) and by Schwimmer et al., (1960). Following this, detailed work on S-containing flavour compounds in *A. cepa* was done by Carson & Wong (1961) where, using gas liquid partition chromatography, they identified several flavour associated S-volatiles. However, it wasn't until 1971 that thiopropanal-S-oxide, which is formed due to alliinase activity on 1-PRENCSO, was identified as the lachrymatory factor in onion by Brodnitz & Pascale in 1971. Following the understanding of the importance of this class of S compounds in determining the commercially appreciated trait of flavour in the bulb, much work was done to elucidate the importance of S fertilization in the accumulation of these flavour precursors (Randle et al., 1995). The sink capacity for secondary sulfur compounds differentiates the S metabolism in *A. cepa* from the model species *Arabidopsis.* Whereas *Arabidopsis* and other members of the family Brassicaceae accumulate sulfated secondary compounds, namely glucosinolates that arise from a bifurcation in the S-assimilation pathway post APS production, *A. cepa* accumulates reduced S compounds and secondary compounds arising from post cysteine synthesis (Kliebenstein et al., 2001; McCallum et al., 2011). Differences in pathway regulation of S assimilation also differs from other species. For instance, sulfur metabolism in *Allium cepa* and *Brassica oleracea* responded differently upon H_2S exposure. As opposed to *B.oleracia,* an increase in secondary sulfur compounds and sulfate was observed in *A. cepa* upon H_2S exposure suggesting differences in the feedback regulation of the pathway (Durenkamp et al., 2007). Furthermore, APS reductase activity was found to be differentially regulated in both species (Durenkamp et al., 2007). *A. cepa,* has also been

shown to form a complex between ATP sulfurylase and APS reductase *in vitro.* However, the existence of this complex has not yet been validated in other species (Cumming *et al.,* 2007). These anomalies, along with other physiological differences, such as the presence of a storage organ in *A. cepa,* unlike *Arabidopsis,* make it an interesting candidate to study the regulation of the S-assimilation pathway and its significance to the species.

1.10 Concluding statement and research hypothesis

A cepa is the fourth most important horticultural export commodity in New Zealand and is a culinary delight all over the world valued for its unique pungent flavor (Aitken & Hewett, 2014). As such, the growing interest in optimizing breeding and producing enhanced flavor has led to an increased interest in the scientific community to unravel the biochemical pathways which confer it its characteristic flavors. There has been much progress in that direction with most of the S assimilation enzymes characterized. Work done by Thomas (2008) suggested that the primary assimilation enzyme AcATPS1, was positively regulated by S supply and not demand driven by internal cysteine, supporting the idea of a feed-forward mechanism. The formation of complex supra-molecules such as ATPS-APSR has also been established *in vitro,* hinting at the possibility of more such interactions in the network (Cumming et al., 2007). Considering the importance of sulfur in plant development, it is also wise to speculate that the pathway is much more tightly regulated in this species; not only by the enzymes involved in S-assimilation, but also through the various integrated pathways such as the nitrogen and carbon-assimilation pathways. A possible cross-talk between another enzyme in the S-assimilation pathway, namely sulfite reductase and a structurally and functionally similar enzyme in the N-assimilation pathway, nitrite reductase, may form an additional regulatory check point in the S assimilation network, with possible recruitment of AcNiR1 during S starvation to assimilate the excess cytotoxic sulfite accumulated in the plant and *vice versa*.

1.10.1 Hypothesis

"1.) A significant cross-talk might exist between the sulfur and nitrogen assimilatory pathways in the S-accumulating species *Allium cepa,* and 2.) A functional redundancy between the sulfite reductase and nitrite reductase (AcSiR1 and AcNiR1) may form as a yet unreported important point of interaction between these two assimilation pathways."

1.10.2 Research objectives

The objective outlined to test the first part of the hypothesis was:

- To investigate, in a controlled factorial experiment using the *A. cepa* CUDH2107 line, the effect of either sulfate depletion or nitrate depletion or both (S x N) on the S and N-assimilation pathways at the transcriptional, and wherever possible, the translational and the metabolite level.

The objectives outlined to test the second part of the hypothesis were:

- To establish substrate redundancy between AcSiR1 and AcNiR1 *in vitro* by expressing and purifying recombinant AcSiR1 and AcNiR1 and determining activity against both sulfite and nitrite for each enzyme.

- To investigate the possibility of an indirect interaction between AcSIR1 and AcNiR1 as enzyme recruitment, by determining expression, accumulation and activity of AcSiR1 and AcNiR1 in leaf and root tissues of *A. cepa* plants obtained from the controlled S x N factorial experiment.

- To test the possibility of indirect interaction, as transient recruitment at a transcriptional level, using the model species *Arabidopsis,* along with the recently characterized *AtSiR1* T-DNA insertion line *sir1-1* (Khan et al., 2010), in a short term factorial experiment (S x N).

- To investigate the possibility of a direct interaction between AcSiR1 and AcNiR1 in the form of a protein-protein interaction *via* an ELISA based solid phase binding assay and a tag free technique isothermal titration calorimetry (I.T.C).

The *A. cepa* line to be used in this thesis is a double haploid line (CUDH2107) obtained from Plant & Food Research, Lincoln. The *Arabidopsis sir1-1* line was a gift from Dr. Markus Wirtz (Centre for Organismal Studies, University of Heidelberg, Germany).

Chapter 2: Materials and methods

2.1 Plant propagation and harvesting methods

2.1.1 Plant material

A double haploid genotype of *A. cepa*, CUDH2107 was obtained from Plant & Food research, Lincoln, NZ (developed in Cornell University, Ithaca, N.Y). A T-DNA insertion line of *AtSiR1, sir1-1* (Khan et al., 2010) was a gift from Dr. Markus Wirtz (Centre for Organismal Studies, University of Heidelberg, Germany).

2.1.2 Plant propagation

Seeds of *A. cepa* CUDH2107 were germinated directly on a sand mixture containing 1 mm diameter sand (K-1 white sand), 2 mm diameter sand (K-2 white sand) and <0.3 mm diameter sand in the ratio 6.6:6.6:1. The K-1 and K-2 grade sand was obtained from Industrial Minerals (NZ) Ltd. and the <0.3 mm diameter sand from J61W silica sand, Industrial Sands, Waikato Ceramics, Hamilton. A total of 48 pots (+3 extra pots labelled as "indicator" to monitor *AcFT4* expression) were arranged randomly in 6 blocks and each pot was harvested once as indicated in the layout below. The arrangement of pots were nitrogen treatment_sulfur treatment_developmental stage at which to be harvested where 1 refers to N+/S+ and 2 refers to N-/S- for treatments and to pre-bulbing and bulbing for stage at which the pot is to be harvested.

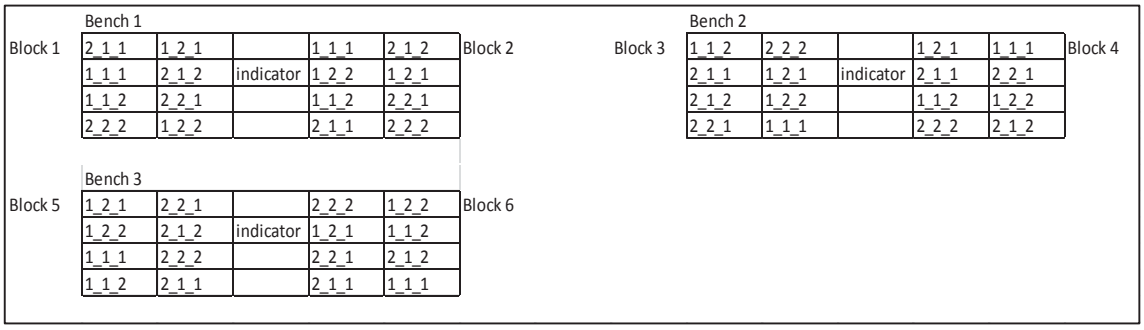

Figure 2.1 layout of the S x N factorial experiment indicating placement of pots in different blocks and stage for harvesting each pot.

For each pot (Daltons, Auckland), 2 kg of sand mix was used. Fifteen seeds were germinated per pot in water for 10 days, after which seedlings were thinned to 6 per pot. After 10 days, the plants were watered with their respective treatments. The media for the –S treatment was modified from Freeman and Mossadeghi, (1967). The –N and the –S-N treatment was

composed by Dr. Stephen Trolove (Plant & Food Research, NZ) such that the concentrations of cations (Ca:K:Mg) and the ratio of NH_4^+:NO_3^- is balanced in each treatment.

	Control	-S	-N	-S-N
(1 X)				
Chemical	[mM]			
KNO_3	6	6	0	0.81
K2SO4	0	0	1.1	0
KH_2PO_4	0	0	0.77	0.77
$NH_4H_2PO_4$	1	1	0.23	0.23
$MgSO_4.7H_2O$	2	0.25	0.9	0.25
$Mg(NO_3)_2.6H_2O$	0	1.75	0	0.25
$Ca(NO_3)_2.4H_2O$	4	2.25	1.64	0.98
IRON-EDTA	0.006	0.006	0.006	0.006

Micronutrient stock solution (80 X)	**gm/L of micronutrient stock solution**
H_3BO_3	2.28
$MnCl_2.4H_2O$	1.44
ZnSO4.7H2O	0.176
CuEDTA	0.26
$Na_2MoO_4.2H_2O$	0.020

Table 2.1 Recipe for different S x N treatments as formulated by Dr. Stephen Trolove

Plants were watered with their respective media everyday between 8-9am with 300 ml of media per pot.

Arabidopsis plants were grown in 96 well (each well 30 x 30 mm) plug trays (PSP limited, Albany, Auckland, NZ) in a mixture of fine grade vermiculite and perlite (Exfoliators PTY. LTD, 3, Dandenong, Victoria, Australia) in a 4:1 ratio. The plug trays were seated inside a holding tray (420 x 310 mm) into which 800 ml of media was poured every alternate day. The media composition used for watering the plants was as described in Hirai et al., (2004). Per plug, eight seeds were germinated in water and were thinned to 1 seedling per plug after successful germination. After thinning the seedlings, plants were watered with control media till 5 weeks from the day of planting after which the treatment was started. Prior to starting the treatment, the plug trays were watered from top with Milli-Q water twice to replace the media, taking care not to flood the plugs.

2.1.3 Growth conditions

A. cepa plants were grown in controlled environment growth rooms at Plant & Food Research, Palmerston North, NZ. For the short day treatment, 10 h/14 h (day/night) light, 25◦/15◦ (day/night) temperature, 70% relative humidity, 700 µmol m^{-2} s^{-1} light intensity and 380ppm CO_2 and red:far red ratio of 1:3 regime was used. For the long day treatment, day length was increased to 14h/10h (day/night) and red:far red ratio was increased to 1:2 to stimulate bulbing.

For *Arabidopsis* short term deprivation experiment, col and *sir1-1* plants were grown under the conditions modified from Khan et al., 2010 at 55% humidity, 180 µmol m^{-2} s^{-1} light intensity, 22.5°C/18°C (day/night) temp, 8.5 h/15.5 h (day/night) photoperiod.

2.1.4 Plant harvesting

For the factorial experiment, 6 pots (6 plants per pot) were harvested and tissues from each pot pooled as a biological replicate for each nutrient treatment at the end of the short day treatment at 32 days post sowing. At the end of the long day treatment, the other six pots remaining per treatment were harvested (6 plants per pot, tissues pooled as a biological replicate). Plant harvests were carried out 3 h into the light period (L+3) for both short day and long day harvests to negate any effects of photoperiod on the expression of genes to be monitored in the experiment. For the pre-bulbing stage at the end of short-day conditions, plants were harvested as the youngest four leaves, pseudo-stem and root. For the bulbing stage at the end of long day conditions, plants were harvested as youngest 4 leaves, bulb and root. The pseudo-stem is defined as the white base of the leaves (approx. 1.5 cm) before the onset of bulbing.

Each tissue from the harvest was blot-dried, weighed and snap-frozen in liquid nitrogen immediately. Tissues were stored at -80°C until further use.

For the *Arabidopsis* experiment, plants were harvested at the end of 5 weeks + 3 days, 4 hours into the light period. Plants were washed with mili-Q water, blot dried, dissected into shoot and root, weighed and snap frozen in liquid nitrogen as soon as possible. Harvested material was stored in -80°C until further use.

2.2 Chemicals used

Unless otherwise stated, the chemicals used in this study were obtained from Sigma-Aldrich company (St. Louis, Mo., US), Duchefa Biochemie BV (Madison, Wi, USA), QIAGEN GmbH (Hilden, Germany). Life Technologies Corp. (Grand Island, NY, USA). Roche Applied Sciences (Roche Diagnostics GmbH, Manheim, Germany) and Bio-Rad Laboratories (Hercules, CA, USA).

2.3 Molecular biology protocols

2.3.1 Nucleic acid isolations

2.3.1.1 Isolation of genomic DNA (gDNA) using the hexadecyltrimethylammonium bromide (CTAB) method

Hundred milligrams of leaf tissue was ground in liquid nitrogen and vortexed in 0.5 ml chilled extraction buffer (0.35 M sorbitol, 0.1 M Tris–HCl, 5 mM ethylenediaminetetraacetic acid [EDTA], pH 7.5, 20 mM $Na_2S_2O_5$). The crude extract was centrifuged at 17,000 g (rpm) for 1 h at 4 °C, and the supernatant was discarded. The pellet was dissolved in 0.2 ml of extraction buffer, 0.3 ml nucleus lysis buffer (0.2 M Tris–HCl, 50 mM EDTA, 2 M NaCl, 2% hexadecyl-trimethyl-ammonium bromide pH 7.5), and 0.1 ml of 5% sarkosyl. The mixture was subsequently incubated for 1 h at 65 °C. Chloroform/isoamylalcohol (24:1 v/v) extraction was performed by adding 0.5 ml of the solvent mixture to the tube, followed by centrifugation at 17,000 rpm for 15 min to separate the aqueous and the organic phase. Clear supernatant was transferred to a clean tube, and DNA was precipitated with an equal volume of ice cold isopropanol and incubated on ice for 20 min before centrifugation at 17,000 rpm for 15 min. The supernatant was decanted, and the pellet was washed with 70% ethanol and air dried for 10 min. The pellet was dissolved in 100 µl of Tris–ethylenediaminetetraacetic acid (TE) buffer containing and gDNA was quantified by by NanoDrop® ND-1000 spectrophotometer (NanoDrop Technologies, Montchenin, DE, USA) (see 2.3.1.4).

2.3.1.2 Isolation of total RNA and quantification

Total RNA was extracted using the Zymogen Quick-RNA™ MiniPrep kit. undred milligrams of tissue was ground in liquid nitrogen and cells were lysed by adding 800 µl of RNA lysis buffer and vortexing for 15 sec. Subsequently samples were centrifuged at 14,000 x g for 1 min at room temperature. gDNA contamination was minimized by transferring the supernatant into Spin-Away™ filter in a collection tube and centrifuging at 10,000 x g for 1 min. After adding equal volume of 100% ethanol, the RNA was isolated by transferring the filtrate to Zymo-spin™ IIICG column in a collection tube and centrifuging at 10,000 x g for 1 min. The filtrate was discarded and 400 µl of RNA prep buffer was added to the column followed by centrifugation at 10,000 x g for 1 min. The RNA was washed by addition of 700 µl of RNA wash buffer followed by centrifugation at 10,000 x g for 1 min. 9. Another 500 µL of RNA wash buffer was added to the column and centrifuged for 2 min at 14,000 x g to remove traces of ethanol. Purified RNA was eluted by addition of 50 µl of DNAse/RNAse free water into the column in a 1.7 ml Eppendorf tube followed by centrifugation at 14,000 x g for 1 min. The RNA was quantified using the Qubit™ RNA Assay Kit (Life Technologies, Carlsbad, USA) using the Qubit® 2.0 Fluorometer.

2.3.1.3 DNAse treatment

For q-RT-PCR experiments, genomic-DNA free RNA was prepared using Roche RNase-free recombinant DNase treatment as follows:

1. Total RNA extracted (2-5 ug) as described in 2.3.1.1, was mixed with 5 µL of 10 x incubation buffer supplied with the enzyme and 1 µL of DNase (10U), 1 µL of Protector RNase inhibitor (10U) before water was added to give a final volume of 48.4 µL.

2. The mixture was incubated at 37°C for 20 min after which the reaction was stopped by the addition of 1.6 µL of 0.25 M EDTA (pH 8.0) and heating at 75°C for 10 min. The final volume was 50 µL.

2.3.2 cDNA synthesis

To synthesize the first strand of cDNA, the Transcriptor First Strand cDNA synthesis kit (Roche) was used with oligo $_{(dT)}$ primer.

Reagents used:

- Transcriptor Reverse Transcriptase (20U/µL)
- Transcriptor RT reaction buffer (5x): 250 mM Tris-HCL, pH 8.5, 150 mM KCL and 40 mM $MgCl_2$.
- Oligo $(dT)_{15}$ primer was used to final concentration of 2.5 µM
- Protector RNase inhibitor (40U/µL)
- dNTP mixture to a final concentration of 1 mM

For obtaining the 3´ UTR region, a 3´ RACE Oligo T Adapter primer was used

The following programme was used for cDNA synthesis:

Steps	Temperature	Time
Denaturation	65 °C	10 min
Incubation	55 °C	30 min
Inactivation	85 °C	5 min

Table 2.2 Temperature and time conditions for cDNA synthesis.

The steps followed were:

- One ug of total RNA was combined with the Oligo $(dT)_{15}$ primer in a 0.2 ml tube and the volume was adjusted to 13 µL with DEPC-treated water.
- The RNA and the primer was denatured at 65 °C for 10 min and placed immediately on ice.
- After this, 7 µL of master reaction mixture containing 5X Transcriptor RT Reaction Buffer, protector RNase inhibitor (40U/µL), 10 mM dNTP-Mix and Transcriptor Reverse Transcriptase (20U/µL) were then added.

- The tubes were placed in Axygen® MaxyGene™ II thermal cycler (Axygen Inc) and cDNA synthesis was carried out at 55°C for 30 min.
- After this the Reverse Transcriptase was heat inactivated at 85°C for 5 min.

2.3.3 Polymerase chain reaction (PCR)

2.3.3.1 Primer design

For isolation of *AcSiR1*and *AcNiR1* sequences, primers were made based on putative matches to *SiR1* and *NiR1* in *Arabidopsis* to the CUDH2107 transcriptome shot-gun sequence database (John McCallum, Plant & Food Research, NZ, *Pers comm.*) (Appendix 3). Each primer was dissolved in DNase/RNase free water to make a stock concentration of 1 mM and was stored in -20°C until required. A working stock was made by diluting the stock concentration 100 fold to a working concentration of 10 µM. The 3´ UTR sequence for *AcSiR1* and *AcNiR1* were obtained by Oligo $(dT)_{15}$ primer was used as a reverse primer with 2 sets of overlapping forward primers designed in the known 3´ region of the sequence.

2.3.3.2 General PCR protocol for amplification of cDNA

Setup:

Forward Primer (10 µM)	
Reverse Primer (10 µM)	1 µL
2 x PCR Master Mix (Promega)	1 µL
DNA polymerase, dNTPs, $MgCl_2$	10 µL
cDNA	1 µL
PCR grade water	7 µL
Total Volume	20 µL

Table 2.3 Reaction set up for generic PCR

The typical PCR programme used was:

Steps	Temperature	Time	Cycle
Initialization	95°C	10 min	
Denaturing	95°C	30-40 sec	1
Annealing	4°C-5°C lower than primer melting temperature	30-40 sec	30
Extension/Elongation	75°C	As per the product size (eg. 1min/per kb)	
Final Extension	75°C	10 min	

Table 2.4 Cycle conditions for generic PCR

2.3.4 Quantitative Real-Time PCR (qRT-PCR)

2.3.4.1 Primer Design

For q-RT-PCR analysis, specific primers (Appendix 4 and 5) were designed according to the requirements of q-RT-PCR such as:

- T_m= 60°C (± 1°C)
- Minimal secondary structure
- Inability to form stable dimers
- Amplicon length of between 100-200 nucleotides.

The primer efficiency for each set was determined by using the LinReg PCR software (Ruijter et al., 2009).

2.3.4.2 Protocol for q-PCR amplification

qRT-PCR was performed using the LightCycler 480 Real-Time PCR (Roche) system and LinReg PCR analysis software. For each cDNA prep (20 x dilution), three technical replicates were performed. SYBR green I (Roche) was used as a florescent dye.

Reaction set-up for qRT-PCR:

Forward primer (10µM)	**0.5 µL**
Reverse Primer (10µM)	**0.5 µL**
2 X LightCycler® 480 SYBR Green I Master Mix	**5 µL**
cDNA	**2.5 µL**
Sterile water	**1.5 µL**
Total volume	**10 µL**

Table 2.5 Reaction set up for qRT-PCR

Ten µL of reaction per technical replicate per well was pipetted into a 96 well plate and the following programme was used in the Light Cycler 480

Steps		**Temperature**	**Time**	**Cycle**
Pre-incubation		95°C	5 min	1
Amplification	Denaturation	95°C	10 sec	
	Annealing	60°C	10 sec	45
	Extension	72°C	10 sec	
Melting curve		95°C	5 min	1
Cooling		40°C		1

Table 2.6 Cycle conditions for qRT-PCR

Relative transcript abundance was determined by comparative quantification to the geometric mean of the two reference genes, *β-tub* and *CYC* for *A. cepa* and *AtUBC9* and *At2g32170* for Arabidopsis (Pfaffl, 2001). Fluorescence measurements were performed at 72°C for each cycle and continuously during the final melting (melting curve).

2.3.5 Agarose gel electrophoresis

As appropriate, amplified fragments of gDNA and cDNA were separated using agarose gel electrophoresis using the following reagents:

- UltraPURE™ agarose (Life Technologies)
- 50 x Tris-acetate-EDTA buffer (TAE)
- Loading dye (0.1M EDTA, pH 8.0, 50% (v/v) Glycerol, 1% (w/v) SDS, 0.025% (w/v) bromophenol blue)]
- Ethidium bromide (10mg/ml)
- HyperLadder™ 1DNA ladder (Bioline, London, UK)

A 1% (w/v) gel was prepared by heating and dissolving 1g of agarose in 100ml of 1 x TAE buffer. A sample well forming comb was inserted and after the polymerization of the gel, running buffer (1 x TAE) was added to the tray until the gel was submerged. The PCR products were then be loaded onto the gel. After this, 5 µL of PCR product was mixed with 2 µL of 0.1% (v/v) loading dye, mixed and loaded onto the wells. The gel was run at 100 V for 45 min. For smaller products like the qRT-PCR amplicons, a 2% (w/v) Tris-Borate-EDTA gel was used to get optimal resolution.

After electrophoresis, the gel was stained with 0.1 ug ml^{-1} ethidium bromide for 10 min and then de-stained with water. The fragments were visualised using a Gel Doc 2000 Gel Documentation System from Bio-rad Laboratories, CA, USA.

2.3.6 Genome-walking methodology for amplifying 5´ regions

2.3.6.1 Creating a genomic DNA library

Genomic DNA library (2.3.1.1) was digested with five blunt cutter restriction enzymes (*Eco*RV*, Sca*1*, Dra*1*, HPA*1*, Stu*1*).* For each digestion, 2.5 ug of gDNA and 8 µl of restriction enzyme (10 U/µl) of restriction enzyme buffer were mixed and standardized to 100 µl with DNase/RNase free water. The mixture was incubated at 37°C overnight. The digestion

reaction was then checked by running 5 µl of the reaction on a 0.5% (w/v) agarose gel and visualizing by using ethidium bromide as described previously (2.3.5).

2.3.6.2 Purification of digested genomic DNA

After digestion, the genomic DNA was digested by addition of equal volume (9 µl) of phenol to each reaction tube and mixing with gentle agitation followed by centrifugation at 10 x 000 g for 1 min at room temperature to separate the aqueous and the organic layers. The aqueous phase was transferred to a fresh tube and an equal volume of chloroform was added, the mixture vortexed and then centrifuged briefly as above. The supernatant was then transferred to a 2 ml fresh tube and 2 volumes of 100% ice cold ethanol was added along 0.3 M NaOAc and 20 ug of glycogen. The mixture was vortexed for 5 sec and centrifuged at 17,000 x g for 10 min. The supernatant was discarded and the pellet was washed with 100 µl of ice cold 70% (v/v) ethanol and centrifuged at 17,000 x g for 5 min. The supernatant was discarded and the pellet was air-dried for 15 min before being dissolved in 20 µl of water.

2.3.6.3 Adapter ligation and product amplification

The adapter sequence was designed to inhibit amplification of non-target products. The 3′ end of the lower strand was blocked by an amine moiety to prevent amplification of the adapter. The ligation reaction for set up separately for each of the digested libraries as follows:

Digested and purified gDNA	**4 µl**
Adapter (25µM)	1.9 µl
10x ligation buffer	1.6 µl
T4 DNA ligase (6U/µl)	0.5 µl
Total volume	8 µl

Table 2.7 Reaction set up for adapter ligation for making genomic DNA library

The reaction mixture was incubated overnight at 16°C and then deactivated by incubating at 70°C for 5 min. The volume of each tube was made up to 80 µl with water.

Primers specific to the known sequence of 5′ UTR were designed such that they would anneal at least 100 bp downstream to the end of the sequence in the antisense orientation

(Appendix 6). This facilitated the alignment of the amplified products with the known sequence. The primers were also selected for a very high melting temperature of around 72°C to facilitate specific binding and reduce background amplification. A primary PCR was first done using each of the digested libraries to check which libraries show amplification and then a secondary PCR was done using the libraries showing amplification.

The primary PCR reaction mixture contained:

10 µM Adapter primer (GM1/NA46 or GM2/NA46)	**1 µl**
GSP1 primer (10 µM)	1 µl
10 x FastSTart High Fidelity Reaction Buffer	5 µl
MgCL2	
10mM dNTOs (200 µM each)	1 µl
gDNA-adapter ligation	1 µl
FastStart Enzyme blend	0.5 µl
Sterile water	40.5 µl
Total	50 µl

Table 2.8 Reaction set up for primary PCR to select positively amplifying libraries

One µl of the product from positive libraries was taken and used as a template for the secondary PCR. The secondary PCR reaction mixture contained:

10 µM Adapter primer (GM3/NA47)	**1 µl**
GSP2 primer (10 µM)	1 µl
10 x FastSTart High Fidelity Reaction Buffer	5 µl
MgCL2	
10 mM dNTOs (200 µM each)	1 µl
gDNA (PCR1 product)	1 µl
FastStart Enzyme blend	0.5 µl
Sterile water	40.5 µl
Total	50 µl

Table 2.9 Reaction set up for primary PCR to amplify region of interest

The primary PCR conditions were:

Steps	Temperature	Time	Cycle
Denaturation	94°C	25 sec	
Primer annealing	72°C	3 min	7
And extension			
Denaturation	94°C		
Primer annealing	67°C		32
And extension			
Final extension	67°C		1
Hold	10°C		1

Table 2.10 Cycle conditions for primary PCR to select positively amplifying libraries

The conditions for the secondary round were the same except the cycle for the first denaturation and annealing was reduced to 5 cycles and the second step denaturation and annealing was reduced to 20 cycles.

2.3.6.4 Genome walking product purification

The amplified products from genome walking were run on 1% (w/v) agarose gel as described in section 2.3.3.3, and distinct bands were cut out after ethidium bromide illumination and purified using the QIAquick® Gel Extraction Kit as per recommended protocol with the kit.

2.3.7 Cloning and plasmid sequencing of PCR amplification products

2.3.7.1 Preparation of competent cells for cloning

Chemically competent cells for transformation were prepared using the DH5α (GIBCO BRL) strain of *E. coli* according to the method of Inoue et al., (1990) with some modifications. The media and reagents used were:

- LB broth containing 1% (w/v) bacto-tryptone (DIFCO Laboratories, Detroit, MI, USA), 0.5% (w/v) bacto-yeast extract (DIFCO Laboratories), 1% (w/v) NaCl, pH 7.5
- 60 mM $Cacl_2$
- Glycerol

Competent cells were prepared as follows:

- Bacterial cells from a glycerol stock were cultured in LB broth (10 ml) at 37°C overnight with shaking (180 rpm).
- The following day, 400µl of the culture was used to inoculate 40 ml of freshly autoclaved LB broth and cells were grown until optical density reached up to 0.4 at 600 nm.
- After this, the cells were pelleted at 3000 x g for 5 min at 4°C and after decanting the supernatant, the pellet was re-suspended in 10 ml of ice-cold 60 mM $CaCl_2$.
- The cells were then incubated on ice for 30 min after which the cells were pelleted again at 3000 x g and re-suspended in 4 ml of 60 mM $CaCl_2$ containing 15 % (v/v) glycerol. Aliquots of 250 µl of the cells were prepared and stored at -80°C until further use.

2.3.7.2 PCR product cloning to pGEM® T Easy vector and transformed plasmid isolation

Sequencing of all the PCR products in the study was done *via* TA cloning into the pGEM® T Easy vector (Promega, WI, USA) (Appendix 7) as per the supplier recommended standard protocol. The presence of insert was confirmed by PCR amplification using insert sequence specific primers. *E. coli* colonies with the insert were then cultured in 10 ml of LB broth overnight at 37°C with 1µl of 1 mg/ml Ampicillin per 10 ml of culture for positive selection. The cells were then pelleted by centrifugation at 17,000 x g for 1 min.

Pelleted transformed cells were then used to extract the plasmid with insert with the High Pure™ Plasmid Isolation Kit as per the manufacturer recommended instructions.

2.3.7.3 Plasmid sequencing

For sequencing, plasmid samples were submitted to the DNA Analysis Facility, Massey Genome Service, Massey University. A standard protocol for automated capillary analysis was followed on the AB13730 DNA analyser (Applied Biosystems, Life technologies).

2.3.7.4 Sequence analysis

The sequence results obtained from the DNA Analysis Facility were analysed and edited using the 4Peaks software (http://nucleobytes.com/index.php/4peaks). The consensus sequence from multiple positive colonies was generated using the ClustalW programme. The consensus sequence was then analysed by using the BLAST and JCVI databases to compare to homologs in other plants species for the genes of interest. The sequences were then translated *in silico* using the 4Peaks software. Translated sequence was analysed for transit peptide sequence and putative localization motifs using the ExPASy ProtParam tool (http://web.expasy.org/protparam/).

2.4 Protein methods

2.4.1 Recombinant protein: Cloning and expression

The directional cloning method was used for cloning *AcSIR1* and *AcNiR1* into the pGEX-6P-3 vector (GE Healthcare) (Appendix 7) and propagated in the BL21 strain of *E. coli.* Specific primers were made for *AcSiR1* and *AcNiR1* with restriction sites included at the 3´ and 5´ end of the sequence. Restriction sites were selected such that they would not occur within the sequence of interest (Appendix 8). For the *AcSiR1* sequence, *Eco*R1 and *Xho*1 restriction sites were included at the 3´ end and the 5´ end of the primer sequence, and for *AcNiR1* amplification *Bam*H1 and *Not*1 restriction sites were introduced. The sequence of interest was then amplified from a cDNA mix using specific primers with restriction sites, visualized on 1% agarose gel and purified using QIAquick® Gel Extraction Kit. The sequence of interest was then ligated into the pGEM-T-EASY® vector (Promega) and propagated in the DH5α (GIBCO BRL) strain of *E. coli.*

For making recombinant fusion protein with glutathione-*S*-trasferase (GST) for expression studies, *AcSiR1* and *AcNiR1* expression, the sequence was digested out of respective pGEM-T-EASY® plasmid using respective restriction endonucleases as mentioned above and

ligated into pGEX-6P-3 vector using BL21 strain of *E. coli* as host. The translation of the inserted gene was induced with the addition of 0.2mM IPTG (AppliChem, Ottoweg, Darmstadt, Germany) and incubation of cells at 14°C overnight at 180 rpm. After the incubation, the cells were centrifuged at 5000 x g for 10 min and the pellet was resuspended in 40 ml of cold lysis buffer (50mM Tris-HCL, 100mM NaCl and 1 mM DTT, pH 7.5). The cells were then lysed using the French press at 7,000 psi and the lysate was centrifuged at 14,000 x g for 10 min. The supernatant was then mixed with a pre-prepared 50% GS4B (GE Healthcare) slurry as per the manufacturer's instructions and incubated with gentle rotation for 2 h at room temperature. The resin was then washed with 15ml of cold lysis buffer thrice with centrifugation at 500 x g betwwen each wash to pellet the resin. The resin was then re-suspended in cleavage buffer containing 50 mM Tris-HCL, 150 mM NaCl, 1 mM Na_2EDTA and 1 mM DTT (pH 7.0). The beads were washed twice more as above. The fusion protein was cleaved from GST by addition of 20 U of PreScission® Protease (GE Healthcare) in 2 ml of and the tube incubated at 4°C overnight, with end to end rotation. The protein was recovered as supernatant the following day by centrifuging the slurry at 500 x g for 5 min at 4°C.

2.4.2 Protein separation by 1-Dimension SDS polyacrylamide gel electrophoresis

2.4.2.1 Sample Preparation

The protein samples were heated in an equal volume of reducing buffer containing 100 mM Tris-HCL, pH 6.8, 20% (v/v) glycerol, 5% Ultrapure™ SDS (Invitrogen Corp, CA, USA), 0.01% (w/v) bromophenol blue and 5% (v/v) 2-mercaptoethanol for 5 min. After this, the samples were centrifuged at 13,000 x g for 1 min, before loading on the gel. Generally 5-10 µl of protein was loaded per well.

2.4.2.2 Gel preparation and gel electrophoresis

Proteins were separated as per their molecular mass as has been described by Laemmli (1970). The proteins were resolved in 12% resolving gel (0.18M Tris-HCL [pH8.8], 0.1% SDS, 12% acrylamide [37:5:1], 0.1% ammonium persulfate and 5 ul of tetramethylethylenediamine).

The gel was submerged in running buffer (0.025 M Tris-HCL, 0.1% SDS, 0.192 M glycine, pH 8.3) and electrophoresis was run at 150 V for 75 min.

2.4.3 Western Analysis

2.4.3.1 Transfer of proteins onto PVDF membrane

Proteins separated by SDS-PAGE (2.4.2.2) were transferred onto a PVDF membrane (PVDF transfer membranes, PerkinElmer Life Sciences Inc., Boston, MA, USA) as described by Towbin et al, 1979 using the Trans-Blot® Electrophoretic transfer cell (Bio-Rad). The membrane, cut to the size of the gel, was first activated by dipping in MeOH and then transfer buffer (25 mM Tris, 190 mM glycine, pH 8.3 containing 10% (v/v) MeOH) and chilled at 4°C prior to use. The cassette was assembled as per the diagram below:

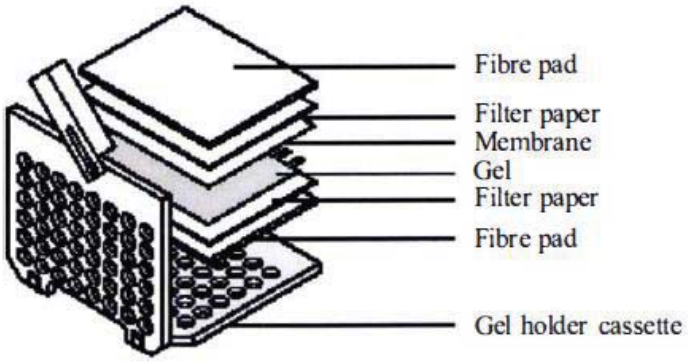

Figure 2.2 Cassette set up for western blotting adapted from Mini Trans-Blot® electrophoretic transfer cell, Instruction manual (Bio-Rad laboratories, Hercules, CA, USA)

The cassette was then transferred to the holder and transfer buffer was poured to cover the top of the cassette and the Bio-Ice™ cooling unit was included. The transfer was conducted at 100 V for 60 min on constant stirring.

2.4.3.2 Detection of proteins by Coomassie Blue staining

Coomassie staining was used to check the accumulation of recombinant proteins and also as an indirect measure to check for equal loading of samples before western blotting for root tissue. To do this, after the electrophoresis, the gel immersed in Coomassie Blue solution containing 0.1% (w/v) Coomassie Brilliant blue (Sigma-Aldrich), 40% (v/v) MeOH and 10% (v/v) EtOH for 30 min after which the gel was destained to remove background stain by washing with 30% (v/v) EtOH until desired contrast was reached. The gel was imaged using the Gel-Doc XR system (Bio-Rad).

2.4.3.3 Probing and detection using specific antibodies

For protein detection using specific antibodies, the PVDF membrane was blocked with blocking solution [12% (w/v) skim milk powder (Pams, The Foodstuffs Co-operative Society Ltd, Wellington, NZ)] in 50 mM phosphate buffer, 250 mM NaCl, pH 7.4, containing for 2 h. The membrane was washed with 50 mL of PBST (phosphate buffer saline with 0.05% (v/v) Tween 20), five times, with 3 min incubation per wash. The membrane was then incubated with protein specific primary polyclonal antibody in a 1:5000 dilution with PBST to a total of 20 ml and incubated for 1.5 h at 35°C. The membrane was then washed with 50 mL of PBST (PBS with 0.05% (v/v) Tween 20), five times, with 3 min incubation per wash. Following this the membrane was incubated with secondary antibody (anti-rabbit) raised in goat and conjugated either with alkaline phosphatase (1:10,000 dilution in PBST) for chromogenic detection or with horseradish peroxidase (1:80,000 dilution in PBST) for chemiluminescense detection (Promega Corp, Madison, WI, USA) for 1 h at 35°C. After incubation, the membrane was washed as before with PBST.

For chromogenic detection, the membrane was finally washed in substrate buffer (100 mM Tris-HCL, pH 9.6, containing 100 mM NaCl and 10mM $MgCl_2$) and then incubated in the dark in developing buffer [100 mM Tris-HCL, pH 9.6, containing 100 mM NaCl, 0.01% (w/v) BCIP, Roche), 0.02% (w/v) NBT, 1% (w/v) DMSO and 8 mM $MgCl_2$] to visualize the protein band of interest. After sufficient contrast was achieved, the reaction was stopped by rinsing the membrane in water.

For Chemiluminescence detection, the membrane was washed in PBST and then incubated with BM Chemiluminescence Western Blotting Substrate (POD) (Roche) as per the supplier's recommendation. The membrane was then placed between two transparency sheets (OfficeMax, Wellington, NZ) and placed inside a FujiFilm BAB cassette (Fujifilm USA

Inc.,Valhalla, NY, USA) making sure that the detection substrate does not seep out from between the transparencies. The X-ray was placed over the BAB cassette in a dark room for required exposure time (usually 1 min) after which it was processed automatically using the X-Ray Film Processor 100 Plus (All Pro Imaging, Hicksville, NY, USA).

2.4.3.4 Production of antibody

Approximately 250 µg of purified AcNiR1/AcSiR1 recombinant protein was emulsified using Freunds incomplete adjuvant and injected into New Zealand white rabbit subcutaneously at several sites on the animal's back. Two more booster injections were given at monthly intervals at the end of which ca. 10 ml of terminal bleed as taken from the rabbit. The bleed was kept at 4 °C overnight and clear serum was collected as supernatant. The serum was further purified by affinity chromatography using Protein G Sepharose 4 Fast Flow resin (GE Healthcare) in 20 mM phosphate buffer as per supplier's instructions.

2.4.4 Isothermal Titration Calorimetry

2.4.4.1 Sample preparation

After purifying the recombinant proteins as described in section 2.4.1.2, the protein samples were dialyzed overnight into ITC buffer containing 50 mM Tris-HCL and 250 mM NaCl, pH 7.5 at 4°C to minimize any noise in the experiment due to difference in pH or buffer composition of the two samples. After dialysis, the protein was recovered and concentrated using Amicon Ultra-0.5 ml centrifugal filters with a 30 kD cut off (Merck Millipore, Manukau, NZ) as per the supplier's recommendation. Recombinant AcSiR1 was concentrated to at least 10 µM and AcNiR1 was concentrated to at least 10 times higher than the AcSiR1 concentration (2.4.4.2), as per a typical run recommended for Microcal™ ITC_{200} System (GE Healthcare). To be able to distinguish signal from noise for uncharacterized proteins, it is recommended that it is recommended that the protein injected (syringe concentration) into the cell (cell concentration) be at least 10 fold higher to begin with and then depending on the signal can subsequently be fine-tuned.

2.4.4.2 Instrument setup and data analysis

The Microcal™ ITC_{200} System (GE Healthcare) was setup and the experiment was run as per the manufacturers recommended procedure using the following settings:

Total injections	**19**
Cell temperature	25
Reference power (µcal/sec)	10
Initial delay (sec)	60
Syringe Concentration (µM)	173.8
Cell concentration (µM)	12.2
Stirring speed (rpm)	1000

Table 2.11 Microcal™ ITC Settings used for protein-protein interaction studies

The data was analysed, curve fitting and graphs plotting was done automatically using the Origin7™ software provided along with ITC_{200} System as per the manufacturer's recommendations.

2.4.5 Solid Phase Binding Assay

The solid phase binding assay was carried out as described in Cumming et al. (2007). The microtitre well was first coated with 1ug/100 µl of recombinant AcNiR1 in buffer containing 50 mM Tris-HCL, 100 mM NaCl (TBS), pH 7.5 at 25°C for 2 h. After incubation, the wells were washed gently with TBS containing 0.05% (v/v) Tween-20 (TBST) and incubated with 200 µl of 0.5% milk powder (Pams) in TBS at 25°C for 2 h or 4°C overnight. Following this the wells were washed gently with TBST and incubated with the secondary protein (AcSiR1 or AcOASTL2) at increasing concentrations from 0 to 2 µg/100 µl at 25°C for 2 hours or 4◦overnight. After this the cells were washed again with TBS and incubated with primary Anti AtSiR1 or the Anti-AcOASTL1 antibody (AcOASTL1 antibody recognized AcOASTL2) for 1 h at 37°C. The wells were washed again as before, and then were incubated with secondary anti-rabbit, alkaline-phosphatase conjugated antibody, for 1 h at 37 °C. The wells were washed post incubation and 100µl of substrate buffer [5 ml of 50 mM $NaHCO_3$, one (5mg) tablet of *p*- nitrophenol phosphate (Sigma-aldrich) and 8 mM $MgCl_2$ pH 9.7] was added per well and absorbance read at 405 nm.

2.4.6 Enzyme analysis

2.4.6.1 Cysteine standard curve

As the AcSiR1 activity was measured indirectly by coupling SiR1 activity with *O*ASTL activity and measuring the amount of cysteine made per unit of time, a cysteine standard curve was generated to use for the conversion of absorbance to amount.

- 1 mM cysteine was prepared and aliquoted into tubes as follows:

Amount (µ mole)	Vol of 1 mM $_{L}$-cysteine	Water
0	0 µl	100 µl
0.01	10 µl	90 µl
0.02	20 µl	80 µl
0.04	40 µl	60 µl
0.06	60 µl	40 µl
0.08	80 µl	20 µl
0.1	100 µl	0 µl

Table 2.12 Set up for cysteine standard curve describing increasing amounts of cysteine used to generate a linear curve

- For each cysteine concentration, a triplicate tube was set up.
- One hundred µl of 20% (w/v) trichloroacetic acid was added and the tubes were centrifuged at 3000 x g for 1 min at room temperature.
- After this, the supernatant was transferred into a new tube and 100 µl of glacial acetic acid and 200 µl of ninhydrin[1] reagent was added.
- The tubes were then heated on a float-rack in a water bath at 100°C for 10 min.
- The tubes were then cooled on ice and 600 µl of 95% (v/v) EtOH was added.
- The absorbance was then read at 546 nm and was plotted against amount to generate the standard curve.

[1]Ninhydrin reagent was made by dissolving 250 mg of ninhydrin in 10 ml of glacial acetic acid:conc HCL (60:40, v/v) and stirring for an hour in the fumehood.

2.4.6.2 Measurement of AcSiR1 activity

AcSiR1 activity was measured using a modified protocol of Brychkova et al. (2012) using dithionite as a reductant and methyl viologen as an electron donor. The assay measures the amount of cysteine made per unit of time. The final 1 ml assay reaction contained 25 mM phosphate buffer, 7 mM methyl viologen, 10 mM *O*-acetylserine, 50 µM $_{L}$-Pyridoxal 5´Phosphate, 2 mM dithioerythritol, ca 1ug of recombinant *Ac*OASTL1 and AcSiR1 extract as required. The reaction was started by the addition of 6 mM sodium dithionite in 150 mM $NaHCO_3$. To stop the reaction, 100 µl of 20% (w/v) trichloroacetic acid was added and samples were centrifuged at 14, 000 x g for 1 min and the supernatant was transferred to a new tube. To this supernatant, 100 µl of glacial acetic acid and 200 µl of ninhydrin reagent were added and tubes were heated on a float-rack in a water bath at 100°C for 10 min. The tubes were then cooled on ice prior to adding 600 µl of 95% (v/v) EtOH. The absorbance was read at 546 nm. The activity was calculated by converting absorbance readings to cysteine using the cysteine standard curve prepared, per unit time.

2.4.6.3 Measurement of AcNiR1 activity

AcNiR activity was measured using a modified protocol of Vega et al., 1980. Nitrite reductase catalyses the six electron reduction of nitrite and formation of NH_4^+ utilizing ferredoxin as electron donor. The enzyme activity was measured as the amount of nitrite converted per unit of time using dithionite as a reductant and methyl viologen as an electron carrier. The reaction mix per ml of assay contained 75 mM Tris-HCL (pH 8), 2 mM sodium nitrite, 0.75 mM methyl viologen, *Ac*NiR1 extract (ca 250 µg for plant extract and 1-2.5 µg for recombinant protein). The reaction was started by the addition of 8.5 mM dithionite in 43.5 mM $NaHCO_3$ at 25°C. The assay was conducted anaerobicaly by flushing the sealed glass tubes with argon gas. At required time- points, the reaction was stopped by vortexing the tubes until the blue color disappeared. Following this, 100 µl of supernatant was taken and added to a fresh 1.7 ml eppindorf® tubes and centrifuges at 13,000 x g for 1 min. For quantification, Griess reagent (20 µl) (Life Technologies, Thermo Fisher Scientific) was added to 30 µl of centrifuged sample in a microtitre plate and vthe volume adjusted to 300 µl with Mili Q water. The absorbance was read at 540 nm. The activity was calculated by converting the absorbance readings to nitrite used with a nitrite standard curve

prepared as per manufacturer's recommendation (Griess reagent kit for nitrite determination, Life technologies).

2.5 Sample preparation metabolomic analysis

2.5.1 Sample preparation for the identification of volatile compounds

For the extraction of volatiles, a protocol adapted for apple skin flavour was employed (Martin Hunt, Plant & Food Research, NZ, *pers comm*). Two g of frozen tissue was added to a 25 ml scintillation *via*l (containing 20 mm x 10 mm stir bar). To this, 4 ml of 25% (w/v) $CaCl_2$ was then added to the sample tube from 5 ml dispenser and the 5.0 ml diethyl ether internal standard (ether is distilled and run through alumina). The sample was capped and stirred at a slow speed for 30 min, avoiding any foam formation at the air interphase. After 30 min, another 0.5 ml of diethyl ether (internal standard) was added and samples stirred for another 90 min. At this point, the stirrers were removed and samples were let to sit for 5 min. After this, the upper phase from the samples was pipetted into a Kimax tube with a screw cap and a pre-measured amount of $MgSO_4$ was added to bond any H_2O present in the ether. The samples were left to dry for an hour. After this, the samples were vortexed once briefly and then centrifuged at 3000 rpm for 5 min. The supernatant was poured off avoiding the salt pelleted at the bottom, into a 10 ml graduated tube and then evaporated under oxygen-free nitrogen down to 2 ml. The sample was then pipetted into a GC vial and labelled and stored in GC vials at -20°C until run on a GC-MS.

The sample run was conducted at Plant & Food Research, Palmerston North, NZ and the normalized data was sent as excel spread sheet for analysis.

2.5.2 Sample preparation for identification of targeted metabolites

For targeted metabolomics, 20 mg of freeze-dried tissue was sent to the Metabolomics Research Group, RIKEN Centre for Sustainable Resource, JAPAN where the samples were run as per standard procedures, as described in the widely targeted metabolomics methodology paper by Sawada et al., (2009). The normalized data was sent back in the form of excel spreadsheets with PCA analysis (section 2.6). For conversion and normalization of targeted metabolomics data, signal to noise of >30 was selected as

detection threshold for metabolites. Areas under the selected peaks were then converted to Log_2 values. For undetected metabolites in a particular sample, missing value was replaced by 0.1. Data was normalized by z-score transformation using the TM4 MEV software (Chu et al., 2008).

2.6 Statistical analysis

The statistical analysis for qRT-PCR and volatile metabolomics was performed using the Microsoft Office Excel 2010 and MiniTab® 16 statistical package. The Student t-test was used to determine significant difference between two data-sets and unless mentioned otherwise, a difference between means at 5% ($p< 0.05$) was considered significant, and indicated as such in the results presented in chapter 3 and 4.

For the targeted metabolome, all statistical analysis was carried using the R-language based online metabolomics suite MetaboAnalyst 2.0 (J. Xia et al., 2012). The venn diagrams were generated using the online venn diagram generator for biological data (BioVenn - a web application for the comparison and visualization of biological lists using area-proportional Venn diagrams; Hulsen et al., 2008). For this, the lists of significantly differeing metabolites between tissues and treatments was generated using the t-test function in Metaboanalyst suite. The threshold for significance was set to < 0.05.

PCA (Principal Component Analysis) is a statistical procedure to simplify and visualize big data-sets. It is represented as a score plot with PC1 at the horizontal axis and PC2 in the vertical axis representing principal and second component. The two percentages represented alongside PC1 and PC2 indicate proportion of variance contributed by the two components. PCA was performed at RIKEN by Dr. Ryo Nakabayashi using SIMCA statistical software package.

Chapter 3: Effects of long term sulfur and/or nitrogen depletion in *A. cepa*

3.1 Experimental design

A factorial S x N experiment was designed (Fig 3.1 A) where seeds were first germinated in water for 7 days and subsequently grown further in control (C, 14 mM N and 2 mM S), S depleted (-S, 14 mM N and 0.25 mM S), N depleted (-N, 3.5 mM N amd 2 mM S) or both S and N depleted (-S-N, 0.25 mM S and 3.5 mM N) media on sand mixture (see section 2.1.2) in a temperature, photoperiod and humidity controlled growth room (see section 2.1.3). Plants were grown in short day conditions for a month, at which point the first harvest (designated the pre-bulbing stage) was undertaken. As the plants still had a shallow root system at this stage and individual root systems were spatially separated from other plants in the same pot, any damage to roots through tangling with adjacent plants was minimized. After this, the remaining pots were then transferred to long day conditions to promote bulbing (see section 2.1.3). The final harvest (designated the bulbing stage) was done after a month in long day conditions (66 days post germination) (see section 2.1.4).

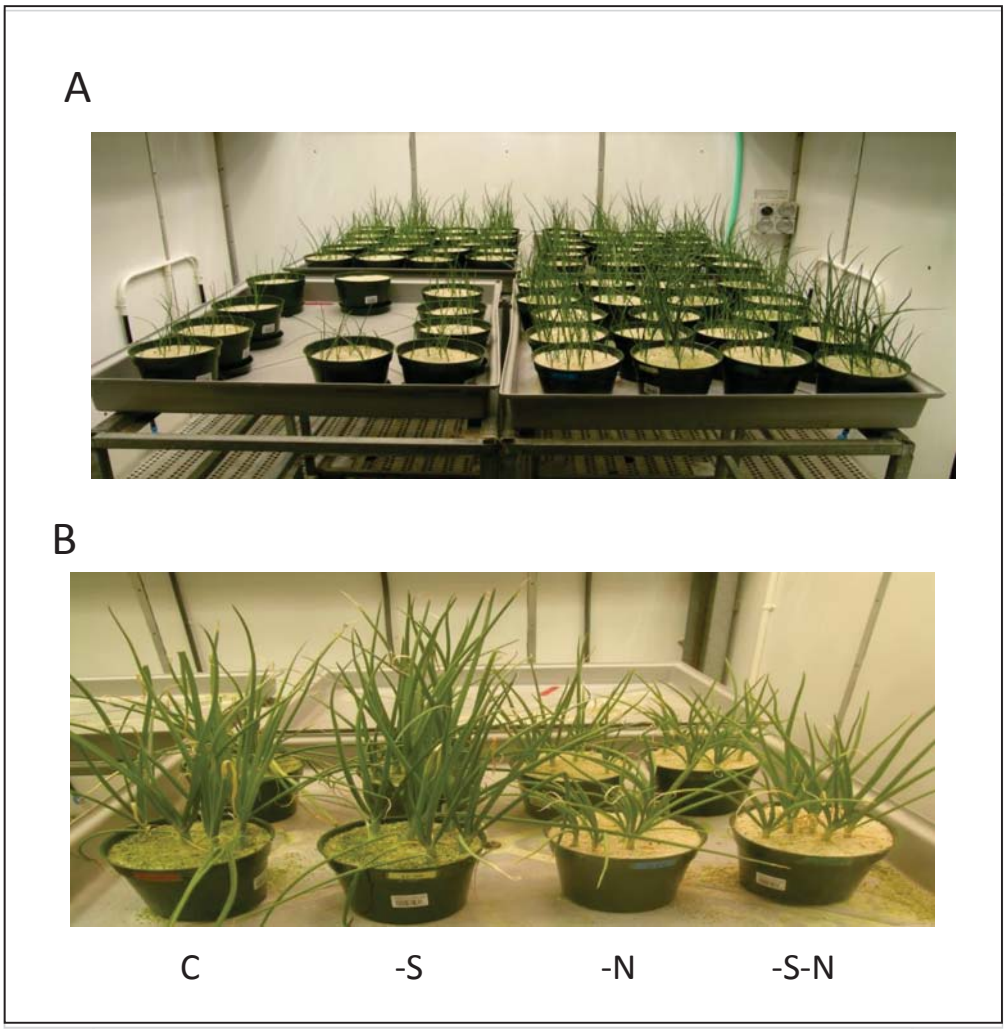

Figure 3.1: Factorial S x N experiment using *A. cepa* . A. Experimental layout of SxN factorial experiment. B. Two month old *A. cepa,* prior to second harvest at the end of 30 days in long day conditions in their respective treatment (C:control, -S: Sulfur depleted, -N: Nitrogen depleted, -S-N: Both sulfur and nitrogen depleted).

3.2 Change in fresh weight of plant tissues in response to S and/or N starvation

3.2.1 Fresh weights and shoot to root ratio at the pre-bulbing stage.

At the pre-bulbing stage, there were no significant differences ($p>0.01$) observed in the total biomass (Fig 3.2 A) or shoot to root ratio (Fig 3.2 C) for the plants grown under the -S treatment when compared with the plants grown under the control treatment. However, the -N treatment and –S-N treatment resulted in a significant reduction ($p<0.01$) of 39% and 27% in total biomass, respectively (Fig 3.2 A). This reduction was mainly due to reduced biomass of the shoot (Fig 3.2 B), as there was no significant ($p>0.01$) reduction in total root biomass in these plants. The decrease in the shoot biomass was also reflected in significant ($p<0.01$) reductions in shoot to root ratios, which were 1.01 for the –N and 1.48 for the –S-N treatments, as compared with 1.95 for the –S and 1.96 for the control treatments.

3.2.2 Fresh weights and shoot to root ratio at the bulbing stage.

The total fresh weight of the bulbing plants grown under the –S treatment tended to be higher than plants grown under the control treatment ($p=0.04$), an effect mediated by the significantly ($p<0.01$) higher root weight (Fig 3.2 E). The two nitrogen-depleted treatments (-N and –S-N) had the largest significant decrease ($p<0.01$) in total fresh weight when compared with the plants grown under the control treatment (Fig 3.2 D). The shoot fresh weights were significantly less ($p<0.01$) for plants grown in both the N-depleted treatments (-N and –S-N), while there was no significant difference in the root fresh weights of plants grown in the –N treatment. However, the fresh weight of the roots from the plants grown in –S-N treatment were significantly higher ($p<0.01$) (Fig 3.2 E).

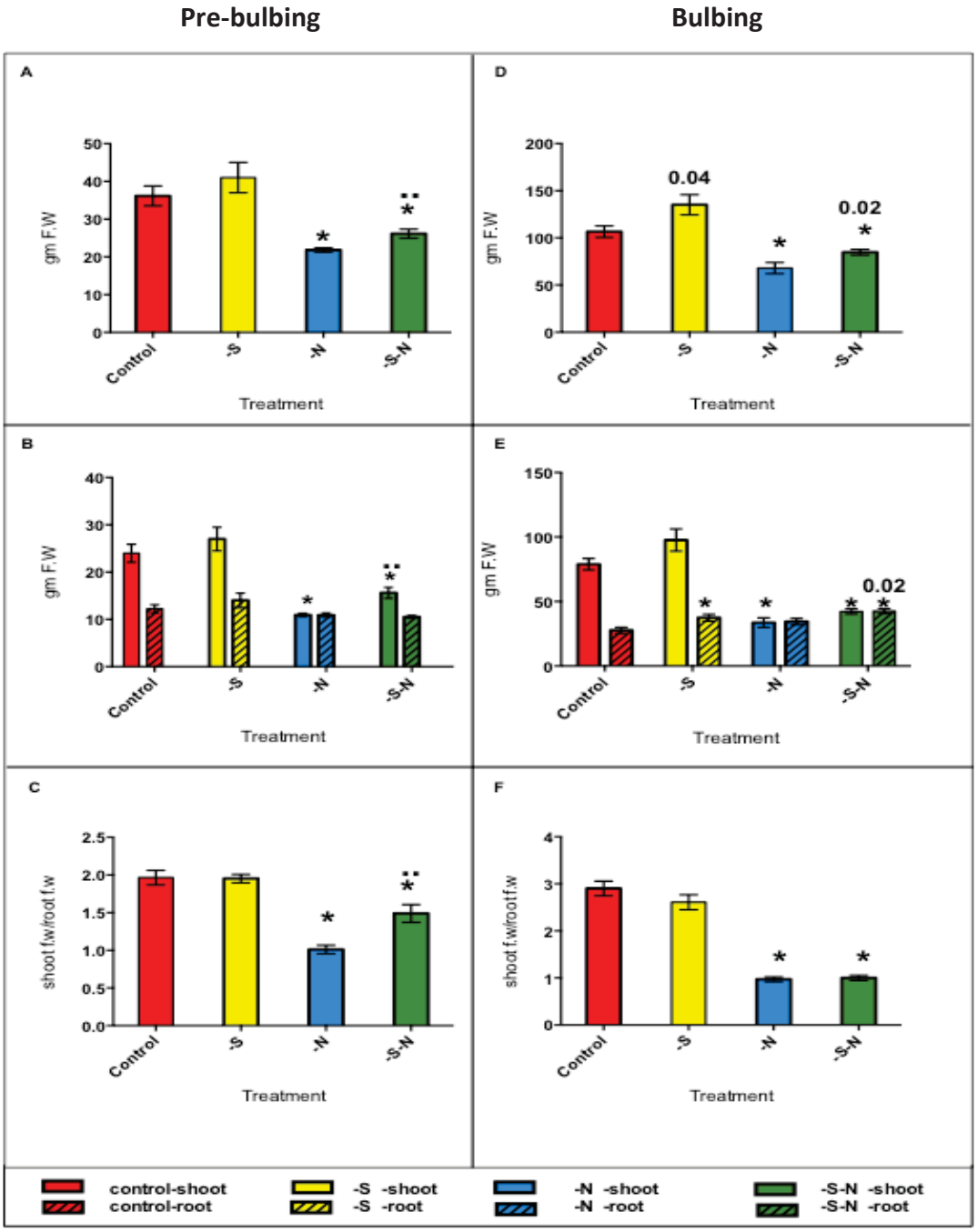

Figure 3.2 *A. cepa* factorial S x N experiment fresh weight measurements. A and D: Total biomass for each indicated treatment. B and E: Fresh weights for shoot and root for each treatment. C and F: Shoot to root ratios for each treatment. The values are mean ± SEM of six biological replicates where each biological replicate comprises tissues pooled from six individual plants. Error bars represent standard error of the mean. (⋆) Denotes significant difference ($p < 0.01$) from control and (¨) indicates significant difference ($p<0.01$) from the –N treatment. P-values >.01 but > 0.05 emphasize general trends.

3.3 Expression of *A. cepa* sulfur and nitrogen assimilatory genes in response to N and/or S depletion

To understand the effect of the S and N depletion treatments on the S and N-assimilation pathways, the transcriptional response of selected genes in each pathway was investigated for each treatment in both the leaf and the root for both the developmental stages (pre-bulbing/ bulbing).

Expression analysis was undertaken for selected genes in the S and N-assimilation pathway using qRT-PCR (see section 2.3.4, appendix 9), such that a broad picture of the whole pathway for each treatment can be captured (Fig 3.3). Relative expression of *putative High affinity Sulfate Transporter1;1 (AcHAST 1.1 LIKE1), adenosine-5´-triphosphate sulfurylase (AcATPS1), adenosine 5´-phosphosulfate reductase (AcAPSR1), adenosine 5´-phosphosulfate kinase (AcAPSK1), sulfite reductase (AcSiR1), sulfite oxidase (AcSOX1)* and *O-acetylserine thiolyase (AcOASTL1, 2* and *3)* was determined for the S-assimilation pathway and root specific *putative nitrate transporter 2;1 like1 (AcNRT2;1LIKE1), nitrate reductase (AcNR1)* and *nitrite reductase (AcNiR1)* was examined for the N-assimilation pathway. The *Flowering locus T4 (AcFT4)* gene, which has been shown to regulate the development of bulb in *A. cepa* (Lee et al., 2013), was used as molecular marker for transition of plants to the bulbing stage upon exposure to long day conditions.

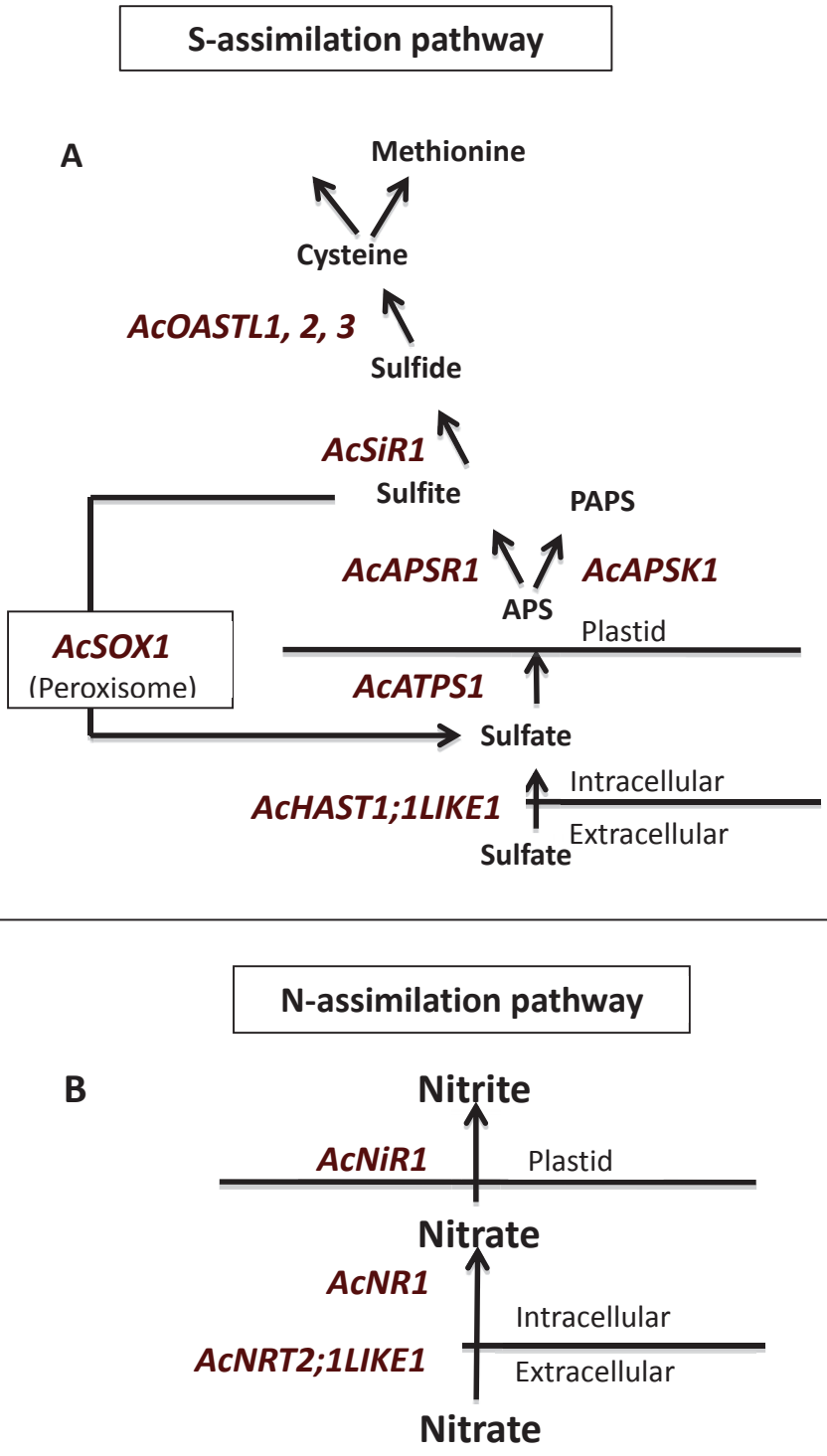

Figure 3.3 Schematic representation of the S and N-assimilation pathway and the genes transcribing the enzymes involved in *A. cepa*. A) S-assimilation pathway. **B)-** N-assimilation pathway. The transcription profile was investigated for all the genes depicted in each pathway for leaf and root tissue from plants grown under each of the four S x N treatments. *AcHAST1;1LIKE1 - Putative high affinity sulfate transporter1;1, AcATPS1- adenosine-5'-triphosphate sulfurylase, AcAPSR1- adenosine 5'-phosphosulfate reductase, AcAPSK1- adenosine 5'-phosphosulfate kinase, AcSiR1- sulfite reductase, AcOASTL1.2.3- O-acetylserine thiolyase1, 2, 3, AcSOX1- sulfite oxidase, AcNRT2;1LIKE1- putative nitrate transporter 2;1, AcNR1- nitrate reductase1, AcNiR1- nitrite reductase1*

3.3.1 Transcriptional response in leaf tissue harvested from plants in the –S treatment

A significantly higher ($p<0.05$) relative transcript abundance of *AcHAST1;1LIKE1* and *AcAPSR1*, the two genes commonly used as markers for the S-starvation response, was observed in leaf tissue from plants grown in the –S treatment and harvested at the pre-bulbing stage (Fig 3.4) . No significant change was observed in the relative transcript abundance of *AcATPS1, AcSiR1, AcSOX1* and the *AcOASTL* genes ($p>0.05$) relative to the control treatment (Fig 3.4, Fig 3.5). The relative transcript abundance of Ac*APSK1* (Fig 3.4), which marks a bifurcation in S pathway leading to sulfation reactions (Rotte & Leustek, 2000), was significantly ($p<0.05$) reduced in the leaves of the plants under the –S treatment when compared with the control treatment. There was no significant difference ($p>0.05$) in comparison to the control treatment in the relative transcript abundance of the N-assimilation pathway genes *AcNR1* and *AcNiR1*when compared to the control treatment (Fig 3.5).

In common with the relative transcript abundance of leaves at the pre-bulbing stage, in the leaf tissue of plants under the –S treatment and harvested at the bulbing stage, and a significantly ($p<0.05$) higher level of expression of *AcHAST1;1 LIKE1* and *AcAPSR1* was observed (Fig 3.4). In contrast, *AcATPS1, AcAPSK1, AcSiR1* and *AcOASTL3* transcripts had significantly lower ($p<0.05$) relative abundance (Fig 3.4, Fig 3.5). The relative transcript abundance of *AcSOX1, AcOASTL1, AcOASTL2, AcNR1* and Ac*NiR1* did not show any significant ($p>0.05$) difference when compared with the control treatment (Fig 3.4 , Fig 3.5).

3.3.2 Transcriptional response in leaf tissue harvested from plants in the –N treatment

In the leaf tissue of plants grown in the –N treatment and harvested at the pre-bulbing stage, there was a slight but significant ($p<0.05$) increase in the expression of Ac*HAST1;1 LIKE1 , AcATPS1, AcAPSR1, AcAPSK1* and *AcSOX1* when compared with leaves harvested from pre-bulbing plants grown in the control treatment (Fig 3.4). No significant ($p>0.05$) change in the relative abundance of *AcSiR1, AcOASTL1* and *AcOASTL3* transcripts, were observed. The relative transcript abundance of *AcOASTL2* showed a slight but significant ($p<0.05$) decline in the leaves of pre-bulbing plants harvested from –N treatment when compared with control treatment (Fig 3.4, Fig 3.5). Transcription of the N-assimilation pathway genes, *AcNR1 and AcNiR* had a significantly lower ($p<0.05$) level of relative

transcript abundance when compared with leaves harvested from plants grown in the control treatment (Fig 3.5 D, E).

At the bulbing stage, with the exception of *AcOASTL1* and *AcNR1,* the transcript abundance of all the genes investigated, namely *AcHAST1;1LIKE1*, *AcATPS1*, *AcAPSR1*, *AcAPSK1*, *AcSiR1*, *AcOASTL2* and *AcOASTL3* were significantly higher ($p<0.05$) in leaf tissue when compared with the control treatment (Fig 3.4) (Fig 3.5). The relative transcript abundance of *AcOASTL1* and *AcNiR1* did not show any significant ($p>0.05$) difference compared to leaves from control treatment (Fig 3.5).

3.3.3 Transcriptional response in leaf tissue harvested from plants in the –S-N treatment

In the leaf tissue at the pre-bulbing stage harvested from plants grown under the –S-N treatments, a significantly ($p<0.05$) higher relative transcript abundance were observed for Ac*HAST1;1LIKE1*, *AcATPS1* and *AcAPSR1* when compared with the relative transcript abundance in leaf tissue from plants in the control treatment (Fig 3.4). However, the relative transcript abundance of *AcSiR1, AcOASTL2* and the two nitrogen N-assimilation pathway genes *AcNR1* and *AcNiR1* was significantly ($p<0.05$) lower compared to leaf tissue of same age from plants grown under the control treatment (Fig 3.4, Fig 3.5). No significant changes were observed in transcript levels of *AcAPSK1, AcSOX1, AcOASTL1* and *AcOASTL3* when compared to pre-bulbing leaf tissue harvested from plants grown under the control treatment (Fig 3.4, Fig 3.5). However, when compared to leaf tissue harvested from plants under the -N treatment, the relative transcript levels for Ac*SOX1* and Ac*APSK1* were significantly lower ($p<0.05$) (Fig 3.4).

In leaf tissue at the bulbing stage, the relative transcript abundance of five out of the total of eleven genes investigated differed when compared to the control treatment, namely Ac*HAST1;1LIKE1, AcAPSR1, AcAPSK1, OASTL2* and Ac*NR1.* All five genes had significantly higher ($p<0.05$) relative transcript abundance (Fig 3.4) (Fig 3.5). No significant difference was observed in the relative transcript levels of the other six genes, namely; *AcATPS1, AcSIR1, AcSOX1, AcOASTL1, AcOASTL3* and *AcNiR1* (Fig 3.4) (Fig 3.5).

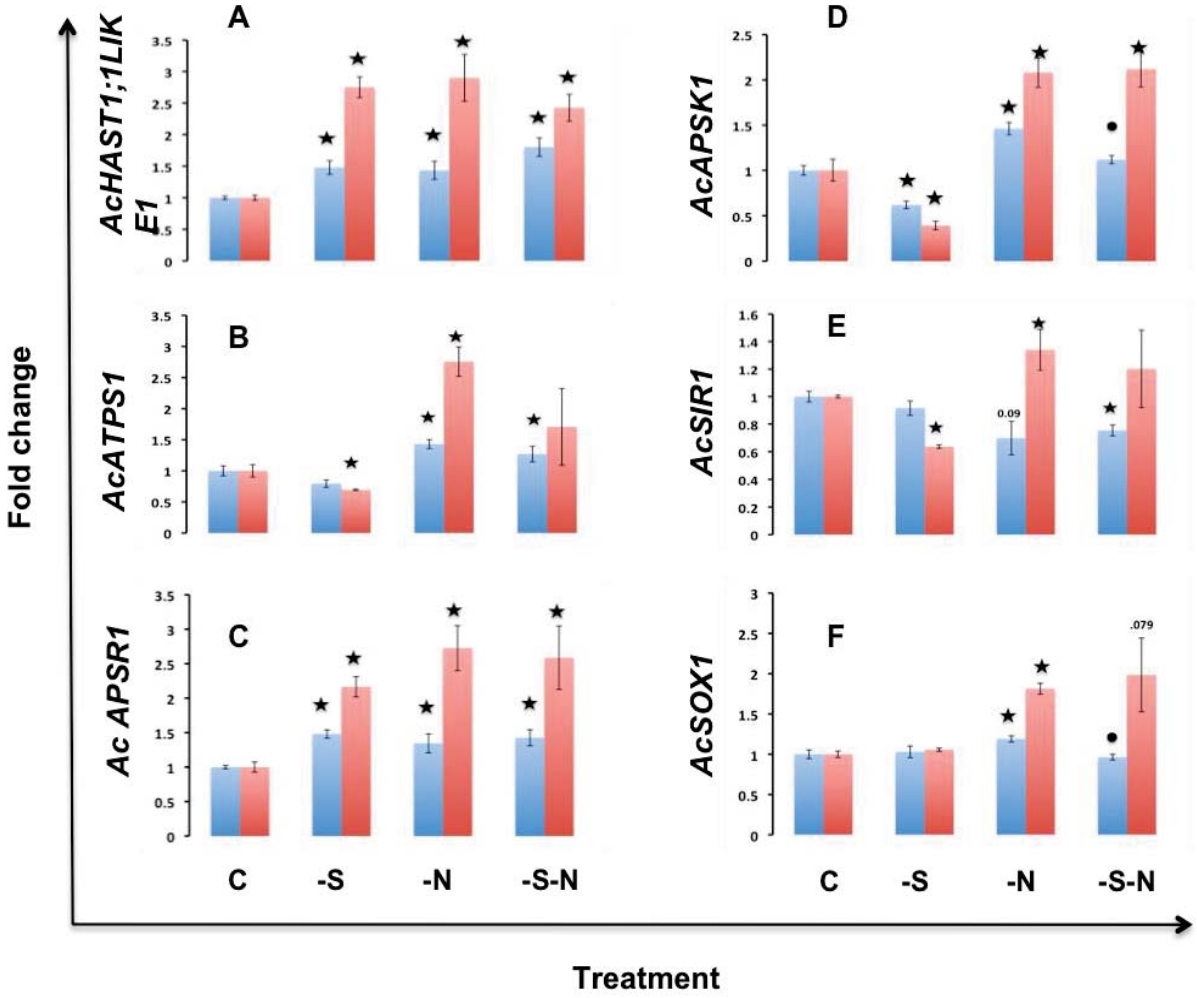

Figure 3.4 Transcriptional changes in the sulfur assimilation pathway in response to S and/or N depletion in leaves harvested at the pre-bulbing (blue bars) and at the bulbing stage (red bars). Relative transcript abundance (fold change) was determined by qRT-PCR and was normalized to control treatment using two internal reference genes *TUBa* and *CYC. AcHAST1;1LIKE1 - Putative high affinity sulfate transporter1;1, AcATPS1- adenosine-5'-triphosphate sulfurylase, AcAPSR1- adenosine 5'-phosphosulfate reductase, AcAPSK1- adenosine 5'-phosphosulfate kinase, AcSiR1- sulfite reductase, AcSOX1- sulfite oxidase*. Bars represent mean ±SEM of three biological replicates. "⋆" indicates statistically significant (P<0.05) differential expression when compared with control plants of the same stage. "•" indicates statistically significant (P<0.05) difference between the -N treatment and the –S-N treatment for the same stage. P-values>0.05 but <0.1 indicate trend towards significant difference.

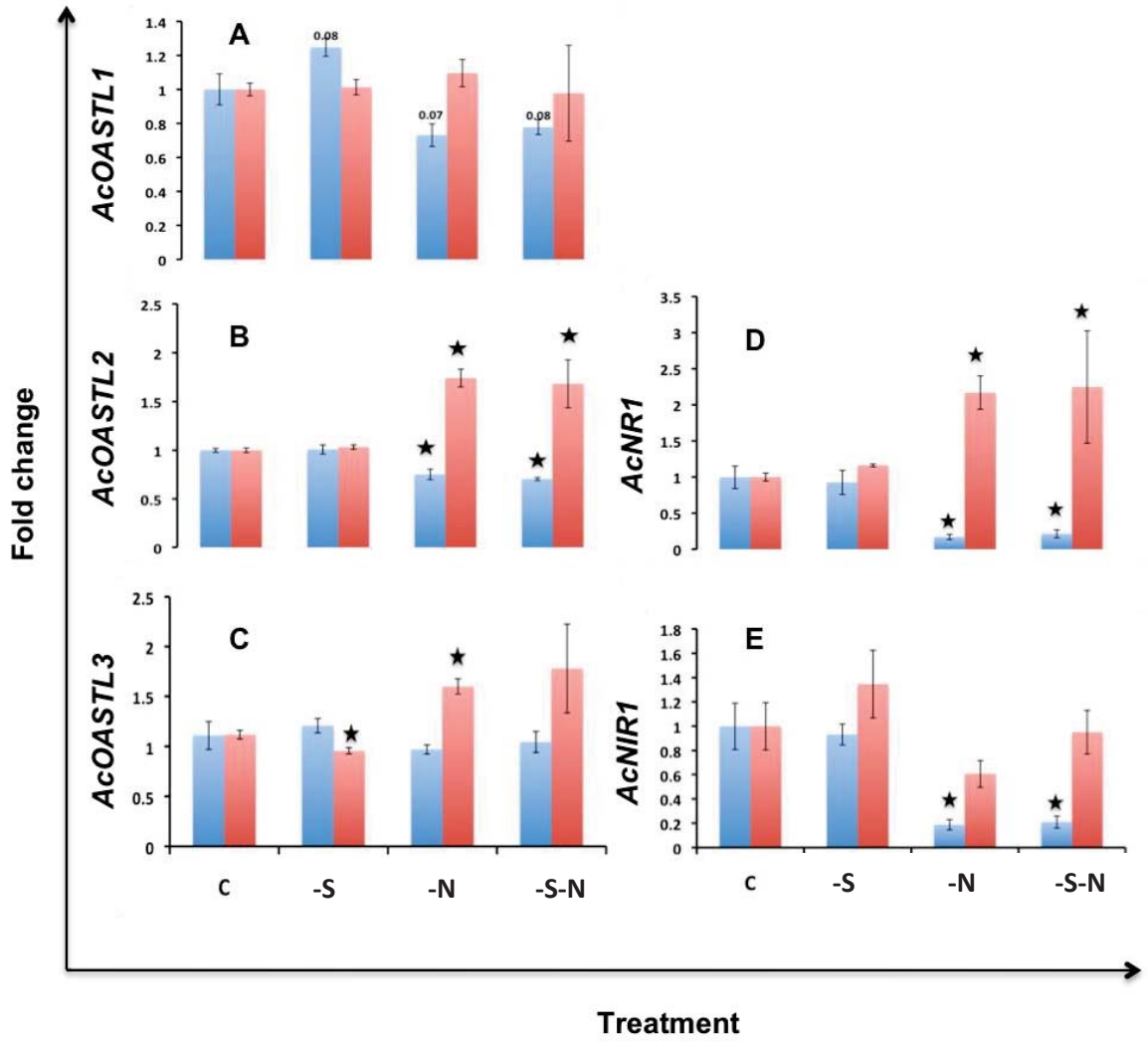

Figure 3.5 Transcriptional changes in the sulfur and nitrogen assimilation pathway in response to S and/or N depletion in leaves harvested at the pre-bulbing (blue bars) and at the bulbing stage (red bars). Relative transcript abundance (fold change) was determined by qRT-PCR and was normalized to control treatment using two internal reference genes *TUBa* and *CYC. AcOASTL1, 2* and *3- O-acetylserine thiolyase1, 2 and 3, AcNR1- nitrate reductase1, AcNiR1- nitrite reductase1.* Bars represent mean ±SEM of three biological replicates. "⋆" indicates statistically significant (P<0.05) differential expression when compared with control plants of the same stage. "•" indicates statistically significant (P<0.05) difference between the -N treatment and the –S-N treatment for the same stage. P-values>0.05 but <0.1 indicate trend towards significant difference.

3.3.4 Transcriptional response in root tissue harvested from plants in the –S treatment

The relative transcript levels of Ac*HAST1;1LIKE1* and *AcAPSR1* were significantly higher ($p<0.05$) in root tissue from plants grown under the –S treatment at the pre-bulbing stage, compared to roots from plants grown under control treatment (Fig 3.6). Whereas the relative transcript abundance of *AcATPS1*, *AcAPSK1*, AcOASTL2*, AcNRT2;1LIKE1* and *AcNiR1* genes were significantly ($p<0.05$) lower (Fig 3.6, Fig 3.7). No change in the relative transcript abundance of *AcSiR1, AcSOX1, AcOASTL1, AcOASTL3* and *AcNR1* was observed in response to –S treatment when compared with expression in plants grown in the control treatments. (Fig 3.6, Fig 3.7).

In response to the –S treatment in the roots of bulbing plants, a significantly higher ($p<0.05$) level of relative transcript abundance for *AcHAST1;1LIKE1, AcAPSR1* and *AcSIR1* was observed (Fig 3.6). In contrast, the relative transcript abundance of *AcATPS1* and *AcAPSK1* transcripts were significantly lower ($p<0.05$) than root tissue harvested from the control treatment at the same developmental stage (Fig 3.6). Relative transcript levels of Ac*SOX1, AcOASTL1, AcOASTL2, AcOASTL3, AcNRT2;1LIKE1, AcNR1* and *AcNiR1* did not show any significant change ($p>0.05$) when compared with the roots harvested from plants grown in the control treatment (Fig 3.6, Fig 3.7) .

3.3.5 Transcriptional response in root tissue harvested from plants in the –N treatment

In the root tissue harvested from plants grown in the -N treatment at the pre-bulbing stage, a slight but significantly higher ($p<0.05$) relative transcript abundance for Ac*APSK1* was observed (Fig 3.6). No significant difference was observed in the relative transcript abundance of *AcOASTL3* (Fig 3.7 C), and The relative transcript abundance of *AcHAST1;1LIKE1*, Ac*ATPS1*, Ac*APSR1*, Ac*SiR1*, Ac*SOX1*, Ac*OASTL1*, Ac*OASTL2*, Ac*NRT2;1LIKE1*, Ac*NR1* and Ac*NiR1* were significantly lower ($p<0.05$) (Fig 3.6) (Fig 3.7).

At the bulbing stage, a significantly higher ($p<0.05$) level of expression of Ac*APSK1* , Ac*SOX1* and Ac*OASTL3* was observed in plants grown in the –N treatment (Fig 3.6) (Fig 3.7). In contrast, the relative expression levels of *AcHAST1;1LIKE1*, *AcATPS*1, *AcAPSR1*, *AcSiR1*, *AcNR1* and *AcNIR1* were significantly ($p<0.05$) lower (Fig 3.6) (Fig 3.7), and the transcript

abundance of Ac*OASTL1, AcOASTL2* and *AcNRT2;1LIKE1* did not show any significant ($p>0.05$) difference when compared with the control treatment (Fig 3.7).

3.3.6 Transcriptional response in root tissue harvested from plants in the –S-N treatment

At the pre-bulbing stage, apart from *AcAPSK1* and *AcNRT2;1LIKE1,* a significantly lower ($p<0.05$) relative transcript abundance was observed for all the other genes investigated when compared with roots harvested from pre-bulbing plants grown in the control media (Fig 3.6) (Fig 3.7). This included *AcHAST1;1LIKE1*, *AcATPS1, AcAPSR1*, *AcSiR1*, *AcSOX1*, *AcOASTL1*, *AcOASTL2*, *AcOASTL3*, *AcNR1* and *AcNiR1* (Fig3.6, Fig 3.7). However, when compared to the –N treatment, a significantly ($p<0.05$) higher transcript abundance of *AcHAST1*;*1LIKE1* and *AcAPSR1* was observed (Fig 3.6). The relative transcript abundance of *AcAPSK1*, which did not show any fluctuation compared to control treatment, were significantly ($p<0.05$) reduced when compared to roots harvested from –N treatment (Fig 3.6).

At the bulbing stage, a significantly ($p<0.05$) higher relative transcript abundance was observed for *AcAPSK1* and *AcOASTL3* as compared with roots of bulbing plants harvested from control treatment. (Fig 3.6, Fig 3.7). In contrast, the transcript abundance of *AcHAST1;1LIKE1*, *AcATPS1*, *AcAPSR1*, *AcSiR1*, *AcNR1*, Ac*NiR1* was significantly ($p<0.05$) lower (Fig 3.6, Fig 3.7). No significant changes in the relative transcript abundance of *AcSOX1*, *AcOASTL1, AcOASTL2* and *AcNRT2;1LIKE* were determined in comparison to roots harvested from plants grown under the control treatment (Fig 3.6, Fig 3.7). When compared with the -N treatment, *AcHAST1;1LIKE1* and *AcAPSR1* had significantly ($p<0.05$) higher relative transcript abundance in the –S-N treatment (Fig 3.6).

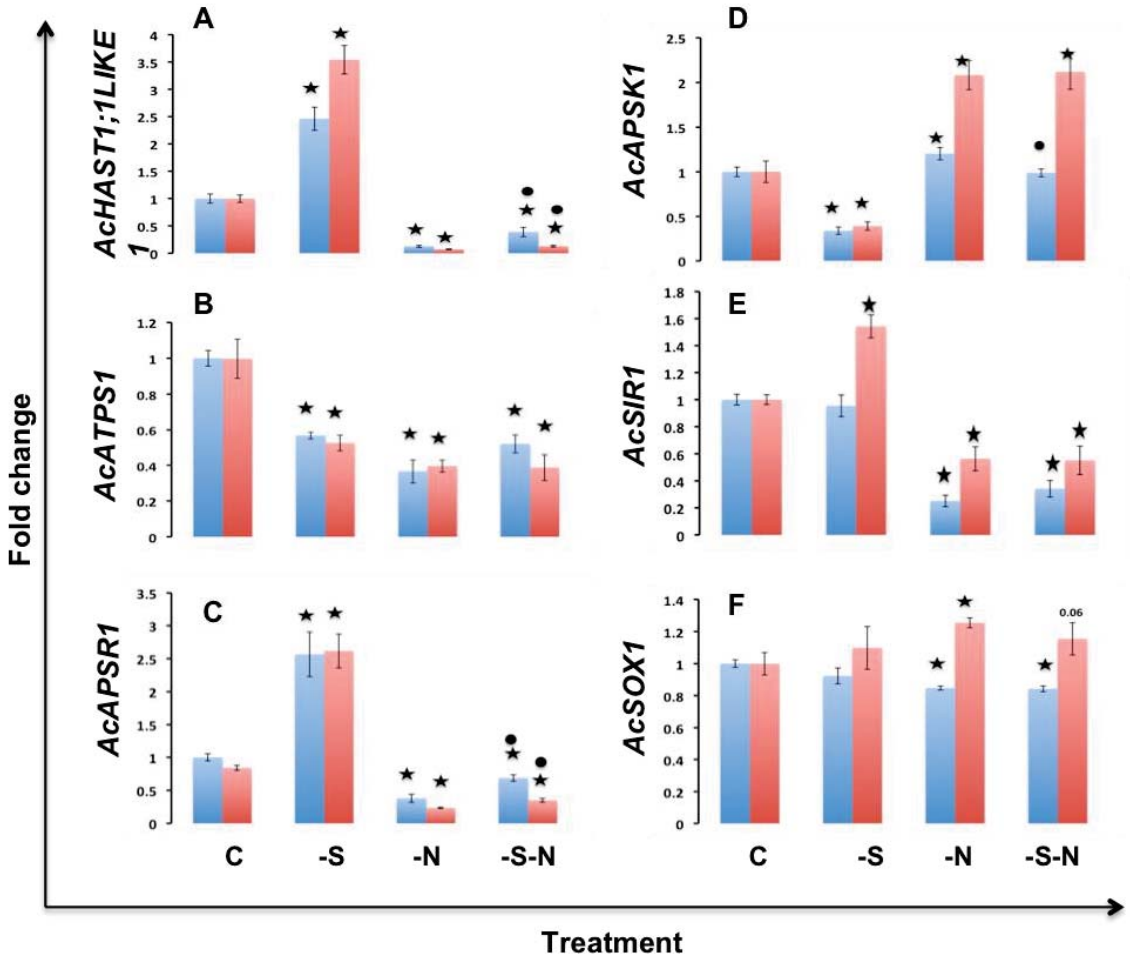

Figure 3.6 Transcriptional changes in the sulfur assimilation pathway in response to S and/or N depletion in roots harvested at the pre-bulbing (blue bars) and at the bulbing stage (red bars). Relative transcript abundance (fold change) was determined by qRT-PCR and was normalized to control treatment using two internal reference genes *TUBa* and *CYC. AcHAST1;1LIKE1 - Putative high affinity sulfate transporter1;1, AcATPS1- adenosine-5'-triphosphate sulfurylase, AcAPSR1- adenosine 5'-phosphosulfate reductase, AcAPSK1- adenosine 5'-phosphosulfate kinase, AcSiR1- sulfite reductase, AcSOX1- sulfite oxidase.* Bars represent mean ±SEM of three biological replicates. "⋆" indicates statistically significant (P<0.05) differential expression when compared with control plants of the same stage. "•" indicates statistically significant (P<0.05) difference between the -N treatment and the –S-N treatment for the same stage. P-values>0.05 but <0.1 indicate trend towards significant difference.

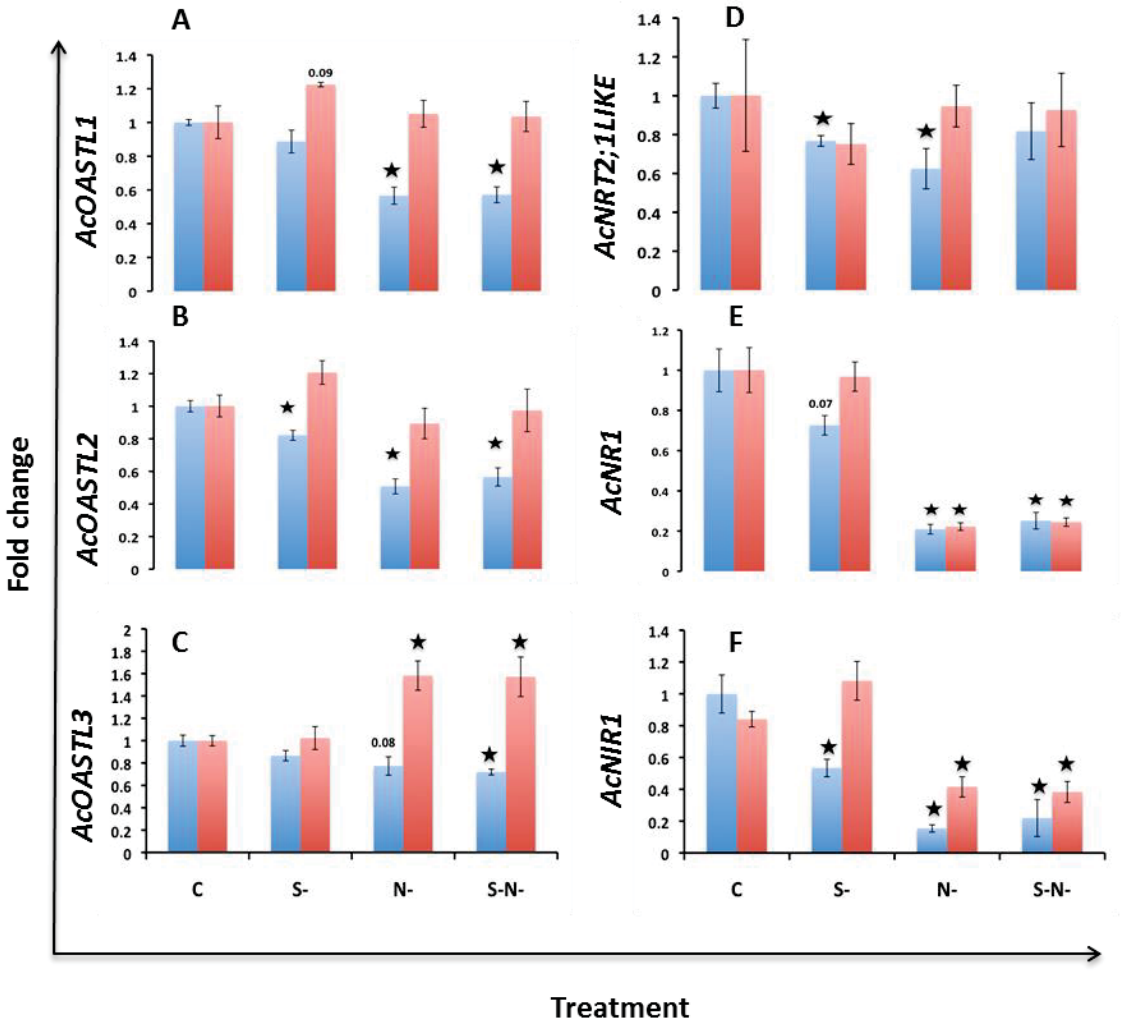

Figure 3.7 Transcriptional changes in the sulfur and nitrogen assimilation pathways in response to S and/or N depletion in roots harvested at the pre-bulbing (blue bars) and at the bulbing stage (red bars). Relative transcript abundance (fold change) was determined by qRT-PCR and was normalized to control treatment using two internal reference genes *TUBa* and *CYC. AcOASTL1, 2* and *3- O-acetylserine thiolyase1, 2 and 3, AcNRT2;1LIKE1- putative nitrate transporter 2;1, AcNR1- nitrate reductase1, AcNiR1- nitrite reductase1.* Bars represent mean ±SEM of three biological replicates. "⋆" indicates statistically significant (P<0.05) differential expression when compared with control plants of the same stage. "•" indicates statistically significant (P<0.05) difference between the -N treatment and the –S-N treatment for the same stage. P-values>0.05 but <0.1 indicate trend towards significant difference.

3.4 Expression of *Flowering locus T4 (AcFT4):* Changes in response to treatment and development.

3.4.1 Response to treatment

A role in bulbing for *AcFT4* has been suggested recently, where the overexpression of the gene has been shown to inhibit bulbing (Lee et al., 2013). Hence *FT4* gene expression was used as an indicator of the successful transition from pre-bulbing to the bulbing stage. The expression in leaf tissue was measured as an indicator as *AcFT4* expression in roots has been shown to be much lower under control conditions (Lee et al., 2013). As expected, under the control treatment, *AcFT4* transcript abundance is markedly reduced upon induction of bulbing, as plants were transferred from short day to long day conditions (2.1.3) (Fig 3.8 B). The expression of *AcFT4* was also found to respond to the -N and the –S-N treatments, where the relative expression was significantly ($p<0.05$) higher in plants grown in the -N and the –S-N treatment when compared with the control treatment. This higher level of relative transcript abundance was also observed at the bulbing stage, with a 9-fold increase in the –N and an 8.3-fold increase in the –N-S treatment (Fig 3.8 A). No significant change in relative transcript abundance level of *AcFT4* was observed in leaf tissue harvested from plants grown under the control and the –S treatment at both the pre-bulbing and the bulbing stages (Fig 3.8 A).

3.4.2 Response to development

The expression of *AcFT4* was also used as a marker gene for bulbing, and so the relative change between the two developmental stages was evaluated separately for each treatment (Fig 3.8 B). In the plants grown in the control and the -S media, the *AcFT4* relative transcript abundance declined significantly ($p<0.05$). However, no significant change in *AcFT4* relative transcript abundance was observed between the two developmental stages in plants grown under the -N and the –S-N treatments.

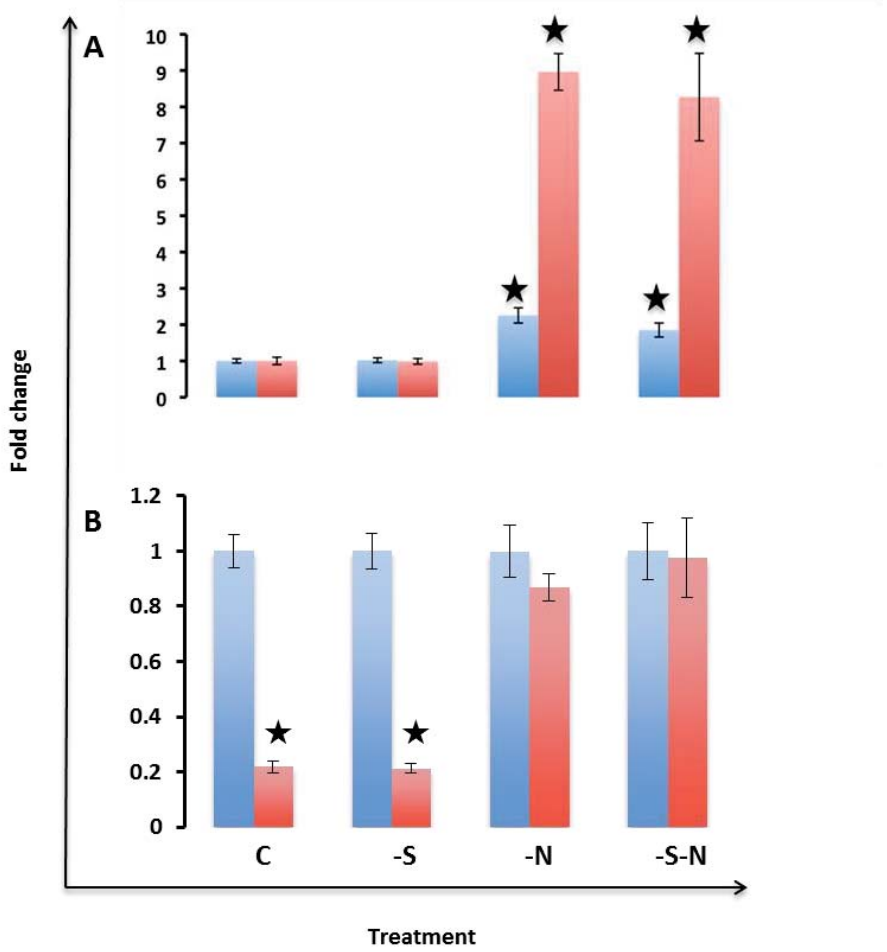

Figure 3.8 Relative expression of *AcFT4* in leaves. A: Change in relative transcript abundance in response to treatment for pre-bulbing and the bulbing stage compared to the control treatment. **B:** Change in relative transcript abundance in response to development comparing pre-bulbing stage with the bulbing stage for each treatment. Transcript abundance was determined by qRT-PCR and was normalized to control treatment for using two reference genes *AcTUBα* and *AcCYC* for **(A)** and to the pre-bulbing stage for each treatment as well as the two reference genes for **(B)** . Bars represent mean ±SEM of three biological replicates where each replicate consists of tissue pooled from 2 biological replicates as described in section 2.1.4 where each replicate consists of tissues pooled from 6 plants. "⋆" denotes statistically significant ($p<0.05$) difference as compared to control treatment for the respective stage (A), as compared to the pre-bulbing stage for the respective treatment (B).

3.5 Expression of sulfur and nitrogen assimilatory genes in response to bulbing under different S x N treatments

To understand the changes in nutritional requirement as the plant progresses from pre-bulbing to bulbing, the expression of the different S and N-assimilation pathway genes in response to bulbing was also determined. For each treatment, the expression at the pre-bulbing stage of each gene was compared with the expression of the same gene at the bulbing stage (Fig 3.9 and 3.10).

3.5.1 Plants grown in the control treatment

In the leaf tissue, *AcAPSK1* was significantly ($p<0.05$) up-regulated at the bulbing stage compared to the pre-bulbing stage (Fig 3.9 A). In contrast, the relative transcript abundance of *AcHAST1;1LIKE1, AcATPS1, AcAPSR1, AcSOX1, AcOASTL2, AcNR1* and Ac*NiR1* declined significantly ($p<0.05$) at the bulbing stage in the leaf tissue. No significant change was observed in the relative transcript abundance of Ac*SiR1*, Ac*OASTL1* and *AcOASTL3* upon bulbing when compared with the pre-bulbing stage in the leaf tissue (Fig 3.9 A).

In the root tissue harvested from bulbing plants grown in the control media, Ac*APSR1* was the only up-regulated gene compared to relative transcript abundance in root tissue at the pre-bulbing stage (Fig 3.9 C). In contrast, the relative transcript levels of Ac*ATPS1, AcAPSK1, AcSiR1, AcSOX1, AcOASTL1, AcOASTL2, AcOASTL3, AcNRT2;1LIKE1, AcNR1* and *AcNiR1* were significantly lower ($p<0.05$) in the roots at bulbing. No significant change between the two developmental stages was seen in the level of *AcHAST1;1LIKE1* transcripts (Fig 3.9 C).

3.5.2 Plants grown in the -S treatment

In the leaf tissue harvested from bulbing plants subjected to the –S treatment, there was a significant ($p<0.05$) increase in the relative transcript abundance of *AcHAST1;1LIKE1* compared to the pre-bulbing stage for the same treatment (Fig 3.9 B). In contrast, all the other genes were significantly ($p<0.05$) down-regulated in roots at bulbing (Fig 3.9 B).

In the root tissue of the plants grown in the -S media and harvested at bulbing, the transcript levels of *AcHAST1;1LIKE1* and *AcAPSR1* were significantly ($p<0.05$) up-regulated

when compared with the pre-bulbing stage (Fig 3.9 D). No significant change was observed in the relative transcript level of *AcSOX1* upon bulbing. Transcript abundance for all other genes investigated, namely *AcATPS1*, *AcAPSK1*, *AcSiR1*, *AcOASTL1*, *AcOASTL2*, *AcOASTL3*, *AcNR1* and *AcNiR1* were significantly ($p<0.05$) lower in leaves harvested at the pre-bulbing stage (Fig 3.9 D).

3.5.3 Plants grown in the -N treatment

In the leaf tissue harvested from plants at the bulbing stage grown under the –N treatment, *AcHAST1;1LIKE1*, *AcATPS1*, *AcAPSK1*, *AcOASTL1* and *AcOASTL3* were significantly ($p<0.05$) up-regulated compared to the pre-bulbing stage (Fig 3.10 E). In contrast, the N-assimilation pathway genes, *AcNR1* and *AcNiR1* were down-regulated at bulbing. The transcript levels of *AcAPSR1, AcSiR1, AcSOX1* and *AcOASTL2* transcript levels did not show any significant ($p>0.05$) change between the two developmental stages (Fig 3.10 E).

In the root tissue, none of the gene transcripts investigated were significantly up regulated, while *AcAPSR1, AcAPSK1, AcSOX1, AcOASTL2* and *AcOASTL3* transcript levels did not show any significant change. However, Ac*HAST1;1LIKE1, AcATPS1, AcSiR1*, *AcOASTL1, AcNR1* and *AcNiR1* were significantly ($p<0.05$) down-regulated at bulbing when compared with leaf tissue at pre-bulbing grown under the same treatment (Fig 3.10 G).

3.5.4 Plants grown in the –S-N treatment

In the leaf tissue, the relative transcript abundance of only Ac*OASTL3* were significantly ($p<0.05$) higher (Fig 3.10 F). The transcript levels of *AcAPSR1, AcAPSK1, AcSiR1, AcSOX1* and *AcOASTL1* remained unchanged upon bulbing under the –S-N treatment. The relative transcript abundance of *AcHAST1;1LIKE1*, *AcATPS1*, *AcAPSR1* and the N-assimilation pathway genes, *AcNR1* and *AcNiR1,* were significantly ($p<0.05$) lower compared to the pre-bulbing stage (Fig 3.10 F).

In common with the leaf tissue at bulbing, *AcHAST1;1LIKE1*, *AcATPS1*, *AcAPSR1*, *AcNR1* and *AcNiR1* were significantly ($p<0.05$) down-regulated along with *AcSiR1* and *AcOASTL1* (Fig 3.10 H). However, *AcSOX1, AcOASTL2* and *AcOASTL3* expression levels remain unchanged (Fig 3.10 H).

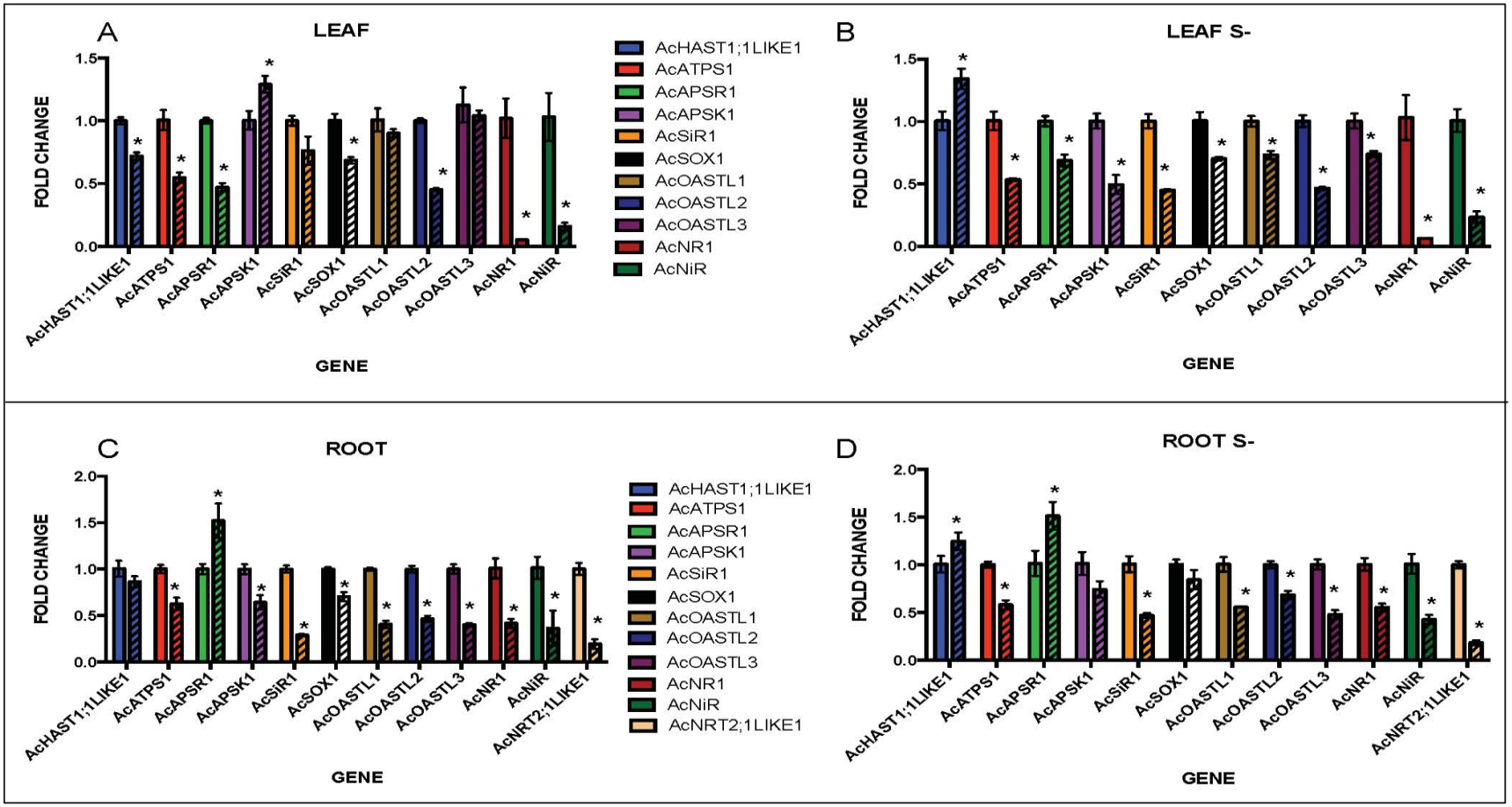

Figure 3.9 Trancriptional changes in the S and the N-assimilation pathway upon bulbing in leaves and roots of plants grown under the control and the –S treatment. Clear bars indicate the pre-bulbing stage and shaded bars indicate the bulbing stage. Fold change was determined by qRT-PCR and data was normalized to expression at the pre-bulbing stage (normalized to unity) for each gene and two reference genes *TUBa* and *CYC*. Bars represent mean ± SEM of three biological replicates. "⋆" indicates statistically significant ($p<0.05$) differential expression when compared with pre-bulbing samples for the same tissue and treatment.

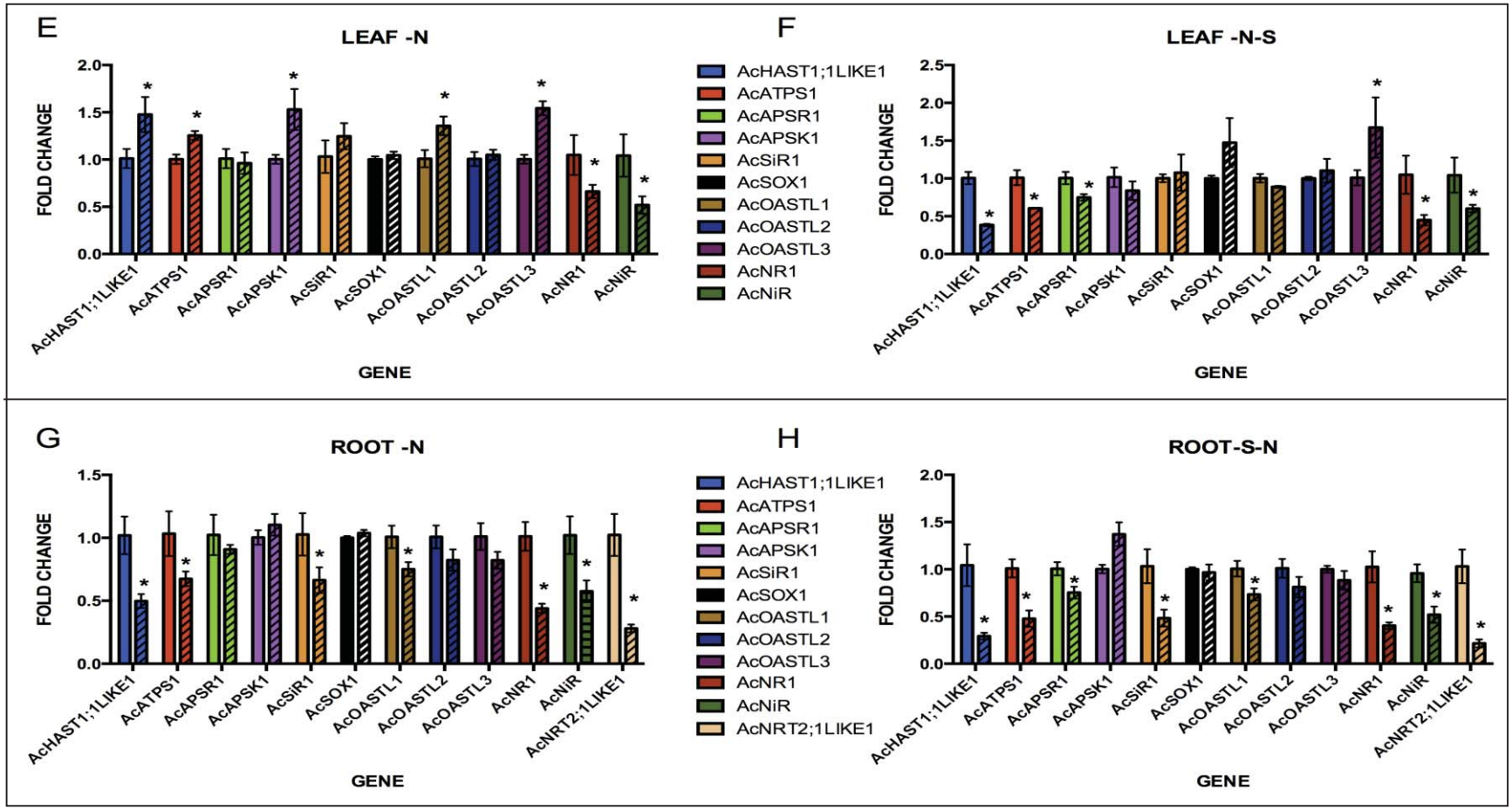

Figure 3.10 Trancriptional changes in the S and the N-assimilation pathway upon bulbing in leaves and roots of plants grown under the -N and the –S-N treatment. Clear bars indicate the pre-bulbing stage and shaded bars indicate the bulbing stage. Fold change was determined by qRT-PCR and data was normalized to expression at the pre-bulbing stage (normalized to unity) for each gene and two reference genes *TUBa* and *CYC*. Bars represent mean ± SEM of three biological replicates. "⋆" indicates statistically significant ($p<0.05$) differential expression when compared with pre-bulbing samples for the same tissue and treatment.

3.6 Metabolome wide responses to factorial S and N depeletion in different tissues of *A. cepa* CUDH2107

3.6.1 Experimental Design

Metabolomics serves as a powerful platform to capture a snapshot of the metabolic status of a plant cell under a defined set of conditions. To elucidate the metabolic networks perturbed by the –S, -N and –S-N treatments in the factorial experiment (see section 3), a widely targeted GC-MS analysis (see section 2.5) was performed on leaf, bulb (pseudo-stem for pre-bulbing stage) and root tissue harvested at the pre-bulbing stage and the bulbing stage. The accumulation of a total of 112 metabolites was determined under all four treatments at both the stages for each tissue (Table 3.2). The significantly ($p<0.05$) differing metabolites in each tissue are depicted as Venn diagrams where the area of each circle is proportional to the total number of significantly ($p<0.05$) changing metabolites (see section 2.6).

As S-containing onion pungency factors are volatile in nature, a GC-MS analysis of the volatiles in leaf tissue at pre-bulbing and bulbing stage, as well as bulbs (bulbing stage only) was also performed.

3.6.2 Changes in composition of volatile compounds in leaf and bulb tissue in response to S and/or N depletion.

Due to limited tissue availability, the volatile GC-MS analysis was only performed on the leaf tissue at the both developmental stages and the bulb. As the pseudo-stem tissue was very limited, it could not be used for volatile identification. A total of 28 volatile compounds were detected by GC-MS (Table3.1) (Appendix 10, 11), out of which nine compounds were found to be S-containing volatiles (Table 3.1) (Dr. Daryl Rowan Plant & Food Research, *pers. comm*.). No nitrogen-containing volatile was identified. Four out of the nine detected S-volatiles (designated C1, C5, C9, C26) (Table3.1) were postulated to be the same compound, dimethylthiophene, based on the theoretical molecular weight match for the each of the compounds (Dr. Daryl Rowan, Plant & Food Research, *pers. comm*.). However, differing treatment specific responses described below, suggest that each may be a separate compound. In this thesis, only the nine S-containing volatiles have been discussed

hereafter. The treatment and the development response of volatiles are represented in the form of a heat-map with each square representing the normalized value relative to the signal for the internal standards used. The most significantly represented volatile in the GC-MS was thiopropanal sulfoxide, an organosulfur Lachrymatory Factor formed by the action of the enzyme lachramatory factor synthase (LFS) on 1-PRENCSO, when it is released on wounding (Randle et al., 1995). Its response to development and treatment was also evaluated independently of other volatiles (Fig 3.12).

	NAME *	SULFUR AS COMPONENT
C1	Dimethylthiophene_10.69	Yes
C2	Compound_2 (unidentified)	No
C3	2-Me 2-pentanal	No
C4	2-methoxy 1,3 dioxlane	No
C5	Dimethylthiophene_10.99	Yes
C6	3,7,11,15-tetramethyl-2-hexadecene	No
C7	6.8min Results	No
C8	3-Mebutyl formate	No
C9	Dimethylthiophene_10.53	Yes
C10	Compound_13 (unidentified)	No
C11	Compound_14 (unidentified)	No
C12	Compound_16 (unidentified)	No
C13	1,2,5-trithiane	Yes
C14	Propenyl dithiopropanoate	Yes
C15	2-mercapto-3,4-dimethyl-2,3- dihydrothiphene	Yes
C16	2-undecanone	No
C17	Compound_21 (unidentified)	No
C18	Compound_22 (unidentified)	No
C19	Compound_23 (unidentified)	No
C20	2-hydroxymethyl...1,4-dithiane	Yes
C21	2-tridecanone	No
C22	BHT	No
C23	3,7,11,15-Tetramethyl-2-hexadecen-1-ol	N o
C24	Compound_3 (unidentified)	N o
C25	Compound_5 (unidentified)	No
C26	Dimethylthiophene_7.8	Yes
C27	Prenyl alcohol	No
C28	Thiopronanal sulfoxide	Yes

Table 3.1 List of volatile compounds detected *via* GC-MS in *A. cepa.* Compounds with sulfur present are denoted with a Yes and ones lacking sulfur as No. *Name given as per the best match for the molecular weight in the Scripps Center for Metabolomics and Mass Spectrometry database (Dr. Daryl Rowan, Plant & Food Research, *pers. comm*.)

3.6.2.1 Comparison of leaf tissue between the pre-bulbing and the bulbing stage

In the leaf tissue harvested from plants at the pre-bulbing stage, the accumulation of two forms of dimethylthiophene (C1, C5) was highest in the control treatment followed by the –S treatment then the –S-N treatment, and the lowest level of accumulation was detected in the –N treatment ($p<0.01$) (Fig 3.11). Accumulation of 1,2,5-trithiane (C13) and the C9 form of dimethylthiophene was highest in the control and then in the –S treatment with the values further decreasing in the –N and –S-N treatment, but there was no significant ($p>0.01$) difference in the values between the two N-depleted treatments. Accumulation of 2-hydroxymethyl-1,4-dithiane (C20) was highest in control and lowest in –S-N treatment. The values for –S and –N treatment were lower than control but did not differ significantly ($p>0.01$) between the treatments. Propenyl dithiopropanoate (C14), 2-mercapto-3, 4-dimethyl-2, 3-dihydrothiphene (C15) and the C26 form of dimethylthiophene did not respond significantly ($p>0.01$) to any of the treatments (Fig 3.11 A).

In the leaf tissue harvested from plants at the bulbing stage, the accumulation pattern of the two forms of dimethylthiophene (C1, C5) was the same as in pre-bulbing leaves. The C9 form of dimethylthiophene, 1, 2, 5-trithiane (C13), 2-mercapto-3,4-dimethyl-2,3-dihydrothiphene (C15), 2-hydroxymethyl.1,4-dithiane (C20) and dimethylthiophene (C26) accumulated highest in control and lowest in the –N and –S-N treatment, with no significant difference in accumulation between the two N-depleted treatments. The levels of propenyl dithiopropanoate (C14), which did not change with the treatment in the pre-bulbing leaves, accumulates in control treatment in leaves of bulbing plants when compared with the three treatments. There is no significant difference ($p<0.01$) in values between the –S, -N and –S-N treatment for C14 (Fig 3.11 A).

3.6.2.2 Variation in thiopropanal sulfoxide in leaf tissue between the two developmental stages

In the leaf tissue harvested at the pre-bulbing stage, thiopropanal sulfoxide levels were significantly ($p<0.01$) different from the control, with the highest levels in the -N and the –S-N samples. For the same samples, the levels dropped significantly and were the lowest in the -S treatment (Fig 3.12 A).

In leaves harvested at the bulbing stage, the highest thioproanal sulfoxide levels were found in the control plants, which were significantly reduced ($p<0.01$) in the –S treatment, -N treatment and were the lowest in –S-N treatment (Fig 3.12 A).

3.6.2.3 Comparison at the bulbing stage between the leaf and the bulb tissue

In the leaf tissue harvested from bulbing plants, all of the nine S-volatile compounds have the highest relative accumulation values in the control treatment followed by the–S treatment and then the two N-depletion treatments. The values for the S-volatiles did not differ significantly between the –N and the –S-N treatments ($p>0.01$), with the exception of the C1 and C5 forms of dimethylthiophene which were significantly higher in leaves harvested from –S-N treatment when compared to the –N treatment ($p<0.01$) (Fig 3.11 B).

However in the bulbs harvested from the same stage, accumulation of C1, C5 and C9 forms of dimethylthiophene, 1,2,5-trithiane (C13), 2-hydroxymethyl...1,4-dithiane (C20) were highest in the control and lowest in the –S treatment. The values for –N and –S-N treatment were significantly lower than control values but did not differ significantly between the two treatments ($p<0.01$). The levels of propenyl dithiopropanoate (C14) did not differ significantly across the treatments. The accumulation pattern of 2-mercapto-3,4-dimethyl-2,3-dihydrothiphene (C15) remained the same between the leaf and the bulb tissue (Fig 3.11 B).

3.6.2.4 Variation in thiopropanal sulfoxide at the bulbing stage between the two tissues, leaf and bulb

Both leaf and bulb harvested at the bulbing stage show the same pattern of levels of thiopropanal sulfoxide, with the highest in the control treatment and the lowest levels in the –S-N treatment ($p<0.01$), compared to all the treatments. The levels of thiopropanal sulfoxide in the -S and the –N treatments are intermediate and so are significantly lower ($p<0.01$) than the control, but higher than the leaves and bulbs from –S-N treatments at bulbing (Fig 3.12 B).

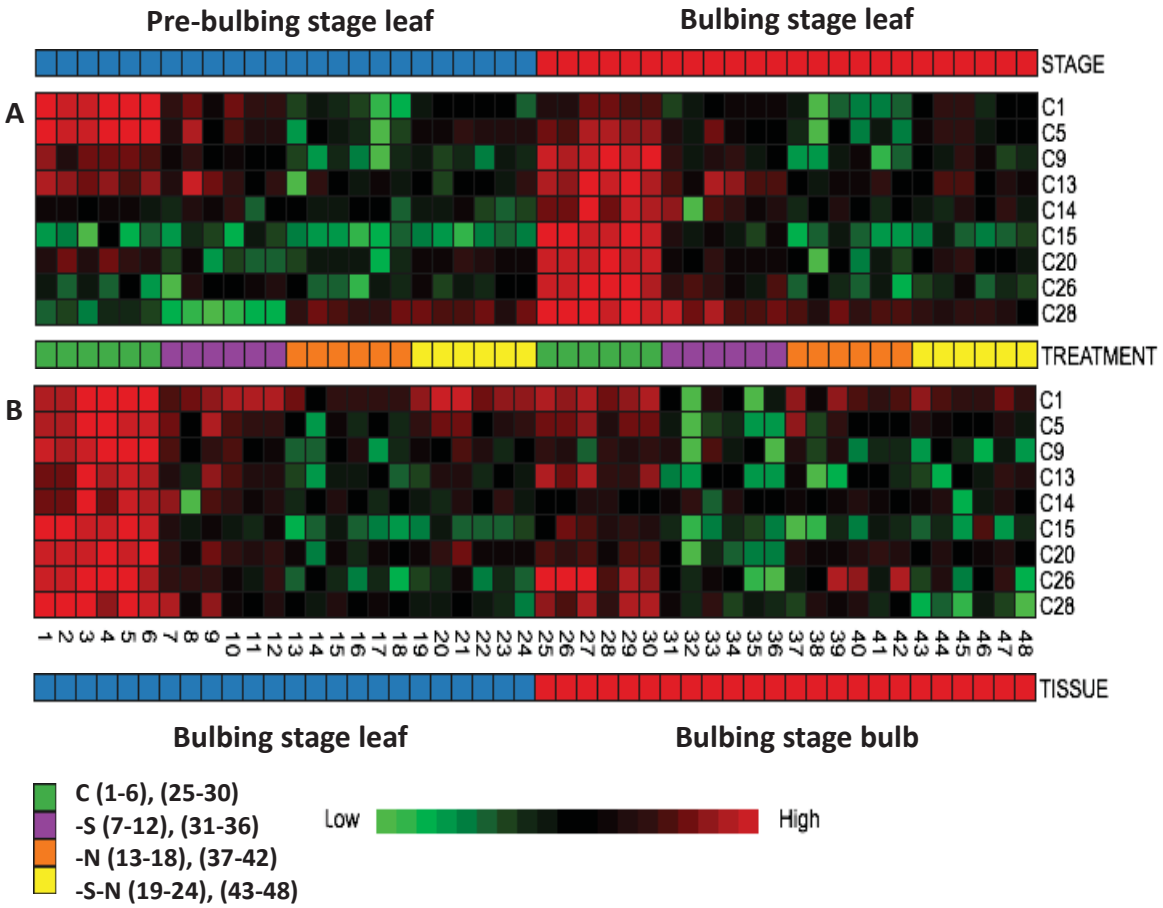

Figure 3.11 Response of S-volatiles to treatment and development as detected by GC-MS, represented as a heat-map. Comparison of Leaf tissue between pre-bulbing and bulbing stage. B- Comparison of leaf and bulb tissue at bulbing stage. Each square (1-48)(4 treatments x 2 stages x 6 replicates) represents $\log_2$ transformed value of a biological replicate for the respective S-volatile compound (C1-C28) (Refer table 3.1). Each treatment (refer color coded key) consists of six biological replicates (n=6) where each biological replicate consists of pooled tissue of six individual plants. The heatmap was generated using the MetaboAnalyst 2.2 online data analysis suite.

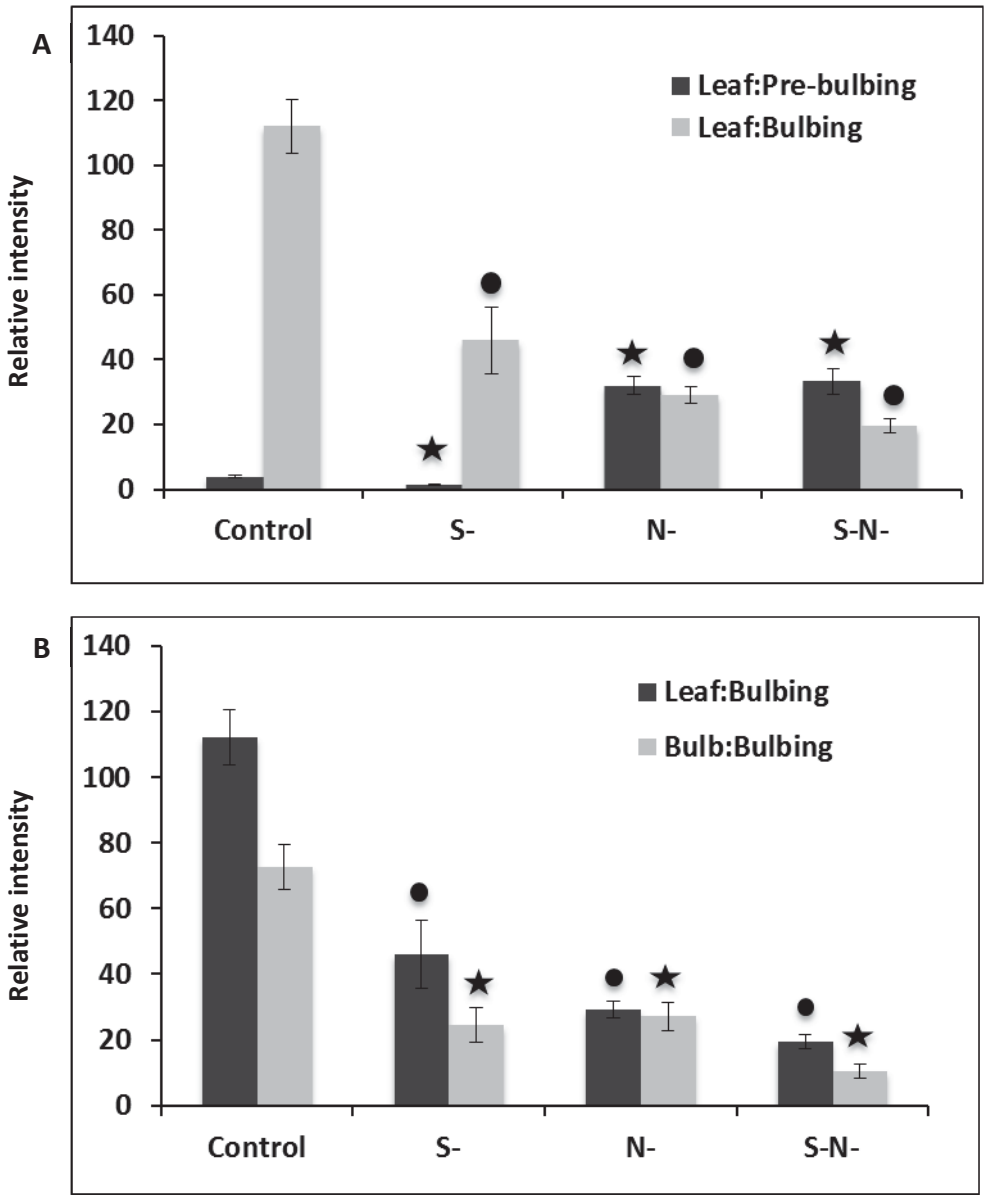

Figure 3.12 Accumulation of thiopropanal sulfoxide in different tissues and response to treatment. A: Comparison of leaf tissue between the two developmental stages, pre-bulbing an bulbing under different treatments **B:** Comparison between the two tissues, leaf and bulb at same stage (bulbing stage) under different treatments.. Bars represent the geometric-mean of six biological replicates (n=6). Error bars represent ± SEM. "⋆" indicates statistically significant difference ($p<0.05$) when compared with A) leaf tissue under control treatment at pre-bulbing stage , B) leaf tissue under control treatment at bulbing stage. "•" indicates indicates statistically significant difference ($p<0.05$) when compared with A) leaf tissue under control treatment at bulbing stage, B) bulb tissue under control treatment at bulbing stage.

3.6.3 Targeted metabolomics expression profile in response to S and/or N depletion

3.6.3.1 Changes in targeted metabolome of plants harvested from –S treatment at the pre-bulbing stage

In the leaf tissue harvested from plants at the pre-bulbing stage grown in the –S media, a total of 22 metabolites differed significantly ($p<0.05$) when compared with leaf tissue from plants grown under the control treatment. Eight out of the 22 metabolites differed exclusively in the leaves (no overlap with any other tissue) and seven of these showed a decline in accumulation (Fig 3.13).

In the pseudo-stem, a total of 36 out of 112 targeted metabolites differed significantly ($p<0.05$), 22 of which responded exclusively in the pseudo-stem. In contrast to leaves at pre-bulbing, 19 out of the significantly differing metabolites showed a higher accumulation. Of the metabolites accumulating exclusively in pseudo-stems under –S treatment, 18 were N-containing compounds, mainly amino acids (Fig 3.13).

In the roots, a total of nine metabolites showed significant ($p<0.05$) difference when compared with roots from pre-bulbing plants grown under the control treatment, three of which differed exclusively in the roots. Two out of these three metabolites, both sugars, showed a higher accumulation whereas tyramine showed a decline in accumulation when compared with roots from control plants at pre-bulbing (Fig 3.13).

A total of eight metabolites showed a significant ($p<0.05$) change in accumulation in both leaves and pseudo-stem. Out of these, seven metabolites identified as amino acids showed a higher accumulation in both the tissues when compared with the same tissues in control treatment. The eighth metabolite, *o*-phosphocoline however, showed a higher accumulation in the pseudo-stem but a decline in accumulation in the leaves (Fig 3.13) (for full list see Appendix 11).

Metabolites which declined in response to the –S treatment in all the tissues included the N and S containing flavour precursors namely; 1-PRENCSO, MCSO, γ-Glu-PRENCSO, cycloalliin, 2-CPGTH and another non flavour associated metabolite $_{DL}$-Pipecolinic acid (Fig 3.13).

3.6.1 Table 3.2 A list of compounds included in the widely-targeted metabolome of *A. cepa* along with the KEGG IDs (Kyoto Encyclopedia of Genes and Genomes) for the compounds (http://www.genome.jp/kegg/).

	Name	KEGG ID		Name	KEGG ID
#1	1-Amino-1-cyclopentanecarboxylic acid	C03969	**#57**	Carbamoyl-D_L-aspartic acid	C00438
#2	4-Hydroxyphenylpyruvic acid	C01179	**#58**	5´-Deoxy-5´-Methylthioadenosine	C00170
#3	(-)-Norepinephrine	C00547	**#59**	sn-Glycero-3-phosphocholine	C00670
#4	1,1-Dimethylbiguanide hydrochloride	C07151	**#60**	$_L$-allo-threonine	C05519
#5	1-Aminocyclopropane-1-carboxylic acid	C01234	**#61**	5-Aminovaleric acid	C00431
#6	Adenine	C00147	**#62**	3-Hydroxypyridine	
#7	Adenosine	C00212	**#63**	$_L$-Threonic acid hemicalcium salt	C01620
#8	Allantoic acid	C00499	**#64**	luteolin-4'-O-glucoside	
#9	$_L$-Histidine	C00135	**#65**	Spiraeoside	
#10	$_L$-Methionine	C00073	**#66**	S-(5´-Adenosyl)-$_L$-methionine chloride	C00019
#11	$_L$-(-)-Phenylalanine	C00079	**#67**	alpha-Methyl-D_L-histidine	
#12	$_L$-Tryptophane	C00078	**#68**	$_L$-Anserine nitrate salt	C01262
#13	$_L$-Tyrosine	C00082	**#69**	o-Phosphocholine	C00588
#14	Sucrose	C00089	**#70**	Trigonelline hydrochloride	C01004
#15	Pyridoxamine dihydrochloride	C00534	**#71**	mucic acid	C00879
#16	Adenosine-5´-monophosphate sodium	C00020	**#72**	$_{DL}$-Pipecolinic acid	C00408
#17	$_D$-Glucosamine-6-phosphate sodium	C00352	**#73**	$_D$-(+)-Raffinose pentahydrate	C00492
#18	2'-Deoxyadenosine monohydrate	C00559	**#74**	$_{DL}$-Glyceric Acid calcium Salt	C00258
#19	Creatine,anhydrous	C00300	**#75**	Petunidin-3-o-beta-glucopyranoside	C12139
#20	Cytidine,cell culture tested	C00475	**#76**	Quercetin-3,4'-o-di-beta-	
#21	$_D$-(-)-Arabinose	C00216	**#77**	$_L$-Leucine	C00123
#22	$_{DL}$-threo-beta-Methylaspartic acid	C03618	**#78**	$_L$-Isoleucine	C00407
#23	Hypotaurine	C00519	**#79**	S-Methylmethionine	
#24	Inosine	C00294	**#80**	Methionine sulfoxide	
#25	$_L$-Asparagine		**#81**	quercetin-3-o-beta-glucopyranoside	C10073
#26	$_L$-Aspartic acid		**#82**	Sodium pantothenate	C00864
#27	$_L$-Glutamic acid		**#83**	alpha-$_D$-Galactose-1-phosphate	C00103
#28	$_L$-Glutamine		**#84**	$_D$-Mannose-6-phosphate	C00275
#29	$_L$-Glutathione (reduced form)	C00051	**#85**	$_D$-Fructose-6-phosphate	C00636
#30	$_L$-Methionine sulfone		**#86**	$_D$(+)-Galactosamine hydrochloride	C02262
#31	$_L$-Ornithine monohydrochloride	C00077	**#87**	$_D$-(+)-Cellobiose_Lactulose	C07064
#32	$_L$-Proline	C00148	**#88**	Melibiose hydrate	C05402
#33	$_L$-Pyroglutamic acid	C01879	**#89**	Cytidine-5´-monophosphate	C00055
#34	$_L$-Serine	C00065	**#90**	$_L$-Iditol	C00392
#35	1-Methylguanidine hydrochloride	C02294	**#91**	$_L$(+)-Arginine	C00062
#36	Pyridoxine	C00314	**#92**	sn-Glycerol 3-phosphoate	C00093
#37	Quisqualic acid	C08296	**#93**	$_D$-(-)-Fructose	C06468
#38	Tyramine	C00483	**#94**	Histamine	C00388
#39	3-Guanidinopropionic acid	C03065	**#95**	Nicotinamide	C00153
#40	beta-Nicotinamide mononucleotide	C00455	**#96**	$_L$-Alanine	C00041
#41	γ-Amino-n-butyric acid	C00334	**#97**	$_L$-Valine	C01826
#42	isorhamnetin-3-o-glucoside		**#98**	$_L$-threonine	C00188
#43	kaempferol-3-o-glucoside	C12249	**#99**	$_L$-2-Aminobutyric acid	C01026
#44	Hyperoside	C10073	**#100**	$_{DL}$-Malic acid	C00497
#45	urocanic acid	C00785	**#101**	$_D$-Xylulose	C00310
#46	N-acetylneuraminic acid	C00270	**#102**	$_L$-Carnitine	C00318
#47	$_N$-acetyl-$_D$-mannosamine	C00645	**#103**	$_{DL}$-2-Aminoadipic Acid	C00956
#48	o-acetyl-$_L$-serine hydrochloride	C00979	**#104**	$_L$-Lysine	C00047
#49	$_L$-saccharopine	C00449	**#105**	$_D$-Alloisoleucine	C01933
#50	$_D$-(+)-Arabitol	C01904	**#106**	$_D$-Melezitose monohydrate	C03661
#51	Maltitol	D04845	**#107**	γ-Glu-PRENCSO	
#52	$_{DL}$-Glyceraldehyde 3-phosphate solution	C00118	**#108**	2-CPGTH	
#53	$_L$-beta-homoglutamine-HCl		**#109**	cycloalliin	
#54	$_L$-beta-homolysine-2HCl		**#110**	PRENCSO	
#55	$_L$-beta-homothreonine		**#111**	MCSO	
#56	o-Acetyl-$_L$-homoserine hydrochloride	C01077	**#112**	alliin	

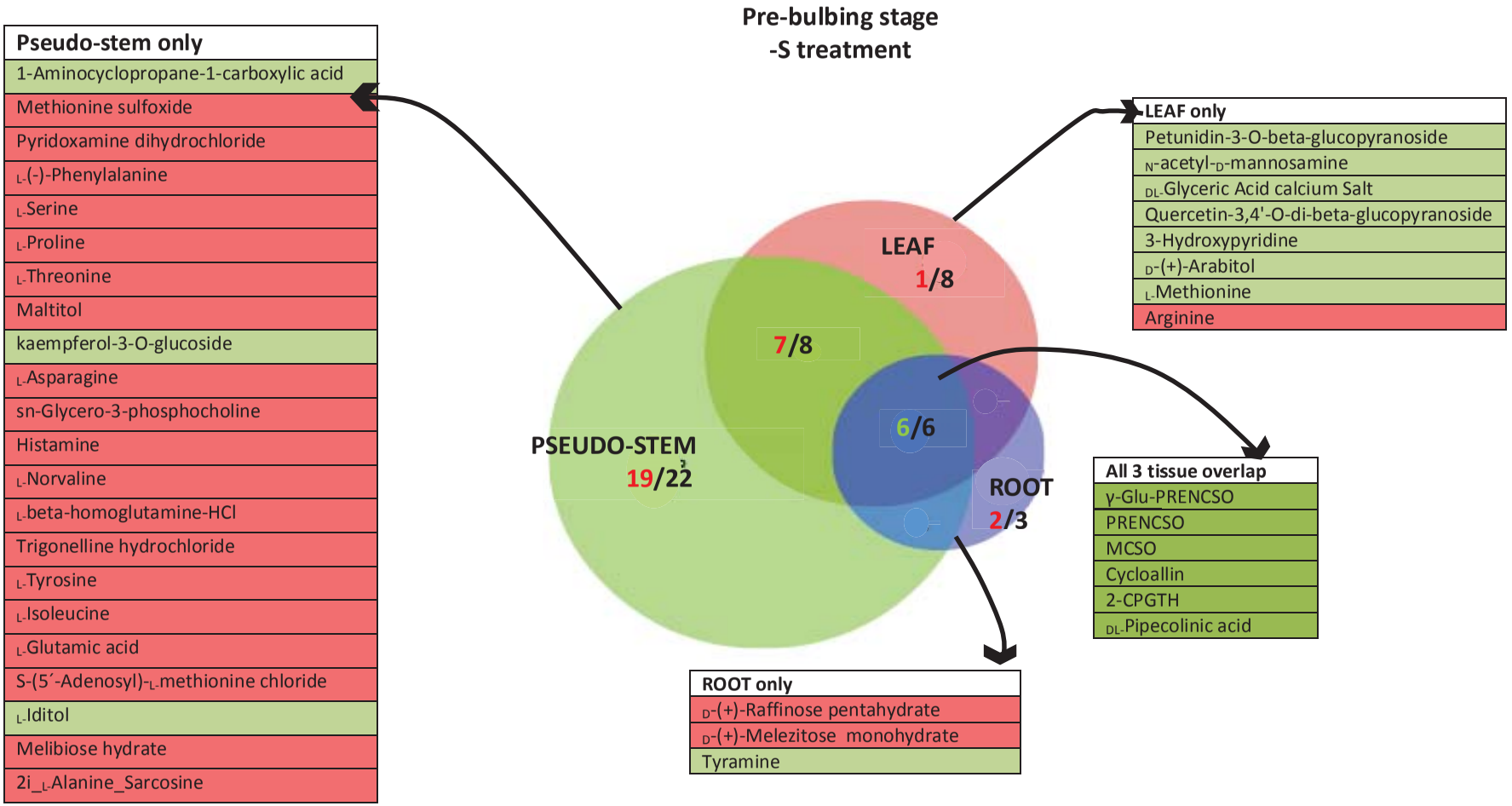

Figure 3.13 Venn- diagram showing significantly (p<0.05) differing metabolites in different tissues in comparison to the control treatment. The overlapping regions show metabolites which differ significantly (p<0,05) in more than one tissue. Red numbers indicate the number of metabolites showing higher accumulation and green numbers indicate a decline in accumulation of metabolites, out of the total number of metabolites (in black) changing in that tissue or overlap region. In the columns, metabolites highlighted in green indicate significant (p<0.05) decline in accumulation and metabolites highlighted in red indicate significant (p<0.05) rise in accumulation.

3.6.1.1 Changes in the targeted metabolome of plants harvested from the–S treatment at bulbing

In the leaf tissue harvested from plants at the bulbing stage grown in the –S media, a total of 54 metabolites differed significantly ($p<0.05$), 39 of which showed an exclusive response only in the leaf tissue (no overlap with any other tissue). All 39 metabolites showed a decline in accumulation and 36 out of these were N-containing amino acids and derivatives (Fig 3.14) (For full list see Appendix 11).

In the bulbs, a total of 17 out of 112 targeted metabolites differed significantly ($p<0.05$), out of which five differed exclusively in the bulbs namely; malic acid, histamine, glucosamine-6-phosphate, hyperoside and quercetin-3,4'-*o*-di-beta-glucopyranoside. Other than histamine, which accumulated in the bulb, all other four metabolites showed a decline in accumulation (Fig 3.14).

In the roots, a total of twelve out of 112 targeted metabolites differed significantly ($p<0.05$) compared to roots from plants of same age under the control treatment. Four of these showed the exclusive response under the –S treatment, only in the roots tissue and all four showed a higher accumulation under the –S treatment (Fig 3.14).

Metabolites responding in both leaf and bulb tissue showed contrasting responses, and comprised exclusively of amino acids. All seven metabolites, common to both the tissues as well as containing N, showed a decline in leaf tissue whereas theses accumulated in the bulb under the –S treatment (Fig 3.14).

In common with the pre-bulbing plants grown under –S treatment, metabolites responding to –S treatment in all tissues at bulbing were the S and N-containing flavour compounds namely γ-Glu-PRENCSO, PRENCSO, cycloalliin and 2-CPGTH (Fig 3.14).

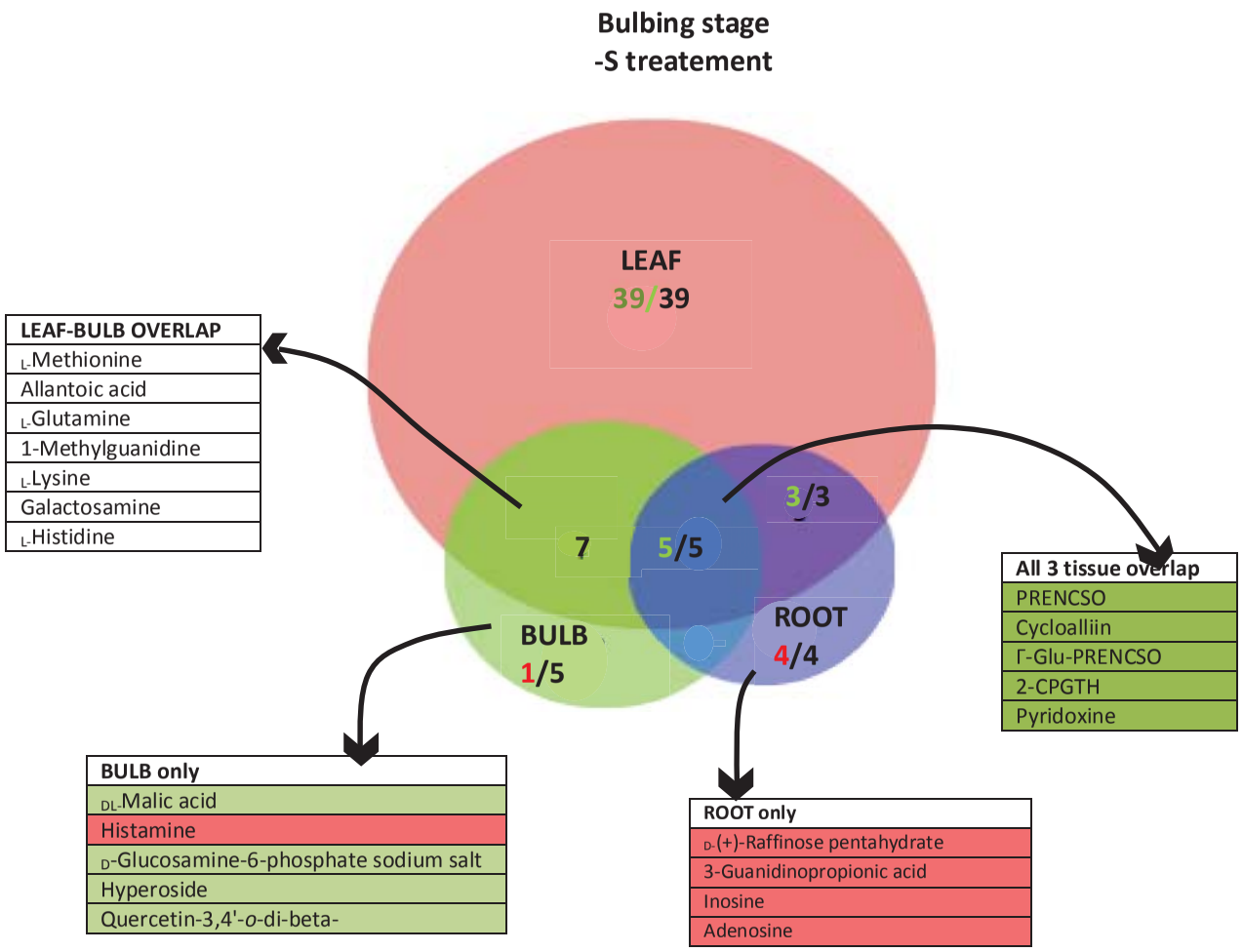

Figure 3.14 Venn- diagram showing significantly (p<0.05) differing metabolites in different tissues in comparison to respective tissues under the control treatment The overlapping regions show metabolites which differ significantly (p<0,05) in more than one tissue. Red numbers indicate the number of metabolites showing higher accumulation and green numbers indicate a decline in accumulation of metabolites, out of the total number of metabolites (in black) changing in that tissue or overlap region. In the columns, metabolites highlighted in green indicate significant (p<0.05) decline in accumulation and metabolites highlighted in red indicate significant (p<0.05) rise in accumulation. The metabolites highlighted in white indicate accumulation in one tissue and decline in the other tissue for the overlap region.

3.6.1.2 Changes in the targeted metabolome of plants harvested from the –N treatment at the pre-bulbing stage

In the leaf tissue, a total of 83 metabolites responded to treatment with significant ($p<0.05$) differences, out of which only eight differed exclusively in the leaves. All of the eight metabolites were N-containing compounds and six showed a decline in accumulation. Two amino acids, $_{N}$-acetyl-$_{D}$-mannosamine which is required to make sialic acids, and quisqualic acid which is a neuroexitator, accumulated under the -N treatment (Fig 3.15).

In the pseudo-stems, a total of 85 out of 112 targeted metabolites differed significantly ($p<0.05$), and ten of these responded exclusively in the pseudo-stem. Out of these, the six N-containing metabolites showed a decline in accumulation, whereas the other four metabolites, all flavonol glucosides, accumulated under the –N treatment (Fig 3.15).

In the roots, a total of 76 out of 112 targeted metabolites differed significantly ($p<0.05$) and three of these showed a decline in accumulation. However, the other four metabolites showed a higher accumulation and were all N-containing compounds namely; galactosamine hydrochloride, beta-nicotinamide mononucleotide, pipecolinic acid and aminoadipic acid (Fig 3.15).

A total of 12 metabolites fluctuated significantly ($p<0.05$) in both leaves and pseudo-stem under the –N treatment. Out of these, three were flavonol-glucosides which showed a higher accumulation in both the tissues. The other nine metabolites showed a decline in accumulation in both the tissues, and eight of these were N-containing compounds (Fig 3.15) (for full list see Appendix 11).

A total of six metabolites fluctuated significantly ($p<0.05$) in both leaves and roots and except for malic acid, which declined in the leaves but accumulated in the roots, the other five metabolites showed a higher accumulation in both the tissues (Fig 3.15) (for full list see Appendix 11).

A total of six metabolites showed significantly ($p<0.05$) differing accumulation in both pseudo-stem and root and five of these showed a higher accumulation. However, allantoic acid accumulated only in the roots and showed a decline in accumulation in the leaves and the pseudo-stem (Fig 3.15) (for full list see Appendix 11).

A much higher number of metabolites, (a total of 57), fluctuated in all the tissues in response to the –N treatment, out of which 10 accumulated in all the tissues under –N treatment. Of these, six were sugars and two were sugar alcohols. Hypotaurine and asparagine were the only N-containing compounds which accumulated in all tissues under the –N treatment at the pre-bulbing stage (Fig 3.15) (for full list see Appendix 11).

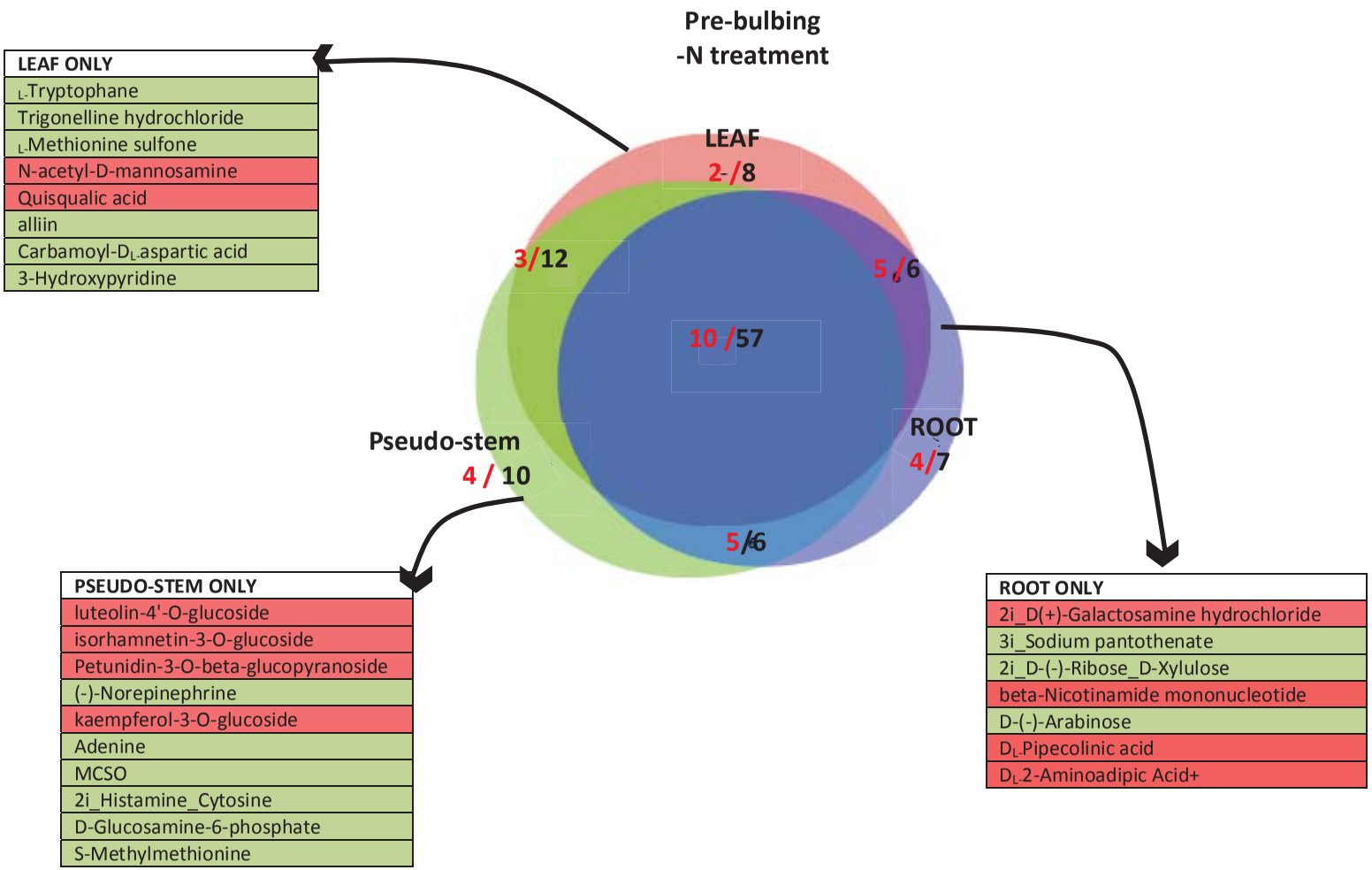

Figure 3.15 Venn- diagram showing significantly (p<0.05) differing metabolites in different tissues in comparison to respective tissues under the control treatment. The overlapping regions show metabolites which differ significantly (p<0,05) in more than one tissue. Red numbers indicate the number of metabolites showing higher accumulation and green numbers indicate a decline in accumulation of metabolites, out of the total number of metabolites (in black) changing in that tissue or overlap region. In the columns, metabolites highlighted in green indicate significant (p<0.05) decline in accumulation and metabolites highlighted in red indicate significant (p<0.05) rise in accumulation.

3.6.1.3 Changes in the targeted metabolome of plants harvested from the –N treatment at bulbing stage

In the leaf tissue, a total of 91 out of 112 targeted metabolites differed significantly ($p<0.05$). Out of these, four differed exclusively in the leaves and in no other. All four were N-containing compounds out of which 3-hydroxypyrisine, 5-aminovaleric acid and 3-guanidinopropinoic acid declined significantly ($p<0.05$) but N-acetyl-mannosamine showed a higher accumulation, in common with the pre-bulbing leaves under the –N treatment (Fig 3.16).

In the bulbs, a total of 87 metabolites were found to differ significantly ($p<0.05$) when compared with the control treatment, and five of these differed exclusively in the bulbs. Out of these, four metabolites, all flavonol glucosides, showed a decline in accumulation whereas glycerol-3-phosphate accumulated in the bulbs under the –N treatment (Fig 3.16).

Out of the 79 significantly ($p<0.05$) differing metabolites in the roots from plants grown under –N treatment and harvested at the bulbing stage, seven fluctuated exclusively in the roots (Fig 3.16). Three out of these, threonic acid, hypotaurine and glyceraldehyde-3-phosphate showed a higher accumulation whereas *o*-acetyl-homoserine, creatine, adenine and kaempferol-3-*o*-glucoside declined in accumulation (Fig 3.16).

A total of 22 metabolites differed in both leaf and bulb tissue, all of which showed a decline in accumulation in both the tissues. Apart from malic acid and petunidin-3-*o*-beta-glucopyranoside, other differing metabolites were all N-containing compounds (Fig 3.16) (for full list see Appendix 11).

Of the metabolites that differed significantly ($p<0.05$) in both bulb and root, all showed a higher accumulation in both the tissues and consisted of sugars and sugar alcohols namely; melibiose hydrate, cellobiose, sucrose, maltitol and iditol (Fig 3.16) (for full list see Appendix 11).

A total of 57 metabolites responded in all tissues under the –N treatment at the bulbing stage when compared to plants at the same developmental stage grown under the control treatment. Only four of these, arabitol, raffinose pentahydrate, fructose and melezitose showed a higher accumulation in all tissues. Ribose and arabinose accumulated only in the leaf tissue and declined in the bulb and the roots whereas 2-alpha-$_{D}$-galactose-1-phosphate, 4-$_{D}$-fructose-6-phosphate and *o*-phosphocholine accumulated only in the roots and declined

in other tissues when compared with the respective tissues of same age grown under the control treatment (Fig 3.16) (for full list see Appendix 11).

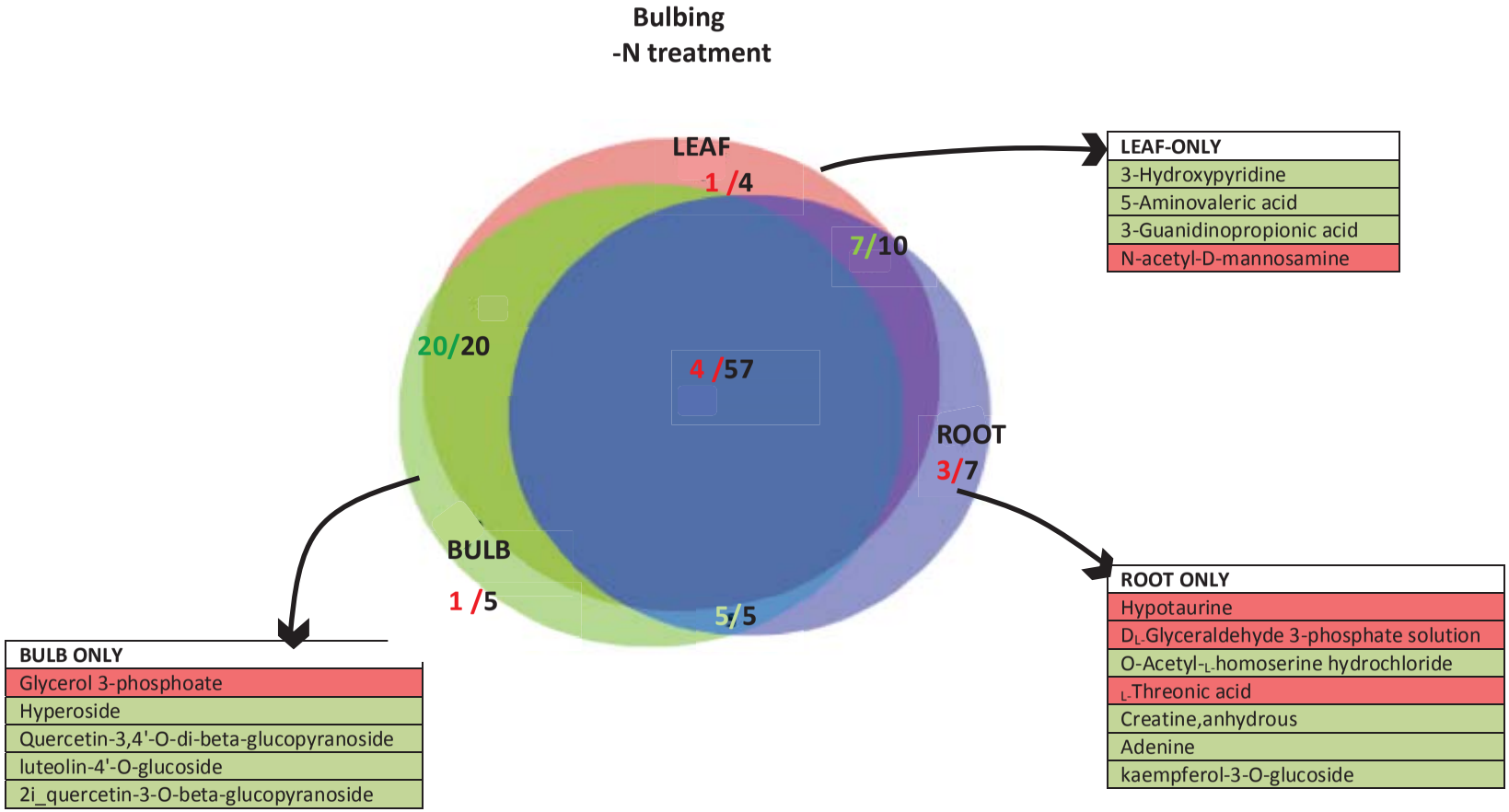

Figure 3.16 Venn- diagram showing significantly ($p<0.05$) differing metabolites in different tissues in comparison to respective tissues under the control treatment. The overlapping regions show metabolites which differ significantly ($p<0.05$) in more than one tissue. Red numbers indicate the number of metabolites showing higher accumulation and green numbers indicate a decline in accumulation of metabolites, out of the total number of metabolites (in black) changing in that tissue or overlap region. In the columns, metabolites highlighted in green indicate significant ($p<0.05$) decline in accumulation and metabolites highlighted in red indicate significant ($p<0.05$) rise in accumulation.

3.6.1.4 Changes in the targeted metabolome of plants harvested from the –S-N treatment at pre bulbing

In the leaf tissue, a total of 72 out of 112 targeted metabolites differed significantly ($p<0.05$). Out of the 72, nine metabolites responded exclusively in the leaves of which only two metabolites, N-acetyl-mannosamine and iditol showed a higher accumulation and the other seven declined when compared with leaves of same aged plants grown under the control treatment (Fig 3.17).

In the pseudo-stem, a total of 81 metabolites were found to differ significantly ($p<0.05$) when compared with the same aged plants grown under the control treatment. Out of these, nine metabolites responded exclusively in the pseudo-stem only, eight of which were N-containing compounds, and all declined in accumulation. In contrast, petunidin-3-o-beta-glucopyranoside showed a higher accumulation in the pseudo-stems under the –S-N treatment when compared with the control treatment (Fig 3.17).

In the roots, a total of 72 metabolites were found to differ significantly ($p<0.05$) when compared with the control treatment. Six out of the 72 differing metabolites, fluctuated exclusively in the roots. Out of these, $_{L}$-tyrosine, ribose and sodium pantothenate showed a decline in accumulation whereas 2-alpha-$_{D}$-galactose-$_{1}$-phosphate, galactosamine hydrochloride and carnitine increased in accumulation when compared with the roots from plants grown under the control treatment (Fig 3.17).

A total of 11 metabolites differed in both leaf and pseudo-stem tissues, out of which the five N-containing compounds showed decline in accumulation, whereas eight showed higher accumulation. Of the higher accumulating metabolites, seven were flavonol glucosides. (For full list see Appendix 11)

A total of five metabolites were common to both leaf and root, out of which trigonelline hydrochloride and methionine sulfoxide showed a decline in accumulation in both tissues and mannose-6-phosphate and fructose-6-phosphate increased in accumulation. In contrast, malic acid showed a decline in the leaves but accumulated in the roots (Fig 3.17) (For full list see Appendix 11).

A total of 14 metabolites responded to the –S-N treatment in both the pseudo-stem and root tissues investigated. Out of these maltitol, cellibiose, melibiose, sucrose and beta-nicotinamide mononucleotide accumulated in all tissues, whereas ornithine

monohydrochloride, arginine, cytidine-5´-monophosphate, leucine, serine, methionine and arabinose showed a decline in accumulation. In contrast, allantoic acid and asparagine declined in the leaves but accumulated in the roots (For full list see Appendix 11).

A total of 47 of the significantly ($p<0.05$) differing metabolites responded in all the tissues investigated, out of which 37 (all N-containing compounds) showed a decline in accumulation in all of the tissues. Hypotaurine and pipecolinic acid were the two N-containing compounds which accumulated in all the tissues in plants grown under the –S-N treatment at the bulbing stage. However, *o*-phosphocholine showed differential accumulation with a decline in the leaves, but accumulation in the pseudo-stem and the root tissue (Fig 3.17) (For full list see Appendix 11).

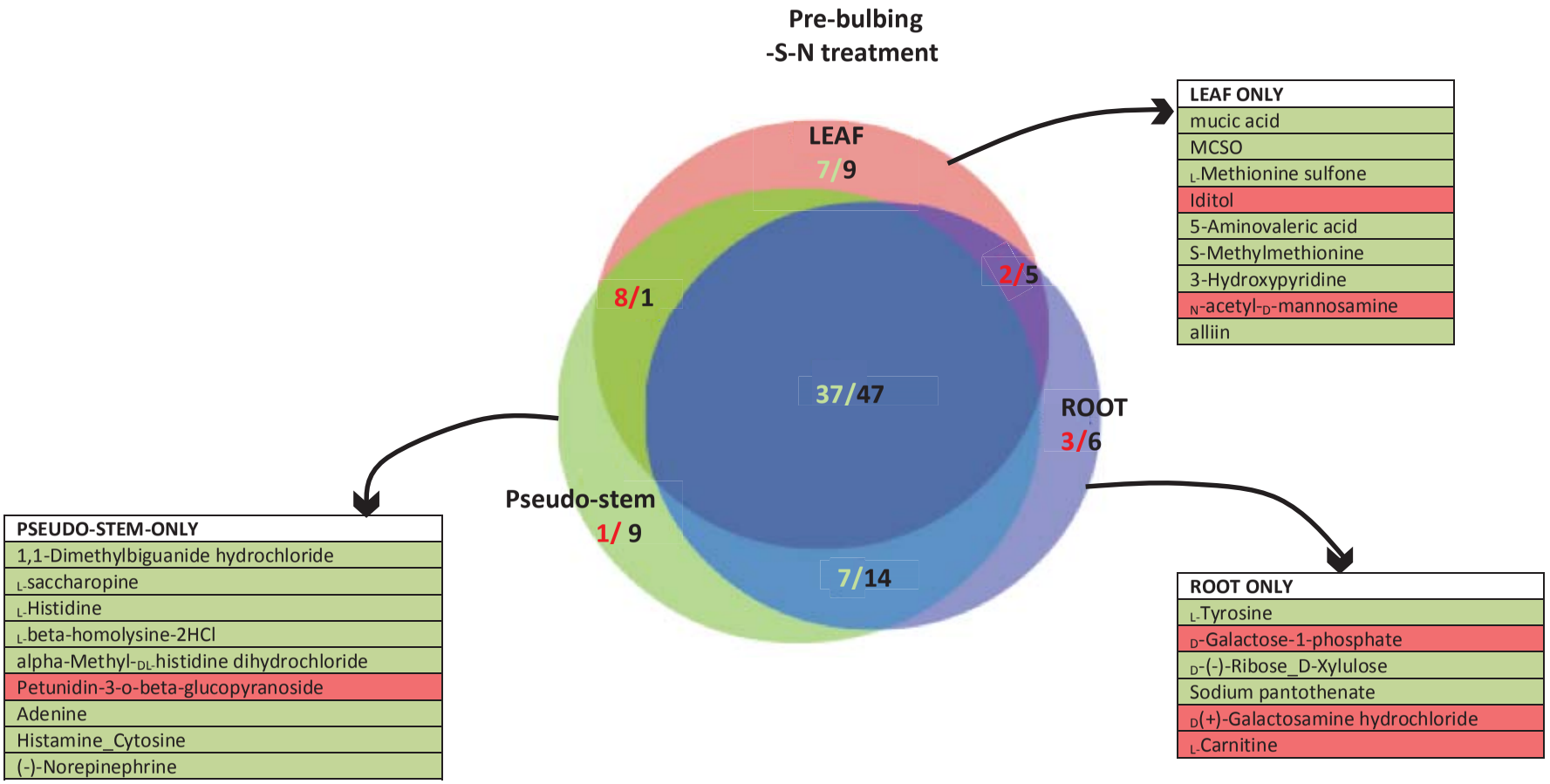

Figure 3.17 Venn- diagram showing significantly (p<0.05) differing metabolites in different tissues in comparison to respective tissues under the control treatment. The overlapping regions show metabolites which differ significantly (p<0.05) in more than one tissue. Red numbers indicate the number of metabolites showing higher accumulation and green numbers indicate a decline in accumulation of metabolites, out of the total number of metabolites (in black) changing in that tissue or overlap region. In the columns, metabolites highlighted in green indicate significant (p<0.05) decline in accumulation and metabolites highlighted in red indicate significant (p<0.05) rise in accumulation.

3.6.1.5 Changes in the targeted metabolome of plants harvested from the –S-N treatment at bulbing stage

In the leaf tissue, a total of 89 out of 112 targeted metabolites differed significantly ($p<0.05$) when compared with leaves from plants grown under the control treatment. Out of the 89, six metabolites responded exclusively in the leaf tissue only, where three showed a higher accumulation and three declined. N-acetyl mannosamine, a N-containing amine was the only N-containing metabolite which showed accumulation under the –S-N treatment exclusively in the leaves (Fig 3.18).

Out of the 86 significantly ($p<0.05$) differing metabolites identified when the bulbs were compared with the control treatment, only glycerol-3-phosphate accumulated exclusively in the bulbs (Fig 3.18).

In the roots, a total of 80 metabolites were found to differ significantly ($p<0.05$) when compared to roots from plants grown under the control treatment, and 6 out of the 80 responded exclusively in the roots. Theronic acid and β-nicotinamide-mononucleotide were among the two accumulating metabolites whereas *O*-acetyl-homoserine, kaempherol-3-*o*-glucoside, isorhamnetin-3-*o*-glucoside and adenine were among the significantly ($p<0.05$) declining metabolites in the roots from plants grown under the –S-N treatment at the bulbing stage (Fig 3.18).

A total of 20 metabolites differed in leaf as well as bulb tissue and all 20 declined in accumulation in both tissues. With the exception of malic acid, all other metabolites differing in both leaf and bulb tissues were N-containing compounds (Fig 3.18) (for full list see Appendix 11).

A total of nine metabolites differed in both leaf and root tissues and seven of these (all N-containing compounds) showed a decline in accumulation. Hypotaurine, an N-containing amino acid and glyceraldehyde-3-phosphate accumulated in leaf and root under the –S-N treatment at the bulbing stage (Fig 3.18) (for full list see Appendix 11).

A total of eleven metabolites differed significantly ($p<0.05$) in both bulb and root when compared with plants grown under the control treatment at the bulbing stage. Seven out of these declined in both the tissues. These were sugars namely melibiose hydrate, cellobiose and sucrose, flavonol glucosides such as hyperoside, quercetin-3-4'-*o*-di-β-glucopyranoside and petunidin-3-*o*-β-glucopyranoside and the N-containing metabolite trigonelline

hydrochloride. However, *o*-phosphocholine, fructose-6-phosphate and mannose-6-phosphate showed a differing accumulation pattern with a decline in the bulb tissue but accumulation in the roots in plants grown under the –S-N treatment at the bulbing stage (Fig 3.18) (for full list see Appendix 11).

A total of 54 metabolites showed fluctuation in all the three tissues, of which 46 were N-containing compounds and all declined in accumulation in all the tissues. Three sugars, fructose, raffinose pentahydrate and melezitose were among the metabolites which accumulated in all tissues under the –S-N treatement at the bulbing stage. Arabinose and ribose accumulated in the leaves, but showed a decline in accumulation in the bulb and the roots whereas galactose-1-phosphate accumulated in the roots only and declined in the leaves and the bulb tissues in the –S-N treated plants when compared to the control treatment. (Fig 3.18) (for full list see Appendix 11).

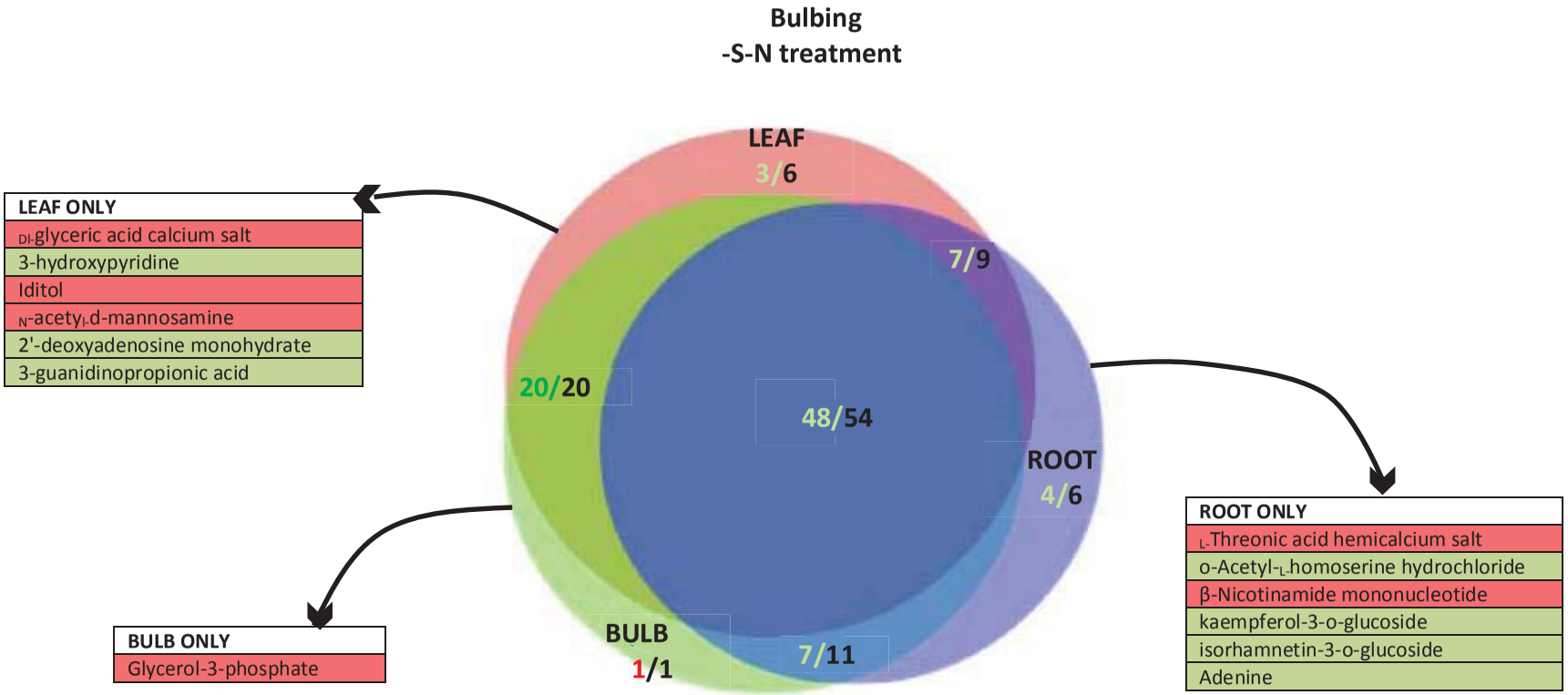

Figure 3.18 Venn- diagram showing significantly (p<0.05) differing metabolites in different tissues in comparison to respective tissues under the control treatment. The overlapping regions show metabolites which differ significantly (p<0,05) in more than one tissue. Red numbers indicate the number of metabolites showing higher accumulation and green numbers indicate a decline in accumulation of metabolites, out of the total number of metabolites (in black) changing in that tissue or overlap region. In the columns, metabolites highlighted in green indicate significant (p<0.05) decline in accumulation and metabolites highlighted in red indicate significant (p<0.05) rise in accumulation.

3.6.2 Changes in the accumulation of key S and N metabolites involved in the S-assimilation pathway in plants grown under the S and/or N treatments.

From the targeted metabolome, changes in accumulation of certain key metabolites involved in the S and N assimilation pathway in response to treatment were highlighted to better elucidate the interdependency of S assimilation pathway on N supply. These included serine which is a precursor amino-acid for cysteine and is metabolized to *o*-acetyl-$_L$-serine by the action of serine acetyltransferase. *o*-acetyl-$_L$-serine provides the carbon backbone which together with sulfide form cysteine (section 1.4.2.4). As *o*-acetyl-$_L$-serine is an N containing metabolite and immediate pre-cursor to cysteine, changes in its accumulation in response to S and/or N depletion might be indicative of the interdependency between the two assimilation pathways. Both glutathione and methionine are made downstream of cysteine and contain both S and N as a component (Figure 3.3).

3.6.2.1 Accumulation of Serine

There was generally no significant ($p>0.05$) change in accumulation of serine in any of the tissues at both, the pre-bulbing as well as the bulbing stage in plants grown under the –S treatment. The exception was in the pre-bulbing pseudo-stem where serine showed a slight but significantly ($p<0.05$) higher accumulation when compared with pseudo-stem of pre-bulbing plants grown under the control treatment.

In plants grown under the –N treatment, serine declined significantly ($p<0.05$) both at the pre-bulbing stage and the bulbing stage in all the tissues. This pattern of decline in accumulation was similar under the –S-N treatment, except for the leaf tissue at pre-bulbing which did not show any significant ($p>0.05$) difference when compared to plants grown under the control treatment (Fig 3.19).

3.6.2.2 Accumulation of *o*-acetyl-$_L$-serine (*O*AS)

In the pre-bulbing stage, there was no change in accumulation of *O*AS under the -S treatment in leaf tissue

. However, in plants grown under the –N treatment, *O*AS declined significantly ($p<0.05$) in all the tissues at both the pre-bulbing and the bulbing stage. There was a similar pattern of decline in all tissues under the –S-N treatment, except in bulbs at the bulbing stage which did not show any significant ($p>0.05$) change in accumulation when compared to bulbs from plants grown under the control treatment (Fig 3.19).

3.6.2.3 Accumulation of reduced Glutathione (GSH)

In plants grown under the –S treatment, there was no change in accumulation of glutathione in any of the tissues examined at the pre-bulbing stage. However at the bulbing stage, only the leaf tissue showed a significant ($p<0.05$) decline in accumulation. Under the –N and the –S-N treatments, glutathione declined significantly ($p<0.05$) in leaf tissue as well as pseudo-stem/bulb for both the pre-bulbing as well as the bulbing stage. In contrast to this, the roots did not show any change in the accumulation of GSH under any treatment (Fig 3.19).

3.6.2.4 Accumulation of methionine

In the plants grown under the –S treatment and harvested at the pre-bulbing stage, methionine declined significantly ($p<0.05$) in the leaf tissue but not in the pseudo-stem and in the roots. However, this pattern changed in plants harvested at bulbing, where methionine declined significantly ($p<0.05$) in both leaves and bulbs, but again did not change in the roots (Fig 3.19).

In plants grown under the –N treatment, methionine declined significantly ($p<0.05$) in all of the tissues examined at both the pre-bulbing and the bulbing stage. This pattern of decline in accumulation was similar in plants grown under the –S-N treatment, except for the leaves in plants at the pre-bulbing stage, where there was no change in accumulation (Fig 3.19).

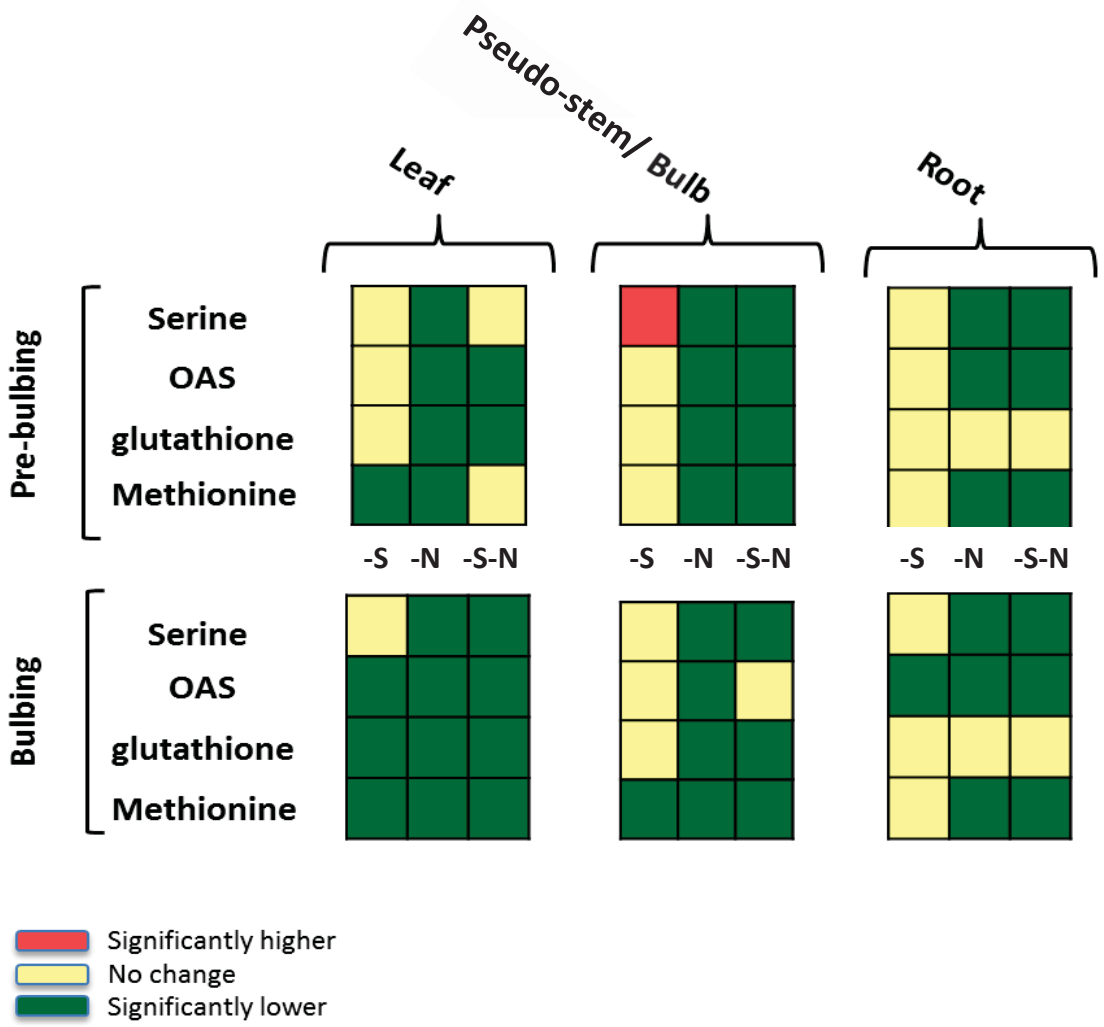

Figure 3.19 Heat-map showing changes in selected S and N metabolites involved in the S-assimilation pathway in different tissues under varying S and N treatments when compared with respective tissues of plants grown under the control treatment. Significant differences were calculated using Student's *t test* with p value threshold of 0.05. Each treatment consisted of six biological replicates (n=6) where each biological replicate comprises of six individual plant tissues pooled together.

3.7 Discussion

The primary objective of this thesis was to examine the long term effects of S depletion on the N-assimilation pathway in *A. cepa* and *vice versa*. A second aim was to investigate the possibility of enzyme redundancy and protein-protein interactions, between the two similar S and N pathway enzymes, sulfite reductase and nitrite reductase as a possible, yet un-reported, point of cross-talk between the two assimilation pathways.

To achieve the primary objective, *A. cepa* (genotype CUDH2107) was grown in a factorial experiment with four different treatments, the control, -S, -N and the –S-N regime (Section 2.1.2). Tissues were harvested at the pre-bulbing and the bulbing stage as leaves, pseudo-stem/bulb (as appropriate) and the root and subsequently used to investigate the effect of each treatment on the transcription of key S and N assimilation genes (Fig 3.3-3.10), as well as the accumulation and activity of specific enzymes (chapter 4). The accumulation of primary metabolites, including a range of N- and S-containing compounds was also measured (Fig 3.11-3.19).

3.7.1 Physiological response of *A. cepa* to long-term SO_4^{2-} and/or NO_3^- depletion

The biomass measurements of plants showed a trend towards a higher total biomass (Fresh weight) under the –S treatment especially during the bulbing stage, when compared to control plants (Fig 3.2 A and D). Further, fresh weight measurements of root and shoot tissues taken separately indicated that this increased total biomass is due to a significantly ($p<0.01$) higher root biomass (Fig 3.2 B and E) suggesting changes in root architecture in response to S depletion. An increase in root biomass under S depletion at the pre-bulbing stage has been previously shown for a low pungency genotype “Texas Grano 348” by McCallum et all. (2011).

A generic response to S starvation in plants is altered root system architecture leading to increased lateral root growth as observed in *Arabidopsis* plants under sulfate deprivation, which has been linked to increase in auxin concentration in the roots *via* increased NITRILASE3 activity (López-Bucio et al., 2003). Although changes in the root system architecture were not looked at in this study, similar changes in root system architecture

have been reported in *A. cepa* previously (Thomas, 2008). It may be, therefore, that the adaptation to depleted external S may also be modulated through changes in local auxin synthesis in *A. cepa,* but this is only speculative as NITRILASE3 activity has not been measured.

In contrast to the –S treatment, a 30% decrease in total biomass in plants harvested at pre-bulbing and a 35% decrease was observed in plants harvested at bulbing stage in response to the –N treatment. This could be attributed entirely to a decrease in shoot biomass (Fig 3.2 B and E), (Fig 3.2 A and D) indicating that the limited N availability to the shoots led to restricted amino acid synthesis and incorporation into proteins. In turn this can lead to a C:N imbalance, restricted metabolic capacity and ultimately reduced growth and biomass (Hermans et al., 2006). Although root morphology was not investigated in this study, it is possible that NO_3^- depletion also led to changes in root system architecture as there was no change in the total root biomass under the –N treatment, but shoot biomass declined indicating a preferential growth of roots over shoots. The contrasting nutrient specific response of the root system architecture can be explained by the effect of NO_3^- availability on lateral and seminal root growth which has been studied in barley (Drew, 1975; Drew & Saker, 1978) and the primary root in *Arabidopsis* (Linkohr et al., 2002). Unlike the root growth response to S depletion, where lateral root growth is induced, N depletion, especially in the form of reduced NO_3^-, leads to an increase in primary root length and decrease in lateral root growth in *Arabidopsis* (Sun et al., 2014). This response is specific to the availability of NO_3^- as the nitrogen source, as the nutrient acts as a signal down-regulating *Arabidopsis nitrate regulated1* (*ANR1*), a MADS-box transcription factor which positively regulates lateral root formation (López-Bucio et al., 2003; Bao et al., 2011; Gan et al., 2012).

The physiological responses observed are a manifestation of the changes in transcription and the metabolome of the plant and hence can be better understood by linking the changes in the biomass to the metabolite accumulation. In this study, long term NO_3^- depletion, led to changes in the accumulation of organic acid in plants (Fig 3.15) (Fig 3.16). Malic acid, an important Krebs cycle intermediate accumulated exclusively in the roots at the pre-bulbing stage, but remained at a level similar to that in roots of control plants upon bulbing. Other organic acids such as aminoadipic acid, allantoic acid, threonic acid and pipecolinic acid also accumulated in the roots (Appendix 11). This tissue specific accumulation of these organic acids could be a part of the metabolic changes triggered to cope with sustained NO_3^- depletion. External malate application has been shown to induce

nitrate uptake in barley seedlings (Chantarotwong et al., 1976) and phloem translocated malate has been shown to induce NO_3^- uptake in intact soyabean plants (Touraine et al., 1992). In keeping with this, *nitrate reductase (NR)* mutants of tobacco, with a high nitrate accumulation, have also been shown to accumulate organic acids and Krebs cycle metabolites (Scheible et al., 1997). Predictably, in this thesis, *AcNR1* as well as *AcNiR1* transcript levels were drastically reduced under the –N and the –S-N treatments further suggesting that this pattern of down-regulation of *NR* transcripts, subsequently leading to organic acid accumulation in the roots, reflects remobilization in primary metabolite accumulation to promote root growth and maximize NO_3^- uptake under sustained NO_3^- depletion (Fig 3.7 E, F).

3.7.2 Decreased sensitivity of *A. cepa* plants to SO_4^{2-} depletion under limiting NO_3^- conditions

To understand the molecular basis of the morphological responses seen in the plants under the various treatments, changes in the relative transcript abundance of genes involved in the S and N-assimilation pathways in response to the N and S treatments were investigated using qRT-PCR.

As summarised in the figure below (Fig 3.20), under sustained SO_4^{2-} depletion, at the pre-bulbing stage, both root and the shoot tissue exhibited significantly ($p<0.05$) increased relative transcript abundance of *AcHAST1;1LIKE1* and *AcAPSR1,* which are generally considered to be S-starvation response marker genes (Hirai et al., 2003; Takahashi et al., 2011). This response was greater in the leaf and root tissue at the bulbing stage (Fig 3.4, 3.6 A, C). Although total S levels could not be determined for the experiment due to limited tissue availability, a downstream effect of S limitation was suggested by the significant decrease in the methionine levels in the leaf tissue, as well as a systemic decline in the accumulation of the major *A. cepa* cysteine sulfoxides and their precursors such as γ-glutamyl-PRENCSO, 2-CPGTH, 1-PRENCSO, and cycloalliin at both the developmental stages (as determined by the widely targeted metabolome analysis; Fig 3.19) (Appendix 11).

The effect of NO_3^- depletion on the S-assimilation pathway was contrastingly different in the roots, where both *AcHAST1;1LIKE1* and *AcAPSR1* had dramatically low relative transcript abundance under the –N treatment, but a higher relative transcript abundance in the shoots in a manner similar to that under the –S treatment. However, unlike the –S

treatment response in the leaf, *AcATPS1, AcSOX1, AcAPSK1* and *AcSiR1* also showed an increase in relative transcript abundance. This was even more striking at the bulbing stage where *AcOASTL2* and *AcOASTL3* also showed an increased relative transcript abundance. This suggests some nutrient specific regulation of the pathway, at least at the transcriptional level (Fig 3.4, 3.6 A, C). The limited relative transcript abundance of *AcHAST1;1LIKE1* in roots, suggested reduced SO_4^{2-} uptake and this was also reflected in the significant ($p<0.05$) reduction of downstream products of the S-assimilation pathway. These included glutathione in the leaf and the bulb tissue, as well as reduction of methionine in leaf, bulb and root tissues at both developmental stages (Fig 3.19).

The hierarchy in response to either SO_4^{2-} or NO_3^- depletion was revealed in plants under the –S-N treatment, where the relative transcript abundance of the S-assimilation pathway genes, *AtHAST1;1LIKE1, AcATPS1, AtAPR1, AcAPSK1, AcSiR1, AvOASTL1, AcOASTLA2* and *AcOASTL3* was similar to that of plants under the –N treatment in both root and leaf tissue, suggesting a decreased sensitivity to limited SO_4^{2-} supply (Fig 3.4 A, C) (Fig 3.6 A, C). Again, the transcriptional response of the S-assimilation pathway correlated well with the metabolome analyses, where the changes in targeted metabolite for plants under the –S-N treatment were similar to that under the –N treatment, rather than those under the –S treatment (Fig 3.15 – 3.18). This was true not only for the accumulation of the direct downstream products of the S-assimilation pathway, such as glutathione and methionine, but also for non S and N containing metabolites such as the sugars, sugar phosphates and sugar alcohols. Flavour and pungency associated precursors such as γ- glutamyl-PRENSCO and 2-CPGTH also showed greater reduction under the –S-N treatment when compared with the –S treatment (Appendix 11, bar plots). As summarized in the PCA for widely targeted metabolites (Fig 3.21), the samples from the –N and the –S-N treatments form tight, overlapping clusters which shift distinctly from the –S and the control treatment along the x- axis (Fig 3.21).

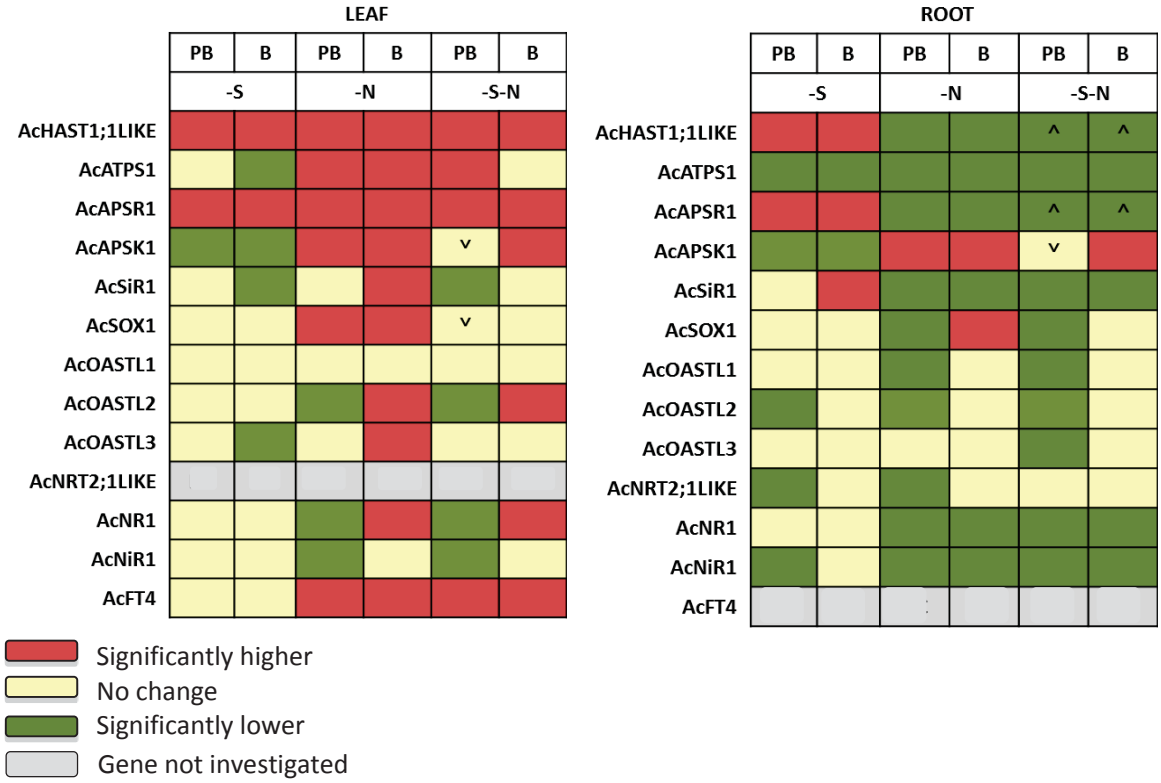

Figure 3.20 Transcriptional response normalized to the control treatment, of S and N assimilation genes investigated in leaf and root tissues at the pre-bulbing (PB) and bulbing (B) stage in response to different treatments (-S, -N, -S-N) (refer colour key for significant differernce). In addition, (^) signifies significant ($p<0.05$) up-regulation compared to the –N treatment and (ˇ) signifies significant ($p<0.05$) down-regulation compared to the –N treatment. Tissue specific genes not investigated in a certain tissue type are indicated by grey boxes.

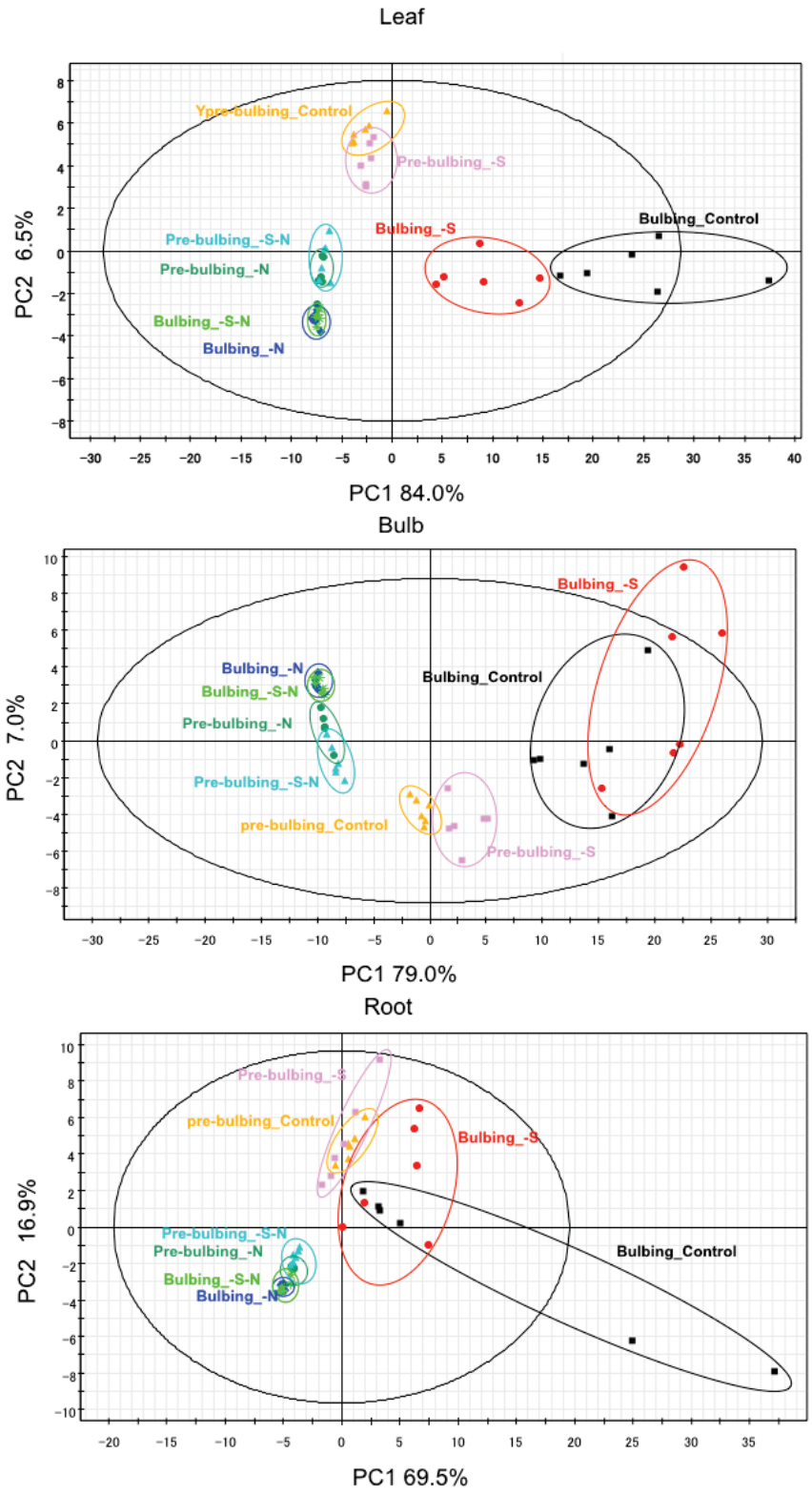

Figure 3.21 Principal component analysis (PCA) showing shift in accumulation of widely targeted metabolites in different tissues under the different S and N treatments at pre-bulbing and bulbing stage generated using the SIMCA statistical package (Ryo Nakabayashi, *pers comm*). Six biological replicates are represented for each tissue where a biological replicate consists of pool of six individual plants. The coloured circles indicate 95% confidence interval for the corresponding age and tissue type (Same colour as the circle, refer to coloured labels in the PCA).

In plants, depletion of either SO_4^{2-} or NO_3^- is known to supress the assimilation pathway of the other element (Koprivova et al., 2000), although the complexity underlying the mechanism for this interaction is still largely unresolved. An inhibitory effect of short term N depletion on S assimilation and *vice versa* has been shown in barley where NO_3^- or SO_4^{2-} depletion reduced the influx of the other element (Clarkson et al., 1989). The reduced influx on NO_3^- was restored by the addition of methionine suggesting its involvement in SO_4^{2-} dependent regulation of N assimilation. Conversely, in *Arabidopsis,* NO_3^- depletion leads to inhibition of the S-assimilation pathway, in both root and shoot as shown by the decline in AtAPR activity and protein accumulation and the cytosolic and plastidic isoforms of At*O*AS-TL following 72 h of NO_3^- depletion (Koprivova et al., 2000). Feeding *O*AS to the plants restored the activity, suggesting that in *Arabidopsis,* regulation of S assimilation by nitrogen is modulated partly through *O*AS. However, under long term NO_3^- depletion (Hirai et al., 2004; Bi et al., 2007), *AtAPR1* and *2* transcripts were unaffected in both root and shoot even though the *O*AS levels were significantly lower, at least in the roots (Hirai et al., 2004). A similar inhibition of the S-assimilation pathway under limiting N supply has been shown in the roots of *B. juncea,* although when both SO_4^{2-} and NO_3^- were depleted the expression of *BjAPR* and *BjATPS* was similar to that observed in the SO_4^{2-} depleted plants (Lee & Kang, 2005). This suggests that in members of *Brasicaceae*, the regulatory effect of N over S assimilation is more drastic under short term depletion before a new metabolic equilibrium is reached.

In *A. cepa* however, as described earlier in the section, the effect of S and N interactions is quite different, both at the transcriptional and at the metabolite level (Fig 3.4- 3.7 and 3.19). This may be due to the unique physiology of *A. cepa,* which undergoes modification at the base of the leaves to form a bulb. This organ serves as a sink tissue for reduced S compounds which can then be mobilized during flowering (Saghir et al., 1965). However, unlike *B. juncea* and *A. thaliana,* which are not bulbing species, this increased nutritional requirement for sulfur in *A. cepa* seems to be regulated highly by NO_3^- nutrition at both the transcriptional and metabolite levels, even under long term NO_3^- depletion. This is highlighted in plants under the –N treatment in this study, where the relative transcript abundance of *AcHAST1;1LIKE1, AcATPS, AcAPSR1, AcSiR1* declined in the roots at pre-bulbing as well as bulbing. This indicates limited SO_4^{2-} uptake and assimilation, but these genes were up-regulated in the shoots, possibly to reflect translocation of increasing amounts of SO_4^{2-} to the shoots. However, expression of group 2 transporters, which are

generally associated with long distance root to shoot transport, was not determined in this study (Takahashi et al., 2000) (Fig 3.6). This repression in roots and elevation in the shoots is also evident at the translational level, where accumulation of AcAPSR1 decreases in the roots but increases in the shoots under the –N treatment, when compared with accumulation in the tissues of the plants grown under the control treatment (Appendix 3).

Another N-nutrition specific response in the S-assimilation pathway is in the transcript profile of *AcAPSK1. APSK* forms a bifurcation in the S-assimilation pathway as the encoded protein shares APS as a substrate with APSR enzyme. Catalysis of APS by APSK leads to production of PAPS, which is the most common co-factor in the sulfotransferase reactions (Lillig et al., 2001). The flux of SO_4^{2-} through the plant is competitively divided between the two branches for S incorporation. As indicated by the factorial experiment in this study and also observed in studies in other plant species, sulfate deprivation leads to reduced *APSK* expression possibly reflecting the preferential direction of S-flux towards cysteine synthesis (Kopriva et al., 2012; Ravilious et al., 2012). However, under the –N and the –S-N treatments, *AcAPSK1* expression increased in both root as well as leaf tissue, while that of *AcATPS1* decreased in the root tissue and increased in leaf tissue. This is the first study, to the author's knowledge, which investigates the response of *APSK* expression in Alliums. Previously, the enzyme encoded (APSK) has been shown to be active in *A. cepa* with a higher specific activity for APS when compared to *Arabidopsis, P.ensyii* and *P. fastigiata* and comparable activity to broccoli florets and leaf tissue (Leung et al., 2012). Given the increase in relative transcript abundance of *AcAPSK1* under N-limiting conditions in *A. cepa,* it is important to establish its contribution in control over the flux of SO_4^{2-} in the plant. Further, as plant APSKs have been shown to be redox regulated (Ravilious et al., 2012b), it is equally important to establish the correlation between the elevated transcript profile, protein accumulation and activity.

Taken together, the results indicate that the nutrient specific differential expression of genes of the S-assimilation pathway in the roots and the shoots seems not to be common in all S-accumulating species. This suggests a species specific regulation of the S-assimilation pathway in *A. cepa.* This difference may also extend to the other members of the Alliums, eg. garlic, which also has storage organ rich in reduced S-compounds. It is important here to note that *AcNR1,* which is a nitrate responsive gene also shows an increase in transcript abundance relative to the control treatment under the –N and –S-N treatment, in leaf tissue at bulbing only. However, this is only an apparent induction as when the developmental response of *AcNR1* is compared (with pre-bulbing for each

treatment as a control for expression at bulbing), there is a sharp decline at bulbing relative to pre-bulbing under the control treatment. The developmental response under the –N treatment shows only a marginal (but significant) decline upon bulbing. Therefore when the comparison across treatments is made, then relative to the bulbing stage in the control treatment, *AcNR1* transcript abundance appears to be elevated. A similar response is also observed for *AcSOX1* at bulbing under the –N treatment in leaf and root tissue (Fig 3.4, 3.5, 3.6, 3.9, 3.10).

A similar transcriptional and post-transcriptional profile does not always indicate a positive correlation with the accumulation of the products of the pathway. Post-translational modifications can also act as another check-point for pathway regulation, modifying the activity of the enzymes, leading to higher or lower accumulation of down-stream products. However, the dominant response to N limitation under the –S-N treatment, as seen in the root expression of *AcHAST1;1LIKE1* and *AcAPSR1* (Fig 3.6 A, C), is also reflected in the metabolome of the plants where accumulation of both untargeted volatile compounds as well as targeted metabolites under the –S-N treatment is similar to that of the –N treatment response suggesting a NO_3^- dependent regulation of S-assimilation pathway in *A. cepa* (Fig 3. 11, 3.17, 3.18).

Conversely, SO_4^{2-} depletion in plants is also known to perturb the N-assimilation pathway. For example, a reduced influx of NO_3^- and lower *NR* expression and subsequent activity of the enzyme encoded was observed in five week old spinach plants when transferred to a SO_4^{2-} free media (Clarkson et al., 2001). A similar inhibition of *NR* relative transcript abundance was seen under long-term SO_4^{2-} depletion in *Arabidopsis,* with intermediate responses at the transcriptome and metabolomic level when both NO_3^- and SO_4^{2-} were limiting (Hirai et al., 2004). However, this was not very evident from the *A. cepa* factorial experiment in this study, as at the transcriptional level, there was only a slight but significant down-regulation in *AcNRT2;1LIKE1* and *AcNiR1* transcripts in the roots only (Fig 3.7). Interestingly at the level of metabolites, there was a significant ($p<0.05$) increase in accumulation of amino acids in the pseudo-stem of the pre-bulbing plants (Fig 3.15). A reason for this could be the altered S:N ratio in the plants and that the excess of N over S is being channelled into amino-acid synthesis. Accumulation of amino acids such as asparagine and glutamine as well as ureides has also been observed in *Arabidopsis* (Nikiforova et al., 2006) and arginine and glutamine accumulates in *N. tabacum* (Klapheck et al., 1982) under short term SO_4^{2-} deprivation. In *N. tabacum,* this also correlated with a decline in protein-synthesis (Klapheck et al., 1982). This indicates that a part of the

excessive accumulation of amino-acids observed in the pseudo-stem and the bulb is possibly also due to a decline in protein-synthesis *via* down-regulation of plastid and ribosomal genes involved in protein synthesis. However, from the targeted metabolome, it is hard to specifically conclude whether this accumulation is in response to a decline in the protein synthesis machinery or through increased protein degradation. Moreover, this response to S limitation seems to contrast with the leaf tissues where a decline in amino acid content is observed. Although it is important to note that this amino acid accumulation is more significant at the pre-bulbing stage, and that the leaf tissue does not show any change in amino acid accumulation at the pre-bulbing stage, at bulbing, a slight decline in the levels of all amino acids investigated is observed. Although the decline was not as drastic as under the –N and the –S-N treatment, it does indicate a degree of inhibition of N assimilation and especially at the bulbing stage, probably due to increased nutritional requirement by the plant at this stage for bulb development. Additional studies measuring the changes in flux of SO_4^{2-} and NO_3^- as the plant transits to bulbing along with expression analyses of genes involved in amino acid synthesis and protein degradation would elucidate if the responses observed in this study are indeed regulated by the increased demand for NO_3^- and SO_4^{2-} at bulbing.

3.7.3 Feed forward mechanism for cysteine accumulation in *A. cepa* highlighted under sustained SO_4^{2-}depletion

O-Acetylserine (*O*AS) is a N-containing precursor of cysteine synthesis synthesized by acetylation of the amino-acid serine, which also links the S-assimilation pathway with N assimilation. In this study, no *O*AS accumulation was observed in plants grown under the –S treatment in any of the tissues, both at the pre-bulbing and the bulbing stage (Fig 3.19). Also, the serine levels remained unaffected under the –S treatment in all tissues and stages except in the pre-bulbing pseudo-stem where a slight but significant ($p<0.05$) accumulation was observed. At the bulbing stage, a decline in accumulation of *O*AS, glutathione as well as methionine was also observed in the leaves. However, the response in the bulb and the roots was not so severe as only methionine levels showed a significant ($p<0.05$) decline in the bulb and *O*AS in the roots (Fig 3.19, Appendix 11: bar plots). This suggests that *O*AS

mediated regulation might only function under short-term SO_4^{2-} limitation and is not in response to sustained limitation in *A. cepa*, especially at bulbing.

Changes in the metabolic profile of other species in response to SO_4^{2-} limitation include accumulation of *O*AS which acts as a hand-break in the feedback regulation of the pathway ultimately leading to the up-regulation of sulfate uptake and assimilation to cope with the limited S availability (Berkowitz et al., 2002; Wirtz & Hell, 2006; Feldman-Salit et al., 2009;). Over a period of time, sustained S-deprivation leads to a decline in the S-containing amino acids cysteine and methionine, as well as other S-metabolites such as glutathione and other sulfated compounds (Takahashi et al., 2011). Again, most of the evidence for the *O*AS-feedback model comes from studies completed on *Arabidopsis* which accumulates secondary S metabolites, mainly glucosinolates (Kliebenstein et al., 2001). However, similar responses to SO_4^{2-} limitation have been observed in soybean (Kim et al., 1999) and rice (Nakamura, Yamaguchi, & Sano, 1999) indicating *O*AS-mediated regulation of the S-assimilation pathway may be a predominant mechanism in plants.

Interestingly, a feed-forward mechanism for S-assimilation in *A. cepa* has been suggested as an explanation of the high levels of cysteine accumulation in the species, particularly during bulbing (McCallum et al., 2011). This is further supported by evidence for a complex formation between AcATPS1 and AcAPSR1 *in vitro* possibly driving the assimilation flux towards accumulation of cysteine (Cumming et al., 2007). Although the existence of ATPS-APSR complex has not yet been examined in other species, a lack of *O*AS accumulation in the tissues examined under the –S treatment even in bulbing plants supports this idea of a feed-forward mechanism in *A. cepa.* However, this might only be true for long term S limitation, and a feed-back regulation might possibly be effective in *A. cepa* under the short term S depletion. The accumulation of serine in the pseudo-stem under the –S treatment could possibly reflect the tail-end of such regulation in pre-bulbing plants, before they switch to a feed-forward mechanism at bulbing. However, it is also equally possible that the serine accumulation may not be linked with feed-back regulation at all as a generic accumulation of other amino acids is also observed in pseudo-stem at the pre-bulbing stage (Fig 3.13). The accumulation of *O*AS is generally thought to feed-back to the S-pathway resulting in transcriptional up-regulation of the pathway (Feldman-Salit et al., 2009; Hesse et al., 2004). However, in this thesis, a dramatic increase in relative transcript abundance of *AcHAST1;1LIKE1* and *AcAPSR1* was observed even without the *O*AS accumulation in both shoot and the root tissue under the –S treatment (Fig 3.4, 3.5, 3.19). In fact, *AcHAST1;1LIKE1* and *AcAPSR1* were up-regulated in shoot tissues even under the –N and

the –S-N treatment when *O*AS accumulation was even lower (Fig 3.4, 3.5). This not only corroborates the regulatory disconnect between the S and N-assimilation pathway in *A. cepa* at the point of incorporation of *O*AS into cysteine; it also indicates that the S-assimilation pathway genes might be feed-back regulated by metabolites down-stream of cysteine synthesis in *A. cepa*.

3.7.4 Suppression of bulbing upon sustained NO_3^- depletion in *A. cepa*

In the present study, to establish successful transition of plants to bulbing stage, the transcript levels of the *Flowering Locus T4 (AcFT4)* gene were monitored as a marker gene for bulbing (Fig 3.8 A) (Lee et al., 2013). As expected, the control plants showed a decrease in *AcFT4* transcript under the LD conditions (bulbing) (Fig 3.8 A). Interestingly, mRNA expression of *AcFT4* also responded to NO_3^- depletion. Under the –N treatment, *AcFT4* relative transcript abundance increased in the leaves at the pre-bulbing stage and was even more heightened at the bulbing stage when compared to leaves from plants grown under the control treatment for each stage (Fig 3.8 A). The regulation of *AcFT4* has been recently characterized in *A. cepa* where the overexpression of the gene has been shown to inhibit bulbing (Lee et al., 2013). The results from this study indicate that under sustained NO_3^- depletion, the nitrate reserves might be insufficient to support bulbing and so the process is supressed by activation of *AcFT4*. This seems even more likely when the response of S and N-assimilation pathway genes to bulbing under the control treatment is compared to bulbing under the –N treatment. As described above, there was a general decline in transcript levels of most genes investigated upon bulbing, when compared to pre-bulbing tissues under the control treatment in both leaf and root tissue (Fig 3.9). However, under the –N treatment, none of the S pathway genes investigated showed a decline upon transition to bulbing in the leaves (Fig 3.10). In fact, there was an increase in the relative transcript levels of *AcATPS1, AcOASTL1* and *AcOASTL3.* The effect of N availability on bulb yield and quality has been shown by many studies where the rate of bulb development is increased up by increasing N availability leading to higher bulb yield. Conversely, a decline in bulb yield is observed under limiting N conditions (Brewster & Butler, 1989; Rezaei et al., 2013). However, the underlying molecular signature of N dependent bulb formation still requires much elucidation. The results from this study add to the general understanding of the transcriptional as well as metabolomic responses involved in bulbing specifically in the S

and N-assimilation pathway. Moreover, this suggests that bulb development may be regulated by a negative feedback mechanism where sustained depletion in N metabolites leads to higher expression of *AcFT4*, thus supressing transition of the plants to the bulbing stage.

3.7.5 Tissue specific and systemic accumulation of certain N and/or S compounds in response to NO_3^- depletion

Metabolomics allows for the screening of a large number of compounds in a single experiment, hence making it possible to understand both systemic and specific responses in plants to a certain treatment. Another by-product of metabolomic profiling is the identification of unexpected compounds and fluctuation in compounds not thought to be directly affected by the treatment. Along with the metabolites traditionally known to fluctuate under S and/or N limitation, some of these were also identified.

Hypotaurine is an intermediate sulfinic acid in the metabolism of taurine, a non-protein S containing amino acid, most abundant in the animal kingdom and red algae but only found in trace amounts in higher plants (L. H. Smith, 1968). The importance of taurine in the animal kingdom has long been established as it is required for many fundamental biological processes such as conjugation of bile acids, antioxidation, osmoregulation, membrane stabilization, and modulation of calcium signaling (Huxtable, 1992). Due to its low abundance in plants and difficulty in detection (Lähdesmäki, 1986), its importance has largely been ignored in plants. It is highly intriguing that the precursor to taurine accumulated in all tissues under the –N and the –S-N treatment at the pre-bulbing stage and in the leaf and root tissue at the bulbing stage (Fig 3.15-3.18). Although there have been a few reports of taurine and hypotaurine synthesis in plants limited mainly to leguminous species (Lähdesmäki, 1986; Pasantes-Morales & Flores, 1991), it has also been reported that exogenous application of taurine has a positive effect on growth of wheat seedlings (Sheng et al., 2004). As this pathway is a divergence from the S-assimilation pathway arising after cysteine is synthesised, it is worth speculating if under sustained NO_3^- depletion, the taurine and hypotaurine assimilation pathway is revived in *A. cepa* to cope with the nutrient deficiency. Hypotaurine could also serve as a S and N reserve for the plant which may be re-mobilized later during flowering. In the light of this study, and given the

importance of taurine in the animal kingdom, it would be interesting to confirm if it also accumulates in *A. cepa* in response to NO_3^- limitation and what its function in plants might be.

Another class of compounds which exhibited tissue specific accumulation were the flavonol glucosides (Fig 3.13, 3.14). An age-dependent, tissue specific accumulation of flavonol glucosides was found in the pseudo-stem at the pre-bulbing stage which declined significantly ($p<0.05$) upon bulbing when compared to bulbs of plants grown under the control treatment. This specific accumulation in the pseudo-stem at the pre-bulbing stage suggests an important function of these compounds in the developmental regulation of bulbing. Flavonol glucosides are known as antioxidants and as protectors against oxidative stress has also been implied. It may be that in *A. cepa,* as the pseudo-stem later develops into a bulb, which is the storage organ, resources are selectively mobilized to protect the pseudo-stem under sustained N depletion. Thus as bulbing is induced as a result of longer photo-period, the continuing N depletion results in the mobilization of resources into flowering instead of bulbing.

Chapter 4: Characterization of the interaction between sulfite reductase (AcSiR1) and nitrite reductase (AcNiR1)

*Ac*SiR and *Ac*NiR are structurally and functionally similar proteins and a single study has reported evidence for redundancy in *S. oleracea* (spinach) (Krueger & Siegel, 1982). To establish if this redundancy exists in *A. cepa,* recombinant *Ac*SiR1 and *Ac*NiR1 were expressed in the *E. coli* strain BL21 and purified the using pGEX-6P3 vector expression system. Substrate replacement studies *in vitro* were conducted using activity assays to test whether each recombinant enzyme can reduce both sulfite and nitrite. The possibility of interaction between the two proteins was also examined using an ELISA-based Solid Phase Binding Assay and also Isothermal Titration Calorimetry (ITC). To investigate if an indirect interaction exists between AcSiR1 and AcNiR1 in the form of enzyme recruitment, mean specific activity and accumulation of *Ac*SiR1 and *Ac*NiR1 in leaf and root tissue in response to the –S, -N and –S-N treatments were also determined. The possibility of a transient recruitment at the transcriptional level was also investigated using *Arabidopsis* wild type (col) and a *SiR1* T-DNA insertion line *SiR1-1* in a controlled, 72 h S x N deprivation experiment (see section 2.1.2).

4.1 Characterization of recombinant *Ac*SiR1 *in vitro*

4.1.1 Recombinant *Ac*SiR1 accumulation

Recombinant GST-tagged mature *Ac*SiR1 was expressed, excluding the chloropastidic signal peptide, in the *E. coli* BL21 strain using the pGEX-6P-3 vector. Recombinant protein was then purified from lysed *E. coli* cells, using glutathione-sepharose beads and the PreScisson protease enzyme then used to cleave the GST tag (Fig 4.1 A) (see section2.4). The theoretical size of the protein, excluding the signal peptide was determined to be 65.70kD (http://web.expasy.org/protparam/). Purified recombinant protein fractionated on a 10% 1D-SDS-PAGE yielded a major band of *ca.* 67 kD, as determined by relative mobility compared to the proteins of known size (protein ladder) fractionated alongside on the same gel (Fig 4.1 B). Antibodies raised against *Arabidopsis* SiR1 (*At*SiR1) which also

recognizes *Ac*SiR1 were used for western blotting. A single major band of a similar size was recognized after cleaving the GST tag (Fig 4.1 C).

4.1.2 Recombinant *Ac*SiR1 activity determination

The enzyme activity of recombinant *Ac*SiR1 was determined using a sulfite-reductase coupled-enzyme assay, which measures the amount of cysteine (nmol) made per unit of time (min) and uses sodium sulfite as substrate (see section 2.4.6.2). The mean specific activity of recombinant *Ac*SiR1 was determined to be 235 ± 17.8 nmol/min/mg protein which was significantly ($p<0.01$) higher when compared with activity determined in a crude leaf extract, at 11.4 nmol/min/mg protein. The activity of recombinant *Ac*SiR1 was also significantly ($p<0.01$) higher than the mean specific activity measured in a *A. cepa* root extract, which was 11.7 ± 1.5 nmol/min/mg protein (Table 4.1).

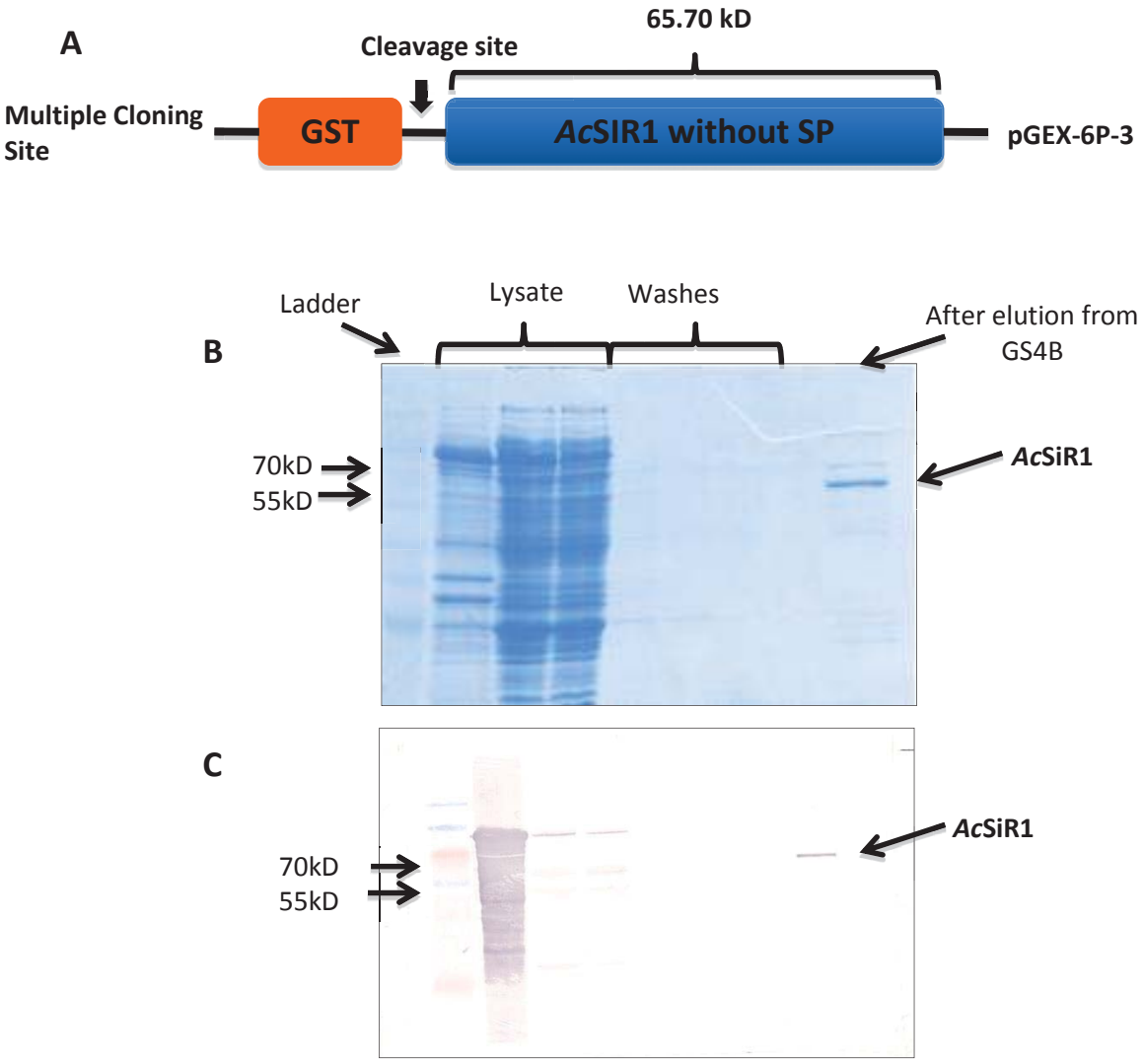

Figure 4.1 Characterization of recombinant AcSiR1. A: Schematic representation of the GST tagged construct for the recombinant protein. The GST tag cleavage site is indicated. B: Coomassie blue stained 10% 1D-SDS-PAGE showing purification of AcSiR1, as indicated, from lysed *E. coli* cells. C: A western blot of showing purified AcSiR1 as a single band recognized by antibodies raised against AtSiR1.

4.2 Characterization of recombinant of *Ac*NiR1 *in vitro*

4.2.1 Recombinant *Ac*NiR1 accumulation

Recombinant full length GST-tagged *Ac*NiR1, excluding the chloropastidic signal peptide, was expressed using the pGEX-6P-3 vector in the *E. coli* BL21 strain and purified using the same method as for *Ac*SiR1 (Fig 4.2 A) (see section2.4). However, as no activity was found for the recombinant protein, it was then expressed with the signal and found to be active. Hereafter, the recombinant AcNiR1 characterized includes the signal peptide. The theoretical size of the protein, including the signal peptide was determined to be 65.9 kD *(http://web.expasy.org/protparam/).* An aliquot of purified recombinant protein fractionated using 12.5% 1D-SDS-PAGE yielded one major band of *ca.* 62 kD (and another lightly staining band of a smaller mass) as determined by relative mobility compared with proteins of known size fractionated alongside on the same gel. Mass-spectrometry analysis of the *ca.* 62kD band confirmed it to be *Ac*NiR1, whereas the minor band was confirmed to be degraded *Ac*NiR1. A minor band above the expected size of the protein was also stained and was confirmed through mass-spectrometry to be *E. coli* chaperone protein DnaK (Fig 4.2 B) Antibodies raised against the purified recombinant *Ac*NiR1, also recognized a single band of *ca.* 65 kD band in western blot analysis in a crude leaf extract from *A. cepa*.. Furthermore, AcNiR1 specific antibody also recognized a single band of a similar size from crude leaf extracts of *N. tabacum* and *A.thaliana* but not from *Trifolium repens* (Fig 4.2 C).

4.2.2 Recombinant *Ac*NiR1 characterization

The enzyme activity of recombinant *Ac*NiR1 was determined using an assay which measures the amount of nitrite (nmol) reduced per unit of time (min) and uses sodium nitrite as substrate (see section 2.4.6.3). The mean specific activity of recombinant *Ac*NiR1 was determined to be 2956.7 ± 87.1 nmol/min/mg protein which was significantly ($p<0.01$) higher when compared with activity determined in a crude extract from *A. cepa* leaves, which was 38.7 ± 14.2 nmol/min/mg protein. The activity of recombinant *Ac*NiR1 was also significantly ($p<0.01$) higher than the mean specific activity measured in a *A. cepa* root extract, which was 54.6 ± 3.4 nmol/min/mg protein (Table 4.1).

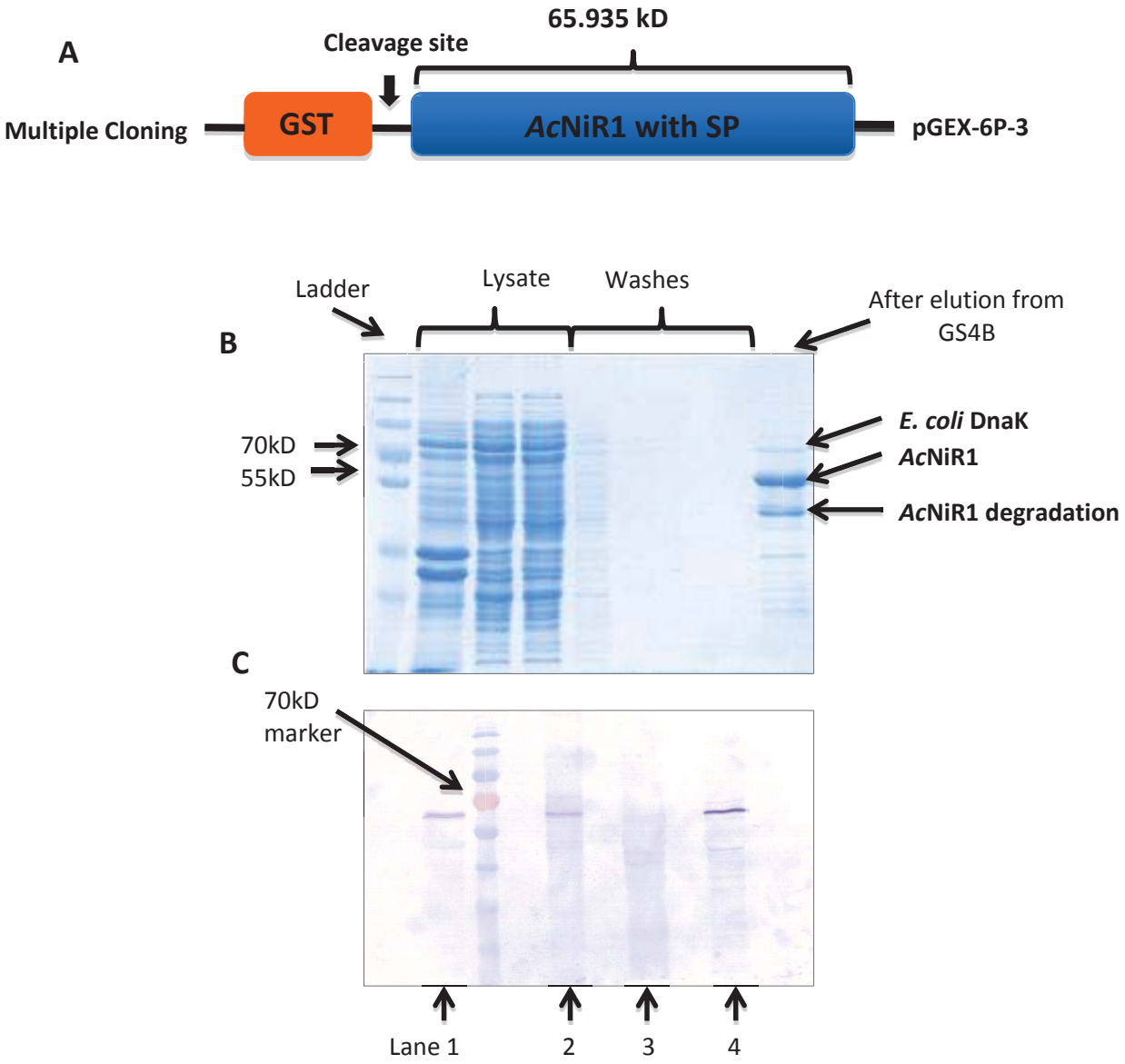

Figure 4.2 Characterization of recombinant AcNiR1. A: Schematic representation of the GST tagged construct for the recombinant protein. The GST tag cleavage site is indicated. B: Coomassie blue stained 10% 1D-SDS-PAGE showing purification of AcNiR1, as indicated, from lysed *E. coli* cells. C: A western blot of showing recognition of a single band of *ca.* 65 kD from crude extracts of *A. cepa* (Lane1), *N. tabacum* (Lane2), *A.thaliana* (Lane 4).Crude extract from *T.repens* was fractionated in lane 3.

4.3 Redundancy in AcSiR and AcNiR substrate specificity

Functional redundancy has been previously demonstrated for purified SiR and NiR from *S. oleracea* extracts (Krueger & Siegel, 1982) where both *So*SiR1 and *So*NiR1 can reduce both substrates (nitrite and sulfite). Recombinant *Ac*SiR1 and *Ac*Nir1 were used to determine if the same phenomenon existed in *A. cepa cv.* CUDH2107. Recombinant protein from a single batch of *E. coli* cells containing the GST fused AcNiR1 construct, with three technical replications, was used to determine the mean specific activity in each case (Table 4.1) (see section 2.4.6.3).

Recombinant *Ac*SiR1, when substituted in the nitrite reductase assay, reduced nitrite and exhibited a mean specific activity of 19.0 nmol/min/mg protein. However, the mean specific activity of *Ac*SiR1 was significantly ($p<0.01$) higher for its physiological substrate sulfite (234.7 ± 17.8 nmol/min/mg protein) (Table 4.1) (see section 2.4.6.3).

Similarly, *Ac*NiR1 was able to reduce sulfite (78.2 nmol/min/mg protein) in a sulfite-reductase specific assay, but this rate was significantly ($p<0.01$) lower than the mean specific activity of *Ac*NiR1 for nitrite (2956.7 ± 87.1 nmol/min/mg protein) (Table 4.1) (see section 2.4.6.2).

AcSiR1 and AcNiR1 activity from recombinant protein and crude extracts

Enzyme	Enzyme activity (nmol/min/mg protein	
	Sulfite as substrate	Nitrite as substrate
Recombinant *Ac*SiR1	234.69±17.81	19.03±2.3
Recombinant *Ac*NiR1	78.23±7.32	2956.69±87.11
Total plant extract-Leaf	11.42±1.04	38.74±14.21
Total plant extract-Root	11.66± 1.47	54.63± 3.37

Table 4.1 Enzyme activity (nmol/min/mg) of AcSiR1 and AcNiR1 as recombinant proteins and crude extract from leaf and root, with sulfite or nitrite as substrate, as indicated. For the crude plant extract the values ±SEM are the means of three biological replicates where each biological replicate comprises a pool of six individual plant tissues.. For the recombinant proteins ±SEM are the means of three chemical replicates where each replicate comprises of a distinct batch of purified recombinant protein.

4.4 Post-transcriptional responses of key S and N assimilation genes in plants grown in S and/or N depleted media.

Tissue from the S and N factorial experiment described in the previous chapter (see section 3.1), was also used to determine changes in the enzyme activity of *Ac*SiR1 and *Ac*NiR1 and protein accumulation in response to the different S and N treatments, both at pre-bulbing and bulbing in leaf and root tissue.

Total protein, extracted from different tissues harvested from plants at the pre-bulbing and bulbing stage, was quantified using the Bradford assay (Bradford, 1976) and 10ug of total protein was used in the enzyme assay to determine sulfite reduction *via* cysteine synthesis. The mean specific activity was calculated from three biological replicates in each case, where tissue pooled from six individual plants comprised one biological replicate (see section 2.4.6.2).

To determine protein accumulation in leaves and roots harvested from plants at pre-bulbing and bulbing, 10 µg of total protein, quantified using the Bradford assay was pooled from six biological replicates, fractionated using 1D-SDS-PAGE and then transferred to a PVDF membrane for western blotting using the anti-AtSiR1 or AcNiR1 antibody as indicated (see section 2.4.2, 2.4.3). Apart from the Bradford assay, coomassie blue staining of the SDS-PAGE which showed a major band of *ca.* 55kD, assumed to be larger subunit of RUBISCO, was also used as a loading control for leaf tissue. (Fig 4.3 A).

4.4.1 Specific activity and accumulation of AcSiR1 in plants grown under the control, -S, -N and –S-N treatments

4.4.1.1 Specific activity and protein accumulation in leaves harvested at the pre-bulbing stage

The highest mean specific activity determined for AcSiR1 was 11.42nmol/min/mg, which was found in leaves harvested from plants grown in the control media. The specific activity was lowest for the leaves harvested from plants grown in the –S media, at 4.73 nmol/min/mg, differing significantly ($p<0,05$) from all the other three treatments. In the

leaves from the –N treatment, the mean specific activity was 8.66 nmol/min/mg which was significantly ($p<0.05$) lower than the control treatment, but higher than the –S treatment. There was no significant ($p<0.05$) difference between the –S-N treatment (10.47 nmol/min/mg) and control (Fig 4.2A). However, when compared with the –N and the -S treatment, the activity in leaves from the –S-N treatment was significantly ($p<0.05$) higher (Fig 4.3 A).

Protein accumulation was quantified using ImageJ software (see section 2.4.3.4). Compared to leaves under the control treatment, the highest relative intensity of AcSiR1 accumulation occured in leaves under the –S-Ntreatment, followed by the –N treatment. Leaves from plants grown under the –S treatment had the lowest AcSiR1 accumulation (Fig 4.3 A)

4.4.1.2 Specific activity and protein accumulation in roots harvested at the pre-bulbing stage

There was no significant ($p<0.05$) difference between mean specific activity of AcSiR1 in roots harvested from plants grown in control (11.66 nmol/min/mg) and the –S media (10.64 nmol/min/mg). However, the specific *Ac*SiR1 activity from roots harvested at bulbing from plants grown in the –N (34.69 nmol/min/mg) and the –S-N (34.22 nmol/min/mg) media was significantly ($p<0.05$) higher than control and the –S treatment (Fig 4.3 B).

In the roots at the pre-bulbing stage, *Ac*SiR1 protein accumulation was the highest under –S treatment compared to control treatment. No protein accumulation was detected in roots under the –N and the –S-N treatments (Fig 4.3 B).

4.4.1.3 Specific activity and protein accumulation in leaf tissue harvested at bulbing stage

In the leaf tissue harvested from plants at the bulbing stage, the pattern for mean specific activity of AcSiR1 remained similar to the pre-bulbing leaf tissue, with the highest activity in control plants (19.15 nmol/min/mg). Under the –S and the –N treatments, the mean specific activity dropped to 12.98 and 15.28 nmol/min/mg respectively, both significantly ($p<0.05$) lower than leaves from plants grown under the control treatment. There was no

significant difference between the control and the –S-N treatment (18.13 nmol/min/mg) but the mean specific activity under the –S-N treatment was significantly higher the –N and the –S treatments (Fig 4.3 A).

AcSiR1 protein accumulation, as detected by western blotting and quantified by the imageJ software (see section 2.4.3.4), showed highest accumulation in leaf extracts from plants grown under the control treatment. Compared to the control treatment, a reduced accumulation of AcSiR1 was observed in leaf extracts harvested from plants under the –S treatment. The –N and the –S-N treatment showed visually lower accumulation of AcSiR1. However, this accumulation in the leaf extracts from the –N and the –S-N treatments was higher when compared to accumulation in the –S treatment (Fig 4.3 A).

4.4.1.4 Specific activity and protein accumulation in roots harvested at the bulbing stage

In a similar pattern to pre-bulbing, the roots harvested at bulbing from control (20.17nmol/min/mg) and the –S treatment (17.55nmol/min/mg) did not show any significant difference ($p<0.05$). However, the activity in roots from the –N (51.97nmol/min/mg) and the –S-N media (40.90nmol/min/mg) was significantly ($p<0.05$) higher when compared with activity in roots at bulbing harvested from control and the –S treatment (Fig 4.3 B).

*Ac*SIR1 protein accumulation was highest in extracts from the –S treatment. No protein accumulation was detected by the ImageJ software in extracts from the –N treatment. Protein accumulation in the –S-N treatment was less than control as well as the –S treatment (Fig 4.3 B).

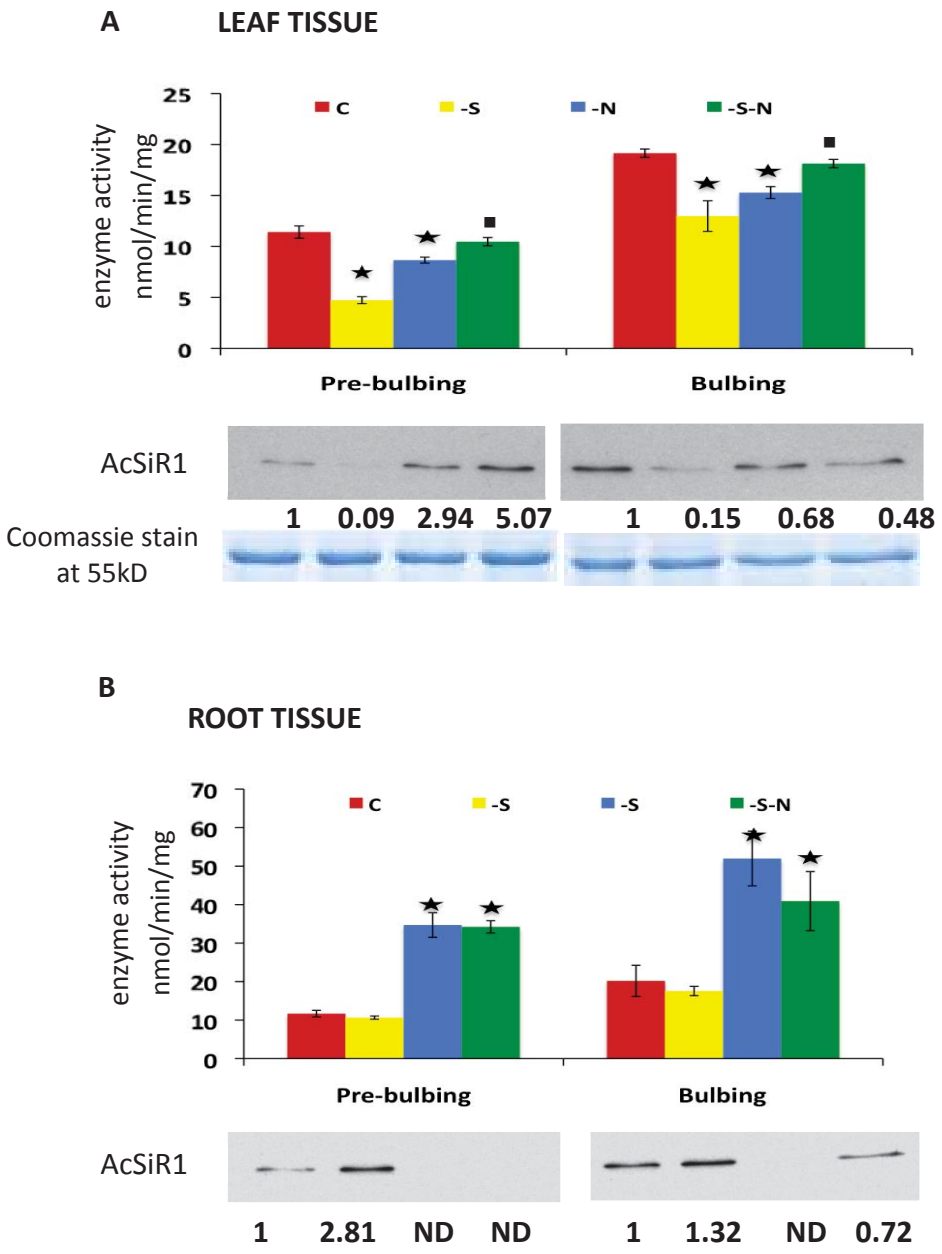

Figure 4.3 Enzyme activity and accumulation of AcSiR1 in total plant protein extracts from the leaf tissue and roots harvested from different N and S treatments. **A**: Activity and accumulation in leaves at pre-bulbing and bulbing stage, as indicated. **B**: Activity and accumulation in roots at pre-bulbing and bulbing stage as indicated. Numbers indicate relative intensity of protein accumulation as calculated by ImageJ software. Bars represent mean ±SEM of three biological replicates where each replicate consists of pooled tissue from 6 individual plants. . "⋆" indicates statistically significant ($P<0.05$) differential expression when compared with control plants of the same stage. "▪" indicates statistically significant ($P<0.05$) difference between the -N treatment and the –S-N treatment for the same stage.

4.4.2 Specific activity of *Ac*NiR1 in plants grown under the control, -S, -N and –S-N treatment

4.4.2.1 Specific activity and protein accumulation in leaf tissue harvested at the pre-bulbing stage

In the leaf tissue, the *Ac*NiR1 mean specific activity was 38.74 nmol/min/mg in control media, 45.20 nmol/min/mg in plants grown in the –S media, 23.96 nmol/min/mg in the –N media and 28.34 nmol/min/mg in the –S-N media. There was no significant ($p>0.05$) difference in any of the four treatments when compared with the control treatment (Fig 4.4 B).

In the leaf tissue harvested from plants at the pre-bulbing stage, the accumulation of *Ac*NiR1, as evaluated using the ImageJ software, was the highest in the –S treatment when compared to control treatment. The extracts from –N treatment had the lowest accumulation of *Ac*NiR1 compared to all other treatments. AcSiR1 accumulation in leaves under the –S-N treatment was slightly lower than the control (Fig 4.4 A).

4.4.2.2 Specific activity and protein accumulation in roots harvested at the pre-bulbing stage

Highest *Ac*NiR1 activity, at 54.63 nmol/min/mg, was determined for roots harvested from plants grown in control media. Under the –S treatment, the mean specific activity was 44.44 nmol/min/mg, which was not significantly different to control treatment. However, in the –N and the –S-N treatment, the mean specific activity was significantly ($p<0.05$) lower than the control treatment at 33.63 and 29.00 nmol/min/mg protein respectively, but there was no significant difference between these two treatment (Fig 4.4 B).

Accumulation of AcNiR1 in the roots at pre-bulbing was similar to the control treatment and the –S treatment. The lowest relative intensity of AcNiR1 accumulation was under the –S-N treatment with a slightly higher accumulation in the –N treatment. (Fig 4.4 B).

4.4.2.3 Specific activity and protein accumulation in leaf harvested at the bulbing stage

In the leaf tissue harvested at the bulbing stage, the *Ac*NiR1 activity was 5.49 nmol/min/mg for the control treatment and 17.37 nmol/min/mg for the –S treatment. Under the conditions of the assay, the activity in the –N and the –S-N treatments was below detection limit when 150ug of total protein was used (Fig 4.4 A).

In protein extracts of leaves harvested at the bulbing stage, AcNiR1 accumulation was slightly higher in all three treatments compared to the control. The highest accumulation was observed in the -S treatment (1.11), followed by the –N (1.09) and the –S-N treatment (1.07) (Fig 4.4 A).

4.4.2.4 Specific activity and protein accumulation in roots harvested at the bulbing stage

In the control treatment, the roots exhibited the highest activity at 63.82 nmol/min/mg, followed by the –S treatment which was significantly ($p<0.05$) lower at 45.88 nmol/min/mg. The specific activity in roots harvested from the –N and the –S-N treatment was 30.94 nmol/min/mg, and 29.08 nmol/min/mg, respectively, and were significantly ($p<0.05$) lower than both the control and the –S treatment (Fig 4.4 B).

In the protein extracts of roots, accumulation of AcNiR1 was similar in the control, the –S treatment and the –N treatment, but slightly higher in –S-N treatment (Fig 4.4 B).

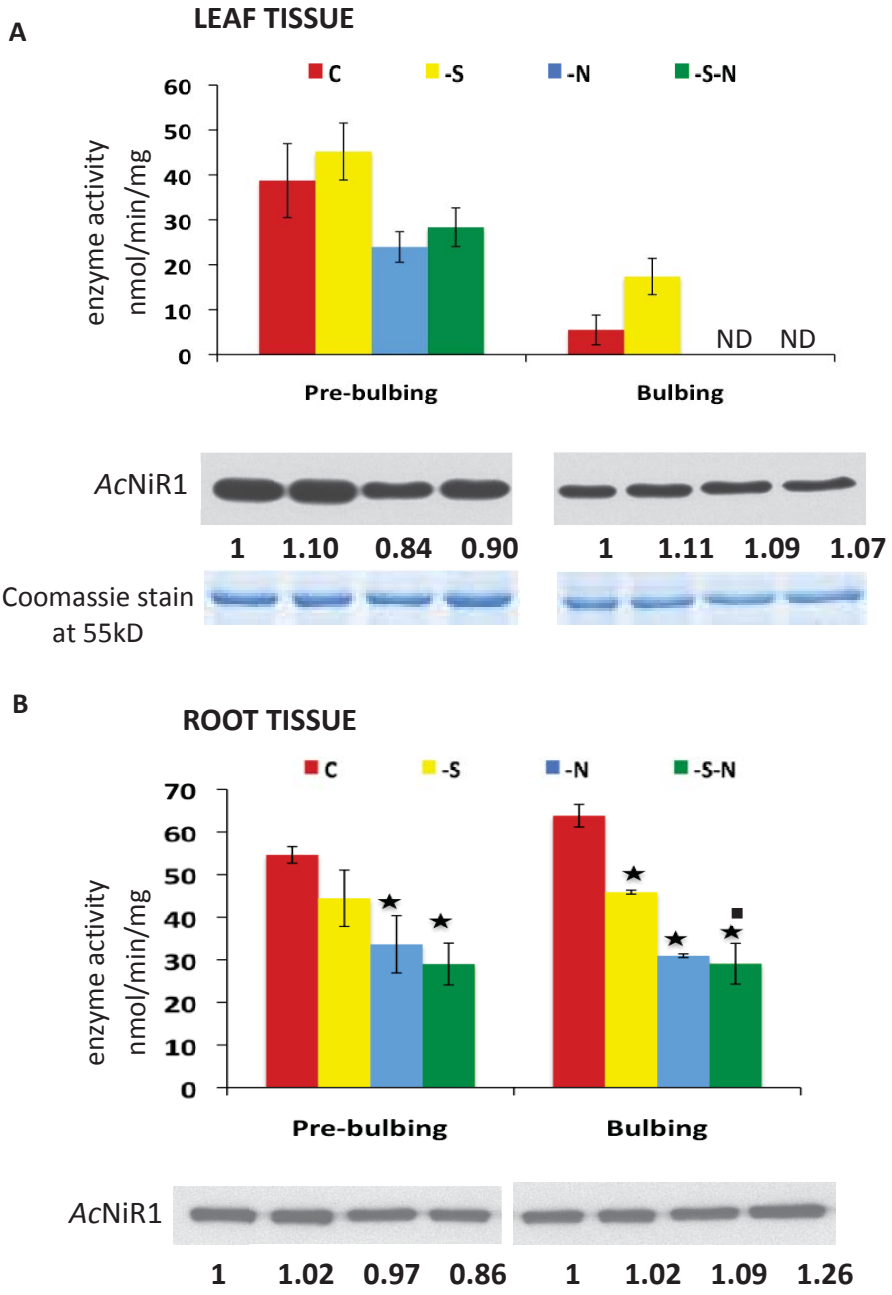

Figure 4.4 Enzyme activity and accumulation of AcNiR1 in total plant protein extracts from the leaf tissue and roots harvested from different N and S treatments. A: Activity and accumulation in leaves at pre-bulbing and bulbing stage, as indicated. **B:** Activity and accumulation in roots at pre-bulbing and bulbing stage as indicated. Numbers indicate relative intensity of protein accumulation as calculated by ImageJ software. Bars represent mean ±SEM of three biological replicates where each replicate consists of pooled tissue from 6 individual plants. "⋆" indicates statistically significant ($P<0.05$) differential expression when compared with control plants of the same stage. "▪" indicates statistically significant ($P<0.05$) difference between the -N treatment and the –S-N treatment for the same stage. "ND" (Not Detected) indicates no measurable enzyme activity.

4.5 Interaction between recombinant *Ac*SiR1 and *Ac*NiR1 *In vitro*

4.5.1 Solid Phase Binding Assay

The putative physical interaction between recombinant *Ac*SiR1 and *Ac*Nir1 was established by the solid phase binding assay (see section 2.4.5). For this, a known constant amount of *Ac*NiR1 protein (1ug) (Cumming et al., 2007) was initially immobilized onto the microtitre plate wells. After subsequent washes, the secondary protein (*Ac*SiR1) was incubated in increasing amounts. *Ac*SiR1 is predicted to bind to *Ac*NiR1 in the case of a positive interaction, which can be detected by adding the specific anti-*At*SiR1 antibody, followed by the addition of alkaline-phosphatase conjugated IgG as secondary antibody. On addition of *p*-nitrophenol phosphate, the positive interaction was seen as a yellow color development measured at 405nm that would therefore increase with increasing amount of secondary (AcSiR1) protein added. The specificity of the interaction and baseline absorbance was established by checking for color development in control wells identical to the test but without 1.) any primary protein (*Ac*NiR1), 2.) any secondary protein (*Ac*SiR1), or 3.) any primary antibody (anti-*At*SiR1 antibody). The solid phase experiments indicated that at pH 7.4, with an increasing concentration of *Ac*SiR1 added, the absorbance (405nm) increased until plateauing at 1ug of *Ac*SiR1. An absence of interaction between two unrelated proteins *Ac*NiR1 and *Ac*OASTL2 was used as a negative control for the experiment, in which no increase in absorbance was detected with increasing amount of AcOASTL2 added (Fig 4.5).

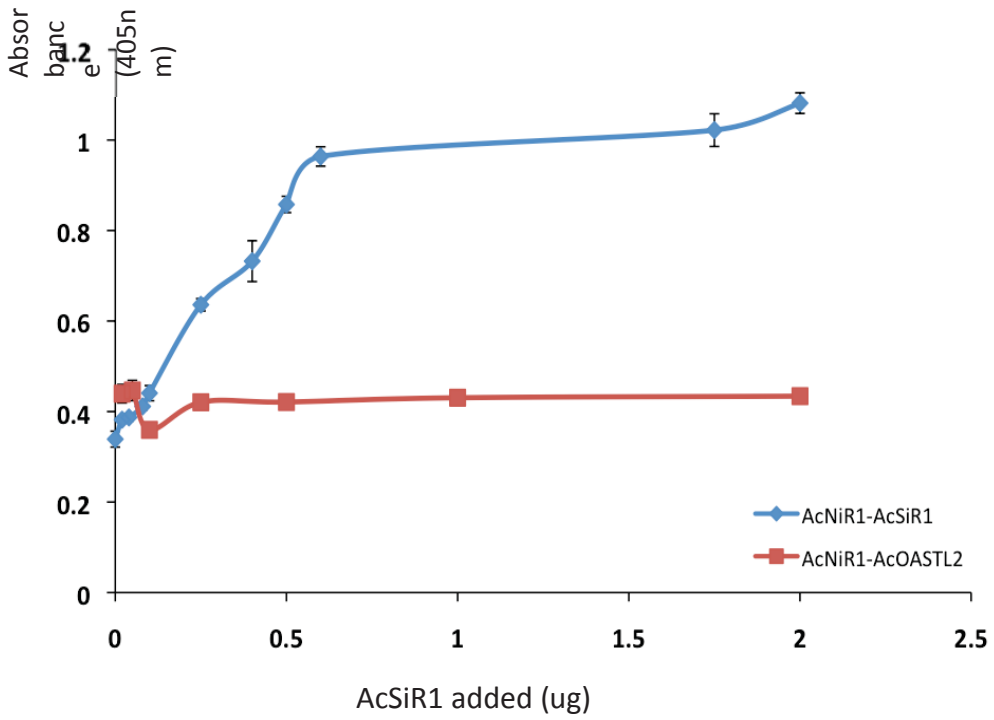

Figure 4.5 Putative interaction between AcNiR1 and AcSiR1 protein using the Solid Phase Binding Assay. Change in absorbance at 405nm in response to increasing amount of AcSiR1 (blue line) and AcOASTL2 (red line) incubation over 1ug of AcNiR1 coated onto the wells. Error bars represent ±SEM for two experimental replicates where each experiment consisted of three technical repeats.

4.5.2 Isothermal Titration Calorimetry (ITC)

ITC is a quantitative technique that measures the change in heat as a result of an interaction between two macromolecules (see section 2.4.4). It can be employed to determine the binding affinity (K_a), binding stoichiometry (n) and enthalpy change (ΔG) associated with the interaction.

ITC was used as a tag-free *in vitro* method to study AcSIR1 and AcNiR1 complex formation and to determine the thermodynamic parameters of the interaction (see section 2.4.4). For this, 19 injections of 2 ul aliquots of 173.8uM AcNiR1 was injected one at a time into a cell containing 220ul of 12.17uM recombinant AcSiR1. The heat change due to mixing of the two proteins was recorded for each injection with respect to a reference cell held at a constant temperature. As the heat change for all injections was minimal and constant, except for injection 14, it indicated that no physical interaction occurred between the two proteins. The abrupt heat change for injection 14 indicates a disturbance probably due to an air bubble (Fig 4.6).

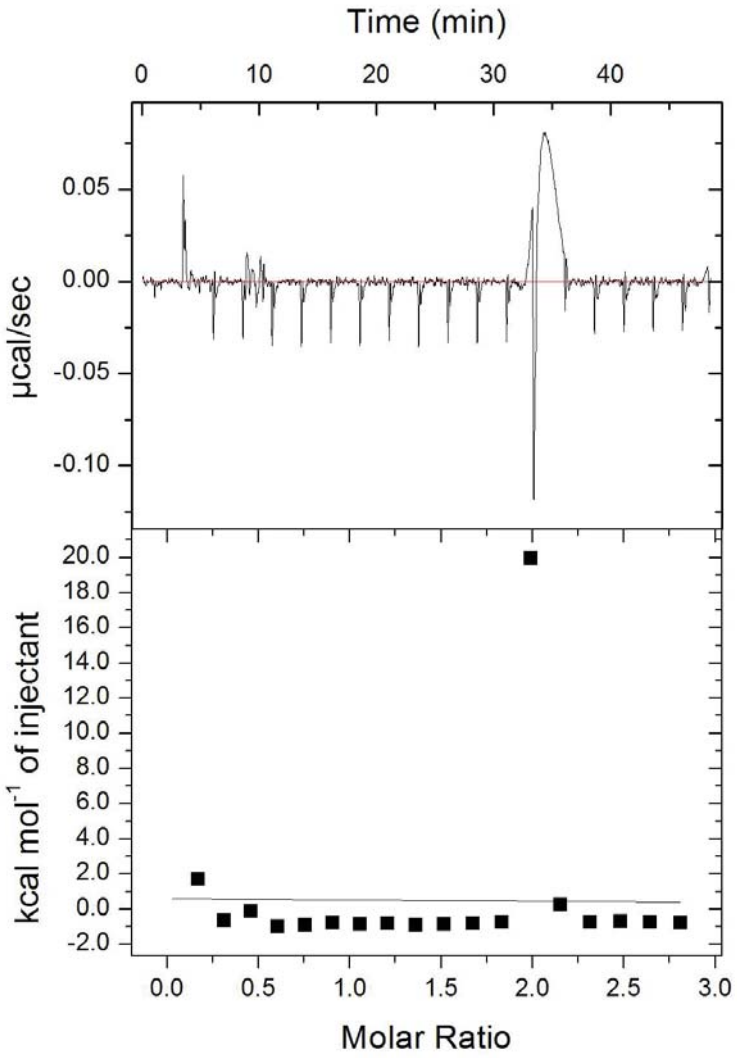

Figure 4.6 Interaction between AcNiR1 and AcSiR analyzed by I.T.C. Two µl injections of 178.3uM AcNiR1 (total 19) injected into 220 µl of 12.17 µM AcSiR1. The minimal and constant heat of dilution (Kcal mol $^{-1}$ of injectant) registered corresponding to each injection (■), indicating no binding between AcSiR1 and AcNiR1. First injection removed from analysis as per data analysis guidelines using the origin software. Spike in injection no. 14 indicates noise due to possible air bubble trapped in the cell.

4.6 Effect of short term S and N depletion on key assimilation genes in *Arabidopsis thaliana* WT and a *sir1-1* line

A sulfite reductase knock-down line, *sir1-1* has recently been characterized in which *AtSiR1* expression was shown to be essential for plant survival (Khan et al., 2010). As this line exhibited AtSiR1 accumulation at only 17% of WT ,this served as an effective tool to test for any perturbations in S and N-assimilation pathway resulting from the AtSiR1 and AtNiR1 interaction or enzyme recruitment in response to S and N treatments.

4.6.1 Experimental design

Five-week old plants of *Arabidopsis thaliana* cv. col (WT) and the t-DNA insertion line *sir1-1* that were grown in complete media, were subjected to sulfur (-S), nitrogen (-N) and coupled sulfur and nitrogen (-S-N) deficient media for 72 hours (Fig 4.7). After this time, shoot and root tissue were harvested for qRT-PCR analysis (see section 2.1.4). Transcripts abundance relative to two reference genes was investigated for the following genes in the S-assimilation pathway: *AtSULTR1;1, AtATPS3 and AtATPS4, AtAPR2, AtSiR1, AtOAS-TL A and AtOAS-TL B.* In the N-assimilation pathway, transcript abundance of *AtNRT2;1, AtNR2* and *AtNiR* was determined (see section 2.3.4) (Appendix 13).

Figure 4.7 Five week old Arabidopsis WT and *sir1-1* plants. WT and *sir1-1* plants , as indicated, grown under control media prior to start of the treatment. Plants were grown in short day (8.5h light/15.5h dark) conditions in 55% humidity with 22°/18° light dark temperature settings

4.6.2 Effect of short term S and N depletion on fresh weight of *Arabidopsis* WT and a *sir1-1* line

4.6.2.1 Changes in fresh weight (FW) in the shoot tissue

In the WT plants after 72 h in the –S treatment, the FW of shoot tissue was significantly ($p<0.05$) higher than fresh weights in the control treatment. No significant changes in FW were observed in shoot tissue from the –N and the –S-N treatment (Fig 4.8 A).

In the *sir1-1* plants, no significant difference was observed in FW of shoots in any of the treatments (Fig 4.8 A).

4.6.2.2 Changes in fresh weight (FW) in the root tissue

In common with the WT shoot tissue, there was a significant ($p<0.05$) increase in the FW of root tissue of plants grown under the –S treatment. A significant ($p<0.05$) increase was also observed in root tissue of plants grown under the –S-N treatment. However, the roots of the plants grown under the –N treatment did not show any change in FW as compared to root tissue of plants grown under the control treatment (Fig 4.8 B).

In the *sir1-1* plants, no significant change was observed in the FW of root tissue in any of the treatments (Fig 4.8 B).

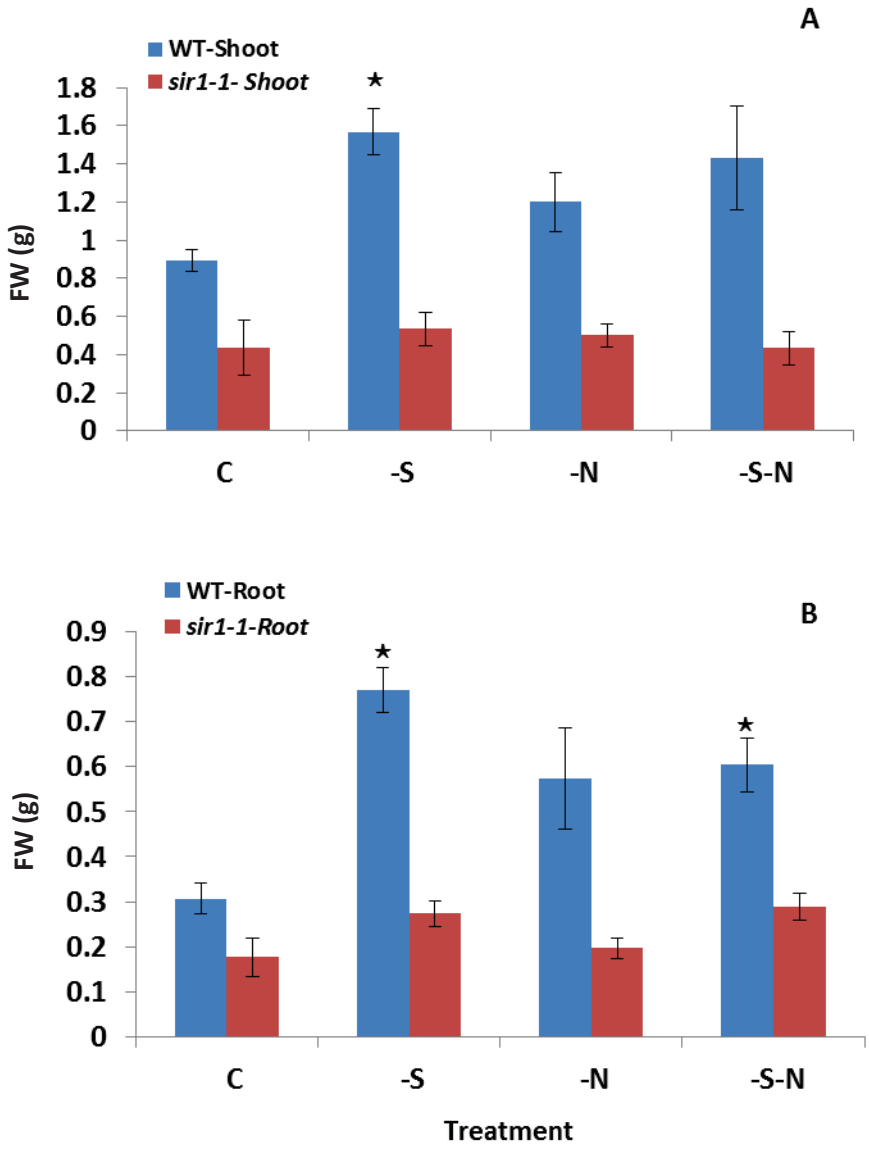

Figure 4.8 Fresh weights of shoot and root tissue after 72 h in each treatment. A: Fresh weights (FW) of shoot tissue of *Arabidopsis* WT (blue bars) and *sir1-1* (red bars). B: Fresh weights of root tissue of *Arabidopsis* WT (blue bars) and *sir1-1* (red bars). Error bars represent mean ±SEM of three biological replicates where each biological replicate comprises of tissues pooled from four individual plants. "★" indicates statistically significant ($P<0.05$) differential fresh weight as compared to control plants of the same genotype.

4.6.3 Relative transcript abundance of S and N-assimilation pathway genes in leaves and roots of *Arabidopsis* (WT and *sir1-1*) after 72 h of treatment

4.6.3.1 Relative expression in plants grown under the –S treatment

In the leaf tissue harvested from the *Arabidopsis* WT plants, relative transcript abundance of *AtOAS-TL A, AtOAS-TL B, AtNR2* and *AtNiR1* was significantly ($p<0.05$) down-regulated (Fig 4.9). There was no significant ($p>0.05$) difference in transcript abundance in any of the other genes investigated, when compared with leaves harvested from plants grown in control media (Fig 4.9).

In the leaf tissue harvested from the *sir1-1* line plants subjected to –S treatment, there were no significant ($p>0.05$) changes observed in any of the gene transcripts examined (Fig 4.9).

In the root tissue harvested from *Arabidopsis* WT plants subjected to the –S treatment for 72 hours, the transcript abundance of *AtAPS3, AtAPS4* and *AtAPR2* was significantly ($p<0.05$) down regulated when compared to roots harvested from plants grown in control media for the same period of time. No change was observed in transcript abundance of the other genes investigated (Fig 4.10).

In the root tissue harvested from the *sir1-1* line plants, the transcript levels of three genes *AtSULTR1;1* AtAPS4 and *AtNR2,* were significantly ($p<0.05$) affected by the –S treatment with higher accumulation when compared to roots from control treatment. No significant change was observed in *sir1-1* plants in any of the other genes investigated (Fig 4.11) (Fig 4.10).

4.6.3.2 Relative expression in plants grown under the –N treatment

In the leaf tissue harvested from *Arabidopsis* WT plants, the relative transcript abundance of *AtAPS3, AtAPS4, AtAPR2*, *AtOAS-TL A*, *AtNR2* and *ATNiR1* was significantly ($p<0.05$) down regulated when compared with *Arabidopsis* WT plants of the same age harvested from the control treatment. No significant change was observed in the transcript

abundance of *AtOAS-TL-B* when compared with *Arabidopsis* WT plants of the same age harvested from control treatment (Fig 4.9).

In the leaf tissue harvested from sir1-1 line plants subjected to the –N treatment for 72 hours, only two genes, *AtAPS4* and *AtAPR2,* showed significant ($p<0.05$) changes and both were down-regulated when compared with *sir1-1* plants of the same age harvested from the control treatment (Fig 4.9).

In the root tissue harvested from the *Arabidopsis* WT plants subjected to the –N treatment for 72 hours, *AtNRT2;1* was the only significantly ($p<0.05$) up regulated gene when compared with roots from the plants grown under the control treatment. In contrast, transcript abundance of *ATAPS3, AtAPS4 ATSIR1* and *AtOAS-TL B* were significantly ($p<0.05$) down regulated when compared with roots from plants grown under the control treatment (Fig 4.11) (Fig 4.10).

In the root tissue harvested from the *sir1-1* plants subjected to the –N treatment for 72 hours, only *AtAPR2* transcripts were significantly ($p<0.05$) down regulated in comparison to roots from *sir1-1* plants grown under the control treatment. The transcript abundance for *AtAPS4, AtOAS-TL B, AtSULTR1;1* , *AtNRT2;1* and *AtNR2* were amongst the significantly ($p<0.05$) up regulated genes (Fig 4.10) (Fig 4.11) .

4.6.3.3 Relative expression in plants grown under the –S-N treatment

In the leaf tissue harvested from *Arabidopsis* WT plants subjected to the –S-N treatment for 72 hours, the relative transcript abundance of all the genes investigated in leaves namely, *AtAPS3, AtAPS4 , AtAPR2 , AtSiR1 , AtOAS-TL A , AtOAS-TL B , AtNR2* from and *AtNiR1* were significantly ($p<0.05$) down regulated when compared with *Arabidopsis* WT plants of the same age harvested from the control treatment. Compared to the relative expression in leaves under the –N treatment, the transcript abundance of *AtAPS3* and *AtAPS4* were significantly ($p<0.05$) up regulated (Fig 4.9).

In the leaf tissue harvested from the *sir1-1* plants, the relative transcript abundance of only *AtAPR2* was significantly ($p<0.05$) down regulated when compared to plants grown in the control treatment. However, in comparison to the relative expression of genes in the –N treatment, *AtAPS3* was significantly ($p<0.05$) down-regulated (Fig 4.9).

In the root tissue harvested from the *Arabidopsis* WT plants, and compared with roots harvested from plants in control treatment, only two gene transcript levels, *AtAPR2* and *AtSiR1,* were significantly ($p<0.05$) down regulated under the -S-N treatment. However, in comparison to roots from plants subjected to the –N treatment, transcripts levels of *AtAPS3, AtAPS4, ATOAS-TL A*, *AtSULTR1;1* and *AtNiR1* were significantly ($p<0.05$) up regulated (Fig 4.10) (Fig 4.11).

In the root tissue harvested from the *sir1-1* plants, *AtAPS4* and *AtOAS-TL B* transcripts were significantly ($p<0.05$) up regulated when compared to roots from the *sir1-1* plants grown in the control treatment. However, the transcript levels of *AtAPR2* were significantly ($p<0.05$) down regulated when compared to roots from *sir1-1* plants grown under the control treatment (Fig 4.10).

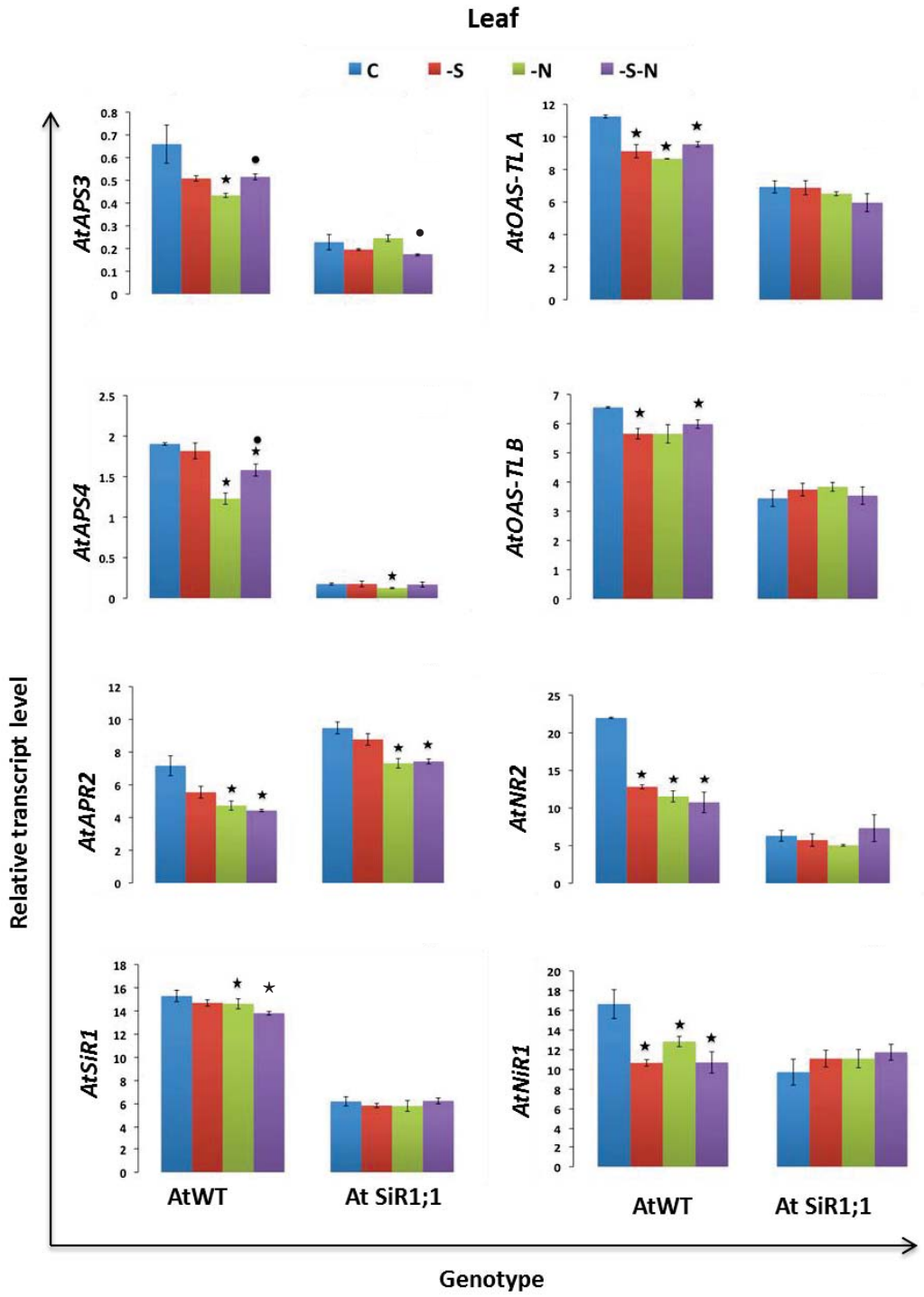

Figure 4.9 Transcriptional changes of genes in the S and N-assimilation pathways in response to S and/or N depletion of leaves of Arabidopsis WT and the *sir1-1 line*. As indicated, the transcript level for each gene relative to housekeeping genes *AtUBC9* and *At2g32170* was determined by qRT-PCR. Error bars represent mean, ±SEM, of three biological replicates where each biological replicate comprises of tissues pooled from four individual plants. "⋆" indicates statistically significant (P<0.05) differential expression as compared to control plants of the genotype. "•" indicates statistically significant (P<0.05) difference as compared to N-depleted treatment for the genotype. *AtAPS- adenosine 5'-triphosphate sulfurylase, AtAPR2- adenosine 5' phosphosulfate reductase 2, AtSiR1- sulfite reductase 1, AtOAS-TL A and B- O-acetylserine thiolyase A and B, AtNR2- nitrate reductase 2, AtNiR1- nitrite reductase1.*

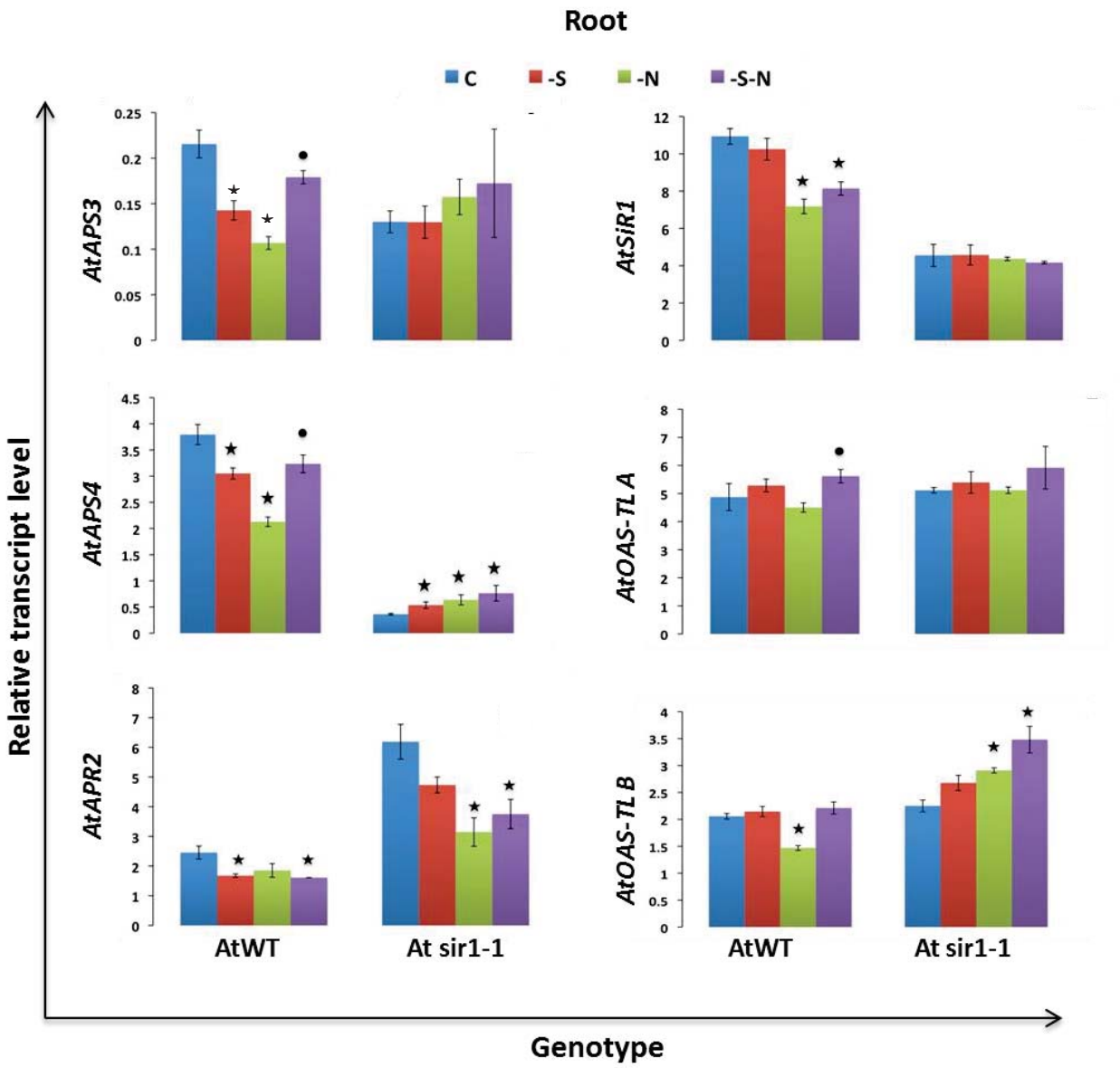

Figure 4.10 Transcriptional changes of genes in the S and N-assimilation pathways in response to S and/or N depletion of roots of Arabidopsis WT and the *sir1-1 line*. As indicated, the transcript level for each gene relative to housekeeping genes *AtUBC9* and *At2g32170* was determined by qRT-PCR. Error bars represent mean, ±SEM, of three biological replicates where each biological replicate comprises of tissues pooled from four individual plants. "⋆" indicates statistically significant (P<0.05) differential expression as compared to control plants of the genotype. "•" indicates statistically significant (P<0.05) difference as compared to N-depleted treatment for the genotype. . *AtAPS- adenosine 5'-triphosphate sulfurylase, AtAPR2- adenosine 5' phosphosulfate reductase 2, AtSiR1- sulfite reductase 1, AtOAS-TL A and B- O-acetylserine thiolyase A and B.*

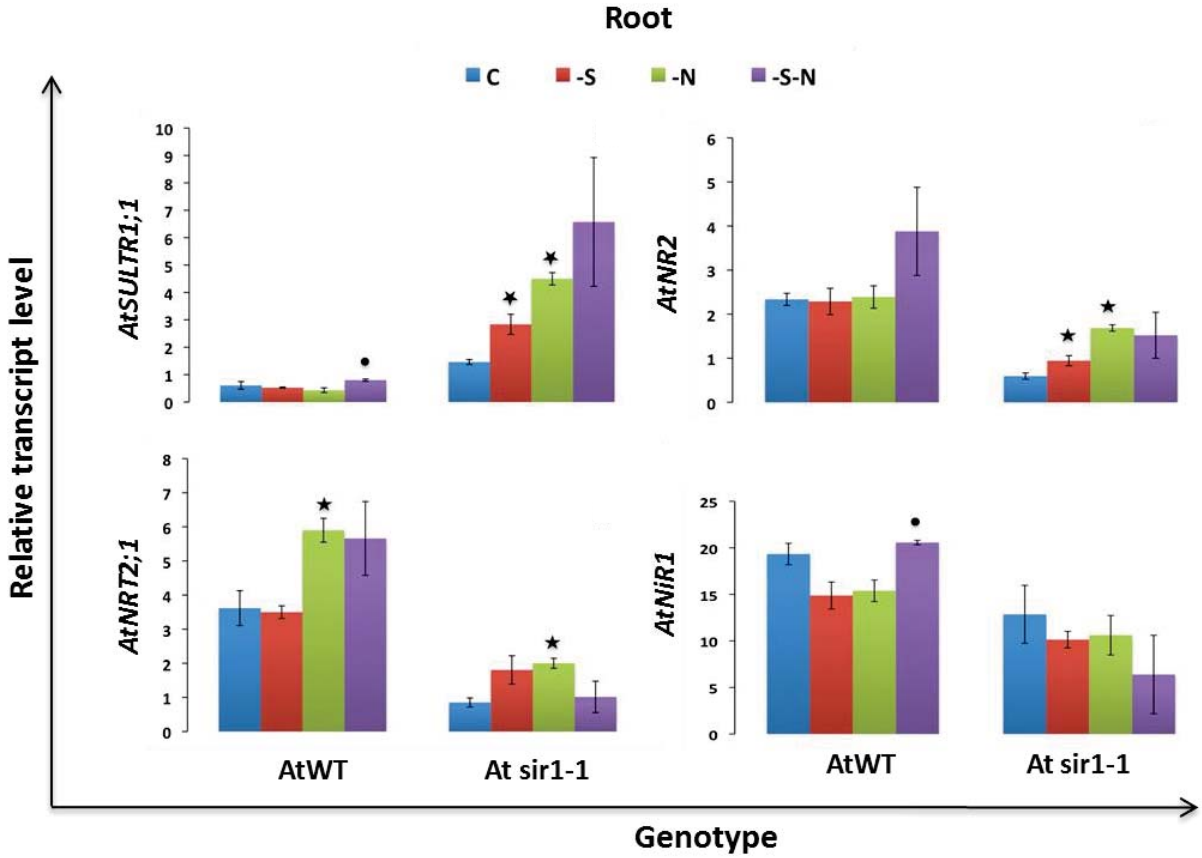

Figure 4.11 Transcriptional changes of genes in the S and N-assimilation pathways in response to S and/or N depletion of root of Arabidopsis WT and the *sir1-1 line*. As indicated, the transcript level for each gene relative to housekeeping genes *AtUBC9* and *At2g32170* was determined by qRT-PCR. Error bars represent mean, ±SEM, of three biological replicates where each biological replicate comprises of tissues pooled from four individual plants. "⋆" indicates statistically significant (P<0.05) differential expression as compared to control plants of the genotype. "•" indicates statistically significant (P<0.05) difference as compared to N-depleted treatment for the genotype. *AtSULTR1;1- sulfate transporter 1;1, AtNRT2;1- nitrate transporter 2;1, AtNR2- nitrate reductase 2, AtNiR1- nitrite reductase.*

4.7 Discussion

4.7.1 Recombinant AcSiR1 and AcNiR1 can reduce both sulfite and nitrite *in vitro*

In both micro-organisms as well as eukaryotes, S and N are taken up as SO_4^{2-} and NO_3^- respectively and are reduced by a series of enzyme-catalysed steps. A common feature in these pathways is the reduction of SO_3^{2-} and NO_2^- by very similar enzymes, sulfite reductase (SiR) and the nitrite reductase (NiR) (Krueger & Siegel, 1982). In higher plants, some enzyme redundancy, albeit with preferential reduction of either SO_3^{2-} and NO_2^-, has been shown in purified plant extracts of spinach (Krueger & Siegel, 1982). As discussed in the previous chapter (see section 3), in *A. cepa,* a preferentially sulfur accumulating species, the S-assimilation pathway does show a dependency on NO_3^- availability. Given the inhibition of the S-assimilation pathway genes in roots by NO_3^- depletion (Fig 3.4), post- translation the enzyme redundancy between AcSiR1 and AcNIR1 could have a further important role during N or S stress, where either enzyme is recruited to provide an increased reduction of SO_3^{2-} or NO_2^-. To test this hypothesis directly, recombinant AcSiR1 and AcNiR1 enzymes were used to establish functional redundancy. As discussed in the results, both genes were initially expressed without the plastidic signal sequence in the *E. coli* expression system. However, recombinant AcNiR1 did not show any activity for either NO_2^- or SO_3^{2-} as substrates. Following this, the putative signal sequence was included and an active recombinant AcNiR1 with functional redundancy with recombinant AcSiR1 was then obtained. An explanation for this may be that some of the amino acids immediately upstream of the predicted signal peptide cleavage site may be a part of the mature protein instead and so essential for correct folding and the activity. Following this, only the precursor protein was used to express recombinant AcNiR1. Recombinant AcSiR1 was active even without the signal peptide and was able to reduce both SO_3^{2-} and NO_2^- (Table 4.1). The recombinant enzymes showed higher specific activity for their physiological substrate with a reduced activity for the secondary substrate in each case. This indicates that although functional redundancy exists *in vitro,* the reduction of the secondary substrate in each case may be affinity dependent (Table 4.1). Studies done using purified SiR and NiR from spinach have shown similar results with SoSiR1 having a much lower K_m for SO_3^{2-}, at 1.2 x 10^{-2} mM, compared to 3.3 mM for NO_2^-. Similarly, for SoNiR1, the Km for NO_2^- was determined at 1.3 x 10^{-3} mM and at 0.8 mM for SO_3^{2-} (Crane & Getzoff, 1996).

Although similar kinetic parameters for AcSiR1 and AcNiR1 were not calculated in this study, such studies would help elucidate the possibility of cross-talk under changing SO_3^{2-} and NO_2^-, *in vivo.*

As the recombinant enzymes can reduce both the substrates, *in vitro*, the next step was to determine if this functional redundancy occurs as an additional point of interaction between the S and the N-assimilation pathway.

Any interaction between AcSir1 and AcNiR1 could be either indirect in the form of enzyme recruitment under S or N depletion to cope with additional requirement of reduced SO_4^{2-} and NO_3^-, or a direct interaction in the form of protein-protein complex formation.

The direct interaction was tested by studying protein-protein interactions *via* a solid phase binding assay and Isothermal Titration Calorimetry (ITC) (see section 2.4.4)

The indirect interaction was tested at the:

1) Transcriptional level, as changes in *AcSiR1* relative expression under the –N treatment and *AcNiR1* relative expression under the –S treatment in the leaves and roots of plants grown under the respective treatments in the factorial experiment (Figs 3.4, 3.6). A previously characterized *Arabidopsis SiR* T-DNA insertion line *sir1-1,* with reduced *SiR* expression as well as activity (Khan et al., 2010), was also used to determine changes in *AtNiR1* relative expression in response to short-term SO_4^{2-} deprivation (Fig 4.9 H, 4.10 D).

2) Translational level, as AcSiR1 and AcNiR1 protein accumulation in plants grown under the –N and the –S treatment in the factorial experiment, respectively (Figs 4.3, 4.4 B).

3) Post translational level as changes in enzyme activity of AcSiR1 and AcNiR1 in the leaves and roots of plants grown under the –N and the –S treatment respectively in the factorial experiment (Figs 4.3, 4.4 B).

4.7.2 The Direct interaction: AcSiR1 and AcNiR1 interaction might be redox regulated in *A. cepa*

Complex formation between enzymes of the same or different pathways has been shown as a regulatory mechanism in plants. For instance, enzymes catalysing the steps of the Calvin cycle can form a multienzyme complex comprising of five different enzymes: ribose-phosphate isomerase, phosphoribulokinase, ribulose-bisphosphae carboxylase/oxygenase, phosphoglycerate kinase and glyceraldehylde-phosphate dehydrogenase (Gontero et al., 1988). The complex regulation of the Calvin cycle is also brought about by individual enzymes interacting with other proteins inside the chloroplast, thus inducing the de-activation of phosphoribulokinase through interaction with a nuclear encoded chloroplast protein CP12 which further interacts with NAD(P)H-glyceraldehyde-3-phosphate dehydrogenase to form a tri-enzyme complex (Wedel et al.,1997). Protein-protein interactions also mediate various protective mechanisms in plants such as the interaction of heat-shock proteins with their target substrate proteins to ensure correct folding and activity of the substrate protein under elevated temperatures (Wang et al., 2004). Within the N and S-assimilation pathway, the cysteine synthase complex is one such well characterized example, and the regulatory mechanism of this has been explained in detail in the Introduction (see section 1.4.2.4). In *A. cepa,* AcATPS1 and AcAPSR1 have also been shown to form a complex *in vitro* (Cumming et al., 2007), although the significance of such a complex in the regulation of the pathway, *in vivo,* has not yet been tested. Given that AcSiR1 and AcNiR1 exhibit substrate redundancy and presumably are co-localized in the plastids due to the presence of plastid localization transit peptides as predicted *in silico* (http://www.cbs.dtu.dk/services/TargetP/), the idea of a complex formation between the two enzymes as a possible regulatory step for either or both assimilatory pathways is possible.

To test for any direct interaction between AcSiR1 and AcNiR1, a solid phase binding assay, performed as described in Cumming et al. (2007), led to an increase in absorbance when increasing amounts of recombinant AcSiR1 were incubated over a constant amount of bound recombinant AcNiR1. The saturation in absorbance increase was reached between 0.6-0.1ug suggesting a 1:1 stoichiometry, beyond which no increase in absorbance was measured (Fig 4.5) (see section 2.4.5). To check if AcNiR1 binds non-specifically to proteins, AcOASTL2 replaced AcSiR1 but no increase in absorbance was noted. This suggests that the binding observed between AcSiR1 and AcNiR1 was not due to any non-specific protein

interaction (Fig 4.6). Following this, a more sensitive measurement was conducted using ITC which is a tag free technique that measures the subtle changes occurring due to heat loss on mixing two biomolecules in solution, with respect to a reference cell with constant temperature (see section 2.4.4).

Although the solid phase suggested a positive interaction between AcSiR1 and AcNiR1, the ITC showed very little heat loss on mixing of recombinant AcNiR1 and AcSiR1 indicating no interaction (Fig 4.6).

The solid phase technique relies on adhering of the primary protein to the inert surface of the wells through hydrophobic interactions of the nonpolar amino acids (Biesiadecki & Jin, 2011). As such, there is a chance of non-specific binding of the secondary protein directly to the inadequately blocked regions of the polystyrene surface. However, a blocking step with a generic milk protein, casein, was included throughout the experiment to avoid any non-specific binding of the secondary protein to the wells. Another negative control with no primary protein added but with blocking of the complete well was also set up to test the efficiency of blocking. Here, absorbance was recorded at background level with no increase upon increasing the secondary protein suggesting that the increase seen in the test experiment is indeed due to some form of specific interaction between the AcSiR1 and AcNiR1. However under the conditions of the ITC procedure, no binding was observed between the two proteins. It is possible that adhering of AcNIR1 to the assay well somehow facilitated the binding to AcSiR1 in a specific manner, as AcOASTL2 did not show any binding under the same conditions. Both the solid phase and ITC experiments were repeated to confirm the results. To resolve this contradictory result, protocols leading to sample preparation were checked to see if there was any difference in buffer composition used in the two experiments. Interestingly, dithiothreitol (DTT) was used in the sample preparation for solid phase but not for ITC (see section 2.4.4). Although the implication of this difference still needs to be tested, it may be that the AcSiR1-AcNiR1 complex formation is redox regulated and the presence of DTT in solid phase experiments led to the required modification in either or both of the proteins resulting in a positive interaction.

Redox regulation of proteins by post-translational modification is an essential mechanism by which plants regulate metabolism and respond to an ever changing environment. This is mediated largely by reactive oxygen (ROS), reactive nitrogen (RNS) and reactive sulfur species (RSS) (Couturier, Chibani, Jacquot, & Rouhier, 2013). A new class of redox

regulation increasingly gaining importance in metabolic regulation is the cysteine based redox regulation mediated by the modification of key cysteine residues (Klomsiri et al., 2011). The sulfhydryl group of the cysteine residues present in proteins represents the most reduced state of sulfur in proteins, and has increasingly been found to be oxidized post-translationally leading to a change in catalytic activity or protein interaction (Klomsiri et al., 2011). A class of proteins found in both prokaryotes and eukaryotes, which is also involved in redox-regulation of proteins by reducing the disulfide-bridges present in certain cysteine containing proteins, is the glutaredoxin-theoredoxin family. In plants these proteins have been shown to post-translationally modulate the activity of many plastid localized membrane proteins including the protein translocon protein TIC55, the precursor NADPH:protochlorophyllide oxidoreductase translocon protein PTC52, and the lethal leaf spot protein LLS1 (Bartsch et al., 2008). Translation, *in silic*o of the *AcSiR1* and *AcNiR1* sequences reveal the presence of 10 and 11 cysteine residues, respectively, four of which are conserved across species between SiR and NiR and are the point of ligation for the 4Fe-4S cluster (Crane & Getzoff, 1996). But other than these, five other cysteine residues are largely conserved amongst the NiRs and four amongst the SiRs (Appendix 5). Hence the possibility of a cysteine based thioredoxin-glutaredoxin mediated redox regulation cannot be completely ruled out. Thus a parallel experiment run with and without DTT using both solid phase assay and ITC could remove ambiguity and confirm the possibility of a redox-regulated interaction between recombinant AcSIR1 and AcNiR1. In the longer term, confirmation of the AcSiR1-AcNiR1 complex *in vivo,* by imaging techniques such as bimolecular fluorescence complementation (BiFC) or Förster resonance energy transfer imagining (FRET imaging) may also be possible (Truong & Ikura, 2001; Bracha-Drori et al., 2004).

4.7.3 The Indirect interaction: AcNiR1 might be recruited into the S pathway under long term NO_3^- depletion in *A. cepa*

The expression, protein accumulation and activity pattern of AcSiR1 and AcNiR1 in the S x N factorial experiment was quite complex and has been summarised in Fig 4.12. In terms of enzyme recruitment in the S-assimilation pathway, AcNiR1 activity would be expected to increase to compensate for reduced AcSiR1 activity under a given treatment. Conversely, for recruitment into the N pathway, AcSiR1 activity would increase to compensate for reduction of AcNiR1 activity. However, it is equally possible that the enzyme recruitment may not be reflected in the enzyme activity as under a given treatment post translational modification in either AcSiR1 or AcNiR1 may alter the substrate affinity in favour of the secondary substrate, thus showing little or no change in activity for the primary substrate.

The transcriptional study showed that the relative expression of *AcSiR1* did not change significantly across the treatments in leaves at the pre-bulbing stage, with only a slight but significant decline in relative expression in the –S-N treatment. However, in the leaves from the bulbing stage, there was a significant reduction in the relative expression of *AcSiR1* in the –S treatment, with a trend towards a higher relative expression in the –N and the –S-N treatment (although, this was only significant for the -N treatment) (Fig 3.4). This may support the possibility of enzyme recruitment into the N pathway to compensate for reduced *AcNiR1* expression and activity. However, for the bulbing stage, this pattern of expression did not agree with the AcSiR1 activity and protein accumulation which was significantly ($p<0.05$) reduced under all three treatments when compared with the control. Interestingly, at the pre-bulbing stage in leaves, higher AcSiR1 accumulation was observed under the –N and the –S-N treatment, again indicating that this may contribute to nitrite reduction in the N pathway under N depletion. However, AcSiR1 activity declined in the –N treatment and was similar to control levels in the –S-N treatment. As discord between protein accumulation and enzyme activity could be a result of post-translational modification without altering the substrate specificity, it is hard to uncouple the changes in protein accumulation and activity from recruitment, from the factorial experiment alone. However, possible enzyme recruitment may occur in the S-assimilation pathway *via* AcNiR1, specifically in the roots at the bulbing stage, where AcSiR1 accumulation is below the limit of detection (under the –N treatment) or very low (under the –S-N treatment), but a

dramatic increase in AcSiR1 activity is observed (Fig 4.3 B). Under the same treatment in the roots, AcNiR1 accumulation is only slightly reduced at the pre-bulbing stage and higher at the bulbing stage. However, reduced activity is observed under both the treatments (Fig 4.4 B).

A future exploration of the correlation between *AcSiR1* and *AcNiR1* relative expression, protein accumulation and activity as well as post-transcriptional regulation possibly through yet unreported microRNA would help dissect the complexity of the transcription and translational pattern exhibited. In plants, S assimilation is regulated at the post transcriptional level by the interplay between the transcription factor SLIM1 and microRNA 395 (mR395) by regulating transcript abundance of *ATPS* and *SULTR2;1* (Kawashima et al., 2011). However, neither *SiR* nor *NiR* have been reported as a target for either *SLIM1* or mir395 suggesting that it is an unlikely explanation for this inconsistency between protein accumulation and enzyme activity.

In this thesis, the possibility of a cross-talk between AcSiR1 and AcNiR1 regulated by the increased demand for reduced cysteine or ammonia under limited S or N availability has been tested. However, given the cytotoxic nature of sulfite and nitrite, it is equally possible that under conditions of excess intercellular sulfite or nitrite, the SiR-NiR redundancy may operate as a rescue mechanism to scavenge sulfite/nitrite. In the S-assimilation pathway, one such scavenger, sulfite oxidase (Z. Xia et al., 2012), has been characterized in detail, but no such scavenger for nitrite other than nitrite reductase has yet been discovered in plants.

	PRE-BULBING			BULBING		
AcSiR1-Leaf						
	-S	**-N**	**-S-N**	**-S**	**-N**	**-S-N**
Gene						
Protein	0.09	2.94	5.07	0.15	0.68	0.48
Activity						
AcSiR1 Root						
	-S	**-N**	**-S-N**	**-S**	**-N**	**-S-N**
Gene						
Protein	2.81	ND	ND	1.32	ND	0.72
Activity						
AcNiR1-Leaf						
	-S	**-N**	**-S-N**	**-S**	**-N**	**-S-N**
Gene						
Protein	1.1	0.84	0.9	1.11	1.09	1.07
Activity					ND	ND
AcNiR1-Root						
	-S	**-N**	**-S-N**	**-S**	**-N**	**-S-N**
Gene						
Protein	1.02	0.97	0.86	1.02	1.09	1.26
Activity						

Significantly high
No change
Significantly low

Figure 4.12 AcSiR1 and AcNiR1 gene expression, protein accumulation and activity under the S x N factorial experiment. Statistically significant ($p<0.05$) changes are depicted with colours (refer colour key). For protein accumulation, numbers indicate relative intensity. as calculated by ImageJ software with accumulation in the control treatment being one.

It is important to note that the activity assays are not enzyme specific, and rather measure the cysteine made per unit time or NO_2^- reduced per unit time, and so it is hard to determine if the activity measured is solely that of AcSiR1 and AcNiR1 respectively. As the specific activity is much higher for a particular substrate in each case (Table 4.1), assays should be specific enough, although a change in substrate affinity due to post-translational modification cannot be ruled out. The inter-changeability of substrate affinity has been clearly illustrated in the work done by Nakayama et al (2000), where a single amino acid substitution at Arg-193 associated with SO_4^{2-} binding in recombinant maize SiR (ZmSiR), led to the inability of the enzyme to reduce SO_4^{2-} and a subsequent increase in affinity for NO_3^- reduction. No studies so far have looked to see if the same is true for NiRs as well, but it does raise an interesting question, given the structural and functional similarities between SiRs and NiRs. Would a post-translational modification in one or more of the conserved amino acids associated with nitrite binding in NiRs similarly lead to an increase in SO_4^{2-} affinity and reduction? Although there has been no direct evidence yet for post-translational modification of NiRs in plants, a large scale identification of proteins binding 14-3-3 proteins did reveal NiR as one of the putative partners as identified by yeast two hybrid screening (Shin et al., 2011). However, this could not be confirmed by immunoprecipitation experiments. 14-3-3 proteins regulate cellular processes by recognizing and binding to phosphoserine phosphorylated proteins (Muslin, Tanner, Allen, & Shaw, 1996). Large-scale identification of the rice and *Arabidopsis* proteome however, did not identify nitrite reductase as a phosphorylated protein (Nakagami et al., 2010) which may suggest that the 14-3-3 binding to NiR could be a false positive. Interestingly, phosphorylation of the both the subunits of the heterodimeric NiR in *Candida utilis* has been shown to modify the activity of the enzyme *in vivo* (Sengupta et al., 1997) suggesting the post-translational modification, leading to modified activity of AcNiR1, may also occur in plants but only under specific conditions. Apart from phosphorylation, other known means of post translational modification such as *S*-nitrosylation, sumoylation and ubiquitylation could also modify NiR activity in plants (Lindermayr & Durner, 2009; Miura & Hasegawa, 2010).

A post-translational mechanism might also explain the anomalous behaviour observed in *A. cepa* roots under the –N and the –S-N treatment where no AcSiR1 protein could be detected at the pre-bulbing stage, but a 3- to 4- fold higher activity was observed (Fig 4.3 B). The trend for AcSiR1 activity was the same at the bulbing stage with no protein being

detected under the –N treatment, although protein accumulation was observed under the –S-N treatment, but this was less than what was measured in the control. Interestingly, when AcNiR1 activity and accumulation was measured in the same tissue, a significant drop was observed in AcNiR1 activity but not in protein accumulation (Fig 4.4 B). It is however counter-intuitive to think that AcNiR1, the transcripts of which are highly down-regulated under the –S-N treatment, would be recruited into the S-pathway for SO_4^{2-} reduction under the –S and the –S-N treatment. As shown by the severe down-regulation of *AcHAST1;1LIKE1* and *AcAPSR1* and decline in methionine pools in the roots under the –N and the –S-N treatment, the S-assimilation pathway is more severely affected by NO_3^- depletion compared to SO_4^{2-} depletion and this may serve as a premise for post translational modification in AcNiR1 leading to higher SO_4^{2-} reduction (Fig 3.4, 3.6 A, C) (Fig 3.19).

A more direct means to resolve the occurance of interaction between AcSiR1 and AcNiR1 would be to knock-down the genes for either of the enzymes and then determine if the expression, accumulation and activity of the other is affected, especially under limiting SO_4^{2-} or NO_3^- conditions. Unfortunately, this could not be achieved for *A. cepa* due to un-predictability of transformation in *A. cepa* and limitations of time.

However, a T-DNA insertion *SiR1* knock-down line in *Arabidopsis (sir1-1)* was recently characterized by Khan et al., 2010 and was kindly gifted by Dr. Markus Wirtz. This served as a convenient tool to further explore if limited S-supply through reduced *AtSiR1* transcription and translation would lead to an up-regulation of *AcNiR1* expression or protein accumulation. As enzyme recruitment may be a transient process, a short-term S and/or N deprivation factorial experiment was set up where post 5 weeks of growth in complete media, plants were transferred into media lacking S, N and both S and N for 72 hours and then harvested as shoots and roots (section 2.1). At the transcriptional level, a 72 hour S-deprivation (-S) treatment did not elevate *AtNiR1* expression in the *sir1-1* line, (Fig 4.9 H, 4.11 D). In fact, there was no significant ($p<0.05$) change in *AtNiR1* expression under any treatment. In contrast, no up-regulation was seen in *AcSiR1* transcripts under the –N treatment in the *sir1-1* line (Fig 4.9 D). This suggests that any recruitment, if occurring at all, is not transcriptionally regulated. As antibodies raised against AcNiR1 also cross-reacted with AtNiR1, protein accumulation of AtNiR1 was also determined in WT as well as *sir 1-1* line under all four treatments (Appendix 12). Contrary to the *AtNiR1* expression in the WT plants, where transcripts were reduced significantly ($p<0.05$) under all three treatments, AtNiR1protein accumulated in all three treatments (-S, -N and –S-N), when compared to accumulation in the control treatment, suggesting some form of post-transcriptional

regulation. However, in the *sir1-1* plants, although no change was observed in the *AtNiR1* expression, accumulation of protein declined under the –S and the –S-N treatment suggesting a SO_4^{2-} deprivation specific response. However, the consequence of this in terms of AcNiR1 activity could not be determined due to limited tissue available (Appendix 4).

Apart from *AtSiR1 and AtNiR1,* the relative expression of other genes involved in the S and N-assimilation pathway was also investigated. This included *AtSULTR1;1, AtATPS3, AtAPS4, AtAPR2, AtOAS-TLA, AtOAS-TLB* in the S-assimilation pathway and *AtNRT2;1* and *AtNR2* in the N-assimilation pathway. Interestingly, the impact of S-deprivation was not very significant on the WT plants as *AtSULTR1;1* and *AtAPR2* transcripts did not show any up-regulation under the experimental conditions (Fig 4.9 C, Fig 4.11 A). However, a small but significant increase was observed in the *AtSULTR1;1* transcripts in the roots, under the –S-N treatment (Fig 4.11 A). This is different to the expression profile observed in experiments done by Hirai et al., 2003 where three week old *Arabidopsis* plants were deprived of S for 48 h. This may be explained by the differences in the experimental setup between the two studies. In experiments done by Hirai et al., plants were grown for three weeks under long day conditions, whereas in this study *Arabidopsis* plants were grown under short-day conditions for five weeks before the onset of treatment. This difference in age and day-length may explain the dampened effect of S-deprivation. Having said that, Rouached et al. (2008) investigated the regulation of *AtSULTR1;1* and *AtSULTR1;2* under varying abiotic stresses and showed that *AtSULTR1;1* transcripts accumulated approximately 4-fold in the first 72 hours of S-deprivation (Fig 4.11 A). The experimental conditions described in the paper are similar to those used in this study, but the experiment was conducted hydroponically whereas in this study a mixture of vermiculite: perlite mixture was used (Fig 4.7) (Section 2.1.2). Although care was taken to wash the vermiculite twice with the respective treatment media, it is possible that not all the media was completely replaced and so some S may still have been available to the plants. Interestingly, the *sir1-1* line did seem to respond more rapidly when compared to WT plants in all the treatments, as *AtSULTR1;1* was highly up-regulated in all the three treatments. However, under the –S treatment, this effect was not evident down-stream as no change was observed in the transcripts of *AtAPS3, AtAPS4, AtAPR2* and *AtSIR1* in the leaf tissue (Fig 4.11 A, Fig 4.9 A, B, C). Accumulation of *O*AS on S-deprivation positively regulates the response of *AtSULTR1;1* and *AtAPR2.* This response might be dependent on a threshold accumulation of *O*AS, beyond which *AtSULTR1;1* and *AtAPR* are up-regulated. In *sir1-1* plants, as *O*AS accumulates even under sulfur sufficient conditions due to low AtSiR1 activity, it may already be at the

threshold limit and is therefore more sensitive to sulfate deprivation. However, there is no consequent up-regulation of *AtAPR2 implying* that the excess of sulfate may be directed to the PAPS pathway *via AtAPSK* (Fig 4.9 C). Measuring the expression of other *AtAPR* as well as *AtAPSK via* qRT-PCR would confirm if excess sulfate being taken up is being diverted to PAPS synthesis and then conversion to glucosinolates.

Although the results from the study do not establish conclusively if the interaction between SiR and NiR occurs *in vivo,* it does provide a basis for speculation as to how this interaction might work. Whether it would have any regulatory function in the S or N pathway under nutrient stress is yet to be investigated.

Chapter 5: General Discussiohn

The main objective of this thesis was to determine the extent of interdependency between the S and N-assimilation pathways at the transcriptional and the metabolite level by quantifying the expression of key genes, accumulation and activity of specific enzymes and accumulation of metabolites under S and/or N limiting conditions. A secondary objective of this thesis was to explore the specific cross-talk between the S and N-assimilation pathways as a direct or indirect interaction between AcSiR1 and AcNiR1.

The up-regulation of the transcript abundance of the genes associated with S-assimilation pathway genes in both the root and the shoot tissue under the –S treatment was observed to be dependent on NO_3^- availability (Fig 3.4-3.7). Moreover, the transcriptional up-regulation of the S-assimilation pathway was not dependent on *O*AS accumulation (Fig 3.19), suggesting a disconnect in the feed-back inhibition of the pathway commonly present in other plant species studied so far (Nakamura et al., 1999; Urano et al., 2000; Berkowitz et al., 2002).

Masking of this S limitation response *via* inhibition of up-regulation of the S-starvation marker genes *AcHAST1;1LIKE1* and *AcAPSR1* was also observed under the –S-N treatment in the roots which subsequently also led to a decline in S-containing metabolites in the leaf tissue as well as the pseudo-stem/bulb tissue(Fig 3.4-3.7; 3.19)(fig 3.17-18). The N-assimilation pathway was also affected by S limitation which was reflected in the exclusive amino acid accumulation in the pseudo-stem and bulb (Table 3.3-3.4).

A more specific investigation with regards to cross-talk between the S and N-assimilation pathway was also undertaken by measuring the redundancy and interaction between AcSiR1 and AcNiR1, *in vitro*. Both the recombinant enzymes were found to be functionally redundant with a higher specific activity for the physiological substrate in each case (Table 4.1). This corroborated the premise for enzyme recruitment between the S and N pathway under high reduced N or S demand. A direct interaction between the two recombinant proteins, however, was supported by the solid phase binding assay but not by ITC (Fig 4.5-4.6). This suggests that even the functional redundancy between AcSiR1 and AcNiR1 may lead to an indirect interaction between the S and N-assimilation pathway but not necessarily through a direct interaction between the two proteins.

Thus based on the results described in this thesis, a tentative model of S and N interactions in *A. cepa* under S or N limiting conditions has been proposed. The model suggests a feed-forward mechanism for cysteine accumulation which is driven by the N-assimilation pathway through a feedback insensitive/less sensitive SAT. There are a lot of known factors regulating the pathway such as microRNA395, transcription factor *SLIM1* and *HY5* and other *MYB* factors (Jonassen et al., 2008; Kawashima et al., 2011) that have not been added to the model for the sake of simplicity. The interactions proposed in the pathway may well be regulated by these factors. However, the extent of their regulation in *A. cepa* still needs to be determined.

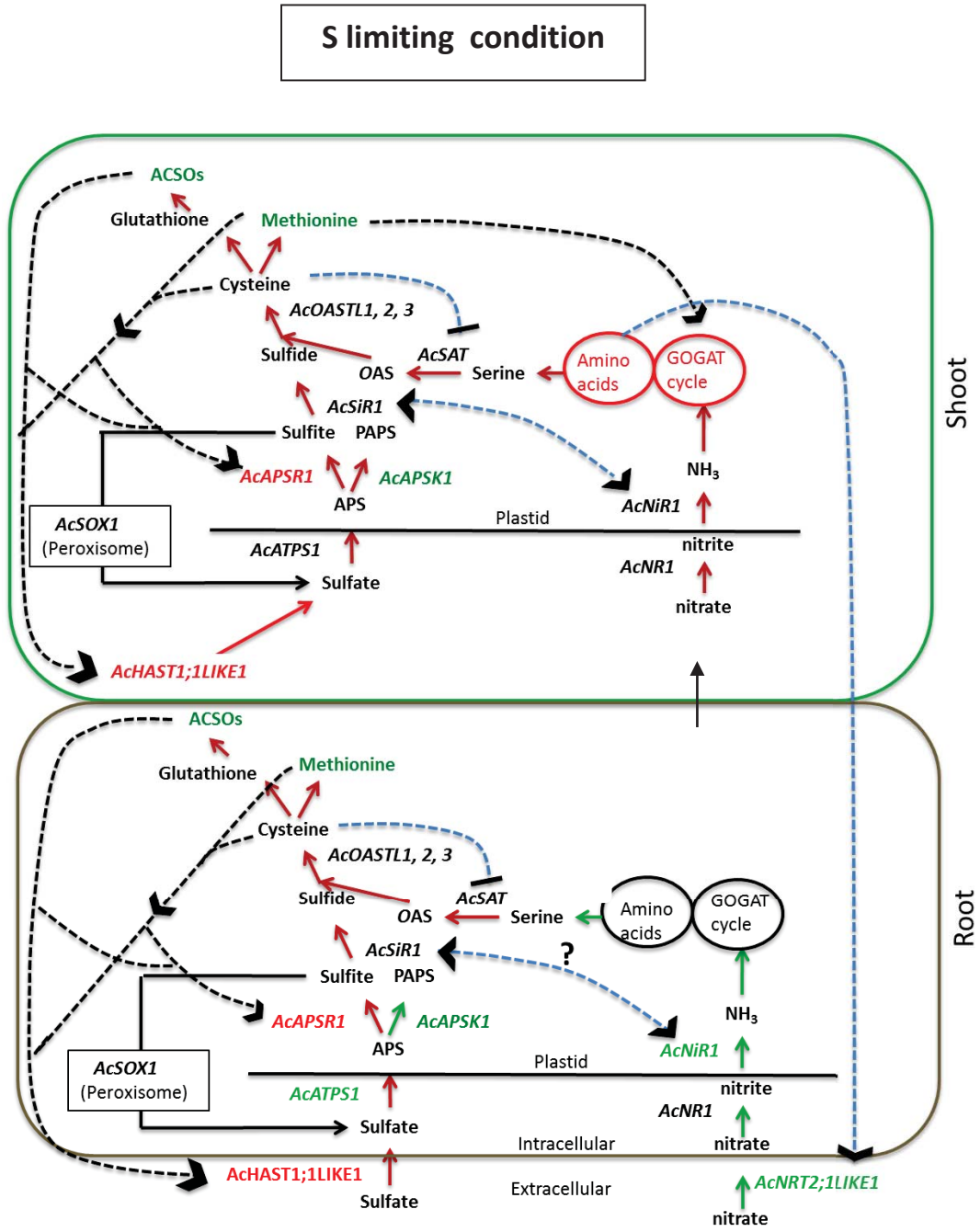

Figure 5.1 Proposed model of the putative interactions between the S and N-assimilation pathways in *A. cepa* root and shoot under S limiting conditions. Higher relative accumulation of genes and metabolites is indicated in red and lower relative accumulation in green. Increased flux in a preferential direction is indicated by red arrow and decline by green. The proposed interactions at the transcriptional level are indicated in black discontinuous lines with the arrow indicating the direction of regulation. The proposed interactions at the enzyme activity level are indicated in blue discontinuous lines. Interaction lines ending in (-) Indicates disruption in interaction.

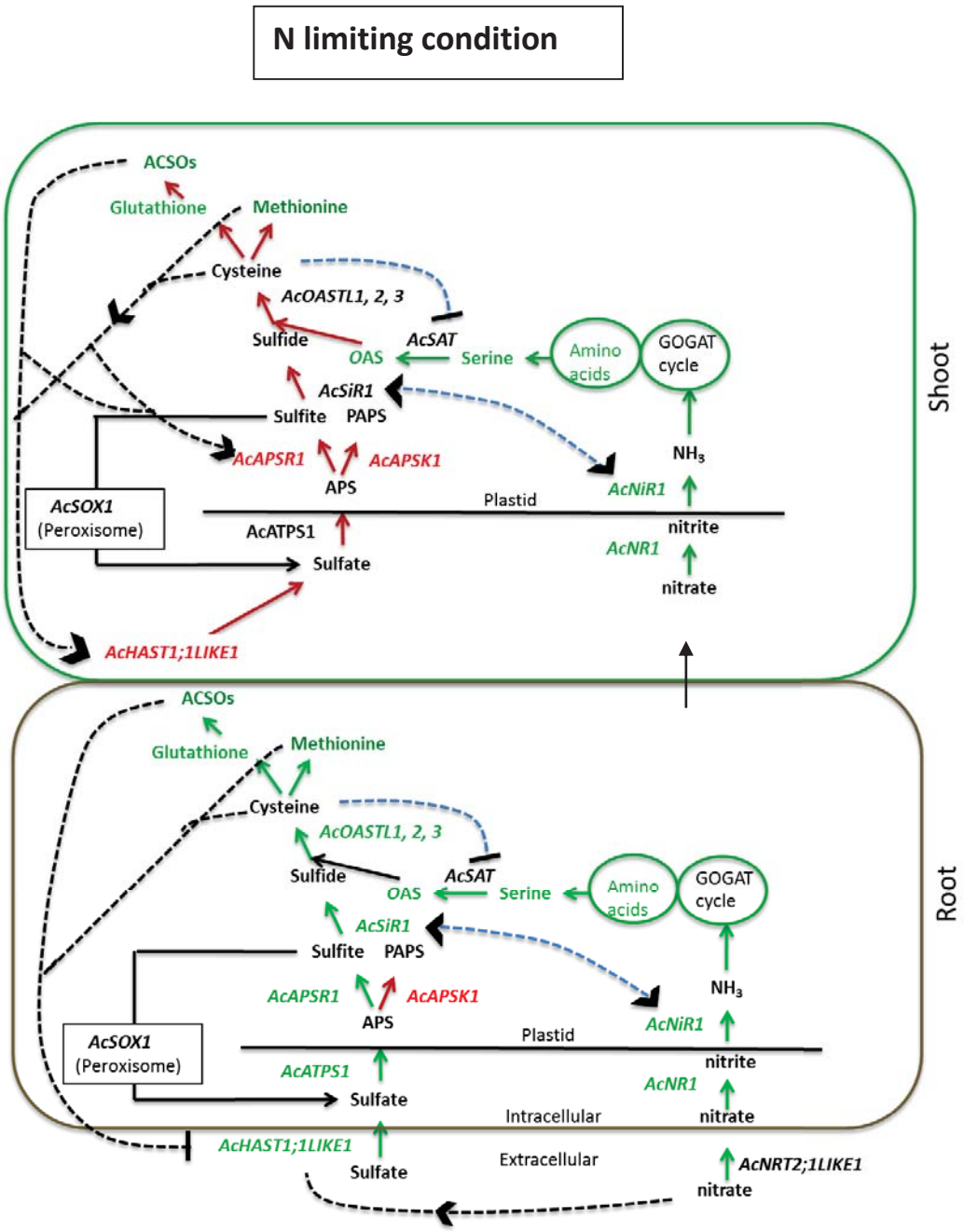

Figure 5.2 Proposed model of the putative interactions between the S and N-assimilation pathways in *A. cepa* root and shoot under N limiting conditions. Higher relative accumulation of genes and metabolites is indicated in red and lower relative accumulation in green. Increased flux in a preferential direction is indicated by red arrow and decline by green. The proposed interactions at the transcriptional level are indicated in black discontinuous lines with the arrow indicating the direction of regulation. The proposed interactions at the enzyme activity level are indicated in blue discontinuous lines. . Interaction lines ending in (-) Indicates disruption in interaction.

.

The proposed model (Fig 5.1, 5.2) describes the possibility of a feed-forward regulation, not under the regulation of *O*AS. However, SAT which forms a complex with *O*ASTL, is also feed-back regulated by cysteine, thus inhibiting the formation of excess *O*AS under non S-limiting conditions where otherwise a higher flux to cysteine would be achieved (Hawkesford & De Kok, 2006). As described by Hawkesford et al. (2006) under such a mechanism, no *O*AS accumulation would occur. Indeed no *O*AS accumulation was observed in the S x N factorial experiment under any of the treatments (Fig 3.19). Therefore, the feed-forward mechanism for cysteine biosynthesis predicts the existence of a cysteine insensitive or less sensitive SAT isoform. Interestingly, a SAT isoform has already been characterized for *A. tuberosum* which exhibits much less sensitivity to inhibition by cysteine (49.7 µM for 50% inhibition) compared to other plant species studied so far (*ca.* 5 µM) (Urano et al., 2000). Given that *A. tuberosum* species accumulates a much higher level of cysteine compared to other species such as *Arabidopsis* and tobacco, the SAT isoform characterized might be responsible for the high accumulation (Urano et al., 2000).

In *A. cepa,* one SAT isoform has been characterized to date which shares 70% identity with SAT5 from *Arabidopsis* and 97% identities with SAT1 from *A. tuberosum* (McManus et al., 2005). However, a cysteine inhibition assay showed 50% inhibition of activity at 3.1 µM cysteine for the *A. cepa* isoform, which is in a similar range as other feed-back sensitive SATs in other plant species (Urano et al., 2000). This indicates that there must be other less cysteine sensitive isoform(s) of SAT present in *A. cepa* genome. Indeed, screening the available Allium cepa CUDHLF2_13740 transcriptome assembly against the *A. tuberosum* SAT5 in the NCBI database revealed some potential candidates (Accession no: GBR001027229 and GBRN01068012) that can be further characterized to test cysteine inhibition dependency.

The apparent dependency of S assimilation on N availability also raises some interesting questions and speculations regarding the domestication history of this ancient crop. There is no clear indication as to when exactly domestication of *A. cepa* began, but its mention in the recorded history dates back to over 4000 years ago making it one of the earliest vegetables to be domesticated (Fritsch & Friesen, 2002). Over the past 4000 years, *A. cepa* has been extensively selected for bigger bulbs with more flavour, which at the biochemical level translates to an S-assimilation pathway with higher flux for cysteine and cysteine derived sulfoxides. However, the flavour precursors in *A. cepa* not only have sulfur, but also

nitrogen as a constituent. Therefore it is worth speculating if by selecting for bulbs rich in S and N containing flavour precursors, *A. cepa* has also been indirectly selected for an increasingly N-dependent S-assimilation pathway? Added to this, the increasing use of N-fertilizers in farming practices would have only reinforced this selection towards greater N-dependency and subsequently, lower N use efficiency. Indeed, an extensive study done by Vitousek et al., (1997), suggested that the increasing use of fossil fuels and N-fertilization in agriculture has led to an alteration of the natural N cycle leading in part to an accelerated loss of plant species adapted to efficient use of nitrogen (Vitousek & Aber, 1997). Other independent studies conducted across the globe, as summarized by Berendse et al have also found a negative correlation between N load and species diversity with more nitrophilous species replacing the more diverse N efficient species such as seen in the composition of herb layer in the forests of Central Europe and southern Sweden (Berendse et al., 1993).

Ideally, a comparison with ancestral parental species or wild un-cultivated relatives of *A. cepa* would reveal differences, if present, in the S-assimilation pathway regulation. Unfortunately, the evolutionary lineage of *A. cepa* is still highly debated and over collecting of the wild species has led to a severe loss of the wild relatives of this species. However, the subgenera *Amerallium* and *Melanocrommyum* are considered to be more ancient lines (Reinhard M Fritsch & Friesen, 2002) and may hold clues to the effect of domestication of the S-assimilation pathway of *A. cepa* and other commercially important members of this genus such as garlic, chives, leeks and bunching onions.

More work characterising the SAT-binding domain deficient *O*ASTL (*O*ASTL1), along with SAT-binding *O*ASTL2 and *O*ASTL3 is underway to determine the localization of these proteins as well as the role of SAT-binding domain *O*ASTL in cysteine synthesis. A preliminary screening of Allium cepa CUDHLF2_13740 transcriptome assembly has revealed putative members of the SAT family, some of which are highly similar to the cysteine resistant *A. tuberosum* SAT. These would be further characterized to establish their sensitivity to cysteine and subsequent role in feed-forward mechanism (McManus et al, unpublished).

Tissues from the S x N factorial experiment were also used to generate an untargeted metabolome. This is currently being analysed to further resolve the intricacy of S and N interactions, along with mapping a global picture of different tissues in *A. cepa* under S and/or N depleted conditions and response to bulbing. Preliminary screening of the untargeted metabolome has shown the accumulation of a number of known beneficial bioactives and so more work cataloguing these nutritionally important metabolites and changes in their accumulation under S and/or N depletion would be done.

To resolve the SiR-NiR interaction, preliminary experiments will be done to understand the effect of DTT as a reducing agent on the protein-protein interaction. As AcNiR1 specific anti-body is now available, specificity of the interaction with increasing recombinant AcNiR1 incubation over bound recombinant AcSiR1 also needs to be determined. Fluorescence tag based interaction assay, may also be done to test for direct interaction *in vivo.* Kinetic parameters and substrate specificity of recombinant *Ac*SiR1 and *Ac*NiR1 for both sulfite and nitrite also need to be determine

References

A. Khan Nafees, Sarvajeet, S., & Shahid, U. (2008). Sulfur Assimilation and Abiotic Stress in Plants. Retrieved from http://books.google.co.nz/books?id=NSdKAAAAQBAJ&dq=sulfur+in+plants+dry+weight&source=gbs_navlinks_s

Aitken, A. ., & Hewett, E. . (2014). *Fresh Facts. New zealand horticulture 2014* (p. 2). The New Zealand institue for Plant and Food Reasearch Ltd. Retrieved from http://www.freshfacts.co.nz/file/fresh-facts-2014.pdf

Awazuhara, M., Fujiwara, T., Hayashi, H., Watanabe-Takahashi, A., Takahashi, H., & Saito, K. (2005). The function of SULTR2;1 sulfate transporter during seed development in Arabidopsis thaliana. *Physiologia Plantarum*, *125*(1), 95–105. doi:10.1111/j.1399-3054.2005.00543.x

Bao, S., An, L., Su, S., Zhou, Z., & Gan, Y. (2011). Expression patterns of nitrate, phosphate, and sulfate transporters in Arabidopsis roots exposed to different nutritional regimes. *Botany*, *89*(9), 647–653. doi:10.1139/b11-053

Bartsch, S., Monnet, J., Selbach, K., Quigley, F., Gray, J., von Wettstein, D., … Reinbothe, C. (2008). Three thioredoxin targets in the inner envelope membrane of chloroplasts function in protein import and chlorophyll metabolism. *Proceedings of the National Academy of Sciences of the United States of America*, *105*(12), 4933–4938.

Berendse, F., Aerts, R., & Bobbink, R. (1993). Atmospheric nitrogen decomposition and its impact on terrestrial ecosystem. In C. C. Vos & P. Opdam (Eds.), *Landscape Ecology of a Stressed Environment* (pp. 104–121). Springer Netherlands.

Berkowitz, O., Wirtz, M., Wolf, A., Kuhlmann, J., & Hell, R. (2002). Use of biomolecular interaction analysis to elucidate the regulatory mechanism of the cysteine synthase complex from Arabidopsis thaliana. *The Journal of Biological Chemistry*, *277*(34), 30629–34. doi:10.1074/jbc.M111632200

Bi, Y.-M., Wang, R.-L., Zhu, T., & Rothstein, S. J. (2007). Global transcription profiling reveals differential responses to chronic nitrogen stress and putative nitrogen regulatory components in Arabidopsis. *BMC Genomics*, *8*, 281.

Bick, J. a, Aslund, F., Chen, Y., & Leustek, T. (1998). Glutaredoxin function for the carboxyl-terminal domain of the plant-type 5'-adenylylsulfate reductase. *Proceedings of the National Academy of Sciences of the United States of America*, *95*(14), 8404–9. Retrieved from http://www.pubmedcentral.nih.gov/articlerender.fcgi?artid=1887594&tool=pmcentrez&rendertype=abstract

Bieker, S., & Zentgraf, U. (2013). Plant Senescence and Nitrogen Mobilization and Signaling, Senescence and Senescence-Related Disorders, Dr. Wang Zhiwei (Ed.), ISBN: 978-953-51-0997-6, InTech, DOI: 10.5772/54392. Available from: http://www.intechopen.com/books/senescence-and-senescence-related-disorders/plant-senescence-and-nitrogen-mobilization-and-signaling

Biesiadecki, B. J., & Jin, J.-P. (2011). A high-throughput solid-phase microplate protein-binding assay to investigate interactions between myofilament proteins. *Journal of Biomedicine & Biotechnology*, *2011*, 421701. doi:10.1155/2011/421701

Bracha-Drori, K., Shichrur, K., Katz, A., Oliva, M., Angelovici, R., Yalovsky, S., & Ohad, N. (2004). Detection of protein-protein interactions in plants using bimolecular fluorescence complementation. *The Plant Journal*, *40*(3), 419–427. doi:10.1111/j.1365-313X.2004.02206.x

Bradford, M. (1976). Rapid and Sensitive Method for Quantification of Microgram Quantities of Protein utilizing principle of Protein-Dye-Binding. *Analytical Biochemistry*, *72*(1-2), 248–254.

Brewster, J. L., & Butler, H. A. (1989). Effects of Nitrogen Supply on Bulb Development in Onion Allium cepa L ., *40*(219), 1155–1162.

Brodnitz, M., & Pascale, J. (1971). Thiopropanal S-oxide: a lachrymatory factor in onions. *Journal of Agricultural and Food Chemistry*, *19*(2), 269–72.

Brychkova, G., Grishkevich, V., Fluhr, R., & Sagi, M. (2013). An essential role for tomato sulfite oxidase and enzymes of the sulfite network in maintaining leaf sulfite homeostasis. *Plant Physiology*, *161*(1), 148–64. doi:10.1104/pp.112.208660

Brychkova, G., Xia, Z., Yang, G., Yesbergenova, Z., Zhang, Z., Davydov, O., … Sagi, M. (2007). Sulfite oxidase protects plants against sulfur dioxide toxicity. *The Plant Journal*, *50*(4), 696–709. doi:10.1111/j.1365-313X.2007.03080.x

Brychkova, G., Yarmolinsky, D., Ventura, Y., & Sagi, M. (2012). A novel in-gel assay and an improved kinetic assay for determining in vitro sulfite reductase activity in plants. *Plant & Cell Physiology*, *53*(8), 1507–16. doi:10.1093/pcp/pcs084

Buchner, P., Parmar, S., Kriegel, A., Carpentier, M., & Hawkesford, M. J. (2010). The sulfate transporter family in wheat: tissue-specific gene expression in relation to nutrition. *Molecular Plant*, *3*(2), 374–89. doi:10.1093/mp/ssp119

Cao, M.-J., Wang, Z., Wirtz, M., Hell, R., Oliver, D. J., & Xiang, C.-B. (2013). SULTR3;1 is a chloroplast-localized sulfate transporter in Arabidopsis thaliana. *The Plant Journal : For Cell and Molecular Biology*, *73*(4), 607–16. doi:10.1111/tpj.12059

Carson, F. ., & Wong, F. F. (1961). The Volatile Flavor Components of Onions. *Journal of Agricultural and Food Chemistry*, *9*(2), 140–143.

Castaings, L., Camargo, A., Pocholle, D., Gaudon, V., Texier, Y., Boutet-Mercey, S., … Krapp, A. (2009). The nodule inception-like protein 7 modulates nitrate sensing and metabolism in Arabidopsis. *The Plant Journal : For Cell and Molecular Biology*, *57*(3), 426–35. doi:10.1111/j.1365-313X.2008.03695.x

Cavallito, C. J., & John, A. N. (1944). Allicin, the Antibacterial Principle of Allium satioum. I. Isolation, Physical Properties and Antibacterial Action. *Journal of the American Chemical Society*, *66*(11).

Chantarotwong, W., Huffaker, R. C., Miller, B. L., & Granstedt, R. C. (1976). In vivo nitrate reduction in relation to nitrate uptake, nitrate content, and in vitro nitrate reductase activity in intact barley seedlings. *Plant Physiology*, *57*(4), 519–22. Retrieved from http://www.pubmedcentral.nih.gov/articlerender.fcgi?artid=542064&tool=pmcentrez&rendertype=abstract

Chu, V. T., Gottardo, R., Raftery, A. E., Bumgarner, R. E., & Yeung, K. Y. (2008). MeV+R: using MeV as a graphical user interface for Bioconductor applications in microarray analysis. *Genome Biology*, *9*(7), R118. doi:10.1186/gb-2008-9-7-r118

Clarkson, D. T., Saker, L. R., & Purves, J. V. (1989). Depression of Nitrate and Ammonium Transport in Barley Plants with Diminished Sulphate Status . Evidence of Co-regulation of Nitrogen and Sulphate Intake, *40*(218), 953–963.

Couturier, J., Chibani, K., Jacquot, J.-P., & Rouhier, N. (2013). Cysteine-based redox regulation and signaling in plants. *Frontiers in Plant Science*, *4*(April), 105. doi:10.3389/fpls.2013.00105

Crane, B. R., & Getzoff, E. D. (1996). The relationship between structure and function for the sulfite reductases. *Current Opinion in Structural Biology*, *6*(6), 744–56. Retrieved from http://www.ncbi.nlm.nih.gov/pubmed/8994874

Crawford, N. M. (1995). Nitrate: nutrient and signal for plant growth. *The Plant Cell*, *7*(7), 859–68. doi:10.1105/tpc.7.7.859

Cumming, M., Leung, S., McCallum, J., & McManus, M. T. (2007). Complex formation between recombinant ATP sulfurylase and APS reductase of Allium cepa (L.). *FEBS Letters*, *581*(22), 4139–47. doi:10.1016/j.febslet.2007.07.062

Drew, M. (1975). Comparison of the effects of a localised supply of phosphate, nitrate, ammonium and potassium on the growth of the seminal root system, and the shoot, in barley. *New Phytologist*. Retrieved from http://onlinelibrary.wiley.com/doi/10.1111/j.1469-8137.1975.tb01409.x/abstract

Drew, M. C., & Saker, L. R. (1978). Nutrient Supply and the Growth of the Seminal Root System in Barley, *29*(109), 435–451.

Droux, M., Ruffet, M. L., Douce, R., & Job, D. (1998). Interactions between serine acetyltransferase and O-acetylserine (thiol) lyase in higher plants--structural and kinetic properties of the free and bound enzymes. *European Journal of Biochemistry / FEBS*, *255*(1), 235–45. Retrieved from http://www.ncbi.nlm.nih.gov/pubmed/9692924

Durenkamp, M., De Kok, L. J., & Kopriva, S. (2007). Adenosine 5'-phosphosulphate reductase is regulated differently in Allium cepa L. and Brassica oleracea L. upon exposure to H2S. *Journal of Experimental Botany*, *58*(7), 1571–9. doi:10.1093/jxb/erm031

Eady, C. C., Kamoi, T., Kato, M., Porter, N. G., Davis, S., Shaw, M., … Imai, S. (2008). Silencing onion lachrymatory factor synthase causes a significant change in the sulfur secondary metabolite profile. *Plant Physiology*, *147*(4), 2096–106. doi:10.1104/pp.108.123273

Feldman-Salit, A., Wirtz, M., Hell, R., & Wade, R. C. (2009). A mechanistic model of the cysteine synthase complex. *Journal of Molecular Biology*, *386*(1), 37–59. doi:10.1016/j.jmb.2008.08.075

Ferreira, R. M., & Teixeira, a R. (1992). Sulfur starvation in Lemna leads to degradation of ribulose-bisphosphate carboxylase without plant death. *The Journal of Biological Chemistry*, *267*(11), 7253–7. Retrieved from http://www.ncbi.nlm.nih.gov/pubmed/1559969

Forde, B. G., & Lea, P. J. (2007). Glutamate in plants: metabolism, regulation, and signalling. *Journal of Experimental Botany*, *58*(9), 2339–58. doi:10.1093/jxb/erm121

Friesen, N., & Fragman-sapir, O. (2014). A new Allium species from section Molium from Israel: A. akirense (Amaryllidaceae). *Phytotaxa*, *173*(May), 140–148.

Fritsch, R. M., & Friesen, N. (2002). *Allium crop science: Recent advances*. CAB International.

Fritsch, R. M., & Friesen, N. (2002). *Allium crop science: recent advances.* CAB International. Retrieved from http://www.cabdirect.org/abstracts/20023117383.html

Gan, Y., Bernreiter, A., Filleur, S., Abram, B., & Forde, B. G. (2012). Overexpressing the ANR1 MADS-box gene in transgenic plants provides new insights into its role in the nitrate regulation of root development. *Plant & Cell Physiology*, *53*(6), 1003–16. doi:10.1093/pcp/pcs050

Girin, T., Lejay, L., Wirth, J., Widiez, T., Palenchar, P. M., Nazoa, P., … Lepetit, M. (2007). Identification of a 150 bp cis-acting element of the AtNRT2.1 promoter involved in the regulation of gene expression by the N and C status of the plant. *Plant, Cell & Environment*, *30*(11), 1366–80. doi:10.1111/j.1365-3040.2007.01712.x

Gontero, B., Cardenas, M. L., & Ricard, J. (1988). A functional five-enzyme complex of chloroplasts involved in the Calvin cycle. *European Journal of Biochemistry / FEBS*, *173*, 437–443. Retrieved from http://onlinelibrary.wiley.com/doi/10.1111/j.1432-1033.1988.tb14018.x/full

Gruhlke, M. C. H., & Slusarenko, A. J. (2012). The biology of reactive sulfur species (RSS). *Plant Physiology and Biochemistry : PPB / Société Française de Physiologie Végétale*, *59*, 98–107. doi:10.1016/j.plaphy.2012.03.016

Hänsch, R., Lang, C., Rennenberg, H., & Mendel, R. R. (2007). Significance of plant sulfite oxidase. *Plant Biology (Stuttgart, Germany)*, *9*(5), 589–95. doi:10.1055/s-2007-965433

Hawkesford, M. J. (2003). Minireview Transporter gene families in plants : the sulphate transporter gene family Ð redundancy or specialization ? *Physiologia Plantarum*, 155–163.

Hawkesford, M. J., & De Kok, L. J. (2006). Managing sulphur metabolism in plants. *Plant, Cell and Environment*, *29*(3), 382–395.

Hawkesford, M. J., & De kok, L. J. (Eds.). (2007). *Sulfur in Plants: An Ecological Perspective Volume 6 of Plant Ecophysiology*. Springer Science & Business Media.

Heeg, C., Kruse, C., Jost, R., Gutensohn, M., Ruppert, T., Wirtz, M., & Hell, R. (2008). Analysis of the Arabidopsis O-acetylserine(thiol)lyase gene family demonstrates compartment-specific differences in the regulation of cysteine synthesis. *The Plant Cell*, *20*(January), 168–185. doi:10.1105/tpc.107.056747

Hell, È. (1997). Review Molecular physiology of plant sulfur metabolism, *49*, 138–148.

Hermans, C., Hammond, J. P., White, P. J., & Verbruggen, N. (2006). How do plants respond to nutrient shortage by biomass allocation? *Trends in Plant Science*, *11*(12), 610–7. doi:10.1016/j.tplants.2006.10.007

Hesse, H., Nikiforova, V., Gakière, B., & Hoefgen, R. (2004). Molecular analysis and control of cysteine biosynthesis: integration of nitrogen and sulphur metabolism. *Journal of Experimental Botany*, *55*(401), 1283–92. doi:10.1093/jxb/erh136

Hirai, M. Y., Fujiwara, T., Awazuhara, M., Kimura, T., Noji, M., & Saito, K. (2003). Global expression profiling of sulfur-starved Arabidopsis by DNA macroarray reveals the role of O-acetyl-l-serine as a general regulator of gene expression in response to sulfur nutrition. *The Plant Journal : For Cell and Molecular Biology*, *33*(4), 651–63. Retrieved from http://www.ncbi.nlm.nih.gov/pubmed/12609039

Hirai, M. Y., Yano, M., Goodenowe, D. B., Kanaya, S., Kimura, T., Awazuhara, M., … Saito, K. (2004). Integration of transcriptomics and metabolomics for understanding of global responses to nutritional stresses in Arabidopsis thaliana. *Proceedings of the National Academy of Sciences of the United States of America*, *101*(27), 10205–10. doi:10.1073/pnas.0403218101

Ho, C.-H., Lin, S.-H., Hu, H.-C., & Tsay, Y.-F. (2009). CHL1 functions as a nitrate sensor in plants. *Cell*, *138*(6), 1184–94. doi:10.1016/j.cell.2009.07.004

Hulsen, T., de Vlieg, J., & Alkema, W. (2008). BioVenn - a web application for the comparison and visualization of biological lists using area-proportional Venn diagrams. *BMC Genomics*, *9*(1), 488. doi:10.1186/1471-2164-9-488

Huxtable, R. J. (1992). Physiological actions of taurine. *Physiol Rev*, *72*(1), 101–163. Retrieved from http://physrev.physiology.org/content/72/1/101

Jonassen, E. M., Lea, U. S., & Lillo, C. (2008). HY5 and HYH are positive regulators of nitrate reductase in seedlings and rosette stage plants. *Planta*, *227*(3), 559–64. doi:10.1007/s00425-007-0638-4

Kamenetsky, R., & Rabinowitch, H. (2006). The genus Allium: A developmental and horticultural analysis. *Horticultural Reviews*. Retrieved from http://books.google.com/books?hl=en&lr=&id=wNZ2ODMVzkkC&oi=fnd&pg=PA329&dq=The+Genus+Allium:+A+developmental+and+horticultural+analysis&ots=wBEZ_b-2qo&sig=KV3dtM5cI0EzvQer3GE6a-Y5P4s

Kataoka, T., Watanabe-Takahashi, A., Hayashi, N., Ohnishi, M., Mimura, T., Buchner, P., … Takahashi, H. (2004). Vacuolar sulfate transporters are essential determinants controlling internal distribution of sulfate in Arabidopsis. *The Plant Cell*, *16*(10), 2693–704. doi:10.1105/tpc.104.023960

Kawashima, C. G., Matthewman, C. a, Huang, S., Lee, B.-R., Yoshimoto, N., Koprivova, A., … Kopriva, S. (2011). Interplay of SLIM1 and miR395 in the regulation of sulfate assimilation in Arabidopsis. *The Plant Journal : For Cell and Molecular Biology*, *66*(5), 863–76. doi:10.1111/j.1365-313X.2011.04547.x

Khan, M. S., Haas, F. H., Samami, A. A., Gholami, A. M., Bauer, A., Fellenberg, K., … Hell, R. (2010). Sulfite reductase defines a newly discovered bottleneck for assimilatory sulfate reduction and is essential for growth and development in Arabidopsis thaliana. *The Plant Cell*, *22*(4), 1216–31. doi:10.1105/tpc.110.074088

Khedim, T., Amirouche, N., & Amirouche, R. (2013). Biosystematics and Plant Genetic Resources: Example from the Genus Allium (Amaryllidaceae) of the Algerian Flora. *Actahort.org*, 19–24. Retrieved from http://www.actahort.org/members/showpdf?booknrarnr=997_1

Kiba, T., Feria-Bourrellier, A.-B., Lafouge, F., Lezhneva, L., Boutet-Mercey, S., Orsel, M., … Krapp, A. (2012). The Arabidopsis nitrate transporter NRT2.4 plays a double role in roots and shoots of nitrogen-starved plants. *The Plant Cell*, *24*(1), 245–58. doi:10.1105/tpc.111.092221

Kim, H., Hirai, M. Y., Hayashi, H., Chino, M., Naito, S., & Fujiwara, T. (1999). Role of O-acetyl-l-serine in the coordinated regulation of the expression of a soybean seed storage-protein gene by sulfur and nitrogen nutrition. *Planta*, *209*(3), 282–9. Retrieved from http://www.ncbi.nlm.nih.gov/pubmed/10502094

Klapheck, S., Grosse, W., & Bergmann, L. (1982). Effect of Sulfur Deficiency on Protein Synthesis and Amino Acid Accumulation in Cell Suspension Cultures of Nicotiana tabacum. *Zeitschrift Für Pflanzenphysiologie*, *108*(3), 235–245. doi:10.1016/S0044-328X(82)80123-2

Kliebenstein, D. J., Kroymann, J., Brown, P., Figuth, a, Pedersen, D., Gershenzon, J., & Mitchell-Olds, T. (2001). Genetic control of natural variation in Arabidopsis glucosinolate accumulation. *Plant Physiology*, *126*(2), 811–25. Retrieved from http://www.pubmedcentral.nih.gov/articlerender.fcgi?artid=111171&tool=pmcentrez&rendertype=abstract

Klomsiri, C., Karplus, P. A., & Poole, L. B. (2011). Cysteine-based redox switches in enzymes. *Antioxidants & Redox Signaling*, *14*(6), 1065–77. doi:10.1089/ars.2010.3376

Klonus, D., Höfgen, R., Willmitzer, L., & Riesmeier, J. W. (1994). Isolation and characterization of two cDNA clones encoding ATP-sulfurylases from potato by complementation of a yeast mutant. *The Plant Journal : For Cell and Molecular Biology*, *6*(1), 105–112.

Kopriva, S., Büchert, T., Fritz, G., Suter, M., Weber, M., Benda, R., … Brunold, C. (2001). Plant adenosine 5'-phosphosulfate reductase is a novel iron-sulfur protein. *The Journal of Biological Chemistry*, *276*(46), 42881–6. doi:10.1074/jbc.M107424200

Kopriva, S., Mugford, S. G., Baraniecka, P., Lee, B.-R., Matthewman, C. a, & Koprivova, A. (2012). Control of sulfur partitioning between primary and secondary metabolism in Arabidopsis. *Frontiers in Plant Science*, *3*(July), 163. doi:10.3389/fpls.2012.00163

Kopriva, S., Mugford, S. G., Matthewman, C., & Koprivova, A. (2009). Plant sulfate assimilation genes: redundancy versus specialization. *Plant Cell Reports*, *28*(12), 1769–80. doi:10.1007/s00299-009-0793-0

Koprivova, a, Suter, M., den Camp, R. O., Brunold, C., & Kopriva, S. (2000). Regulation of sulfate assimilation by nitrogen in Arabidopsis. *Plant Physiology*, *122*(3), 737–46. Retrieved from http://www.pubmedcentral.nih.gov/articlerender.fcgi?artid=58909&tool=pmcentrez&rendertype=abstract

Kopsell, D. E., & Randle, W. M. (1999). Changes in the S -alk (en) yl Cysteine Sulfoxides and their Biosynthetic Intermediates during Onion Storage. *Journal of American Society of Horticulture Science*, *124*(2), 177–183.

Krueger, R. J., & Siegel, L. M. (1982). Spinach siroheme enzymes: Isolation and characterization of ferredoxin-sulfite reductase and comparison of properties with ferredoxin-nitrite reductase. *Biochemistry*, *21*(12), 2892–904. Retrieved from http://www.ncbi.nlm.nih.gov/pubmed/7104302

Kupiecki, F. P., & Virtanen, A. I. (1960). Cleavage of alkylcysteine sulfoxides by an enzyme in onion (Allium cepa). *Acta Chemica Scandinavica*, *14*, 1913–1918.

Kusano, M., Fukushima, A., Redestig, H., & Saito, K. (2011). Metabolomic approaches toward understanding nitrogen metabolism in plants. *Journal of Experimental Botany*, *62*(4), 1439–53. doi:10.1093/jxb/erq417

Lähdesmäki, P. (1986). Determination of taurine and other acidic amino acids in plants. *Phytochemistry*, *25*(10), 2409–2411. doi:10.1016/S0031-9422(00)81707-0

Lee, B.-R., Koprivova, A., & Kopriva, S. (2011). The key enzyme of sulfate assimilation, adenosine 5'-phosphosulfate reductase, is regulated by HY5 in Arabidopsis. *The Plant Journal : For Cell and Molecular Biology*, *67*(6), 1042–54. doi:10.1111/j.1365-313X.2011.04656.x

Lee, R., Baldwin, S., Kenel, F., McCallum, J., & Macknight, R. (2013). FLOWERING LOCUS T genes control onion bulb formation and flowering. *NATURE COMMUNICATIONS*, *10*(1038).

Lee, S., & Kang, B. S. (2005). Interaction of Sulfate Assimilation with Nitrate Assimilation as a Function of Nutrient Status and Enzymatic Co-Regulation in Brassica juncea Roots. *Journal of Plant Biology*, *48*(September), 270–275.

Lejay, L., Wirth, J., Pervent, M., Cross, J. M.-F., Tillard, P., & Gojon, A. (2008). Oxidative pentose phosphate pathway-dependent sugar sensing as a mechanism for regulation of root ion transporters by photosynthesis. *Plant Physiology*, *146*(4), 2036–53. doi:10.1104/pp.107.114710

Leung, S. C. S., Smith, D., Chen, R., Mccallum, J. A., Mckenzie, M., & Mcmanus, M. T. (2012). Characterization of Adenosine 5' -Phospho-Sulfate Kinase (APSK) Genes from Higher Plants. In L. J. De Kok, L. Tabe, M. Tausz, M. J. Hawkesford, R. Hoefgen, M. T.

McManus, … E. Schnug (Eds.), *Sulfur Metabolism in Plants* (pp. 67–70). Dordrecht: Springer Netherlands. doi:10.1007/978-94-007-4450-9

Li, Y.-F., Zheng, Y., Jagadeeswaran, G., & Sunkar, R. (2013). Characterization of small RNAs and their target genes in wheat seedlings using sequencing-based approaches. *Plant Science : An International Journal of Experimental Plant Biology*, *203-204*, 17–24. doi:10.1016/j.plantsci.2012.12.014

Liang, G., Yang, F., & Yu, D. (2010). MicroRNA395 mediates regulation of sulfate accumulation and allocation in Arabidopsis thaliana. *The Plant Journal : For Cell and Molecular Biology*, *62*(6), 1046–57. doi:10.1111/j.1365-313X.2010.04216.x

Lillig, C. H., Schiffmann, S., Berndt, C., Berken, A., Tischka, R., & Schwenn, J. D. (2001). Molecular and catalytic properties of Arabidopsis thaliana adenylyl sulfate (APS)-kinase. *Archives of Biochemistry and Biophysics*, *392*(2), 303–10. doi:10.1006/abbi.2001.2453

Lillo, C., & Appenroth, K.-J. (2001). Light Regulation of Nitrate Reductase in Higher Plants: Which Photoreceptors are Involved? *Plant Biology*, *3*(5), 455–465. doi:10.1055/s-2001-17732

Lindermayr, C., & Durner, J. (2009). S-Nitrosylation in plants: pattern and function. *Journal of Proteomics*, *73*(1), 1–9. doi:10.1016/j.jprot.2009.07.002

Linkohr, B. I., Williamson, L. C., Fitter, A. H., & Leyser, H. M. O. (2002). Nitrate and phosphate availability and distribution have different effects on root system architecture of Arabidopsis. *The Plant Journal : For Cell and Molecular Biology*, *29*(6), 751–760. doi:10.1046/j.1365-313X.2002.01251.x

López-Bucio, J., Cruz-Ramírez, A., & Herrera-Estrella, L. (2003). The role of nutrient availability in regulating root architecture. *Current Opinion in Plant Biology*, *6*(3), 280–287. doi:10.1016/S1369-5266(03)00035-9

Lukat, P., Rudolf, M., Stach, P., Messerschmidt, A., Kroneck, P. M. H., Simon, J., & Einsle, O. (2008). Binding and reduction of sulfite by cytochrome c nitrite reductase. *Biochemistry*, *47*(7), 2080–6. doi:10.1021/bi7021415

Lunn, J., Droux, M., Martin, J., & Douce, R. (1990). Localization of ATP sulfurylase and O-acetylserine (thiol) lyase in spinach leaves. *Plant Physiology*, 1345–1352. Retrieved from http://www.plantphysiol.org/content/94/3/1345.short

Masclaux-Daubresse, C., Daniel-Vedele, F., Dechorgnat, J., Chardon, F., Gaufichon, L., & Suzuki, A. (2010). Nitrogen uptake, assimilation and remobilization in plants: challenges for sustainable and productive agriculture. *Annals of Botany*, *105*, 1141–1157. doi:10.1093/aob/mcq028

McCallum, J., Thomas, L., Shaw, M., Pither-Joyce, M., Leung, S., Cumming, M., & McManus, M. T. (2011). Genotypic variation in the sulfur assimilation and metabolism of onion (Allium cepa L.) I. Plant composition and transcript accumulation. *Phytochemistry*, *72*(9), 882–887. doi:10.1016/j.phytochem.2011.03.006

McManus, M. T., Joshi, S., Searle, B., Pither-Joyce, M., Shaw, M., Leung, S., … McCallum, J. (2012). Genotypic variation in sulfur assimilation and metabolism of onion (Allium cepa L.) III. Characterization of sulfite reductase. *Phytochemistry*, *83*, 34–42. doi:10.1016/j.phytochem.2012.07.028

McManus, M. T., Leung, S., Lambert, A., Scott, R. W., Pither-Joyce, M., Chen, B., & McCallum, J. (2005). Molecular and biochemical characterisation of a serine acetyltransferase of onion, Allium cepa (L.). *Phytochemistry*, *66*(12), 1407–16. doi:10.1016/j.phytochem.2005.04.034

Mengel, K., Kirkby, E. A., Kosegarten, H., & Appel, T. (2001). Sulphur. In K. Mengel, E. A. Kirkby, H. Kosegarten, & T. Appel (Eds.), *Principles of Plant Nutrition* (pp. 435–452). Springer Netherlands.

Meyer, C., & Stitt, M. (2001). Nitrate Reduction and signalling. *Plant Nitrogen*, 37–59.

Miura, K., & Hasegawa, P. M. (2010). Sumoylation and other ubiquitin-like post-translational modifications in plants. *Trends in Cell Biology*, *20*(4), 223–32. doi:10.1016/j.tcb.2010.01.007

Mugford, S. G., Yoshimoto, N., Reichelt, M., Wirtz, M., Hill, L., Mugford, S. T., … Kopriva, S. (2009). Disruption of adenosine-5'-phosphosulfate kinase in Arabidopsis reduces levels of sulfated secondary metabolites. *The Plant Cell*, *21*(3), 910–27. doi:10.1105/tpc.109.065581

Muslin, A. J., Tanner, J. W., Allen, P. M., & Shaw, A. S. (1996). Interaction of 14-3-3 with Signaling Proteins Is Mediated by the Recognition of Phosphoserine. *Cell*, *84*(6), 889–897. doi:10.1016/S0092-8674(00)81067-3

Nakagami, H., Sugiyama, N., Mochida, K., Daudi, A., Yoshida, Y., Toyoda, T., … Shirasu, K. (2010). Large-scale comparative phosphoproteomics identifies conserved phosphorylation sites in plants. *Plant Physiology*, *153*(3), 1161–74. doi:10.1104/pp.110.157347

Nakamura, T., Yamaguchi, Y., & Sano, H. (1999). Four rice genes encoding cysteine synthase: isolation and differential responses to sulfur, nitrogen and light. *Gene*, *229*(1-2), 155–61. Retrieved from http://www.ncbi.nlm.nih.gov/pubmed/10095115

Nakayama, M., Akashi, T., & Hase, T. (2000). Plant sulfite reductase: molecular structure, catalytic function and interaction with ferredoxin. *Journal of Inorganic Biochemistry*, *82*(1-4), 27–32. doi:10.1016/S0162-0134(00)00138-0

Nikiforova, V. J., Bielecka, M., Gakière, B., Krueger, S., Rinder, J., Kempa, S., … Hoefgen, R. (2006). Effect of sulfur availability on the integrity of amino acid biosynthesis in plants. *Amino Acids*, *30*(2), 173–83. doi:10.1007/s00726-005-0251-4

Ohyama, T., Minagawa, R., Ishikawa, S., Yamamoto, M., & Hung, N. V. P. (2012). Soybean Seed Production and Nitrogen Nutrition.

Pasantes-Morales, H., & Flores, R. (1991). Taurine content of Mexican beans. *Journal of Food Composition and Analysis*, *4*(4), 322–328. doi:10.1016/0889-1575(91)90018-2

Pfaffl, M. W. (2001). A new mathematical model for relative quantification in real-time RT-PCR. *Nucleic Acids Research*, *29*(9), e45. Retrieved from http://www.pubmedcentral.nih.gov/articlerender.fcgi?artid=55695&tool=pmcentrez&rendertype=abstract

Prosser, I. M., Purves, J. V, Saker, L. R., & Clarkson, D. T. (2001). Rapid disruption of nitrogen metabolism and nitrate transport in spinach plants deprived of sulphate. *Journal of Experimental Botany*, *52*(354), 113–21. Retrieved from http://www.ncbi.nlm.nih.gov/pubmed/11181720

Randle, W. M., Lancaster, J. E., Shaw, M. L., Sutton, K. H., Hay, R. L., & Bussard, M. L. (1995). Quantifying Onion Flavor Compounds Responding to Sulfur Fertility-Sulfur Increases Levels of Alk (en) yl Cysteine Sulfoxides and Biosynthetic Intermediates. *Journal of Smerican Society of Sorticulture Science*, *120*(3), 1075–1081.

Ravilious, G. E., Nguyen, A., Francois, J. a, & Jez, J. M. (2012a). Structural basis and evolution of redox regulation in plant adenosine-5'-phosphosulfate kinase. *Proceedings of the National Academy of Sciences of the United States of America*, *109*(1), 309–14. doi:10.1073/pnas.1115772108

Rezaei, E. E., Kafi, M., & Bannayan, M. (2013). Nitrogen and Cultivated Bulb Weight Effects on Radiation and Nitrogen-Use Efficiency , Carbon Partitioning and Production of Persian Shallot (Allium altissimum Regel .), *2013*(10), 225–232.

Rotte, C., & Leustek, T. (2000). Differential subcellular localization and expression of ATP sulfurylase and 5'-adenylylsulfate reductase during ontogenesis of Arabidopsis leaves indicates that cytosolic and plastid forms of ATP sulfurylase may have specialized functions. *Plant Physiology*, *124*(2), 715–24. Retrieved from http://www.pubmedcentral.nih.gov/articlerender.fcgi?artid=59176&tool=pmcentrez&rendertype=abstract

Rouached, H., Secco, D., & Arpat, a B. (2009). Getting the most sulfate from soil: Regulation of sulfate uptake transporters in Arabidopsis. *Journal of Plant Physiology*, *166*(9), 893–902. doi:10.1016/j.jplph.2009.02.016

Ruijter, J. M., Ramakers, C., Hoogaars, W. M. H., Karlen, Y., Bakker, O., van den Hoff, M. J. B., & Moorman, a F. M. (2009). Amplification efficiency: linking baseline and bias in the analysis of quantitative PCR data. *Nucleic Acids Research*, *37*(6), e45. doi:10.1093/nar/gkp045

Saghir, A., Mann, L., & Yamaguchi, M. (1965). Composition of volatiles in Allium as related to habitat, stage of growth, and plant part. *Plant Physiology*, *40*(4), 681–685. Retrieved from http://www.ncbi.nlm.nih.gov/pmc/articles/PMC550361/

Saito, K. (2004). Sulfur Assimilatory Metabolism . The Long and. *Metabolism Clinical And Experimental*, *136*(September), 2443–2450. doi:10.1104/pp.104.046755.Figure

Sanda, S., Leustek, T., Theisen, M. J., Garavito, R. M., & Benning, C. (2001). Recombinant Arabidopsis SQD1 converts udp-glucose and sulfite to the sulfolipid head group precursor UDP-sulfoquinovose in vitro. *The Journal of Biological Chemistry*, *276*(6), 3941–6. doi:10.1074/jbc.M008200200

Sawada, Y., Akiyama, K., Sakata, A., Kuwahara, A., Otsuki, H., Sakurai, T., … Hirai, M. Y. (2009). Widely targeted metabolomics based on large-scale MS/MS data for elucidating metabolite accumulation patterns in plants. *Plant & Cell Physiology*, *50*(1), 37–47. doi:10.1093/pcp/pcn183

Scheible, W. R., Gonzalez-Fontes, a., Lauerer, M., Muller-Rober, B., Caboche, M., & Stitt, M. (1997). Nitrate Acts as a Signal to Induce Organic Acid Metabolism and Repress Starch Metabolism in Tobacco. *The Plant Cell*, *9*(5), 783–798. doi:10.1105/tpc.9.5.783

Schwimmer, S., Carson, J. F., Makower, R. U., Mazelis, M., & Wong, F. F. (1960). Demonstration of aliinase in a protein preparation from onion. *Experientia*, *16*(10), 449–450.

Sekine, K., Sakakibara, Y., Hase, T., & Sato, N. (2009). A novel variant of ferredoxin-dependent sulfite reductase having preferred substrate specificity for nitrite in the unicellular red alga Cyanidioschyzon merolae. *The Biochemical Journal*, *423*(1), 91–8. doi:10.1042/BJ20090581

Sengupta, S., Subbarao Shaila, M., & Ramananda Rao, G. (1997). A novel autophosphorylation mediated regulation of nitrite reductase in Candida utilis. *FEBS Letters*, *416*(1), 51–56. doi:10.1016/S0014-5793(97)01166-6

Shibagaki, N., & Grossman, A. R. (2010). Binding of cysteine synthase to the STAS domain of sulfate transporter and its regulatory consequences. *The Journal of Biological Chemistry*, *285*(32), 25094–102. doi:10.1074/jbc.M110.126888

Shin, R., Jez, J. M., Basra, A., Zhang, B., & Schachtman, D. P. (2011). 14-3-3 Proteins Fine-Tune Plant Nutrient Metabolism. *FEBS Letters*, *585*(1), 143–7. doi:10.1016/j.febslet.2010.11.025

Smith, L. H. (1968). Biochemistry and Physiology of Taurine and Taurine Derivatives, *48*(2).

Smith, V. H., & Schindler, D. W. (2009). Eutrophication science: where do we go from here? *Trends in Ecology & Evolution*, *24*(4), 201–7. doi:10.1016/j.tree.2008.11.009

Sun, H., Tao, J., Liu, S., Huang, S., Chen, S., Xie, X., … Xu, G. (2014). Strigolactones are involved in phosphate- and nitrate-deficiency-induced root development and auxin transport in rice. *Journal of Experimental Botany*, eru029–. doi:10.1093/jxb/eru029

Takahashi, H., Kopriva, S., Giordano, M., Saito, K., & Hell, R. (2011). Sulfur assimilation in photosynthetic organisms: molecular functions and regulations of transporters and assimilatory enzymes. *Annual Review of Plant Biology*, *62*, 157–84. doi:10.1146/annurev-arplant-042110-103921

Takahashi, H., Watanabe-Takahashi, A., Smith, F. W., Blake-Kalff, M., Hawkesford, M. J., & Saito, K. (2000). The roles of three functional sulphate transporters involved in uptake and translocation of sulphate in Arabidopsis thaliana. *The Plant Journal : For Cell and Molecular Biology*, *23*(2), 171–82. Retrieved from http://www.ncbi.nlm.nih.gov/pubmed/10929111

Thomas, Ludivine, A. (2008). *Regulation of sulfur assimilation in onion (Allium cepa L.)*. Massey University.

Tomatsu, H., Takano, J., Takahashi, H., Watanabe-Takahashi, A., Shibagaki, N., & Fujiwara, T. (2007). An Arabidopsis thaliana high-affinity molybdate transporter required for efficient uptake of molybdate from soil. *Proceedings of the National Academy of Sciences of the United States of America*, *104*(47), 18807–12. doi:10.1073/pnas.0706373104

Touraine, B., Muller, B., & Grignon, C. (1992). Effect of Phloem-Translocated Malate on NO(3) Uptake by Roots of Intact Soybean Plants. *Plant Physiology*, *99*(3), 1118–23. Retrieved from http://www.pubmedcentral.nih.gov/articlerender.fcgi?artid=1080591&tool=pmcentrez&rendertype=abstract

Towbin, H., Staehelin, T., & Gordon, J. (1979). Electrophoretic transfer of proteins from polyacrylamide gels to nitrocellulose sheets: procedure and some applications. *Proceedings of the National Academy of Sciences of the United States of America*, *76*(9), 4350–4354. doi:10.1073/pnas.76.9.4350

Truong, K., & Ikura, M. (2001). The use of FRET imaging microscopy to detect protein–protein interactions and protein conformational changes in vivo. *Current Opinion in Structural Biology*, *11*(5), 573–578. doi:10.1016/S0959-440X(00)00249-9

Tsay, Y.-F., Chiu, C.-C., Tsai, C.-B., Ho, C.-H., & Hsu, P.-K. (2007). Nitrate transporters and peptide transporters. *FEBS Letters*, *581*(12), 2290–300. doi:10.1016/j.febslet.2007.04.047

Urano, Y., Manabe, T., Noji, M., & Saito, K. (2000). Molecular cloning and functional characterization of cDNAs encoding cysteine synthase and serine acetyltransferase that may be responsible for high cellular cysteine content in Allium tuberosum. *Gene*, *257*(2), 269–77. Retrieved from http://www.ncbi.nlm.nih.gov/pubmed/11080593

Vega, J., Cárdenas, J., & Losada, M. (1980). *Photosynthesis and Nitrogen Fixation - Part C*. *Methods in Enzymology* (Vol. 69, pp. 255–270). Elsevier. doi:10.1016/S0076-6879(80)69025-9

Vitousek, P., & Aber, J. (1997). Human alteration of the global nitrogen cycle: sources and consequences. *Ecological Applications*, *7*(November 1996), 737–750.

Wang, W., Vinocur, B., Shoseyov, O., & Altman, A. (2004). Role of plant heat-shock proteins and molecular chaperones in the abiotic stress response. *Trends in Plant Science*, *9*(5), 244–52. doi:10.1016/j.tplants.2004.03.006

Watanabe, M., Hubberten, H.-M., Saito, K., & Hoefgen, R. (2010). General regulatory patterns of plant mineral nutrient depletion as revealed by serat quadruple mutants disturbed in cysteine synthesis. *Molecular Plant*, *3*(2), 438–66. doi:10.1093/mp/ssq009

Wedel, N., Soll, J., & Paap, B. K. (1997). CP12 provides a new mode of light regulation of Calvin cycle. *Proceedings of the National Academy of Sciences of the United States of America*, *94*(September), 10479–10484.

Wirtz, M., & Hell, R. (2006). Functional analysis of the cysteine synthase protein complex from plants: structural, biochemical and regulatory properties. *Journal of Plant Physiology*, *163*(3), 273–86. doi:10.1016/j.jplph.2005.11.013

Xia, J., Mandal, R., Sinelnikov, I. V, Broadhurst, D., & Wishart, D. S. (2012). MetaboAnalyst 2.0--a comprehensive server for metabolomic data analysis. *Nucleic Acids Research*, *40*(Web Server issue), W127–33. doi:10.1093/nar/gks374

Xia, Z., Sun, K., Wang, M., Wu, K., Zhang, H., & Wu, J. (2012). Overexpression of a maize sulfite oxidase gene in tobacco enhances tolerance to sulfite stress via sulfite oxidation and CAT-mediated H2O2 scavenging. *PloS One*, *7*(5), e37383. doi:10.1371/journal.pone.0037383

Xia, Z., Wu, K., Zhang, H., Wu, J., & Wang, M. (2014). Sulfite Oxidase is Essential for Timely Germination of Maize Seeds upon Sulfite Exposure. *Plant Molecular Biology Reporter*. doi:10.1007/s11105-014-0760-y

Xu, G., Fan, X., & Miller, A. J. (2012). Plant nitrogen assimilation and use efficiency. *Annual Review of Plant Biology*, *63*, 153–82. doi:10.1146/annurev-arplant-042811-105532

Yi, H., Galant, A., Ravilious, G. E., Preuss, M. L., & Jez, J. M. (2010). Sensing sulfur conditions: simple to complex protein regulatory mechanisms in plant thiol metabolism. *Molecular Plant*, *3*(2), 269–79. doi:10.1093/mp/ssp112

Yoshimoto, N., Inoue, E., Saito, K., Yamaya, T., & Takahashi, H. (2003). Mediates Re-Distribution of Sulfur from Source to Sink Organs in Arabidopsis 1. *Plant Physiology*, *131*(April), 1511–1517. doi:10.1104/pp.014712.plasmamembranes

Zhang, B., Pasini, R., Dan, H., Joshi, N., Zhao, Y., Leustek, T., & Zheng, Z. (2014). Aberrant gene expression in the Arabidopsis SULTR1 ; 2 mutants suggests a possible regulatory role for this sulfate transporter in response to sulfur nutrient status, 185–197. doi:10.1111/tpj.12376

Zhao, M.-G., Chen, L., Zhang, L.-L., & Zhang, W.-H. (2009). Nitric reductase-dependent nitric oxide production is involved in cold acclimation and freezing tolerance in Arabidopsis. *Plant Physiology*, *151*(2), 755–67. doi:10.1104/pp.109.140996

Zheng, D., Han, X., An, Y., Guo, H., Xia, X., & Yin, W. (2013). The nitrate transporter NRT2.1 functions in the ethylene response to nitrate deficiency in Arabidopsis. *Plant, Cell & Environment*, *3*, 1328–1337. doi:10.1111/pce.12062

Zuber, H., Davidian, J., Aubert, G., Aime, D., Belghazi, M., Lugan, R., … Gallardo, K. (2010). The Seed Composition of Arabidopsis Mutants for the Group 3 Sulfate Transporters Indicates a Role in Sulfate. *Plant Physiology*, *154*(October), 913–926. doi:10.1104/pp.110.162123

Appendices

Appendix 1: Full protein sequence alignment for AcSiR1 and AcNiR1 using the PROMALS server (http://prodata.swmed.edu/promals/promals.php). The blue denotes conserved α-helix and the red colour denotes conserved β sheet. Green lines denote the predicted transit peptide for each sequence

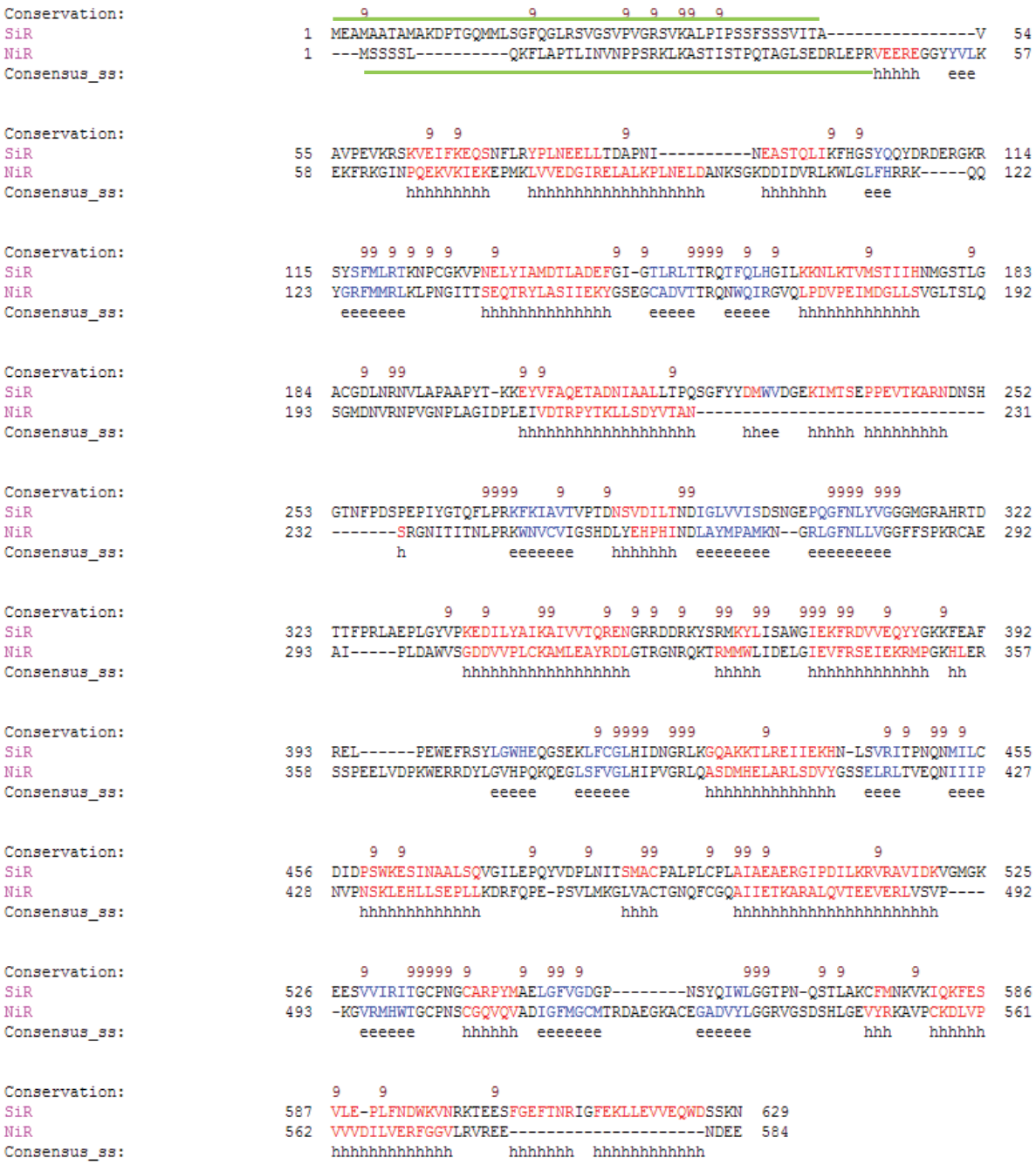
Conservation:
SiR
NiR
Consensus_ss:

Appendix 2: CLUSTAL alignment of SiR and NiR sequences from various monocots and dicots showing conserved residues (highlighted in red box) and conserved secondary structure designated as consensus_ss. In the secondary structure, the blue colour and letter e stands for α-helix and the red colour and letter h for β sheet. The sequences are grouped into two based on sequence similarity with the group representative sequence ID in magenta.

Appendix 3: Sequences of primers used for amplification of AcSiR1 and AcNiR1

Primer name	Forward
SiR-F	ATGGAAGCGATGGCGGCGA
SiR-R	TTAATTTTTAGAACTATCCCACTGCTC
SIRmature-F	GTTATTACGGCTGTAGCTGTTCC
NiR3´RACE-F1	TGTCCTAATAGTTGCGGGCA
NiR3´RACE-F2	ATATTGGGTTTATGGGGTGC
NiR-mature-F	GTCGAAGAAAGGGAAGGAG
NIR-RT-Reverse	CAAACCTCTCGACCAAAATAT

Appendix 4: Sequences of primers used for q-RT-PCR (*A. cepa*)

Gene	Forward	Reverse
Cyclophilin	CAAACGCTGGACCTGGAAC	TCTCAATGGCTCGCACAAC
αTubulin	GATAAACTACCAGCCTCCGA	CAAACACTTCAGCCACACTC
AcHAST1;1LIKE1	ACCTGTCACTGATATAGACACC	CATCACCGCCTCATCAACT
AcATPS1	CTGAGTTCCTCCAAACACTTCA	ACAAGCAAAACCCTCTTCCTCT
AcAPSR1	CGACTCAAAAGACAGCACC	GCTCTCCATACCCTGACAA
AcAPSK1	CATACAGAAGAGACCGTGATGC	GTTCAATGGTTGCTCATAGGG
AcSiR1	CTCTGCCTCTATGTCCACTA	GCCATCACCAACAAACCCTA
AcSOX1	GCTGAGACAGGCAACAAATC	CAGGAACAACAACACGCA
AcOASTL1	CGAAAGAAGGATGTTGCTC	GTGTAGTGTGTTCCAGGGTTT
AcOASTL2	TGAGCCTACCGAAAGCAA	ATAACCCTTCTTGAAGTGCCA
AcOASTL3	CCTACAAGCGGTAACACG	GCAACCTTTGAT TCCCAATAA T
AcNRT2;1	CCAATAGGAAGTTGAATGAGAATGG	CATTTGCTCACACCATGTATCTC
AcNR1	CGTTGTTTATGCGAACCG	TATCCTCAGACCCACCCAT
AcNiR1	ATCACAACAAGCGAGCAGACT	TCCATAATCTCAGGCACATCAG
AcFT4	TGAAATAGGAGGTGTACCAAGAAT	TTCCGAAACTACCATCCATATTTG
AcCyclophilin	CAAACGCTGGACCTGGAAC	TCTCAATGGCTCGCACAAC
AcαTubulin	GATAAACTACCAGCCTCCGA	CAAACACTTCAGCCACACTC

Appendix 5: Sequences of primers used for q-RT-PCR (*A. thaliana*)

Gene	Forward	Reverse
At2G32170	ATCGAGCTAAGTTTGGAGGATGTAA	TCTCGATCACAAACCCAAAATG
AtUBC9	TCACAATTTCCAAGGTGCTGC	TCATCTGGGTTTGGATCCGT
AtSULTR1;1	TGGGTGGAATTGGCAAACTA	GACTCCTTGTTTATCAGCACG
AtAPS3	GCGGCGGATTTGCCGAGAGT	CCCACGAAGAGGACTAGCCCAAC
AtAPS4	AGCGAAGGCTGGGCAAGTCC	AGCCGTCTTCGAGCCGGAAC
AtAPR2	AAAAGAGCTCCACGGGCTAT	GAGATGTTGATTCACTCATGTCG
AtSiR1	GGGATCCCCAGCATTCTAAA	CTCCTAGCCAAACCTGATAGC
AtOAS-TL1	ACAGAACGCAAACGTCAAGCTG	GCTTCCCACCGGATAGAATAGCAC
ATOAS-TL2	AGGAAGGCTTGTTGGTTGGT	C TGGAAAAGCTGGGTCGAG
AtNRT2;1	CCATGGGAGTTGAGTTGAGCACTG	GTGGAGCTTCAAGTGAAACCTGTC
AtNR2	AACTCGCCGACGAAGAAGGTTG	GGGTTGTGAAAGCGTTGATGGG
AtNiR1	CAACCCTCAGAAACAAGAA	TTCTTGTTTCTGAGGGTTGAC

Appendix 6: Sequences of primers used for genome walking for *AcNiR1* amplification

Primer name	Forward
GM1 (with NA46)	TGGTTCAAGCCTGTCTTCGCT
GM3 (with NA47)	GCTAGGAATTTTGGAGAGAG

Appendix 7: Plasmid Vector map for p-GEM®-T EASY and p-GEX-6-P3

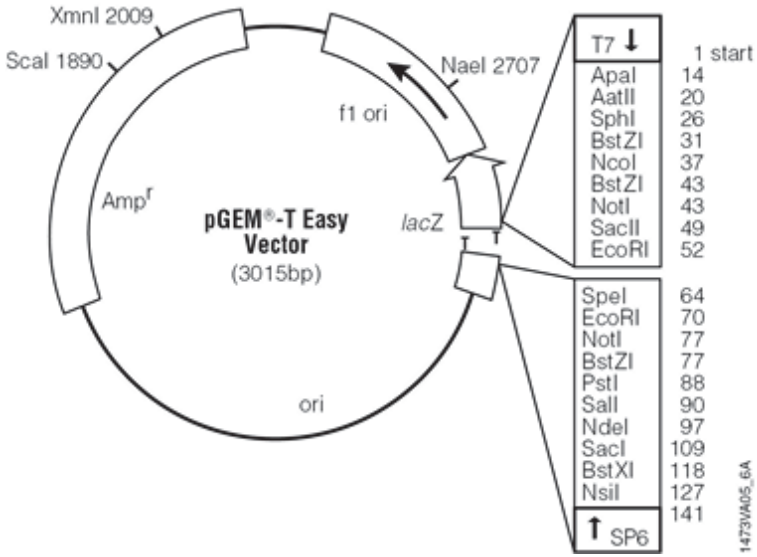

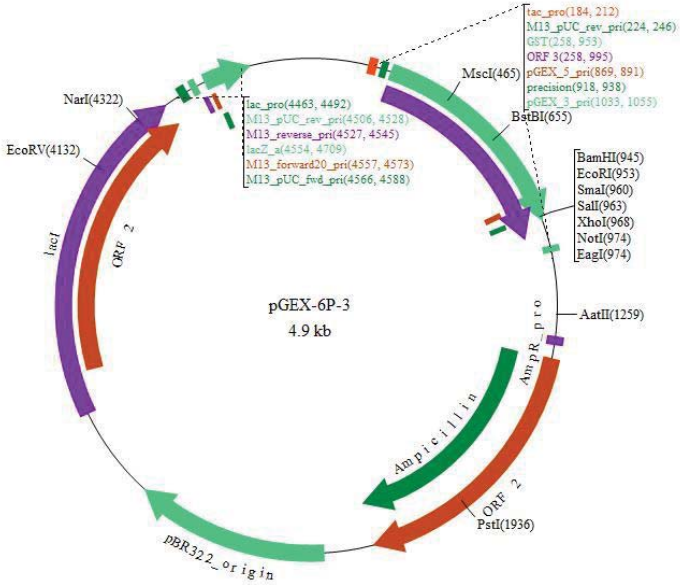

Appendix 8: Sequences of primers used for pGEX cloning

Primer name	Forward
pGEX-SiR-F	GACGACGAATTCATTGGAAGCGATGGCG
pGEX-SiR-R	GACGACGAATTCTTAATTTTTAGAACTATCCCACTGCT
pGEX-NiR-F	GACGACGGATCCATGTCTTCATCCTCTCTC
pGEX-NiR-R	GACGACGCGGCCGCTTTATTCCTCATCGTTCTC
pGEX-NiR-2F (mature)	GACGACGGATCCGTCGAAGAAAGGGAAGGA

Appendix 9: Gene accession numbers for *A. cepa*

Gene	Accession no.
AcHAST1;1LIKE1	AF458090
AcATPS1	AF403295.1
AcAPSR1	AF212155.1
AcAPSK1	JR848333
AcSiR1	JX020763.1
AcSOX1	JR845533.1
AcOASTL1	GBGJ01075644
AcOASTL2	GBRO01036168
AcOASTL3	GAAO01016265
AcNRT2;1LIKE1	GAAO01014042
AcNR1	GBGJ01079536
AcNiR1	GBGJ01123998
AcαTubulin	JR845462.1

Appendix 10: Heatmap of changes in response to the S x N treatments in the factorial experiment in 28 volatile metabolites identified in *A. cepa* leaf and bulb tissue. Values are calculated relative to control using the Metaboanalyst 2.0 online metabolomics data analysis suite

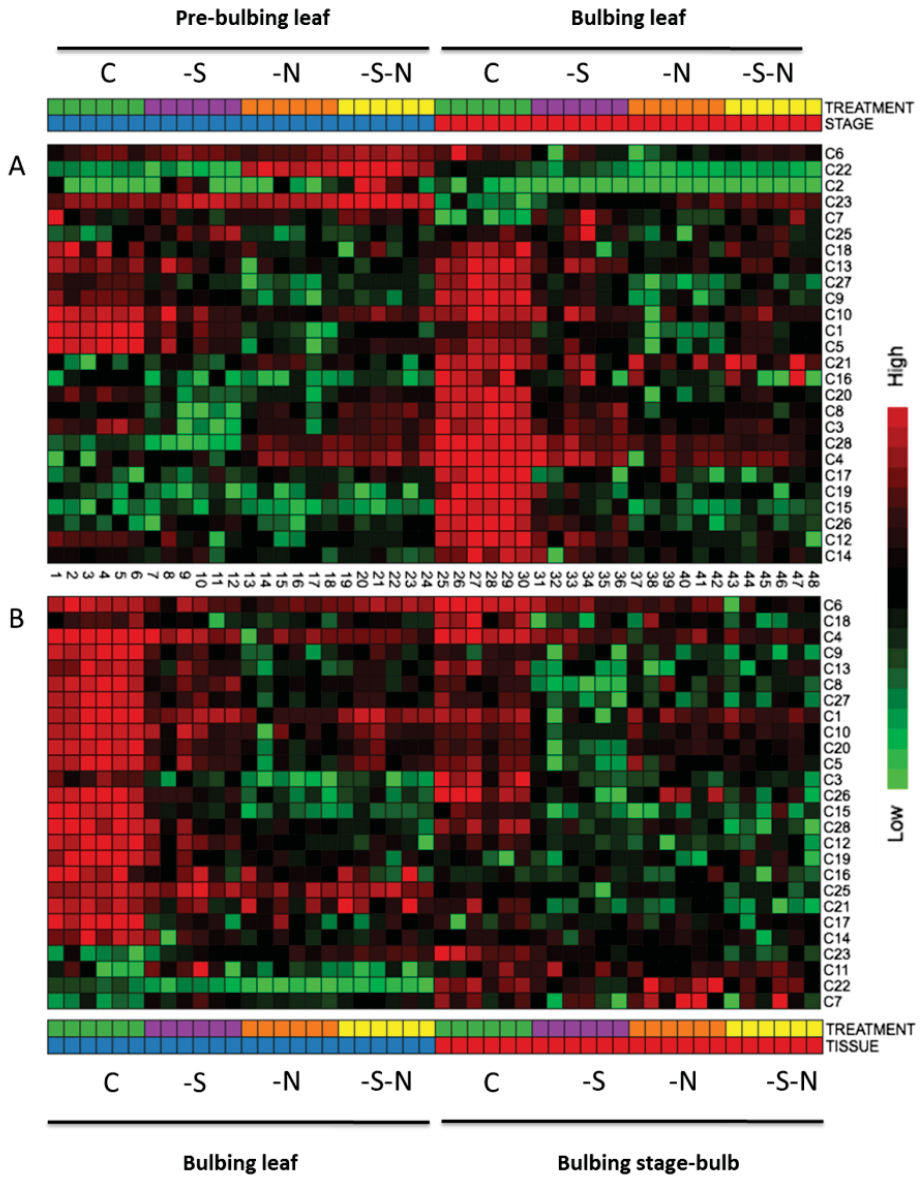

Appendix 11: Raw Targeted metabolomics and volatile quantification data (refer CD attached) A: Bar plots denoting intensity of accumulation of targeted metabolites in leaf (L), pseudostem/bulb (B) and root (R) at pre-bulbing (Y) and bulbing stage (M). B: Raw data for targeted metabolomics detailing intensity of accumulation for each metabolite in different tissues at pre-bulbing and bulbing stage along with treatment key and KEGG ID list for the targeted metabolome. C: List of metabolites differing significantly ($p<0.05$) in intensity of accumulation when compared to control treatment for each tissue at pre-bulbing and bulbing stage. The list was subsequently used to generate Venn diagrams using BioVenn application.

Appendix 12: Protein accumulation of AtSiR1 and AtNiR1 in the WT and *sir1-1* line of in leaf tissue as revealed by western analyses using anti-AtSiR1 and anti-AcNiR1 antibody respectively. Relative protein accumulation values are indicated as calculated by ImageJ software.

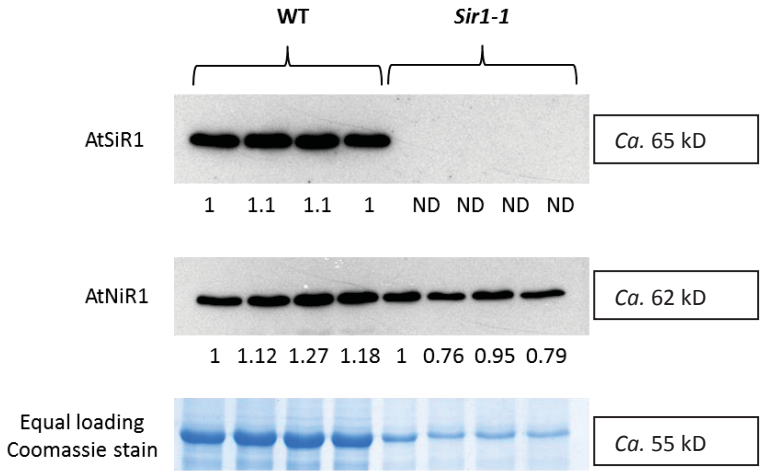

Appendix 13: Gene accession number for *A. thaliana*

Gene	Forward
At2G32170	NM_179854
AtUBC9	NM_179131
AtSULTR1;1	NM_116931.2
AtAPS3	U59738.1
AtAPS4	AF110407.1
AtAPR2	AF016283.1
AtSiR1	NM_120541.3
AtOAS-TL1	NM_117574.3
ATOAS-TL2	NM_001202816.1
AtNRT2;1	NM_100684.2
AtNR2	NM_103364.2
AtNiR1	NM_127123.2